R-13-08

Investigation of backfill candidate materials

Torbjörn Sandén, Siv Olsson, Linus Andersson,
Ann Dueck, Victor Jensen, Emelie Hansen

Clay Technology AB

Anna Johnsson, ÅF Industry AB

September 2014

Svensk Kärnbränslehantering AB
Swedish Nuclear Fuel
and Waste Management Co

Box 250, SE-101 24 Stockholm
Phone +46 8 459 84 00

ISSN 1402-3091
SKB R-13-08
ID 1379245

Investigation of backfill candidate materials

Torbjörn Sandén, Siv Olsson, Linus Andersson,
Ann Dueck, Victor Jensen, Emelie Hansen

Clay Technology AB

Anna Johnsson, ÅF Industry AB

September 2014

Keywords: Bentonite, Backfill, Geotechnical properties, Hydraulic conductivity, Mineralogy.

Abstract

The reference technique for backfilling the deposition tunnels in the KBS-3V concept is to use pre-compacted bentonite blocks together with a filling of bentonite pellets close to the tunnel wall. A robot will emplace the blocks one by one in the tunnel and bentonite pellets will be blown into the remaining slot between blocks and rock.

Three batches of candidate backfill materials were delivered between 2010 and 2012; 250 tons of bentonite from Ashapura, India in 2010, 100 tons of bentonite from Ibeco, Greece in 2011 and 600 tons of bentonite from Ashapura, India in 2012. The materials were used for tests of both the block and pellet manufacturing In addition, investigations of the material properties have been made in laboratory. This report contains the results of these investigations.

The performed tests can be divided into three parts:

1. **Acceptance control.** Some of these tests have been done on all big bags and some on every fifth or tenth and included determinations of the water content, swell index and CEC. The control of Asha 2012 also included determinations of the liquid limit and the granule size distribution.
2. **Hydro-mechanical tests.** These tests included determinations of the swelling pressure and hydraulic conductivity, the strength of compacted samples, compressibility of saturated backfill and also a study of how compacted bentonite is influenced when exposed to high relative humidity.
3. **Chemical and mineralogical analyses** of the bentonites and determination of the exchangeable cations.

The acceptance control showed that the Ibeco 2011 batch is a homogeneous bentonite, which fulfills the requirements regarding water content and granule size distribution. The swell index, liquid limit and CEC indicated that the amount of swelling minerals in this bentonite is moderate. The two batches from Asha consist of a more heterogeneous material. The requirements regarding water content are not fulfilled and the scatter in the determinations is large. The requirement on the granule size distribution is also not fulfilled, additionally both batches contain about 20% of aggregates that are much larger than stipulated.

The swell index for both Asha batches was higher than for the Ibeco bentonite. The Asha batch from 2012 had higher swell index than the batch from 2010. The scatter in the results of the liquid limit determination is very large, especially for samples of Asha 2012 from the last two-hundred big bags out of a total of five-hundred. There was also a clear difference in the results of the CEC determinations made on the two batches; the average CEC is similar for the two Asha batches (85 and 87 meq/100 g), but the variation in CEC is larger among the samples of Asha 2010 than 2012.

The swell index, liquid limit and CEC indicated that the amount of swelling minerals in both Asha batches was rather high. It should, however, be remembered when assessing the quality of the three batches that the Asha bentonite is sodium dominated, whereas the Ibeco bentonite is calcium dominated, which should result in different swelling capacities for the bentonites.

The grain density of the Ibeco bentonite was 2,723 kg/m^3 (N=5, std.dev=27.4) and of the two Asha batches 2,917 (N=5, std.dev=22.1) and 2,928 (N=5, std.dev=7.2) kg/m^3, respectively. The values are in agreement with earlier measurements on similar materials.

The Ibeco benonite had lower swelling pressure and higher hydraulic conductivity than expected. At low dry densities, below 1,350 kg/m^3, piping seemed to occur in some of the samples, resulting in very high hydraulic conductivity. To further understand the test results, bentonite from the Ibeco batches 2004 and 2008, investigated previously, was re-tested, which resulted in similar hydraulic conductivity and swelling pressure as determined earlier for these batches. The batch from 2011 was apparently of lower quality (lower smectite content) than the batches from 2004 and 2008, as indicated already in the acceptance control.

The compression properties of the saturated Asha 2010 bentonite was determined in two oedometer tests, one saturated with water with a salinity (Total Dissolved Solids) of 1% and the other with

3.5% salinity. The deformation of the samples was almost proportional to the vertical stress up to 3,200 kPa, which was the maximum stress applied in the tests. The evaluated compression modules were almost the same for both samples, 19 MPa and 18 MPa respectively, which means that the salinity of the pore water had little effect upon the compressibility.

The strength of compacted blocks of bentonite from the two Asha batches was investigated by unconfined one-dimensional compression tests and beam tests. The results show, as expected, a clear influence of the density on the maximum stress at failure and also of the water content of the samples. The results also indicate that blocks manufactured in full scale, with a water content of 20% and a dry density of 1,700 to 1,750 kg/m^3, will have high strength. Tests made on blocks of the as-delivered Asha 2010 batch resulted in rather low strength of the beams, but after crushing of the material before block compaction, the strength doubled, which demonstrates the effects of granule size distribution on the strength.

The influence of high relative humidity on compacted blocks was investigated on compacted specimens (d=50 mm, h=30 mm) with initial water content of 20% and dry density of about 1,700 kg/m^3, which were placed in vessels with a relative humidity of either 100% or 75%. One test was performed to determine the water uptake, another to determine expansion and cracking. The absorption rate at high relative humidity was higher than at low relative humidity, where almost no water was absorbed. Cracking was observed on the specimens exposed to high relative humidity while the specimens exposed to 75% RH were little affected since they were almost at equilibrium with their surrounding.

The exchangeable cation pool of the samples of both Asha batches was sodium-dominated (~50%), and had calcium as the second most abundant cation. The Ibeco-bentonite, which contained more than 20% Ca/Mg carbonates, was calcium-dominated (45%), and the proportions of sodium and magnesium were almost equal.

The chemical analyses of the bentonites included determinations of total sulphur, total carbon and acid-soluble carbon. The latter carbon fraction emanates primarily from carbonates. The total sulphur content varied from a minimum of < 0.02% S in samples of Asha 2010 to a maximum of 0.19% S in samples of Asha 2012. Gypsum was detected by XRD-analysis in several of the latter samples, suggesting that the major fraction of sulphur existed as sulphate. All samples contained carbonates, but the highest acid-soluble carbon content, 3%, was found for the Ibeco bentonite. In the samples of Asha 2010 and Ibeco 2011, the difference in total and acid soluble carbon contents was small. In the samples of Asha 2012, the total carbon content was systematically somewhat higher than the acid-soluble carbon content, indicating that small amounts of organic carbon might exist.

The major oxide composition, evaluated as oxide ratios, displayed a significant scatter among the Asha samples, demonstrating the heterogeneity of this bentonite. In contrast, the same ratios for the Ibeco samples were relatively constant.

The mineralogy was determined by XRD-analyses of randomly oriented powders and evaluated quantitatively by use of the Siroquant software. Despite the heterogeneity of the Asha bentonite, the average mineralogy of the two batches was similar. The average smectite content of the samples of Asha 2010 was 74%, and that of the samples of Asha 2012 76% (the latter analysed at CSIRO, Australia). SKB´s requirements stipulate that a candidate tunnel backfill bentonite should have a montmorillonite content between 50 and 60%, with an accepted range of 45 to 90%. Like montmorillonite, the smectite in the Asha bentonite is dioctahedral, but XRD-examination of random powders is inadequate for distinguishing the members in the montmorillonite–beidellite series at species level.

All samples of Ibeco 2011 contained high amounts (~20%) of dolomite and calcite. No potassium-bearing phase was detected in the XRD-traces, and yet the potassium content of the bentonite was fairly high. Detailed investigations of Ibeco bentonite delivered in 2004 and 2008 indicated that the smectite in these batches was interstratified with illitic layers. Interstratified illite/smectite may consequently exist also in the bentonite batch from 2011, but the available data are inadequate for identification of mixed-layers. Therefore, the calculated average smectite content of Ibeco 2011, 64%, may include an unknown, but probably small, proportion of illite/smectite mixed-layers.

Sammanfattning

Referensmetoden för återfyllning av deponeringstunnlar i KBS-3V-konceptet innefattar stapling av förkompakterade bentonitblock på en bädd av bentonitpellets. Blocken staplas ett och ett av en robot enligt ett förutbestämt mönster och pelletar blåses därefter in i de återstående spalterna mellan block och bergvägg.

Tre sändningar av potentiella återfyllningsmaterial levererades 2010 (250 ton bentonit från Ashapura, Indien), 2011 (100 ton bentonit från Milos, Grekland) och 2012 (600 ton bentonit från Ashapura, Indien) för tester av block- och pellettillverkning. Förutom dessa tester har även bestämningar av olika materialparametrar utförts i laboratorium. Denna rapport innehåller resultaten från laboratorieundersökningarna.

De undersökningar som gjorts kan delas upp i tre delar:

1. **Mottagningskontroll.** Tester har utförts på ett stort antal prover som har tagits från de olika storsäckar som materialet levererades i. Testerna omfattade bl a bestämning av vatteninnehåll, svällindex och CEC. Kontrollen av Asha 2012 innefattade även bestämning av flytgräns och kornstorleksfördelning.
2. **Hydromekaniska tester.** Dessa tester innefattade bestämning av svälltryck och hydraulisk konduktivitet, hållfasthet hos kompakterade prov, kompressibilitet hos vattenmättad återfyllning samt en undersökning av hur kompakterade lerprov påverkas vid exponering för hög relativ fuktighet.
3. **Kemiska och mineralogiska undersökningar.** Denna del innefattade XRD-analys, bestämning av utbytbara katjoner samt kemisk analys av materialen.

Resultaten från mottagningskontrollen visar att materialet från Ibeco 2011 är en homogen bentonit som uppfyller kraven när det gäller vatteninnehåll och kornstorleksfördelning. Resultaten från bestämningarna av svällindex, flytgräns och CEC indikerar emellertid att andelen svällande mineral i denna bentonit är ganska låg. De två sändningarna från Asha består av en mer inhomogen bentonit. Kraven när det gäller vatteninnehåll och kornstorleksfördelning är inte uppfyllda och spridningen i resultat är stor. I båda sändningarna har ungefär 20 % av materialet en större kornstorlek än vad som utlovats. Svällindex för dessa båda sändningar är högre än för Ibeco bentoniten och sändningen från 2012 har högre svällindex än den från 2010.

Spridningen i resultat från bestämningarna av flytgräns på Asha levererat 2012 är mycket stor, speciellt för de sista 200 säckarna av de totalt 500 levererade. Det finns också en tydlig skillnad när det gäller CEC för de två sändningarna från Asha. Variationen i CEC är väsentligt större för Asha 2010 än Asha 2012. Förklaringen till denna skillnad kan vara heterogeniteten hos Asha-bentoniten, vilken medfört problem att ta ut representativa prov. Emellertid visar svällindex, flytgräns och CEC att andelen svällande mineral i bentoniten är hög i båda sändningarna från Asha. Vid en kvalitetsbedömning av de tre sändningarna måste hänsyn tas till att Asha är en natriumdominerad bentonit vilket bör resultera i högre svällningskapacitet jämfört med Ibeco 2011, som är kalciumdominerad.

Korndensiteten var 2 723 (N=5, SD=27,4) kg/m^3 för Ibeco 2011, och 2 917 (N=5, SD=22,1) och 2 928 (N=5, SD=7,2) kg/m^3 för de två Asha-leveranserna. Dessa värden överensstämmer med tidigare mätningar på material från dessa leverantörer.

Svälltrycket var lägre och den hydrauliska konduktiviteten högre än väntat för Ibeco 2011. Vid låga densiteter, under 1 350 kg/m^3, verkade piping uppstå under mätningen, vilket resulterade i mycket höga hydrauliska konduktiviteter. För att få mer förståelse för resultatet repeterades tester med material från tidigare leveranser, 2004 och 2008, vilket resulterade i liknande värde på svälltryck och hydraulisk konduktivitet som tidigare hade bestämts för dessa material. Det kunde därmed fastställas att leveransen från 2011 var av lägre kvalitet än de från 2004 och 2008, vilket även indikerats i de tester som gjordes inom mottagningskontrollen.

Kompressionsegenskaperna hos den mättade bentoniten (Asha 2010) bestämdes genom två ödometerförsök, varvid ett av proven mättades med vatten med en salthalt på 1 % och det andra med 3,5 %.

Kompressionskurvorna efter det att ett nytt laststeg lagts på har en typisk form för denna typ av bentonitleror. Deformationen var nästintill proportionell mot den vertikala lasten upp till 3 200 kPa, vilket var den maximala last som lades på. De utvärderade kompressionsmodulerna var nästan samma för båda försöken, 18 och 19 MPa, vilket tyder på att salthalten hos porvattnet inte har någon större betydelse för kompressibiliteten hos materialet.

Hållfastheten hos kompakterade block undersöktes med enaxliga tryckförsök samt balkförsök. Dessa undersökningar gjordes på material från de båda leveranserna från Asha. Resultaten visar som väntat en tydlig inverkan av både densitet och vatteninnehåll när det gäller maximal hållfasthet. Resultaten tyder på att block tillverkade i full skala med ett vatteninnehåll på 20 % och med en densitet på 1 700–1 750 kg/m^3 av detta material har hög hållfasthet. Testerna visade också att kornstorleks-fördelningen hos bentoniten är viktig för hållfastheten efter kompaktering. Okrossad bentonit av Asha 2010 gav ganska låg hållfasthet hos balkarna, men efter krossning av materialet kunde balkar med betydligt högre hållfasthet tillverkas.

Kompakterade prov (D=50 mm, H=30 mm) av krossat material från Asha 2010 placerades i behållare där relativa fuktigheten styrdes till antingen 75 % eller 100 %. Startvatteninnehållet sattes till 20 % och torrdensiteten till 1 700 kg/m^3. Dessa tester gjordes i syfte att bestämma vattenupptag, expansion samt eventuell sprickbildning. Efter en testtid på 93 dagar var vatteninnehållsgradienten hos proven placerade i hög relativ fuktighet mindre än 2 % och motsvarande torrdensitetsgradient var mindre än 25 kg/m^3. Sprickor kunde observeras hos de prov som exponerats för hög relativ fuktighet medan provet placerat i 75 % inte hade påverkats så mycket då fuktigheten nästan befann sig i jämvikt med provets fuktighet.

Hos båda leveranserna av Asha-bentonit dominerades de utbytbara katjonerna av natrium (~50 %), följt av kalcium. Ibeco-bentoniten, som innehöll mer än 20 % Ca/Mg-karbonater, dominerades av kalcium (45 %), och hade ungefär lika proportioner av natrium och magnesium.

Sulfid, svavel och organiskt kol anses vara potentiellt skadliga i förvarsmiljön, men några gränsvärden för dessa ämnen i återfyllnadsmaterial har inte fastställts. De kemiska analyserna av bentoniterna inkluderade bestämningar av totalsvavel, totalkol samt syralösligt kol, d.v.s. karbonatkol.

Det totala svavelinnehållet varierade från < 0,02 % S i proven Asha 2010 till som mest 0,19 % i vissa prov av Asha 2012. Gips detekterades i flera av de senare proven, vilket tyder på att större delen av svavel föreligger som sulfat. Samtliga prov innehöll karbonatkol men högst halt, ca 3 % C,uppmättes för Ibeco-bentoniten. Skillnaden mellan halten totalkol och syralösligt kol var liten i proven av Asha 2010 och Ibeco, medan proven av Asha 2012 generellt hade en något högre halt av totalkol än av syralöslig kol, vilket kan tyda på att organiskt kol förekommer i dessa prov (0,24 % C som högst).

Den kemiska sammansättningen, utvärderad som oxidkvoter, visade stor spridning för Asha-proven, vilket speglar inhomogeniteten hos denna bentonit, medan samma kvoter för Ibeco-proven var relativt konstanta.

Mineralogin bestämdes genom XRD-analys av oorienterade pulverprov och utvärderades kvantitativt med hjälp av programvaran Siroquant. Trots inhomogeniteten hos Asha-bentoniten var totalmineralogin liksom den genomsnittliga smektithalten hos de båda leveranserna likartad: Asha 2010 innehöll 74 % smektit och Asha 2012 76 % (den senare analyserad hos CSIRO, Australien). SKB föreskriver att ett tunnelåterfyllnadsmaterial ska ha en montmorillonithalt mellan 50 och 60 % med en accepterad variation från 45 till 90 %. Smektiten i Asha-bentoniten är dioktaedrisk, liksom montmorillonit, men tillgängliga data är otillräckliga för identifikation av de dioktaedriska smektiterna i montmorillonit-beidellitserien till speciesnivå.

Alla prov av Ibeco-bentonit hade hög halt (~20 %) av dolomit och kalcit. Trots att bentonitens kaliumhalt var förhållandevis hög kunde inga kaliumförande mineral detekteras. Detaljerade undersökningar har dock visat att smektiten i tidigare leveranser av Ibeco-bentonit varit blandskiktad med illit. Blandskiktad illit/smektit kan således förekomma även i den bentonit som levererats 2011, men en röntgenundersökning av enbart bulkprov ger inte tillräckligt underlag för identifiering av blandskikt. Den beräknade genomsnittliga smektithalten hos Ibeco 2011, 64 %, kan därför inkludera en viss, men förmodligen liten, andel illit/smektit blandskikt.

Contents

1 Introduction

The reference technique for backfilling the deposition tunnels in the KBS3-V concept is to use pre-compacted bentonite blocks together with a filling of bentonite pellets close to the tunnel wall, see Figure 1-1. The blocks will be emplaced one by one by a robot, programmed to stack blocks in the tunnel according to a pre-designed pattern. When one six-meter section of the deposition drift is filled with blocks, bentonite pellets will be blown into the remaining slot between blocks and rock. This procedure will be repeated until the tunnel is filled.

The investigations described in this report have been performed within SKB's project System Design of Backfill abbreviated ÅSKAR. One of the main objectives has been to investigate different backfill candidate materials and to assess whether they fulfill the requirements.

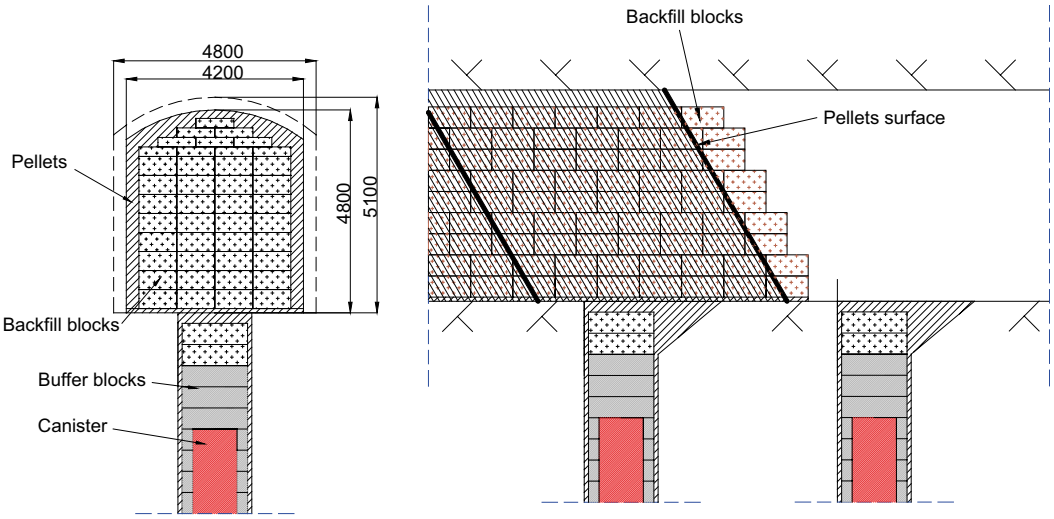

Figure 1-1. *Schematic showing the outlines of the backfilling.*

2 Materials and requirements

2.1 General

Three different batches of candidate backfill materials delivered to SKB between December 2010 and June 2012 have been investigated. The tests can be divided into three parts:

1. Acceptance control.
2. Hydro-mechanical parameters.
3. Mineralogical and chemical investigations.

2.2 Bentonites tested

The following bentonites were tested (see photo provided in Figure 2-1):

1. **Ibeco RWC-BF 2011** (abbreviated Ibeco 2011 in the text) is a material that originates from Milos in Greece. Ibeco is the name of the company producing the material, RWC stands for Radioactive Waste Clay and BF stands for Back Fill. It is a natural calcium bentonite with medium montmorillonite content. 100 tons were delivered (81 big bags) in spring of 2011. The manufacturer's data sheet is provided in Appendix 1.
2. **Asha NW BFL-L 2010** (abbreviated Asha 2010 in the text) is produced by Ashapura Minechem Co. The bentonite is quarried in the Kutch area on the northwest coast of India. The bentonite is sodium dominated with a montmorillonite content of about 70%. 250 tons were delivered (200 big bags) in winter 2010. The manufacturer's data sheet is provided in Appendix 2.
3. **Asha NW BFL-L 2012** (abbreviated Asha 2012 in the text). As above but the bentonite should according to the order have been crushed to a granule size distribution more suitable for the block manufacturing. 600 tons were delivered (480 big bags) in summer 2012.
4. **Minelco** is a Greek bentonite quarried on the island of Milos. The material is a sodium activated bentonite imported by the Swedish company LKAB, who use it in the steel production process. The material tested was taken from the storage at Äspö HRL. The Minelco material was introduced late in the process as an alternative material since severe problems were detected with the quality of the blocks made of Asha 2010. Development of the block manufacturing technique solved these problems, however. A limited number of tests were made with this bentonite.

Two previous deliveries of Ibeco RWC-BF are discussed in this report. The materials were delivered in 2004 and 2008 and are abbreviated Ibeco 2004 and Ibeco 2008 in the text. The material investigations are presented in Johannesson et al. (2010) and Olsson and Karnland (2009).

2.3 Material requirements

In the backfill production report (SKB 2010), the requirements placed on the bentonites as well as the installed and saturated backfill are listed. One of the aims of the investigations performed was to check that these requirements are fulfilled. Other reasons are e.g. to check that manufactured backfill blocks have a sufficiently high strength, so that they can be handled during the installation phase and to investigate how prone they are to cracking upon exposure to high relative humidity.

Figure 2-1. *Photo showing the different materials tested.*

The requirements can be compiled as follows:

Bentonite material

- The montmorillonite content should be between 50 and 60%. Accepted range is between 45 and 90%.
- Potentially harmful substances are sulfide, sulfur and organic carbon. No thresholds have been set regarding the content of these substances.
- The following should be measured and documented: dominant cation, CEC, sulfide, sulfur, organic carbon, and accessory minerals.

Installed backfill

- The hydraulic conductivity should be less than 10^{-10} m/s.
- The swelling pressure should be more than 0.1 MPa.
- The backfill should have a compressibility that ensures a saturated density of 1,950 kg/m^3 of the buffer.
- The backfill should not contain substances that may cause harmful buffer degradation or canister corrosion.
- The barrier functions of the backfill shall be maintained over the long term.

2.4 Ordering of material

The three batches of material delivered were ordered with the following requirements set for them:

Asha 2010 and Ibeco 2011:

- Granule size distribution between 0–5 mm.
- Maximum 20% particle size < 0.063 mm.
- Water content 16 ±1.5%.
- Montmorillonite content > 55%.

Asha 2012:

- Granule size distribution: All granules smaller than 3 mm.
- Water content 16 ±1.5%.
- Montmorillonite content > 55%.

3 Summary of tests performed

3.1 General

The screening and characterization testing of the bentonites has varied with time and an overview of the type of tests completed is provided in Table 3-1, 3-2 and 3-3.

All three batches of bentonite were delivered in big bags, which were numbered to facilitate their sampling.

The work was carried out in accordance with the activity plans AP TD KBP1003-10-043, AP TD KBP1003-10-026 and AP TD KBP1003-10-031. The activity plan is one of SKB's internal controlling documents.

3.2 Acceptance control

Water content, swell index and CEC have been used as an acceptance control for all three batches delivered. For the latest batch, Asha 2012, it was decided to also test the liquid limit and the granule size distribution. The liquid limit is a rather simple and fast test, which gives some indication about the amount of swelling minerals in the clay. The reason for also testing the granule size distribution was that the performed block compaction tests in full scale with the Asha 2010 material had shown that this parameter is of great importance for the quality of the blocks. A compilation of the acceptance control tests that have been performed is provided in Table 3-1.

3.3 Hydro-mechanical tests

The main focus of the tests was on the two batches of material from Ashapura (Asha), since the hydro-mechnical properties of the material had not been tested earlier. Hydro-mechnaical properties had been tested on the previous Ibeco deliveries, Ibeco 2004 and Ibeco 2008, see Johannesson et al. (2010) and Olsson and Karnland (2009), therefore only basic tests were performed on Ibeco 2011. The Minelco material was introduced in the test plan as an alternative material and only a slection of tests were conducted on the material.

A compilation of the hydro-mechanical tests performed is provided in Table 3-2.

Table 3-1. Tests included in the acceptance control of the three batches.

Acceptance control test	Asha 2010	Ibeco 2011	Asha 2012
Water content	Yes	Yes	Yes
Swell index	Yes	Yes	Yes
Liquid limit	*	*	Yes
CEC-Cation exchange capacity **	Yes	Yes	Yes
Granule size distribution	*	*	Yes

*Some single determinations have been made but not as a part of the acceptance control.

**These tests have been done as a part of the acceptance control but are of course also important for the chemical and mineralogical analysis.

Table 3-2. Performed hydro-mechanical tests.

Hydro-mechanical tests	Asha 2010	Ibeco 2011	Asha 2012	Minelco
Grain density	Yes	Yes	Yes	
Swelling pressure	Yes	Yes	Yes	Yes
Hydraulic conductivity	Yes	Yes	Yes	Yes
Compressibility of the saturated backfill	Yes			
One dimensional compression tests			Yes	
Beam tests	Yes		Yes	
Relative humidity induced swelling	Yes			

3.4 Chemical and mineralogical tests

Chemical and mineralogical tests were performed on material from all three batches of backfill candidate material delivered. Some of the tests results reported in this document were from other SKB projects or other laboratories; see Table 3-3, but in order to give a complete picture of the materials they are also presented here.

Table 3-3. Performed chemical and mineralogical tests.

Chemical and mineralogical analyses	Asha 2010	Ibeco 2011	Asha 2012	Minelco
Exchangable cations (EC)	Yes*	Yes	Yes	
Element analysis (EA)	Yes*	Yes	Yes	
Iron content (CBD)	Yes			
XRD-x-ray diffraction analysis	Yes*	Yes	Yes**	
Siroquant quantitative XRD analysis	Yes*	Yes	Yes**	

*Most of these tests have been performed within another SKB project but are also presented in this report.

**The sample preparation for these tests was performed at Clay Technology AB but the analyses were performed at CSIRO, Australia.

4 Acceptance control

4.1 General

In order to collect information regarding the bentonite quality and variations within the delivered batches, samples were taken from all big bags delivered and subsequently characterized.

The acceptance controls have included the following measurements:

- Water content.
- Swell index.
- Liquid limit.
- CEC.
- Granule size distribution.

The quality testing strategy has not been the same for all batches, but evolved with time and experience in material characterisation. For example, determinations of the liquid limit and the granule size distribution were added in the control of the latest batch from Asha but were not done for other materials.

Table 4-1 shows a compilation of the type and the number of tests performed in the acceptance control. The liquid limit and granule size distribution were determined for a few samples of Asha 2010 and Ibeco 2011, but the determination was not a real part of the overall acceptance control testing.

4.2 Sampling strategy

Each of the big bags delivered weighed approximately 1,250 kg. Samples weighing about 500 g were taken from the upper part of each of the bags after removal of the surface layer. Larger samples, 5 to 30 kg, were also taken for determinations of the granule size distribution and for the more comprehensive investigations.

4.3 Water content

4.3.1 General

The water content of the clay is important when manufacturing blocks or pellets. The three batches of material were ordered with water contents somewhat lower than the one required for the block compaction, in order to facilitate adjustment of the water content during mixing.

4.3.2 Method

The water content is defined as mass of water per mass of dry substance in %. The dry mass is obtained from drying the wet specimen at 105°C for 24 h. This definition is used in this report and is common in geotechnical contexts. Care should however be taken to ensure that suppliers understand this definition when orders are placed.

Table 4-1. Number of tests done and test types within the acceptance control.

Batch of bentonite	Number of big bags	Water content	Swell index	Liquid limit	CEC	Granule size distribution
Asha 2010	200	200	40	*6	89	*3
Ibeco 2011	81	81	17	*1	36	*2
Asha 2012	500	500	25	100	100	25

*The determination was not a part of the acceptance control.

Determination of the water content has been performed as follows:
A sample of about 20 g was placed in an aluminum baking tin and the bulk mass (m_b) of the powder was determined by use of a laboratory balance. The powder was dried in an oven for 24 hours at a temperature of 105°C. The dry solid mass (m_s) of the powder was then determined immediately after removal and the water mass (m_w) calculated according to Equation 4-1:

$$m_w = m_b = m_s \quad (4\text{-}1)$$

The water content (w) of the sample was calculated according to Equation 4-2:

$$w = \frac{m_w}{m_s} \quad (4\text{-}2)$$

4.3.3 Test matrix

The water content was determined for material from all big bags delivered. In total, 200 samples were taken from the Asha 2010 batch, 81 from the Ibeco 2011 batch and 500 from the Asha 2012 batch. The sampling and determination of the water content was performed and planned together with staff from Äspö HRL.

4.3.4 Results

The results of the water content measurements are presented in Figure 4-1 and a compilation is provided in Table 4-2. The complete data set for all measurements are also provided in Appendix 3, 4, and 5. The variation in water content was somewhat higher for the two batches delivered from Ashapura compared to the batch from Ibeco. The results show that when the material is to be used for block manufacturing in full scale, or pellet manufacturing, it will be necessary to have access to mixers in order to adjust the water content. It is, however, important that the ordered material has water content lower than the required, since it is easy to add water during a mixing process while drying of large amounts of clay is more difficult and energy intensive.

The requirement regarding water content was set to 16±1.5% for the as-delivered bentonite batches. The two batches from Asha have water contents very close to the required. The batch from Ibeco had higher water content than desired.

The Ibeco 2010 batch is a homogeneous bentonite and the scatter in measurements of water content in the delivered big bags is limited. The two batches from Asha consist of a more heterogeneous material. The requirement regarding water content is not fulfilled and the scatter in the determinations is large, especially for the last two-hundred big bags of the Asha 2012 batch where the scatter seems to increase compared to the first three-hundred big bags.

Table 4-2. Statistics on the water content determinations.

Batch of bentonite	Average water content, %	Max. water content, %	Min. water content, %	Standard deviation, %
Asha 2010	16.2	20.1	13.3	1.2
Ibeco 2011	20.3	22.2	17.9	0.9
Asha 2012	16.2	24.9	12.4	1.2

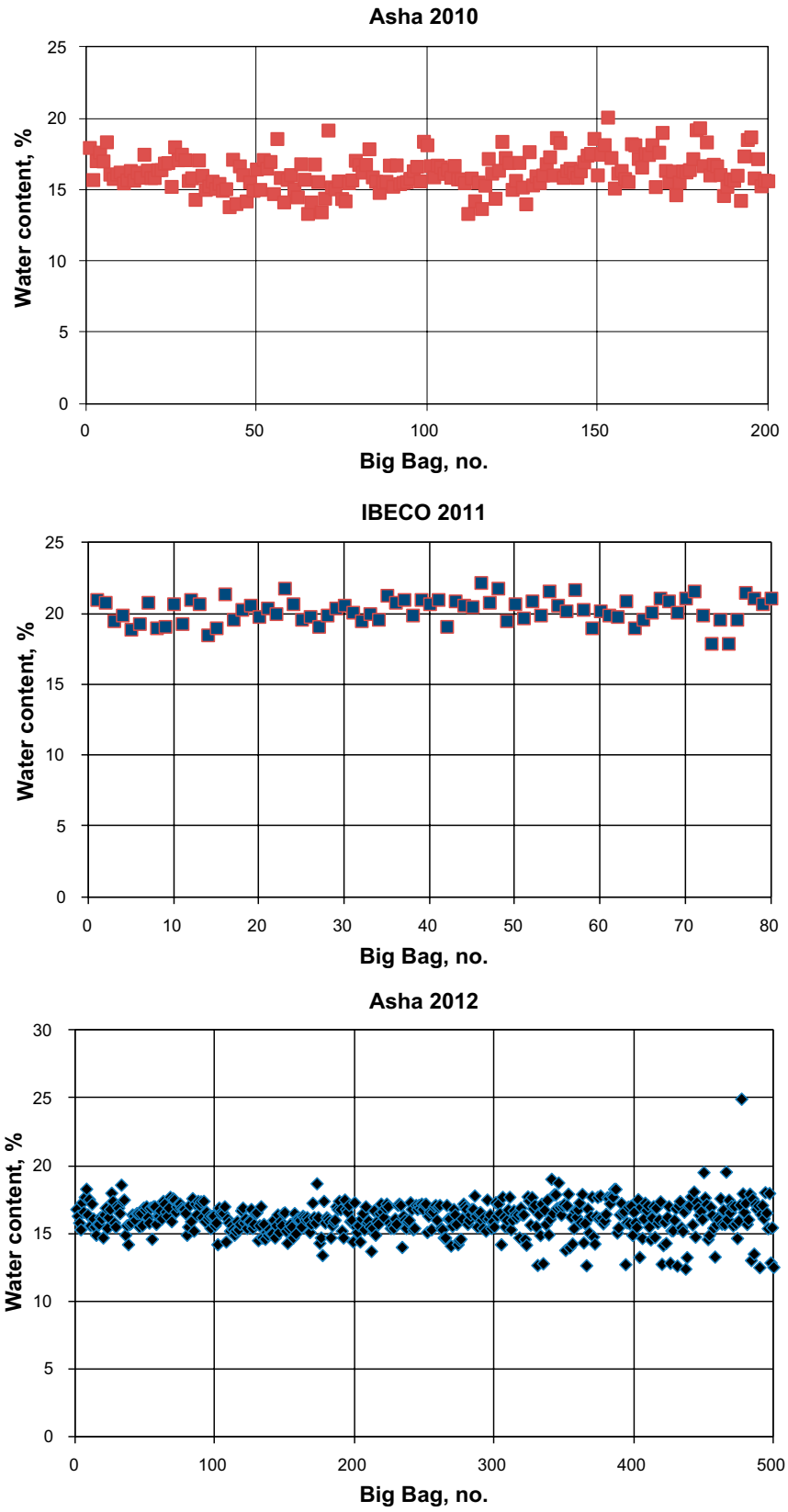

Figure 4-1. *Water content determinations for the three delivered batches plotted versus big bag number.* ***Upper****: Asha 2010,* ***Middle****: Ibeco 2011,* ***Lower****: Asha 2012.*

4.4 Swell index

4.4.1 General

The general swelling characteristics of clays can be determined with a swell index measurement.

4.4.2 Method

The swell index was determined according to a standard, ASTM D 5890. Two grams (2.00 g) of the dry clay is transferred in small portions into a 100 ml graduated cylinder filled with de-ionized water. The volume occupied by the swelled clay is recorded after 24 hours to provide the volumetric swelling capacity.

4.4.3 Test matrix

The swell indices have been determined for the following batches:

- **Asha 2010.** Measurements have been performed on material from every fifth big bag (40 samples).
- **Ibeco 2011.** Measurements have been performed on material from every fifth big bag (17 samples).
- **Asha 2012.** Measurements have been performed on material from twenty-five selected big bags (25 samples).

4.4.4 Results

The results are presented in Figure 4-2 and a compilation is provided in Table 4-3. The complete data set for all measurements is also provided in Appendix 6, 7, and 8. The Ibeco 2011 bentonite has the lowest swelling potential with an average value of 4.0 ml/g. The bentonite from Asha delivered in 2012 has higher swelling potential than the bentonite delivered in 2010 (7.3 ml/g in average 2012 compared to 5.1 ml/g 2010).

The standard deviation is very similar for the two batches from Asha, 0.5 and 0.6 ml/g respectively. The Ibeco bentonite has a lower standard deviation, 0.3 ml/g.

A number of additional determinations of the swell index were performed with the as-delivered Asha 2010 material:

1. The raw material was sorted in coarse and fine granules and four tests were made on each of this sorted material.
2. Two tests were made with material after citrate-bicarbonate-dithionite (CBD) extraction (Mehra and Jackson 1960) see Section 5.2 for details.

The results from the extra determinations (Table 4-4) show that the amount of swelling materials is higher in the coarse material which is consistent with the results obtained in Olsson et al. (2013). The two CBD samples showed a free swelling similar to the untreated material even if one of the samples had a value somewhat higher than the range determined at the acceptance control, see Table 4-3.

Table 4-3. Statistics on the swell index determinations.

Batch of bentonite	Number of samples	Average swelling index, ml/g	Max. swelling index, ml/g	Min. swelling index, ml/g	Standard deviation, ml/g
Asha 2010	40	5.1	6.4	4.2	0.6
Ibeco 2011	17	4.0	4.6	3.5	0.3
Asha 2012	25	7.3	8.5	6.3	0.5

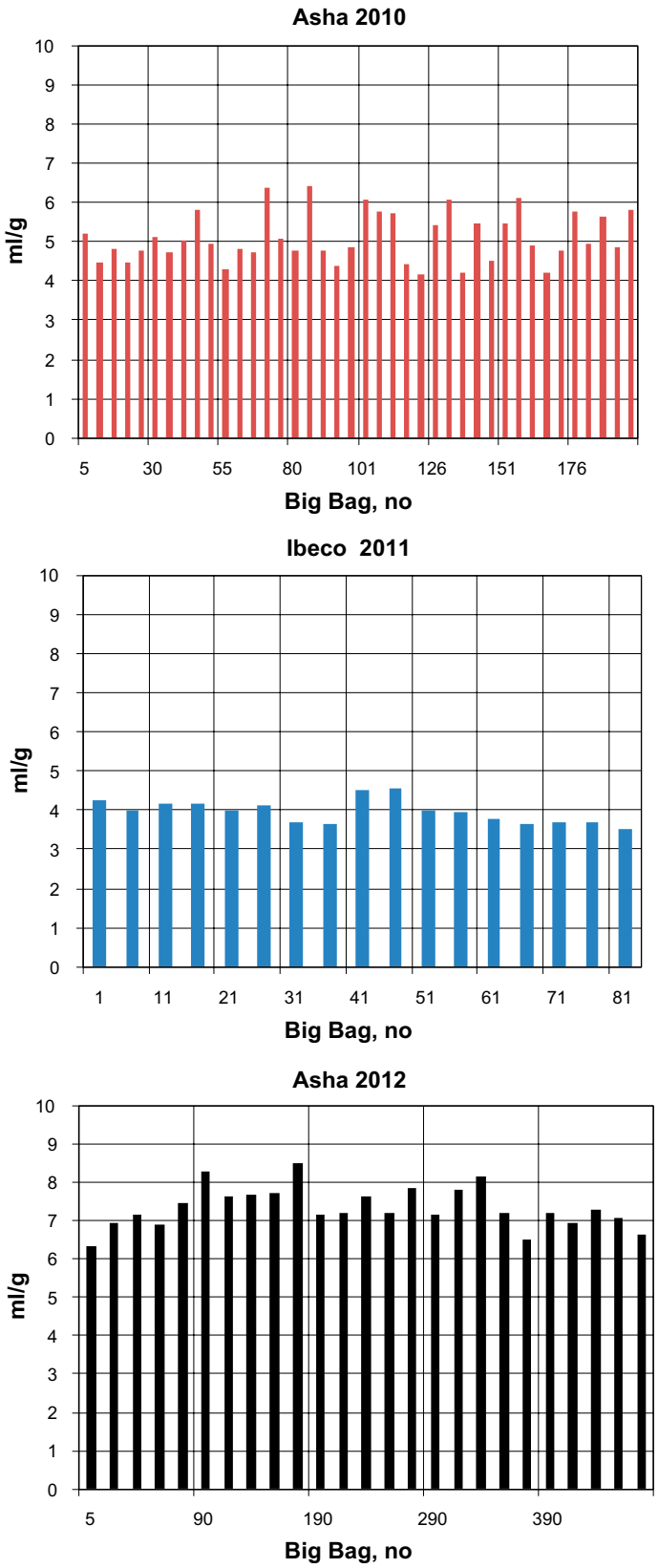

Figure 4-2. *Swell index for the three delivered batches plotted versus big bag number.* ***Upper****: Asha 2010,* ***Middle****: Ibeco 2011,* ***Lower****: Asha 2012.*

Table 4-4. Swell index determinations on sorted and CBD treated, respectively, samples of Asha 2010.

Sample	Big Bag no.	Free swelling ml/g
Coarse 1	Asha 113	9.1
Coarse 2	Asha 113	12.9
Coarse 3	Asha 113	6.5
Coarse 4	Asha 113	9.1
Fine 1	Asha 113	5.1
Fine 2	Asha 113	5.1
Fine 3	Asha 113	5.8
Fine 4	Asha 113	5.8
CBD 1	Asha 113	7.1
CBD 2	Asha 113	5.9

4.5 Liquid limit

4.5.1 General

The liquid limit for a bentonite is defined as the water content at which a soil changes from plastic to liquid behaviour. In this application, the test is used mainly as an index test in order to estimate the amount of swelling minerals in specific clays.

4.5.2 Method

The liquid limit was determined with the fall-cone method which is based on the measurement of the penetration into the clay sample of a standardized cone of specific mass. The method is described in the standard concering methods for laboratory testing of soil (SIS-CEN ISO/TS 17892-12:2007). Bentonite does not act like ordinary clays, which led to some modification to the standard technique. Changes were made with respect to the mixing procedure and the resting period after mixing. The preparation technique used also varied somewhat due to the large variation in granule size between the three batches, see descriptions in next sections. The determinations were made according the following procedure:

1. Weigh 125 g of pure water (de-ionised) in a glass beaker.
2. Stir the water by use of an electrical propeller mixer.
3. Slowly pour down approximately 28 g of bentonite material into the stirred water.
4. Mix thoroughly for another two minutes.
5. Fill a plastic cup with the bentonite paste and smoothen the surface.
6. Cover the bentonite paste in the beaker with a plastic bag, and the cup with a cap, and place it to rest for 24 h.
7. Drop the cone three times, read the penetration depth by use of the magnifying glass, and calculate the average penetration depth.
8. Take approximately 5 g of paste from the impact location and determine its water content (w) according to Equation 4-2.
9. Determine the liquid limit according to the one-point method according to the standard concering methods for laboratory testing of soil (SIS-CEN ISO/TS 17892-12:2007).

Asha 2010

Six samples of Asha 2010 were tested. The raw material was ground manually by use of a mortar, mixed with water to a suitable consistency and thereafter transferred to the sample holder. The clay was covered with a plastic film in order to avoid drying and was then left for 24 hours before the liquid limit was determined by the fall cone method.

Ibeco 2011

Sample preparation as above but samples were not ground before mixing with water (data on the granule size distribution is given in Section 4.7).

Asha 2012

Due to the large variations in the results (see Section 4.5.4) it was decided to perform the tests with Asha 2012 in two different ways:

1. **Asha crushed**. The as-delivered material was ground in a laboratory mill. The material was mixed with water to a suitable consistency and thereafter transferred to the sample holder. The clay was covered with a plastic film in order to avoid drying and was then left for 24 hours before the liquid limit was determined by the fall cone method. This method is the same as used with Asha 2010 but an electric mill, instead of mortar, was used for the grinding.
2. **Asha as-delivered.** The as-delivered material was mixed with water to a suitable consistency. The clay was after that left for 24 hours and was then mixed again. With this procedure all large grains disintegrated and the clay had a rather smooth consistency. After the second mixing the sample was transferred to the sample holder, covered with plastic film and then left for another 24 hours before the liquid limit was determined by the fall cone method.

4.5.3 Test matrix

The liquid limit was used as a part of the acceptance control for the Asha 2012 batch. A total number of 100 determinations were made, 50 with each of the preparation methods, see description above. A few determinations of the liquid limit were made also on samples taken from the two other batches of material.

4.5.4 Results

The results of the measurements are presented in Figure 4-3 and a compilation is provided in Table 4-5. The complete data set for all measurements are also provided in Appendix 9 and 10.

Studying the results from the measurements made on the Asha 2012 bentonite it is obvious that the variation in results is very large. Interesting is that this batch was delivered with two different boats; one boat carrying 300 big bags and the next boat 200 big bags. The results presented in Figure 4-3, shows clearly that the variation in achieved results increases for the last 200 big bags delivered. The reason for this is probably that this bentonite has been excavated from another part of the deposit. The variations observed using the two test methods are very similar which shows the reliability of the method. The tests performed with crushed material (blue dots in Figure 4-3) shows, however, higher values in average, 186% compared to 160% for the as-delivered material. This behavior indicates that there may be some degree of cementation in the material.

Table 4-5. Statistics on the liquid limit determinations.

Material	Number of samples	Average liquid limit, %	Max. liquid limit, %	Min. liquid limit, %	Standard deviation, %
Asha 2010	6	198	227	176	17.7
Ibeco 2011	1	116			
Asha 2012 (1)	50	186	265	141	26.2
Asha 2012 (2)	50	160	225	120	22.8

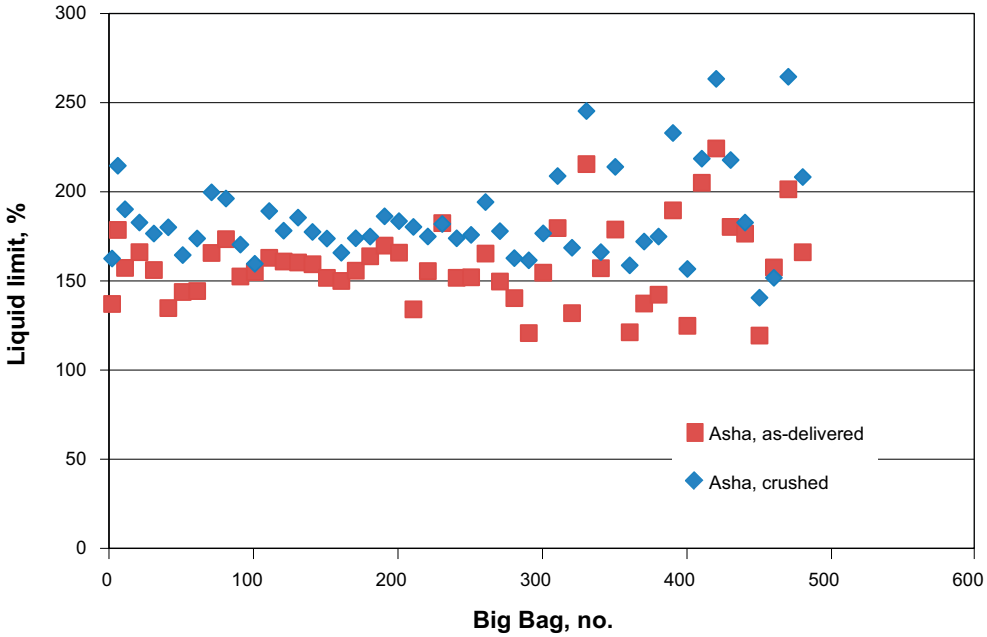

Figure 4-3. *Liquid limit determined for 100 samples taken from the Asha 2012 batch plotted versus big bag number.*

4.6 Cation Exchange Capacity (CEC)

4.6.1 General

The cation exchange capacity (CEC) of a bentonite is primarily determined by the charge of the predominant clay mineral smectite, which has a permanent negative layer charge caused by ion substitutions in the structure. The negative layer charge is balanced by exchangeable cations located between the smectite layers. Negative charge can be generated also on structural "edge" sites consisting of silanol, $–Al\text{-}OH_2$ or $–Fe\text{-}OH_2$ groups. The charge of such sites is pH-dependent and its relative importance for CEC of smectites is generally low but may be of significance – at appropriate pH – for the CEC of, for instance, oxyhydroxides and organic phases that may exist in bentonite. The layer charge of the smectite, and the nature of the charge-balancing interlayer cations, are of importance for the swelling behavior, and, accordingly, for several of the hydro-mechanical properties of a bentonite.

4.6.2 Method

The cation exchange capacity was determined by exchange with copper(II)triethylenetetramine (Cu-trien), following the procedure of Meier and Kahr (1999), modified according to Ammann et al. (2005) to ensure complete exchange. Sample mass and Cu-trien concentration were matched to ascertain that the maximum adsorption of the index cation should not exceed ~60%. In testing, 0.4 g of the ground sample was fully dispersed in 50 ml deionised water by ultrasonic treatment and shaking. 20 ml of ~20 mM Cu-trien solution was added to the suspension, which was left to react for 30 minutes on a vibrating table. After centrifugation the light absorbance of the supernatant at 620 nm was measured using a spectrophotometer (Shimadzu) and CEC was calculated on the basis of the uptake of Cu-trien by the clay. The water content of the clay was determined for a separate sample dried at 105°C to a constant weight. All CEC determinations were done at least twice.

4.6.3 Test matrix

The CEC determination was part of the acceptance control for all three batches of bentonite, although the number of samples taken from each of the batches varied. Moreover, some of the analyses of the Asha 2010 bentonite were performed and reported within another SKB project (Olsson et al. 2013) but the results are included also here. The batches were sampled as follows:

- **Asha 2010**. Every fifth big bag was sampled by filling a 1L polyethene bottle (see also below). In total, 40 samples were taken.
- **Ibeco 2011**. Every fifth big bag was sampled by filling a 1L polyethene bottle. In total, 18 samples were taken.
- **Asha 2012.** Every tenth big bag was sampled by filling a 1L polyethene bottles. In total, 50 samples were taken.

In order to obtain a smaller, representative sample for the laboratory tests, the 1L-sample was reduced to approximately 100 ml by repeated splitting. Thereafter, the sample for analysis was homogenized by grinding the sample in a ball mill. Seven of the samples of Asha 2010 were delivered to the laboratory in 250 ml polyethene bottles. These samples weighed from 170 to 230 g each and were subsequently homogenized by grinding the entire sample (details in Olsson et al. 2013).

Three randomly selected samples of the Asha 2010 bentonite (numbers 70, 113 and 125), were divided into five subsamples for repeatability tests (conditions: same laboratory, apparatus and operator, short time between tests).

4.6.4 Results

The results of CEC testing are presented in Figure 4-4 and in Appendix 11 to 13. Some descriptive statistical measures are compiled in Table 4-6, and the results of the repeatability test performed on three samples of the Asha 2010 bentonite are given in Table 4-7.

Table 4-6. Descriptive statistics on CEC determinations of bentonite samples of Asha 2010, Ibeco 2011 and Asha 2012. Previous CEC-determinations performed on single samples of the batches Asha 2004, Asha 2008, Ibeco 2004, and Ibeco 2008 are included for comparison (from Olsson and Karnland 2009).

Batch of bentonite	Number of samples	Number of analyses	Mean CEC value (meq/100 g)	Max. CEC value (meq/100 g)	Min. CEC value (meq/100 g)	Standard deviation (meq/100 g)
Asha 2010	40	89	86.8	96	79	4.7
Ibeco 2011	18	36	65.4	69	62	2.0
Asha 2012	50	100	84.8	89	81	1.5
Asha 2004	1	3	97	98	96	
Asha 2008	1	3	89	90	89	
Ibeco 2004	1	3	73	74	73	
Ibeco 2008	1	3	71	73	69	

Table 4-7. Repeatability test of the CEC determination, performed on five subsamples of Asha 2010-70, Asha 2010-113, and Asha 2010-125, respectively.

Sample id	CEC_1	CEC_2	CEC_3	CEC_4	CEC_5	CEC_{mean}	st.dev.
	meq/100 g						
Asha 2010-70	84	84	84	83	83	83.5	0.6
Asha 2010-113	85	84	85	85	84	84.7	0.8
Asha 2010-125	89	89	89	88	89	88.8	0.4

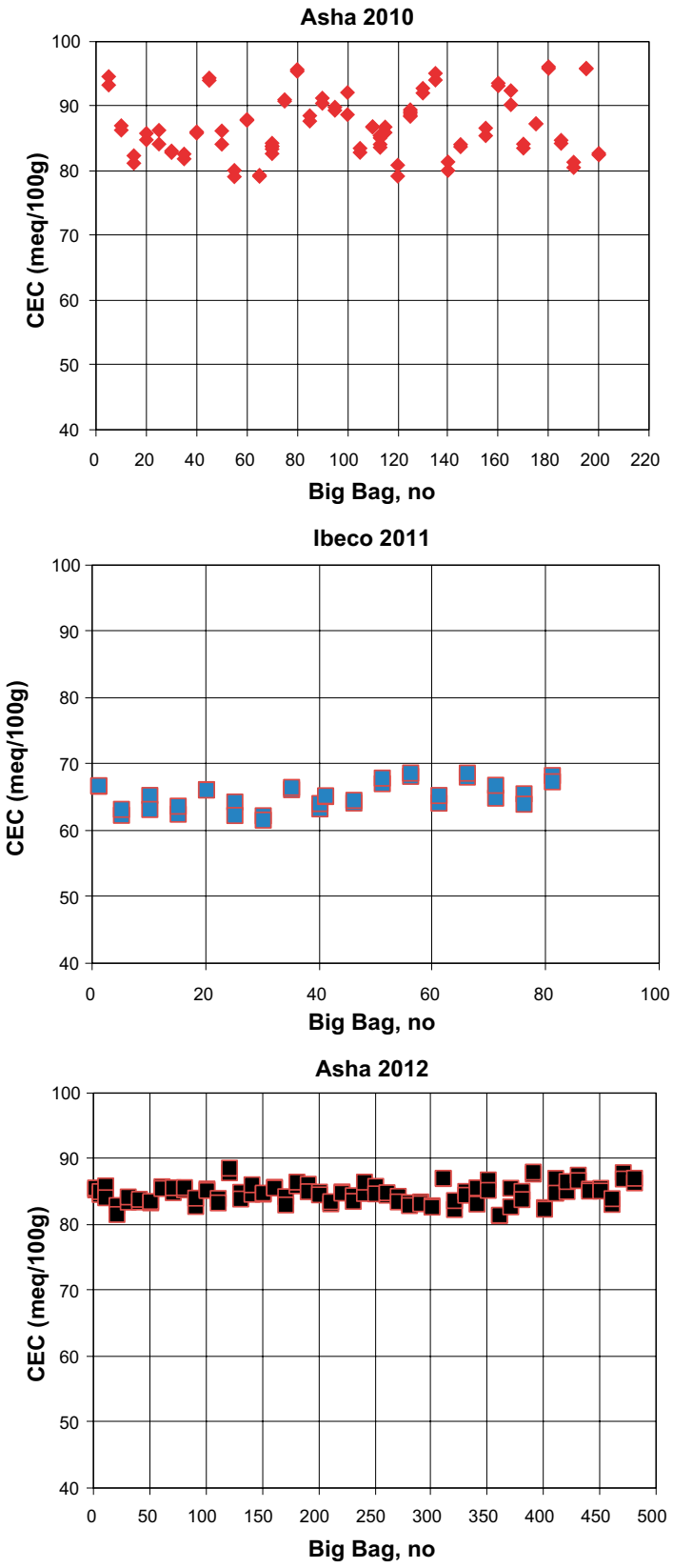

Figure 4-4. *CEC values for the three batches of bentonite plotted versus the bag number.* ***Upper****: Asha 2010,* ***Middle****: Ibeco 2011,* ***Lower****: Asha 2012.*

The average CEC of the Ibeco 2011 bentonite is 65 meq/100 g, which is within the range specified by the producer, 60±10 meq/100 g (Appendix 1) but somewhat lower than CEC reported for single samples of the batches from 2004 and 2008 (data from Olsson and Karnland (2009) included in Table 4-6). Both batches of Asha bentonite have higher mean CEC-values, 85 and 87 meq/100 g, than the Ibeco bentonite, which is consistent with their higher smectite content. It should also be noted that iron oxides/oxyhydroxides are ubiquitous in the Asha samples, and occur not only as discrete phases, but are also closely associated with the clay minerals, on the surfaces of which they may form coatings, thereby modifying the properties of the clay minerals, particularly the ion exchange behavior, but perhaps also their swelling and hydraulic behaviour.

The standard deviation (1σ) in the CEC determination was similar for the samples of the Ibeco 2011 and the Asha 2012 bentonite (2.0 and 1.5 meq/100 g, respectively), whereas the variation in CEC of the Asha 2010 bentonite was much larger (st.dev. 4.7 meq/100 g). This range of variation is significantly larger than the normal scatter in the Cu-trien method, as highlighted by the repeatability tests (Table 4-7), and as was demonstrated in inter-laboratory reproducibility tests of the Cu-trien method (Dohrmann et al. 2012a).

In the "as delivered state" the Asha 2010 bentonite was a heterogeneous material, as indicated by large grain-size variations among the samples; hard bentonite aggregates > 2 mm represented more than 50% of the material in some samples (cf. Figure 4-5). As for all heterogeneous materials, one of the most important factors in establishing a specific property is to obtain a small, representative sample for laboratory tests. In order to assess uncertainties related to material heterogeneity, Olsson et al. (2013) performed separate analyses on bentonite aggregates > 2 mm sorted by colour. The smectite proportion was found to be higher in these hard aggregates than in the fine-grained matrix of the bentonite, and, accordingly, a particle-size segregation during handling/sampling of the bag of bentonite may be pertinent to the representativeness of a test sample.

4.7 Granule size distribution

4.7.1 General

The granule size distribution of the raw material is an important parameter in order to produce backfill blocks of high quality (e.g. consistent density, high strength). The batch from Ashapura delivered in 2010 contained a large amount of rather big and hard granules which affected the block quality, especially the block edges which became very brittle. After crushing the material to a more suitable distribution there was a remarkable improvement of the block quality. At the same time it is important not to have a material containing only fines, which makes the material handling more difficult regarding dust etc and also makes the de-airing of the material more difficult. If large amounts of compressed air are trapped in the blocks, the risk for cracks is much higher.

The ordering of a new batch of material from Ashapura in 2012 therefore included a requirement that the material should be crushed to a granule size smaller than 3 mm.

4.7.2 Method

A sample of about 5 kg was taken from each of the big bags selected for this test. In order to get a smaller representative sample for the sieving, a 500 g subsample was obtained by use of a sample splitter.

The sieving was made using standard sieves but instead of using the vibrator the sieving was done manually in order to avoid crushing of the granules. This is not a standard method but since the interesting part was the size of the granules and not of the individual grain, this was judged to be the most suitable method.

4.7.3 Test matrix

Determination of the granule size distribution was a part of the acceptance control for the Asha 2012 batch. Samples were taken from twenty-five different big bags. The granule size distribution was

also determined for the two other batches delivered i.e. Asha 2010 and Ibeco 2011; three samples were taken from the Ibeco 2011 and two from the Asha 2010 batches. In addition, the granule size distribution of the crushed Asha 2010 was determined.

4.7.4 Test results

The results of the measurements of granule size distribution for Asha 2010, the crushed Asha 2010 and Ibeco 2011 are provided in Figure 4-5 and in Tables in Appendix 14 and 15. As described earlier, the as-delivered Asha 2010 contained a rather large amount of big and rather hard granules which affected the block quality and this was the reason for crushing this material.

As shown in the graph, Asha 2010 may contain as much as 40 to 60% granules larger than 2 mm.

The results for samples of the Asha 2012 batch are presented in the two charts in Figure 4-6. The granule size distribution is very similar to that of the batch delivered in 2010. A visual inspection indicated that the material had been crushed between two rollers with a gap spacing of ~3 mm. This procedure had disintegrated, or reshaped, the large granules but at the same time new granules had been formed with a thickness of 3 mm and of various lengths and widths. This is the explanation for the similar granule size distribution determined for the two batches. The newly formed granules seem however, somewhat softer and later compaction tests have shown that the block quality was improved.

The data on the granule size distribution have been used for calculating the average percentage finer by weight passing different mesh sizes, see Table 4-8. In addition the maximum and minimum percentage passing the different mesh sizes are presented together with the standard deviation. The calculated average, the maximum and the minimum amount are presented in the chart provided in Figure 4-7.

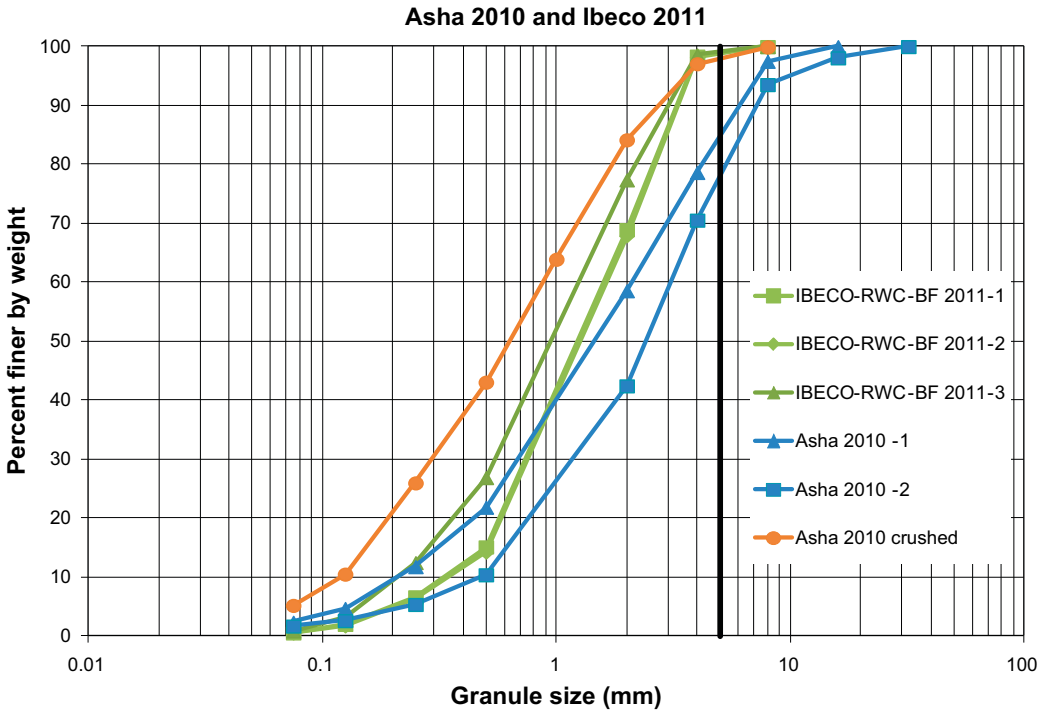

Figure 4-5. *Granule size distribution for Asha 2010, crushed Asha 2010 and Ibeco 2011. The black line shows the maximum granule size required.*

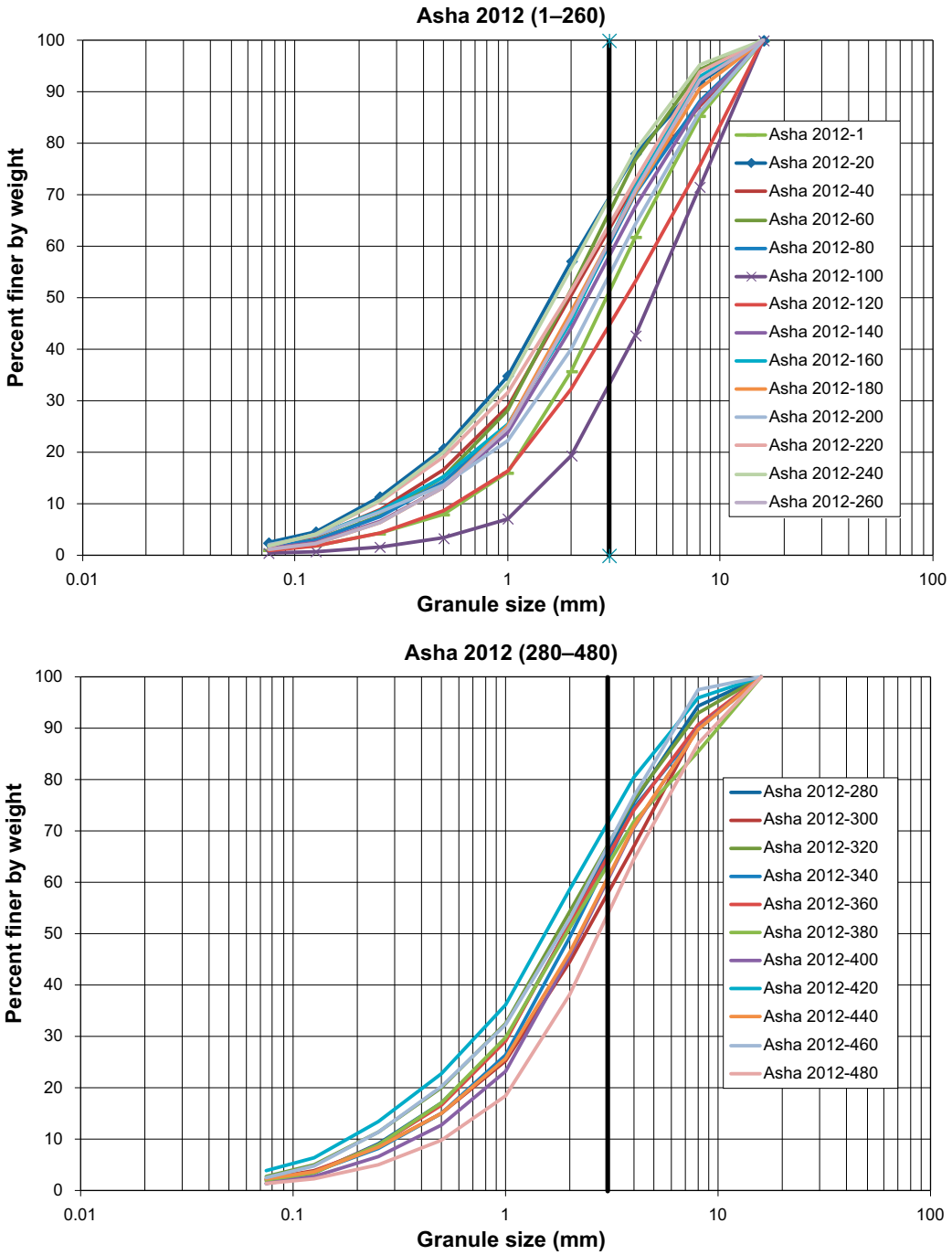

Figure 4-6. *Granule size distribution for twenty-five samples of Asha 2012. The upper diagram shows sample 1 to 260 and the lower sample 280 to 480. The black line shows the maximum granule size required.*

Table 4-8. Statistics on the granule size distribution of the Asha 2012 material. N=25.

Mesh, mm	Average amount of material passing, %	Maximum amount of material passing, %	Minimum amount of material passing, %	Standard deviation, %
16	100.0	100.0	100.0	0.0
8	89.5	97.6	71.6	5.8
4	70.2	80.5	42.7	8.3
2	46.7	58.6	19.4	8.6
1	26.1	36.3	7.2	6.6
0.5	15.0	22.7	3.3	4.4
0.25	8.1	13.4	1.7	2.6
0.125	3.4	6.4	0.8	1.2
0.075	1.8	3.9	0.5	0.7

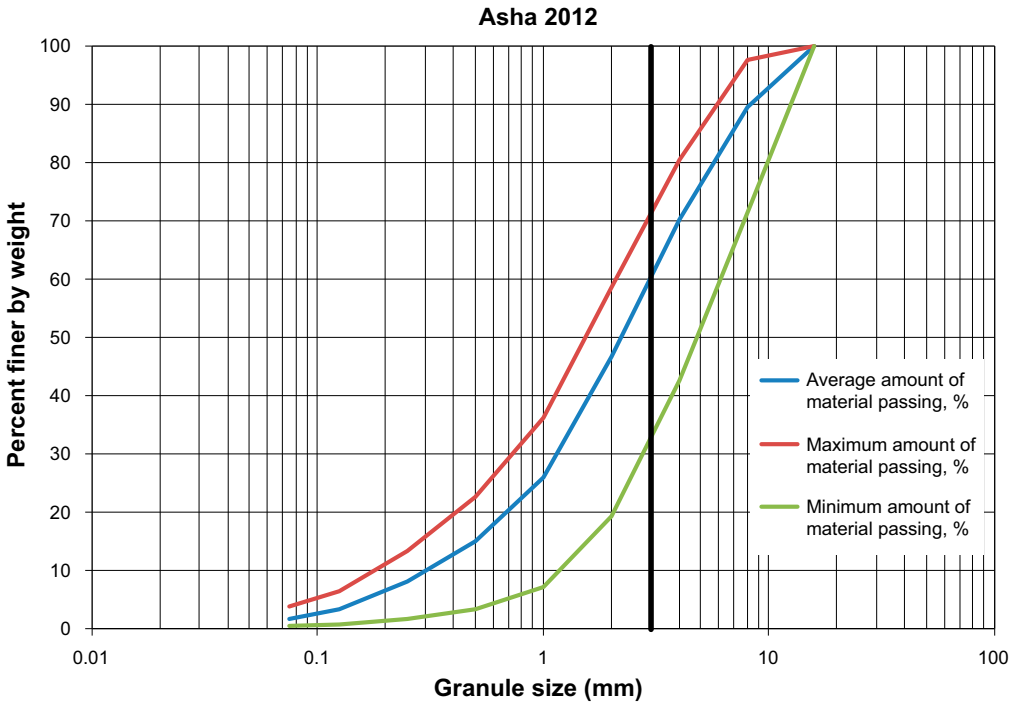

Figure 4-7. *Calculated average, maximum and minimum granule size distribution for twenty-five samples from Asha 2012. The black line shows the maximum granule size required.*

5 Chemical and mineralogical analyses

5.1 General

The chemical composition and mineralogy of random samples from the three bentonite batches were determined by some selected standard methods relevant in quality assessments of bentonites. In addition to chemical and quantitative X-ray diffraction analyses, determinations were made of the composition of the exchangeable cation pool and of the CBD-extractable iron content (the latter only for the iron-rich Asha bentonite). The purpose was to validate conclusions based on CEC and hydromechanical properties of the bentonites and to evaluate their conformity to the reference backfill material, which is bentonite clay with a nominal montmorillonite content of 50–60 weight % and an accepted variation within 45–90% (SKB 2010).

5.2 Exchangeable cations

5.2.1 General

The negative layer charge of smectite is balanced primarily by reversibly adsorbed, i.e. exchangeable, cations in the interlayer region. In natural bentonite the exchangeable cation pool is generally a mixture of mono- and divalent cations, mainly Na^+, K^+, Mg^{2+}, and Ca^{2+}. The valence of the charge compensating cations will affect properties such as swelling and dispersion behavior of the smectite, which motivates that a discrimination is made between, for instance, Na-dominated and Ca-/Mg-dominated bentonites in quality assessments of bentonites based on their hydro-mechanical properties.

5.2.2 Method

Soluble minerals like gypsum and calcite will dissolve in the aqueous Cu-trien solution, which makes this extractant unsuitable for determining the exchangeable cations. Therefore, the exchangeable cations were extracted by three successive displacements with ammonium in an alcoholic solution (0.15 M NH_4Cl in ~80% ethanol) according to a procedure originally recommended for CEC determinations of gypsiferous/calcareous soils (e.g. Belyayeva 1967).

Using a modified procedure of Belyayeva (1967) 0.8 g of the ground sample was shaken for 30 minutes in approximately one third of a total volume of 50 ml of the extractant. After centrifugation, the supernatant was collected. This treatment was repeated three times. After evaporation of the alcohol and adjustment of the volume of the residual supernatant with deionised water, the concentration of Ca, Mg, Na, and K was determined by use of an ICP-AES equipment at the Department of Biology, Lund University. The water content of the bentonite was determined for a separate sample.

5.2.3 Test matrix

The composition of the exchangeable cation pool was determined for randomly selected samples of all three batches of bentonite. Most of the analyses of the Asha 2010 bentonite were performed and reported within another SKB project (Olsson et al. 2013) but the results are also included here. The batches were sampled as follows:

- **Asha 2010.** Nine big bags, number 10, 15, 40, 55, 60, 70, 100, 113, and 125, were sampled. Sample 70 was divided into five subsamples for a repeatability test.
- **Ibeco 2011.** Four big bags, number 1, 15, 25 and 30, were sampled.
- **Asha 2012.** Five big bags, number 80, 180, 280, 380, and 480, were sampled.

Further information about the physical sampling of the big bags for materials subsequently used in laboratory test is given in Section 4.2.

5.2.4 Results

The data on the exchangeable cations extracted by exchange with ammonium in alcohol solution are compiled in Table 5-1. Some descriptive statistical measures are given in Table 5-2, which also includes the results of the repeatability test performed on sample 70 of the Asha 2010 bentonite.

All samples of Asha bentonite are sodium-dominated, and have calcium as the second most abundant cation. However, the variation between individual samples is significantly larger than the scatter in the repeatability test performed on sample 70 of Asha 2010 (Figure 5-1 and Table 5-1) and also than the scatter obtained in inter-laboratory reproducibility tests of the method (Dohrmann et al. 2012b).

The Ibeco-bentonite, which contains more than 20% Ca/Mg carbonates, is calcium-dominated (45%), and the proportions of sodium and magnesium are almost equal. Potassium is a minor component of the cation pool in all samples, but the proportion is higher in the Ibeco bentonite than in the Asha bentonite. The variation between individual samples is smaller for the Ibeco samples than for the Asha samples, which is consistent with the more homogeneous character of the Ibeco bentonite.

Table 5-1. Exchangeable cations extracted by exchange with NH_4^+ in alcohol solution.

Sample id	Ca meq/100 g	%	K meq/100 g	%	Mg meq/100 g	%	Na meq/100 g	%	Σ cations meq/100 g
Asha 2010-10	30.9	32	0.6	0.7	18.3	19	46.6	48	96
Asha 2010-15	25.7	28	0.8	0.9	16.2	18	49.8	54	93
Asha 2010-40	30.4	32	0.7	0.8	18.9	20	44.7	47	95
Asha 2010-55	28.2	31	0.9	1.0	17.5	20	43.0	48	90
Asha 2010-60	31.8	32	0.8	0.8	19.5	20	46.9	47	99
Asha 2010-70:1	26.8	29	0.7	0.8	17.1	18	48.4	52	93
Asha 2010-70:2	26.3	28	0.8	0.8	17.2	18	49.8	53	94
Asha 2010-70:3	27.1	29	0.8	0.8	17.1	18	49.8	53	95
Asha 2010-70:4	27.4	29	0.8	0.8	17.5	18	49.3	52	95
Asha 2010-70:5	27.1	29	0.8	0.8	17.3	18	49.8	52	95
Asha 2010-100	30.9	31	0.8	0.8	18.9	19	48.9	49	99
Asha 2010-113	21.8	26	0.4	0.4	12.6	15	48.8	58	84
Asha 2010-125	24.1	28	0.4	0.4	16.0	18	47.0	54	88
Ibeco 2011-1	33.4	46	1.4	1.9	17.7	24	20	28	73
Ibeco 2011-15	30.9	45	1.3	2.0	16.6	24	19.4	29	68
Ibeco 2011-25	31.5	45	1.3	1.9	17.3	25	20.1	29	70
Ibeco 2011-30	29.4	44	1.3	2.0	16.7	25	20	30	68
Asha 2012-80	26.0	29	0.6	0.6	12.6	14	50.3	56	90
Asha 2012-180	31.8	35	0.5	0.6	13.7	15	44.5	49	91
Asha 2012-280	34.8	37	0.5	0.5	14.5	16	43.2	46	93
Asha 2012-380	32.4	36	0.5	0.5	13.1	15	44.0	49	90
Asha 2012-480	27.3	29	0.5	0.5	12.9	14	52.5	56	93

Table 5-2. Descriptive statistics on the exchangeable cations.

	Cation	Mean	Std.dev. meq/100 g	Max. value	Min. value
Asha 2010 (N=13)	Ca	27.6	2.87	32	22
	Mg	17.3	1.75	20	13
	K	0.7	0.15	0.9	0.4
	Na	47.9	2.17	50	43
	Sum	93	4.4	99	84
Asha 2010-70 (N=5) repeatability test	Ca	26.9	0.40	27	26
	Mg	17.3	0.17	17	17
	K	0.8	0.02	0.8	0.7
	Na	49.4	0.59	50	48
	Sum	94	0.8	95	93
Ibeco 2011 (N=4)	Ca	31.3	1.66	33	29
	Mg	17.1	0.52	18	17
	K	1.3	0.05	1.4	1.3
	Na	20.0	0.32	20	19
	Sum	70	2.2	73	68
Asha 2012 (N=5)	Ca	30.5	3.67	35	26.0
	Mg	13.4	0.75	15	13
	K	0.5	0.03	0.6	0.5
	Na	46.9	4.21	53	43
	Sum	91	1.7	93	90

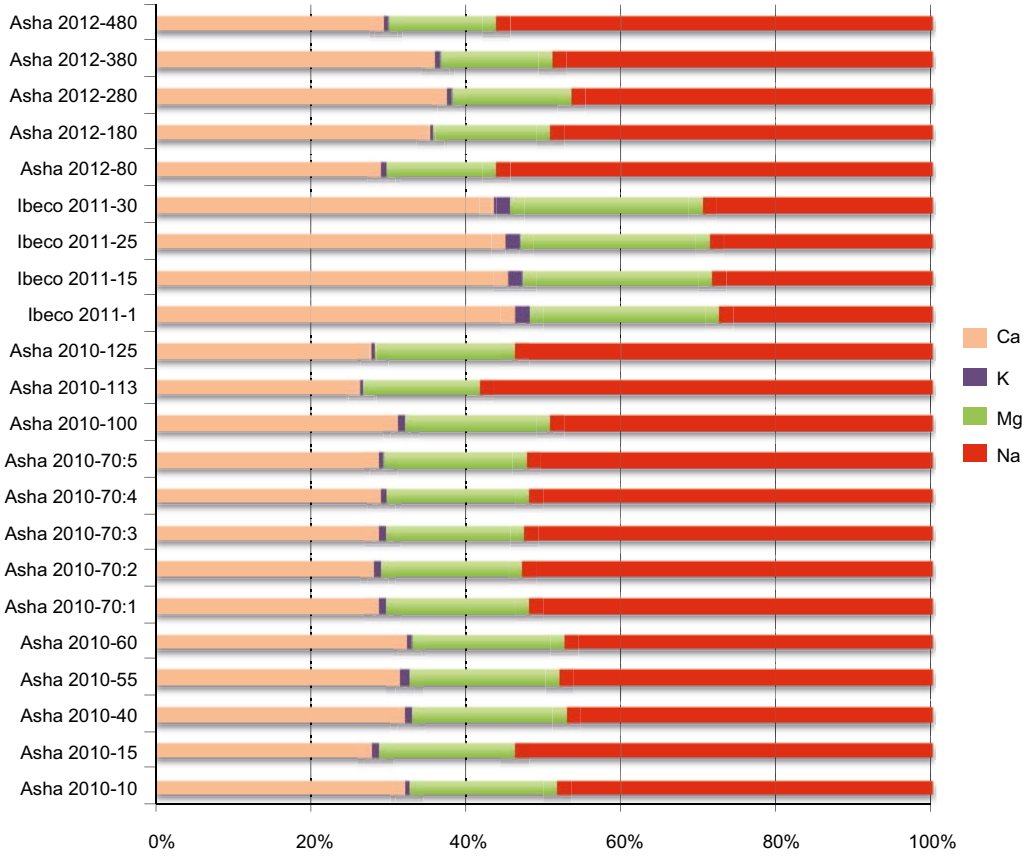

Figure 5-1. *The relative cation distribution in bentonite samples of Asha 2010, Ibeco 2011 and Asha 2012.*

As can be expected, the highest cation sums are found among those samples of Asha, which have the highest CEC-values (cf. Appendix 11–13). However, the sum of cations exceeds the CEC-values in most of the samples (Figure 5-2) and this fact reflects the problems inherent with extraction methods for exchangeable cations: an alcohol solution certainly minimizes dissolution of gypsum and calcite, but non-reactive solutes and easily soluble salts, such as chlorides and carbonates of alkali metals, if present, will dissolve in this extractant and, thus, contribute to the measured exchangeable cation pool. Small amounts (< 1%) of halite (NaCl) are indicated in the X-ray diffractograms of most of the Asha samples (cf. Section 5.5 and Appendix 16). Halite dissolution during extraction will necessarily result in excessive cation sums and inflated values for "exchangeable" sodium (0.1% NaCl is equivalent to 1.7 meq Na/100 g).

5.3 Determination of "free" iron oxides (the CBD-method)

5.3.1 General

The total iron content of the Asha bentonite is almost three times higher than that of the Ibeco bentonite, which reflects differences in their parent rock composition. According to XRD-data goethite, hematite, and maghemite/magnetite are, apart from smectite, the major crystalline, Fe-bearing phases in the Asha bentonite. Iron may, however, also exist as poorly crystalline phases, which are amorphous to X-rays. The CBD-extractable iron fraction was therefore determined in order to estimate the quantity of the latter iron-phases, which cannot be identified or evaluated quantitatively by XRD-analysis.

5.3.2 Method

The content of "free" iron oxides in the Asha bentonite was determined by the CBD-method (citrate-bicarbonate-dithionite) of Mehra and Jackson (1960). While crystalline iron oxides of larger grain-size, such as lithogenic magnetite, are little affected, poorly crystalline and/or very fine-grained forms of the iron oxides/oxyhydroxides (e.g. hematite, maghemite, lepidocrocite, goethite, ferrihydrite and other hydrous ferric oxides) can be extracted more or less selectively by this method, which employs sodium dithionite for the reduction of ferric iron, sodium bicarbonate as a buffer at neutral pH, and sodium citrate as a complexing agent for iron.

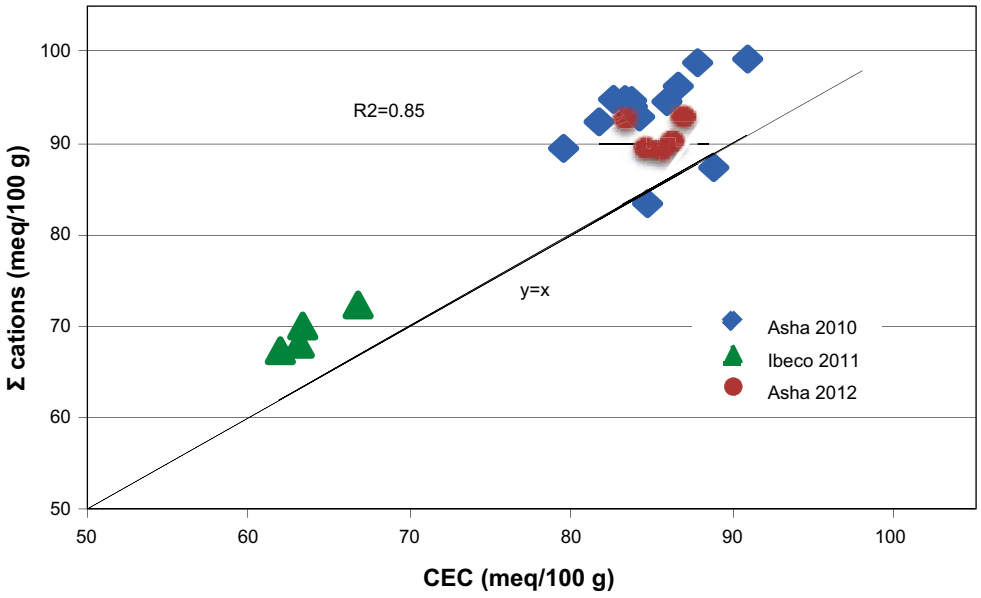

Figure 5-2. Plot of the sum of cations against the CEC of the samples.

The procedure follows the recommendation of Jackson (1975). Na-citrate (0.3 M) and $NaHCO_3$ (1M) were added at a ratio of 8:1 to the pre-weighed, dried sample in a centrifuge tube and the temperature of the suspension was brought to 75–80°C in a water-bath. Na-dithionite was added by means of a pre-calibrated spoon and the mixture was stirred for 5 minutes. The addition of dithionite was repeated twice, or until no reddish coloration of the clay was visible. After centrifugation the supernatant was collected in a volumetric flask. Fe, Mg and Si were determined by ICP-AES at the Department of Biology, Lund University. Si and Mg were included to provide some idea about the contribution by suspended and/or dissolved silicates.

5.3.3 Test matrix

The CBD-extractable iron content was determined for the Asha bentonite, the dark reddish to brownish colour of which is imparted by secondary iron oxyhydroxides. The Ibeco bentonite was not analysed since previous investigations of this bentonite (Ibeco 2004 and 2008) had shown that the CBD-extractable iron content was negligible.

A sample of Asha 2010 from big bag number 113 was divided into five subsamples, which were extracted separately in order to test the repeatability of the CBD-method.

The test sample was the same as used for the CEC-determination (Section 4.6).

5.3.4 Results

The results of the CBD-extraction are given in Table 5-3 in which previous results for the Asha and Ibeco batches from 2004 and 2008 are included for comparison (data from Olsson and Karnland 2009). The results for sample Asha 2010-113 suggest that 4–4.5% Fe_2O_3 is derived from extractable hydrous iron oxides and oxyhydroxides. The fact that these iron phases generally are amorphous to X-rays implies that quantitative mineralogical evaluations based on XRD-profiles of the bentonite tend to underestimate their abundance, and as a consequence of mineral content normalisation to 100% based on diffraction data the crystalline phases are likely to be overestimated. The presence of an amorphous mineral component also has the potential to cause the bentonite to show compromised physical and mechanical behaviours since the bentonite may be prevented from swelling freely in the presence of available water. The swell index of sample Asha 113 determined before and after CBD-extraction (Table 4-4) suggests, however, that such effects of the amorphous iron phases are marginal.

Table 5-3. CBD-extractable iron, silica and magnesium expressed as oxides in weight percent of the dry matter. Previous determinations of CBD-extractable iron in single samples of the batches Asha 2004, Asha 2008, Ibeco 2004 and Ibeco 2008 are included for comparison (from Olsson and Karnland 2009).

Sample id	CBD-extract. Fe_2O_3 %	CBD-extract. SiO_2 %	CBD-extract. MgO %
Asha 2010-113:1	3.96	0.19	0.37
Asha 2010-113:2	4.10	0.20	0.37
Asha 2010-113:3	3.90	0.19	0.36
Asha 2010-113:4	4.51	0.22	0.37
Asha 2010-113:5	4.63	0.22	0.24
mean	**4.22**	**0.20**	**0.34**
st.dev.	**0.33**	**0.01**	**0.06**
Asha 2004	3.96		
Asha 2008	3.95		
Ibeco 2004	0.33		
Ibeco 2008	0.15		

5.4 Chemical composition of the bentonites

5.4.1 General

The composition of a bentonite mined from one and the same deposit may vary on a vertical and horizontal scale, depending on the complexity in the genesis and geological history of the deposit. Chemical analysis is a relatively cost effective way to monitor compositional variations within and between different bentonite batches delivered from the same producer. Random samples of all three batches were therefore analysed for major and minor elements. Total sulphur, total carbon and inorganic carbon were also included in the analysis because bentonite often contains sulphide and sulphate minerals. These minerals are potential sources of S^{2-}, the sulphates through reaction with sulphate-reducing bacteria if appropriate carbon and enegy sources for bacterial growth are available. Because S^{2-} is a metal corrosive in anoxic environments, sulphide, sulphur and organic carbon in the various repository compartments are considered potentially harmful, although no threshold values have been set for these substances in SKB´s requirements on a candidate tunnel backfill bentonite (SKB 2010).

Data regarding inorganic carbon and sulphur are useful also as a check of plausibility in quantitative evaluations of the carbonate and sulfate/sulphide minerals by XRD-analysis.

5.4.2 Methods

The chemical composition of the bentonite samples was determined by ICP emission and mass spectroscopy at a certified laboratory (ACME Analytical Laboratories, Canada), using standard techniques for silicate analysis ($LiBO_2/Li_2B_4O$ fusion followed by nitric acid digestion). These analyses include major, minor and trace elements (incl. rare earth elements, REE). Loss on ignition (LOI) was determined as the weight loss upon ignition of the sample at 1,000°C.

Total carbon and sulphur were determined by evolved gas analysis (EGA) at the same laboratory by combustion of the samples in a Leco furnace, equipped with IR-detectors. Carbonate carbon was determined as CO_2 evolved on treatment of a subsample with hot 15% HCl.

5.4.3 Test matrix

The chemical composition of the bentonite was determined for the following samples of the three bentonite batches:

- **Asha 2010.** Seven big bags, number 10, 15, 40, 55, 60, 70 and 100 were sampled. After homogenization of the samples by grinding, sample 70 was divided into five subsamples for a repeatability test. All chemical analyses of the Asha 2010 bentonite were performed and reported within another SKB project (Olsson et al. 2013). The results reported here are from this investigation.
- **Ibeco 2011.** Five bags, number 1, 15, 20, 25 and 30, were sampled.
- **Asha 2012.** Five bags, number 80, 180, 280, 380 and 480, were sampled.

The test samples were the same as for the CEC-determination (cf. sampling in Chapter 4).

Table 5-4. Chemical composition of the bentonite samples from the batches Asha 2010, Ibeco 2011 and Asha 2012. Major, minor and trace elements by ICP-AES or -MS, S and C by evolved gas analysis. DL=detection limit.

Sample id	SiO_2 %	Al_2O_3 %	Fe_2O_3 %	MgO %	CaO %	Na_2O %	K_2O %	TiO_2 %	P_2O_5 %	MnO %	Cr_2O_3 %	LOI %	Sum %	C_{tot} %	S_{tot} %	CO_2 %
DL	0.01	0.01	0.04	0.01	0.01	0.01	0.01	0.01	0.01	0.01	0.002	5.1	0.01	0.02	0.02	0.02
Asha 2010-10	43.36	15.55	11.89	2.84	4.21	1.38	0.09	0.97	0.23	0.15	0.025	19.1	99.84	0.73	< 0.02	2.55
Asha 2010-15	42.09	16.54	13.24	2.41	3.20	1.47	0.1	1.09	0.15	0.17	0.026	19.3	99.83	0.41	0.02	2.06
Asha 2010-40	44.00	16.01	11.47	2.78	3.63	1.37	0.09	1.02	0.17	0.13	0.028	19.1	99.85	0.46	< 0.02	1.99
Asha 2010-55	42.07	14.24	11.81	2.91	6.40	1.33	0.17	0.90	0.29	0.24	0.024	19.4	99.83	0.95	0.02	3.66
Asha 2010-60	43.69	15.89	11.86	2.88	4.19	1.38	0.10	0.99	0.20	0.14	0.026	18.5	99.83	0.78	< 0.02	2.54
Asha 2010-70:1	42.74	16.23	12.12	2.62	3.62	1.51	0.10	1.00	0.17	0.17	0.024	19.5	99.83	0.60	0.05	2.26
Asha 2010-70:2	42.73	16.08	12.39	2.61	3.51	1.47	0.10	1.04	0.15	0.15	0.025	19.6	99.82	0.59	0.03	2.46
Asha 2010-70:3	43.20	16.11	12.08	2.60	3.41	1.48	0.10	1.07	0.15	0.15	0.024	19.5	99.84	0.58	0.02	2.14
Asha 2010-70:4	42.85	16.07	12.26	2.56	3.68	1.47	0.12	1.03	0.16	0.16	0.025	19.4	99.83	0.58	< 0.02	2.07
Asha 2010-70:5	42.90	15.9	12.13	2.57	3.73	1.45	0.10	1.01	0.14	0.15	0.025	19.5	99.84	0.59	< 0.02	2.20
Asha 2010-100	43.83	15.03	10.81	3.11	4.17	1.39	0.18	0.85	0.50	0.14	0.021	19.8	99.86	0.55	< 0.02	2.04
mean all (N=11)	**43.04**	**15.79**	**12.01**	**2.72**	**3.98**	**1.43**	**0.11**	**1.00**	**0.21**	**0.16**	**0.025**	**19.3**		**0.62**		**2.36**
stdev	**0.65**	**0.64**	**0.60**	**0.20**	**0.87**	**0.06**	**0.03**	**0.07**	**0.11**	**0.03**	**0.002**	**0.3**		**0.15**		**0.48**
mean 70 (N=5)	**42.88**	**16.08**	**12.20**	**2.59**	**3.59**	**1.48**	**0.10**	**1.03**	**0.15**	**0.16**	**0.025**	**19.5**		**0.59**		**2.23**
stdev	**0.19**	**0.12**	**0.13**	**0.03**	**0.13**	**0.02**	**0.01**	**0.03**	**0.01**	**0.01**	**0.001**	**0.1**		**0.01**		**0.15**
Ibeco 2011-1	42.90	13.50	4.73	6.15	9.73	0.86	0.56	0.55	0.14	0.18	0.002	20.5	99.75	3.21	0.11	11.81
Ibeco 2011-15	42.16	13.20	4.70	6.22	10.14	0.91	0.57	0.53	0.13	0.18	< 0.002	21.0	99.74	3.41	0.09	12.46
Ibeco 2011-20	42.33	13.17	4.71	6.25	10.06	0.91	0.57	0.53	0.13	0.18	0.002	20.9	99.77	2.78	0.08	11.32
Ibeco 2011-25	42.63	13.22	4.85	6.16	9.87	0.96	0.62	0.52	0.09	0.19	< 0.002	20.6	99.68	3.34	0.10	12.31
Ibeco 2011-30	42.04	13.08	4.81	6.37	10.56	0.93	0.56	0.52	0.13	0.20	< 0.002	20.5	99.72	3.13	0.09	13.16
mean (N=5)	**42.41**	**13.23**	**4.76**	**6.23**	**10.07**	**0.91**	**0.58**	**0.53**	**0.12**	**0.19**		**20.7**		**3.17**	**0.09**	**12.21**
stdev	**0.35**	**0.16**	**0.07**	**0.09**	**0.32**	**0.04**	**0.03**	**0.01**	**0.02**	**0.01**		**0.2**		**0.25**	**0.01**	**0.69**
Asha 2012-80	48.33	18.28	13.95	2.66	3.48	1.76	0.11	1.05	0.11	0.16	0.032	9.8	99.74	0.65	0.12	1.49
Asha 2012-180	48.22	18.51	13.69	2.77	3.44	1.58	0.10	1.01	0.12	0.13	0.036	10.2	99.78	0.55	0.19	1.54
Asha 2012-280	47.41	19.45	13.42	2.63	3.50	1.47	0.08	1.06	0.10	0.14	0.037	10.4	99.77	0.70	0.14	1.78
Asha 2012-380	47.84	19.23	13.78	2.71	3.26	1.57	0.11	1.03	0.10	0.13	0.038	9.9	99.74	0.54	0.10	1.64
Asha 2012-480	46.30	17.25	17.67	2.80	2.78	1.84	0.11	1.02	0.11	0.20	0.029	9.6	99.76	0.55	0.07	1.60
mean (N=5)	**47.62**	**18.54**	**14.50**	**2.71**	**3.29**	**1.64**	**0.10**	**1.03**	**0.11**	**0.15**	**0.034**	**10.0**		**0.60**	**0.12**	**1.61**
stdev	**0.82**	**0.87**	**1.78**	**0.07**	**0.30**	**0.15**	**0.01**	**0.02**	**0.01**	**0.03**	**0.004**	**0.3**		**0.07**	**0.05**	**0.11**

Table 5-4 continued.

Sample id	B_a mg/kg	Be mg/kg	Co mg/kg	Cs mg/kg	Ga mg/kg	Hf mg/kg	N_b mg/kg	R_b mg/kg	S_n mg/kg	Sr mg/kg	Ta mg/kg	Th mg/kg	U mg/kg	V mg/kg	W mg/kg	Zr mg/kg
DL	1	1	0.2	0.1	0.5	0.1	0.1	0.1	1	0.5	0.1	0.2	0.1	8	0.5	0.1
Asha 2010-10	41	< 1	54.1	0.2	16.1	2	8.9	4.2	< 1	229.5	0.5	1.8	0.6	228	0.6	83.5
Asha 2010-15	80	< 1	67.1	0.3	16.7	2.6	10.2	5.1	< 1	190.2	0.5	1.9	0.6	252	< 0.5	91.4
Asha 2010-40	39	< 1	51.7	0.3	15.7	2.2	9.3	4	< 1	210	0.6	2.1	0.4	220	< 0.5	78.2
Asha 2010-55	77	< 1	71.3	0.2	14.4	2.2	7.9	6.4	< 1	252.9	0.5	1.9	0.6	221	< 0.5	84.5
Asha 2010-60	40	< 1	60.4	0.3	15.5	1.6	9.6	4.4	< 1	214.7	0.7	1.8	0.5	216	< 0.5	70.8
Asha 2010-70:1	88	< 1	69.5	0.3	15.7	1.7	9.7	5.1	< 1	209.6	0.5	1.8	0.4	218	0.6	78.3
Asha 2010-70:2	67	< 1	70.1	0.2	15.5	1.8	10.6	5.3	< 1	215.5	0.5	3.4	0.6	225	< 0.5	85.8
Asha 2010-70:3	54	< 1	57.8	0.2	14.3	2.2	10.8	5.2	< 1	216.7	0.6	1.9	0.5	215	< 0.5	85.9
Asha 2010-70:4	57	< 1	58.4	0.2	14.8	2.2	9.6	5.4	< 1	206.3	0.5	1.8	0.5	215	< 0.5	83.8
Asha 2010-70:5	77	< 1	53.9	0.2	13.9	2	9.4	4.9	< 1	232.4	0.5	3.1	0.6	217	< 0.5	82.4
Asha 2010-100	49	< 1	49.8	0.2	14.6	2.2	8.2	6.4	< 1	209.9	0.5	1.5	0.4	150	< 0.5	67.2
mean all (N=11)	**61**		**60.4**	**0.2**	**15.2**	**2.1**	**9.5**	**5.1**		**217.1**	**0.5**	**2.1**	**0.5**	**216**		**81.1**
stdev	**18**		**7.9**	**0.1**	**0.9**	**0.3**	**0.9**	**0.8**		**16.4**	**0.1**	**0.6**	**0.1**	**24.3**		**7.0**
mean 70 (N=5)	**69**		**61.9**	**0.2**	**14.8**	**2.0**	**10.0**	**5.2**		**216.1**	**0.5**	**2.4**	**0.5**	**218**		**83.2**
stdev	**14**		**7.4**	**0.04**	**0.8**	**0.2**	**0.6**	**0.2**		**10.1**	**0.04**	**0.8**	**0.1**	**4.1**		**3.1**
Ibeco 2011-1	731	4	7.5	9.6	14.6	3.2	6.5	38.3	1	139.4	0.5	7.8	5.1	103	0.8	133.0
Ibeco 2011-15	879	1	8.0	9.2	14.1	3.1	6.2	36.9	1	143.8	0.5	8.0	5.1	99	0.6	130.8
Ibeco 2011-20	620	3	8.5	9.6	13.8	3.3	6.3	37.2	< 1	143.1	0.4	7.7	5.1	101	0.6	134.7
Ibeco 2011-25	1,245	< 1	7.9	10.2	13.9	3.3	7.2	37.6	< 1	164.7	< 0.1	6.9	5.4	126	0.9	139.9
Ibeco 2011-30	1,129	3	8.9	9.5	14	3.2	6.4	37.6	1	151.6	0.4	7.7	5.2	94	0.7	138.0
mean (N=5)	**921**	**3**	**8.2**	**9.6**	**14.1**	**3.2**	**6.5**	**37.5**		**148.5**	**0.5**	**7.6**	**5.2**	**105**	**0.7**	**135.3**
stdev	**263**	**1**	**0.5**	**0.4**	**0.3**	**0.1**	**0.4**	**0.5**		**10.1**	**0.1**	**0.4**	**0.1**	**12.4**	**0.1**	**3.7**
Asha 2012-80	80	< 1	90.0	0.3	17.9	2.2	9.4	6	< 1	522.7	0.5	1.8	0.6	265	< 0.5	86.9
Asha 2012-180	50	1	81.0	0.3	16.4	2.2	9.5	5.3	< 1	264.5	0.5	1.6	0.7	254	< 0.5	73.9
Asha 2012-280	66	< 1	91.1	0.2	18.7	2.2	9.7	5.1	< 1	319.3	0.6	2.0	0.7	279	0.5	83.1
Asha 2012-380	65	1	89.6	0.3	17.8	1.9	8.6	5.7	< 1	503.3	0.6	1.7	0.6	259	0.5	76.9
Asha 2012-480	216	2	87.3	0.4	15.6	2.3	9.3	6.1	< 1	277.9	0.6	2.2	0.8	250	< 0.5	87.4
mean (N=5)	**95**		**87.8**	**0.3**	**17.3**	**2.2**	**9.3**	**5.6**		**377.5**	**0.6**	**1.9**	**0.7**	**261**		**81.6**
stdev	**68**		**4.0**	**0.07**	**1.3**	**0.2**	**0.4**	**0.4**		**125.5**	**0.05**	**0.2**	**0.1**	**11.3**		**6.0**

Table 5-4 continued.

Sample id	Y mg/kg	La mg/kg	Ce mg/kg	Pr mg/kg	Nd mg/kg	Sm mg/kg	E_u mg/kg	G_d mg/kg	T_b mg/kg	Dy mg/kg	Ho mg/kg	Er mg/kg	Tm mg/kg	Y_b mg/kg	L_u mg/kg	Sc mg/kg
DL	0.1	0.1	0.1	0.02	0.3	0.05	0.02	0.05	0.01	0.05	0.02	0.03	0.01	0.05	0.01	1
Asha 2010-10	41.4	14.7	20.8	3.42	16.2	3.63	1.36	4.90	0.95	5.96	1.38	3.98	0.58	3.63	0.55	47
Asha 2010-15	61.4	23.3	24.4	5.29	22.3	5.17	1.96	7.74	1.38	8.70	2.13	6.13	0.89	5.66	0.83	50
Asha 2010-40	37.4	13.2	19.7	3.27	13.6	3.37	1.38	4.74	0.90	5.86	1.27	3.74	0.59	3.58	0.55	48
Asha 2010-55	46.3	16.0	20.4	3.70	14.5	4.08	1.50	5.26	1.01	6.42	1.46	4.60	0.68	4.25	0.71	45
Asha 2010-60	44.3	15.0	21.3	3.67	15.9	4.06	1.49	5.53	1.04	6.17	1.54	4.37	0.66	4.34	0.63	48
Asha 2010-70:1	47.9	18.0	21.7	3.92	16.2	4.26	1.46	5.99	1.02	6.64	1.53	4.34	0.64	4.06	0.63	49
Asha 2010-70:2	63.4	20.0	27.0	4.69	20.2	4.62	1.57	7.03	1.21	7.57	2.01	5.30	0.78	4.92	0.80	48
Asha 2010-70:3	52.0	21.0	24.1	4.39	16.1	4.28	1.48	6.12	1.06	7.11	1.70	4.47	0.66	4.19	0.66	48
Asha 2010-70:4	49.1	19.8	23.2	4.33	19.2	4.47	1.63	6.07	1.13	6.72	1.68	4.75	0.66	4.49	0.64	48
Asha 2010-70:5	49.1	20.2	25.8	4.41	18.9	4.4	1.51	6.09	1.05	6.55	1.57	4.29	0.69	4.13	0.66	47
Asha 2010-100	38.0	13.0	19.5	3.11	13.9	3.36	1.28	4.65	0.89	5.67	1.32	4.09	0.61	3.61	0.59	44
mean all (N=11)	**48.2**	**17.7**	**22.5**	**4.02**	**17.0**	**4.15**	**1.51**	**5.83**	**1.06**	**6.67**	**1.60**	**4.55**	**0.68**	**4.26**	**0.66**	**47**
stdev	**8.4**	**3.5**	**2.5**	**0.67**	**2.8**	**0.55**	**0.18**	**0.96**	**0.14**	**0.87**	**0.27**	**0.67**	**0.09**	**0.62**	**0.09**	**1.7**
mean 70 (N=5)	**52.3**	**19.8**	**24.3**	**4.35**	**18.1**	**4.41**	**1.53**	**6.26**	**1.09**	**6.92**	**1.70**	**4.63**	**0.69**	**4.36**	**0.68**	**48**
stdev	**6.4**	**1.1**	**2.1**	**0.28**	**1.9**	**0.15**	**0.07**	**0.43**	**0.08**	**0.42**	**0.19**	**0.41**	**0.06**	**0.35**	**0.07**	**0.7**
Ibeco 2011-1	14.9	22.3	41.6	4.68	17.9	3.28	0.91	2.78	0.44	2.59	0.51	1.68	0.25	1.65	0.26	11
Ibeco 2011-15	15.8	21.6	41.8	4.67	17.5	3.34	0.81	2.71	0.46	2.59	0.52	1.76	0.26	1.72	0.29	11
Ibeco 2011-20	15.7	21.6	40.6	4.56	17.3	3.27	0.85	2.82	0.44	2.64	0.55	1.70	0.27	1.74	0.29	10
Ibeco 2011-25	17.4	24.2	43.8	5.17	19.8	3.82	0.87	3.17	0.49	2.95	0.57	1.91	0.30	2.17	0.31	11
Ibeco 2011-30	16.9	21.4	41.6	4.62	17.9	3.19	0.87	2.98	0.46	2.72	0.55	1.76	0.29	1.85	0.28	11
mean (N=5)	**16.1**	**22.2**	**41.9**	**4.74**	**18.1**	**3.38**	**0.86**	**2.89**	**0.46**	**2.70**	**0.54**	**1.76**	**0.27**	**1.83**	**0.29**	**11**
stdev	**1.0**	**1.2**	**1.2**	**0.25**	**1.0**	**0.25**	**0.04**	**0.18**	**0.02**	**0.15**	**0.02**	**0.09**	**0.02**	**0.21**	**0.02**	**0.5**
Asha 2012-80	75.9	29.7	27.9	6.73	26.9	7.05	2.69	9.62	1.89	10.98	2.71	8.19	1.14	7.06	1.11	52
Asha 2012-180	65.7	27.0	25.1	6.21	25.7	6.58	2.59	9.07	1.77	10.02	2.53	7.49	1.04	6.56	1.03	53
Asha 2012-280	85.5	31.7	27.4	7.50	31.3	8.14	3.10	10.95	2.20	12.61	3.37	9.76	1.40	9.29	1.40	54
Asha 2012-380	77.7	31.1	30.5	7.03	29.2	7.45	2.90	10.39	2.10	12.39	3.02	8.93	1.29	8.12	1.28	54
Asha 2012-480	69.3	27.0	37.8	6.32	27.7	6.60	2.47	9.00	1.76	10.75	2.62	7.82	1.11	7.48	1.11	48
mean (N=5)	**74.8**	**29.3**	**29.7**	**6.76**	**28.2**	**7.16**	**2.75**	**9.81**	**1.94**	**11.35**	**2.85**	**8.44**	**1.20**	**7.70**	**1.19**	**52**
stdev	**7.7**	**2.2**	**4.9**	**0.53**	**2.2**	**0.65**	**0.25**	**0.85**	**0.20**	**1.11**	**0.34**	**0.91**	**0.15**	**1.06**	**0.15**	**2.5**

Table 5-4 continued.

Sample id	Mo mg/kg	Cu mg/kg	P_b mg/kg	Z_n mg/kgg	Ni mg/kg	As mg/kg	C_d mg/kg	S_b mg/kg	B_i mg/kg	A_g mg/kg	A_u mg/kg	H_g mg/kg	T_l mg/kg	S_e mg/kg
DL	0.1	0.1	0.1	1	0.1	0.5	0.1	0.1	0.1	0.1	0.5	0.01	0.1	0.5
Asha 2010-10	0.2	117	1.3	88	41.3	0.6	< 0.1	< 0.1	< 0.1	< 0.1	1.5	< 0.01	< 0.1	< 0.5
Asha 2010-15	0.2	132.7	1.6	104	46.4	< 0.5	< 0.1	< 0.1	< 0.1	< 0.1	2.1	< 0.01	< 0.1	0.5
Asha 2010-40	0.2	119.3	1.4	91	39.8	< 0.5	< 0.1	< 0.1	< 0.1	< 0.1	3.0	< 0.01	< 0.1	< 0.5
Asha 2010-55	0.4	144.4	2.8	97	60.3	0.6	0.1	< 0.1	< 0.1	< 0.1	3.6	< 0.01	< 0.1	< 0.5
Asha 2010-60	0.2	118.8	1.6	91	43.2	< 0.5	0.1	< 0.1	< 0.1	< 0.1	1.9	< 0.01	< 0.1	< 0.5
Asha 2010-70:1	0.3	130.4	2.0	96	46.5	< 0.5	0.1	< 0.1	< 0.1	< 0.1	3.9	< 0.01	< 0.1	< 0.5
Asha 2010-70:2	0.3	126.6	3.3	95	54.8	0.6	< 0.1	< 0.1	< 0.1	< 0.1	27.1	< 0.01	< 0.1	< 0.5
Asha 2010-70:3	0.3	131.8	2.3	97	51.0	< 0.5	< 0.1	< 0.1	< 0.1	< 0.1	20.1	< 0.01	< 0.1	< 0.5
Asha 2010-70:4	0.3	136.8	2.0	101	47.2	< 0.5	< 0.1	< 0.1	< 0.1	< 0.1	5.1	< 0.01	< 0.1	< 0.5
Asha 2010-70:5	0.2	137.1	1.9	97	48.9	0.7	0.2	< 0.1	< 0.1	< 0.1	6.9	< 0.01	< 0.1	0.5
Asha 2010-100	0.2	111.8	2.2	76	43.7	< 0.5	1.4	< 0.1	< 0.1	< 0.1	1.1	< 0.01	< 0.1	< 0.5
mean all (N=11)	**0.3**	**127.9**	**2.0**	**94**	**47.6**						**6.9**			
stdev	**0.07**	**10.1**	**0.60**	**8**	**6.04**						**8.55**			
mean 70 (N=5)	**0.3**	**132.5**	**2.3**	**97**	**49.7**						**12.6**			
stdev	**0.04**	**4.5**	**0.6**	**2**	**3.3**						**10.4**			
Ibeco 2011-1	0.2	11.6	7.3	29	6.6	2.6	< 0.1	< 0.1	0.3	< 0.1	< 0.5	0.28	0.2	0.7
Ibeco 2011-15	0.2	9.2	7.5	33	7.1	3.8	< 0.1	< 0.1	0.3	< 0.1	< 0.5	0.07	0.3	< 0.5
Ibeco 2011-20	0.1	10.9	8.5	29	8.4	2.8	0.1	< 0.1	0.3	< 0.1	0.6	0.10	0.2	0.5
Ibeco 2011-25	0.1	10.4	7.6	32	7.0	2.3	0.2	< 0.1	0.3	< 0.1	< 0.5	0.07	0.2	1.3
Ibeco 2011-30	< 0.1	9.6	7.8	27	7.6	2.8	< 0.1	< 0.1	0.3	< 0.1	< 0.5	0.09	0.3	1.1
mean (N=5)	**0.2**	**10.3**	**7.7**	**30**	**7.3**	**2.9**			**0.3**			**0.12**	**0.2**	**0.9**
stdev	**0.06**	**1.0**	**0.5**	**3**	**0.7**	**0.6**			**0.0**			**0.09**	**0.05**	**0.4**
Asha 2012-80	0.2	136.5	1.7	152	65.5	< 0.5	0.2	< 0.1	< 0.1	< 0.1	< 0.5	< 0.01	< 0.1	0.6
Asha 2012-180	0.2	140.2	1.7	153	67.0	< 0.5	0.2	< 0.1	< 0.1	< 0.1	2.2	< 0.01	< 0.1	0.8
Asha 2012-280	0.3	143.9	1.6	160	71.9	< 0.5	0.3	< 0.1	< 0.1	< 0.1	1.1	< 0.01	< 0.1	< 0.5
Asha 2012-380	0.3	134.9	1.4	159	68.1	< 0.5	0.2	< 0.1	< 0.1	< 0.1	1.8	< 0.01	0.1	< 0.5
Asha 2012-480	0.4	139.6	2.0	124	65.9	< 0.5	0.3	< 0.1	< 0.1	< 0.1	5.4	< 0.01	< 0.1	1.1
mean (N=5)	**0.3**	**139.0**	**1.7**	**150**	**67.7**		**0.2**				**2.2**			
stdev	**0.08**	**3.5**	**0.2**	**15**	**2.6**		**0.05**				**1.9**			

5.4.4 Results

The chemical composition of the samples from the three batches of bentonite is given in Table 5-4.

Sulphur. The total sulphur content is close to or below the detection limit (0.02%) in all samples of Asha 2010 (N=11). According to results of aqueous leachates, reported in Olsson et al. (2013), the major fraction of sulphur exists as sulphate, probably gypsum.

The samples of Ibeco 2011 (N=5) have higher total sulphur content (0.08–0.11% S) than Asha 2010. Gypsum was detected in the XRD-profile of some of the samples, although allocation of all sulphur to gypsum ($CaSO_4 \times 2H_2O$) suggests that the maximum content that can exist is 0.6%.

The highest total sulphur content is found among the samples of Asha 2012 (range 0.07–0.19% S). If all sulphur is allocated to gypsum, the maximum value for this mineral would correspond to 1%, and gypsum is detectable in several of the XRD-traces of the samples scanned in the as-received state (Appendix 16).

Carbon. The total carbon content of the samples of Asha 2010 ranges from 0.41 to 0.95% C, and is more or less equal to the acid soluble carbon content (Figure 5-3; acid-soluble carbon is expressed as CO_2 in Table 5-4), suggesting that the predominant source of carbon is a carbonate phase. Sample 55 has the maximum acid-soluble carbon content, which corresponds to 8% $CaCO_3$ if all acid-soluble carbon is allocated to calcite (cf. the XRD results).

The total carbon content of the five samples of Asha 2012 ranges from 0.54 to 0.70% C. The acid-soluble carbon content is systematically somewhat lower (values plot below the y=x-line in Figure 5-3), which suggests that other carbon sources than carbonates may exist. If so, a probable source is organic matter. The remnant carbon content (i.e. total minus acid-soluble carbon) is 0.24% C at a maximum.

The samples of Ibeco 2011 (N=5) are distinguished by very high contents of acid-soluble carbon (3.04–3.49% C), which stoichiometrically corresponds to 15–18% CO_3^{2-}, and is paralleled by high CaO and MgO contents. Thus, the chemical data suggest that the carbonate fraction consists of both Ca and Mg carbonates, which is confirmed by the XRD-analysis showing that dolomite ($CaMg(CO_3)_2$) and calcite ($CaCO_3$) together make up more than 20% of the samples. The acid-soluble carbon content is essentially equal to the total carbon content, although acid-soluble C exceeds total C in two samples (values plot above the y=x-line in Figure 5-3), which is an obvious analytical error, probably attributable to an increased scatter in the analysis at high carbon contents.

Major oxides. Due to large variations in LOI, which represents the amount of volatiles (including adsorbed water) in the samples, comparisons of the major oxide composition are preferably based on ratios of the oxides rather than percentage values.

The SiO_2/Al_2O_3 ratio (Figure 5-4) of the samples of the Asha bentonite varies from 2.4 to 3. This range of variation is larger than the scatter in the repeatability test performed on sample Asha 2010-70 and demonstrates the heterogeneity of the Asha material. In contrast, the same ratio for the samples of Ibeco 2011 show much more constant values.

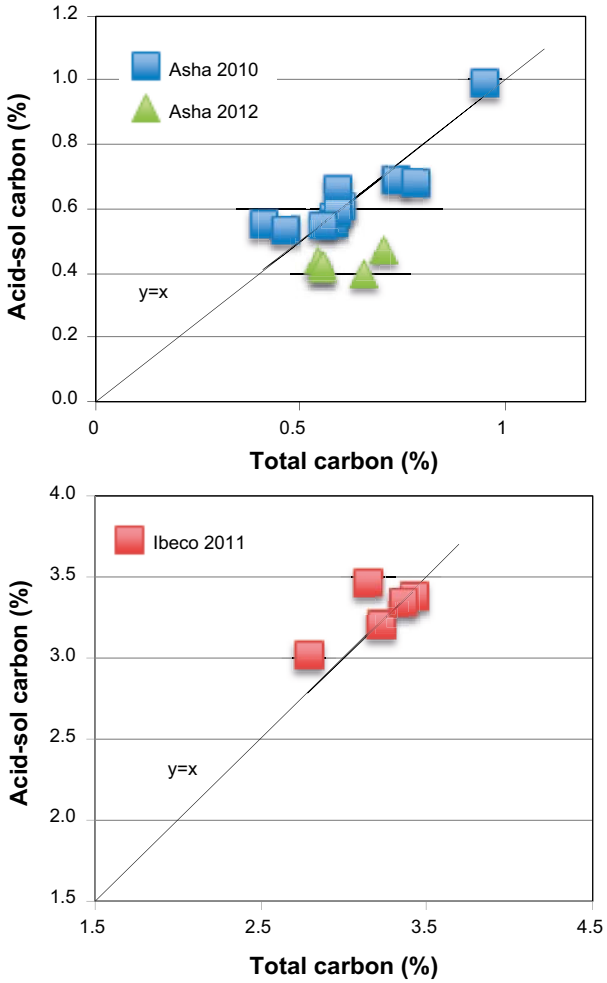

Figure 5-3. *Plot of acid-soluble carbon against total carbon in the bentonite samples of the batches Asha 2010, Asha 2012 and Ibeco 2011. Notice the difference in scale of the diagrams. Implications of the y=x-line discussed in the text.*

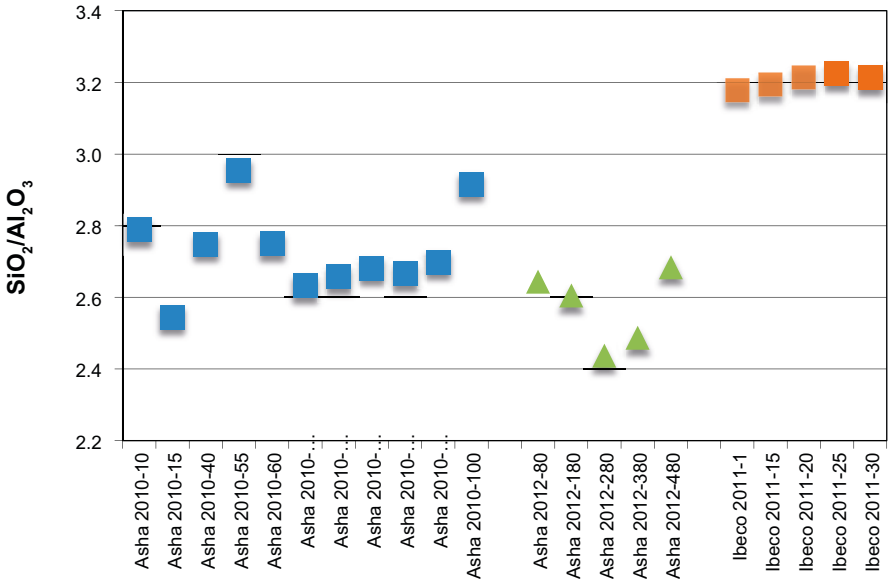

Figure 5-4. *The SiO_2/Al_2O_3 ratio of the bentonite samples Asha 2010, Asha 2012 and Ibeco 2011.*

The total iron content in the Asha bentonite is approximately three times higher than in the Ibeco bentonite. Accordingly, the Al_2O_3/Fe_2O_3 ratio of samples of the two batches of Asha bentonite is significantly lower than that of the Ibeco bentonite (Figure 5-5). The scatter around the mean is almost in the same range for all three bentonite batches, except for one conspicuous "outlier" among the samples of Asha 2012, which has an exceptionally high iron content. The results of the repeatability test performed on sample Asha 2010-70 and included in Figure 5-5 show that the analytical scatter is small.

A major fraction of magnesium in the Ibeco bentonite originates from dolomite and the magnesium content is more than twice as high as that of the Asha bentonite. While the Al_2O_3/MgO ratio is more or less constant for the samples of Ibeco bentonite (Figure 5-5- lower diagram), the population of Asha samples displays a significant scatter, again demonstrating the heterogeneity of this bentonite. The ratio of five subsamples of Asha 2010-70, used for a repeatability test, is included in the diagram.

5.5 X-ray diffraction analysis

5.5.1 Method

The mineralogical composition was determined by X-ray diffraction analysis of randomly oriented powders at two laboratories using different equipment with different X-ray tubes and slightly different sample preparation. Samples of Asha 2010 and Ibeco 2011 were analysed at Clay Technology AB, Lund, whereas samples of Asha 2012 were analysed at CSIRO, Australia.

The procedures utilised at the two laboratories are described below.

Clay Technology AB.

The randomly oriented specimens used in x-ray diffraction analyses were prepared after grinding 3 g of the bulk material to a grain-size < 10 µm by use of an agate mortar. After equilibration at ambient relative humidity, the powders were lightly pressed into stainless steel sample holders and scanned in the 2θ interval 2–66° with a step size of 0.05° 2θ and a counting time of 5 seconds.

A Seifert 3000 TT X-ray diffractometer with CuKα radiation and automatic divergence slit was used for the X-ray diffraction analyses.

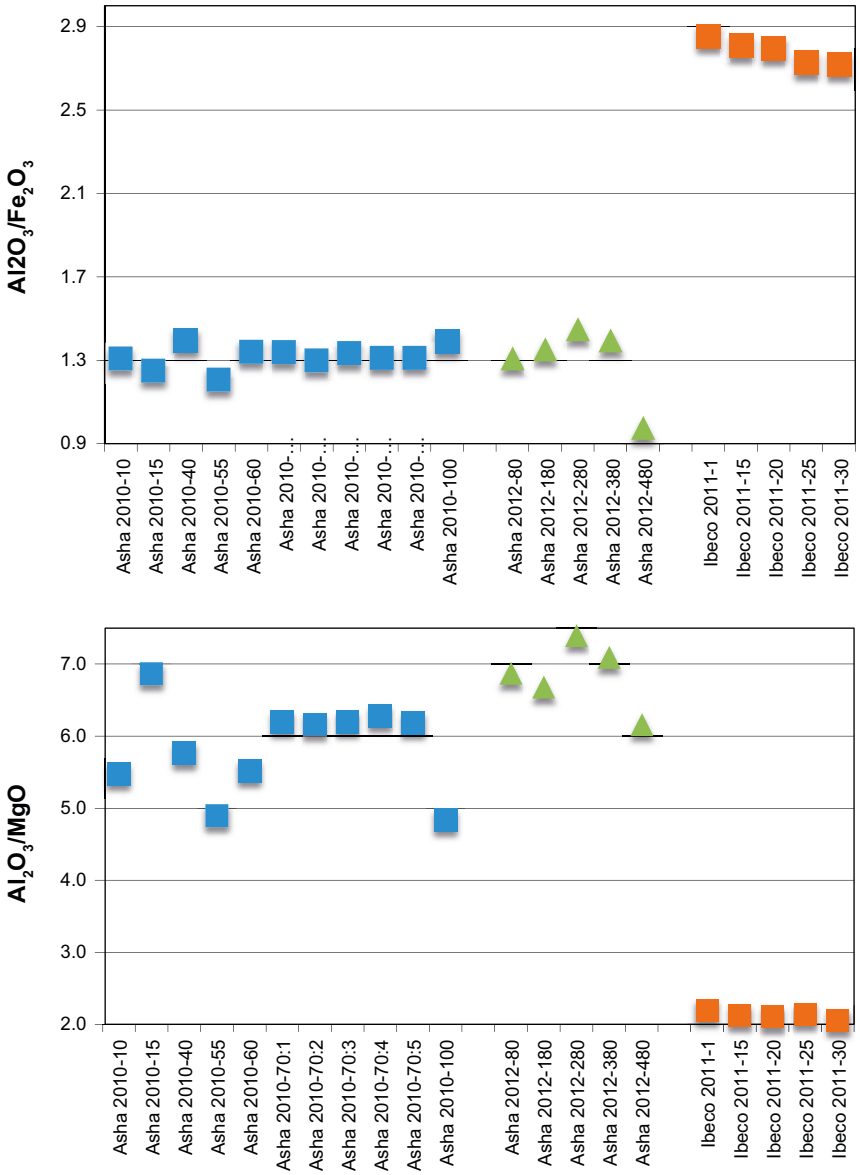

Figure 5-5. *The ratios Al_2O_3/Fe_2O_3 (upper diagram) and Al_2O_3/MgO (lower diagram) of the bentonite samples of Asha 2010, Asha 2012 and Ibeco 2011.*

Mineral identifications were made by comparison of the diffractograms of the randomly oriented powders with the Siroquant v.30h database, Sietronics Pty Ltd. Subsequently, mineral quantification was made by use of the Siroquant Analytical Software, version 3. The modelling is principally based on a Rietveld refinement method of least squares fit of calculated to measured XRD profiles (Rietveld 1969). The method is described in general and also used for montmorillonite in Taylor and Matulis (1994). The results are normalised to 100%, and hence do not include estimates of unidentified or amorphous materials.

CSIRO

A 1.5 g sub-sample was ground for 10 minutes in a McCrone micronizing mill under ethanol. The resulting slurry was oven dried at 60°C then thoroughly mixed in an agate mortar and pestle before being lightly pressed into a stainless steel sample holder for X-ray diffraction analysis.

The XRD patterns of the as received samples showed swelling clay minerals present and hence were Ca saturated twice using 1M $CaCl_2$ followed by water- then ethanol wash before oven drying at 60°C (samples were centrifuged at 6,000 rpm after each step). This resulted in a Ca-saturated smectite phase

being present and simplified subsequent mineral quantification and identification. The oven-dried samples were thoroughly mixed with an agate mortar and pestle before being lightly back pressed into stainless steel sample holders to achieve random orientation of the mineral particles for XRD analysis.

XRD patterns were recorded with a PANalytical X'Pert Pro Multi-purpose Diffractometer using Fe filtered Co Ka radiation, auto divergence slit, 2° anti-scatter slit and fast X'Celerator Si strip detector. The diffraction patterns were recorded in steps of 0.016° 2 θ with a 0.4 second counting time per step, and logged to data files for analysis.

Quantitative analysis was performed on the XRD data using the commercial package SIROQUANT from Sietronics Pty Ltd. The results are normalised to 100%, and hence do not include estimates of unidentified or amorphous materials.

5.5.2 Test matrix

The three batches of bentonite were sampled as follows:

- **Asha 2010.** Seven big bags, number 10, 15, 40, 55, 60, 70 and 100 were sampled. Sample 70 was used for a repeatability test of the preparation and analysis of random powders. All mineralogical analyses of the Asha 2010 bentonite were performed and reported within another SKB project (Olsson et al. 2013). The results reported here are from this investigation.
- **Ibeco 2011.** Five big bags, number 1, 15, 20, 25 and 30, were sampled.
- **Asha 2012.** Samples were taken from every twentieth big bag from number 20 to 480 including number 1, i.e. in total 25 bags. All samples of Asha 2012 were prepared and analysed at CSIRO, Australia.

5.5.3 Results

Asha 2010

To test the reproducibility in the preparation and X-ray-analysis of random powders, sample Asha 2010-70 was ground in two batches. Two random powders were prepared of batch 1 (A and B batch 1 in Figure 5-6) and three of batch 2 (A, B and C batch 2 in Figure 5-6).

The XRD-profile of sample B batch 2 displays a peak of low intensity at 18.3° 2θ (d=0.485 nm), probably derived from gibbsite ($Al(OH)_3$), which can barely be detected in the rest of the subsamples of Asha 2010-70. Some variation is seen also in the intensities of the strongest peaks of quartz and calcite, probably as an effect of variations in particles size and/or heterogeneous mixing of the samples, which are factors of major importance in the diffraction of X–rays by mixed powders. The acceptable particle size depends on the composition of the material and the radiation used, but for most powders of clay, the optimal particle size should be less than 2 μm. However, in general it is necessary to accept a larger particle size rather than to use prolonged grinding, which may create amorphous surface layers and lattice distortions in minerals, resulting in reduced reflected X-ray intensity and peak broadening. Brindley and Brown (1980) report, for instance, that for ground quartz, a maximum intensity is obtained for particles in the 2–10 μm range.

The results of the quantitative evaluation of the mineralogy of the five subsamples of Asha 2010-70 are given in Table 5-5. The general reproducibility is quite good, considering that some of the observed scatter may represent actual variations among the powders, as described above.

Diffraction profiles of random powders of all samples of Asha 2010 are shown in Figure 5-7, in which the peak positions of the major accessory minerals are indicated together with the values d(001) and d(060) of the smectite. Basal spacings in the range 1.25–1.28 nm are typical of the monolayer hydrate of Na-smectites, which are stable at a relative humidity below 60–70%. Peak asymmetry towards the low angle side, as displayed in some of the samples, may arise when the interlayer cation pool is a mixture of mono- and divalent cations (cf. Section 5.1). A value of 0.150 nm for d(060) is typical of dioctahedral smectites.

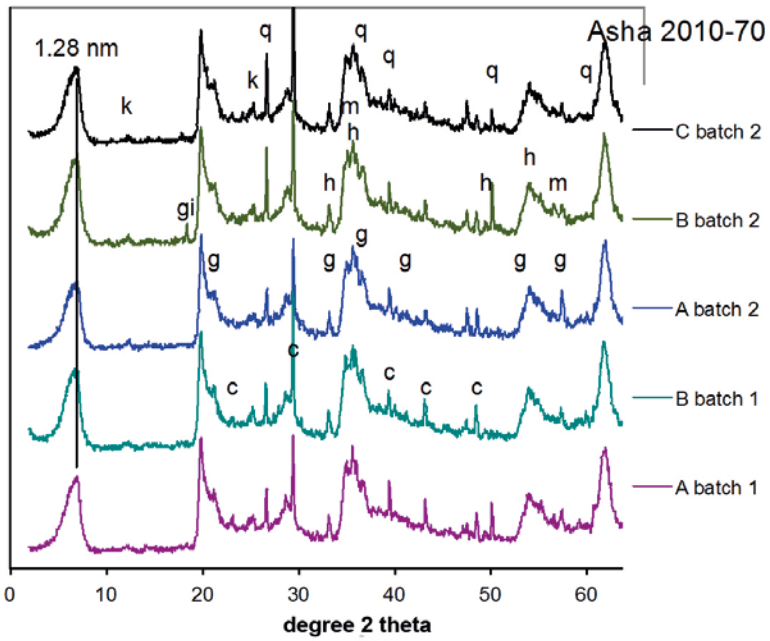

Figure 5-6. *Repeatability test: XRD-profiles of powders of Asha 2010-70, ground in two batches and scanned as five random preparations. The position of the strongest peaks of the major accessory minerals is indicated: c=calcite; g=goethite; gi=gibbsite; h=hematite; k=kaolin mineral; m=magnetite/maghemite; q=quartz. The position of the (001) smectite peak is also indicated at 1.28 nm. CuKα radiation was used.*

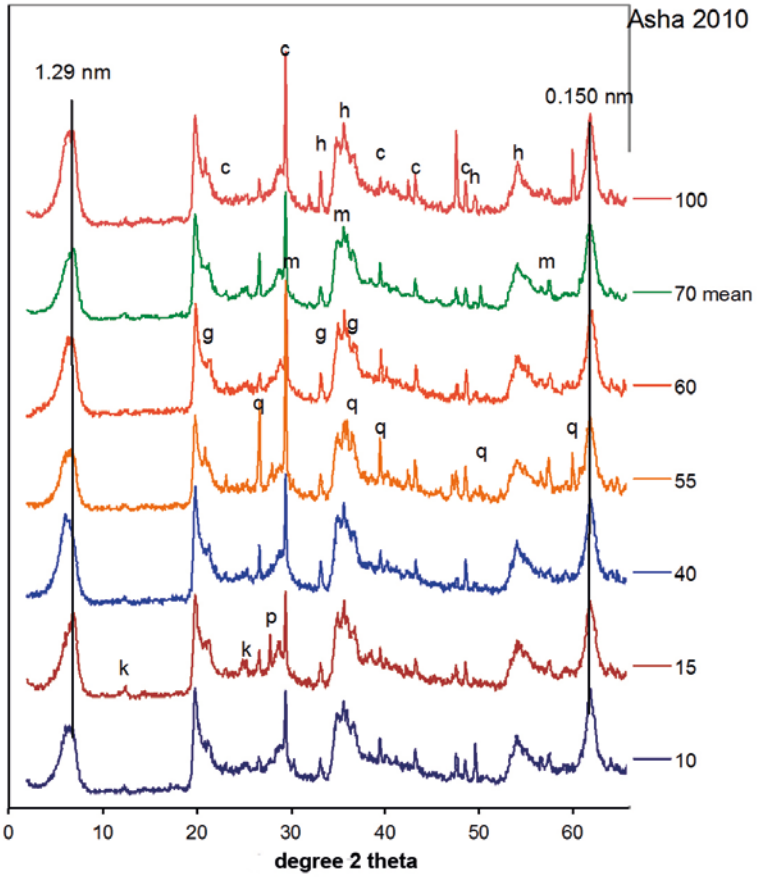

Figure 5-7. *XRD-profiles of random powders of Asha 2010. The position of the strongest peaks of the major accessory minerals is indicated: c=calcite; g=goethite; h=hematite; k=kaolin mineral; m=magnetite/maghemite; p=plagioclase; q=quartz. The positions of the smectite peaks (001) at 1.29 nm and (060) at 0.150 nm are also indicated. CuKα radiation was used.*

Consistent with the chemical data, the XRD-data clearly show that the content of calcite varies among the samples and is most abundant in sample 55. Similarly, the quantity of quartz is at a maximum in this sample, while close to the detection limit of the XRD-method in most of the other samples.

The XRD-analyses also indicate that the abundance and type of iron oxide minerals varies among the samples: sample 100, which has a reddish colour, has the maximum content of hematite, whereas goethite predominates in the yellowish brown sample 55. Also a magnetic phase, magnetite or maghemite, exists in the samples but the distinction between these minerals by XRD analysis is difficult due to the overlap of their strongest diffraction peaks. Poorly crystalline and/or very fine-grained iron oxyhydroxides are amorphous to X-rays, which implies that the iron phases tend to be underestimated in quantitative evaluations.

The results of the quantitative evaluation according the standard procedure described in the Siroquant manual are summarised in Table 5-5. In the analyses, the main minerals were identified by their typical main peaks in the XRD diffractograms (Figure 5-7 and 5-8), and the presence of less common minerals were checked by comparison with synthetic patterns created from the database. In this process, it is of course important not to overlook the existence of a mineral phase since this will introduce a general error equal to the content of the overlooked mineral. On the other hand, the number of possible but uncertain mineral phases should be minimized, due to the risk for accidental fit with scatter in the diffractograms, which thereby apparently reduces the content of existing phases. This also implies that phases with a calculated low content (~1%) generally must be considered uncertain. Distinction between intermediate members of the plagioclase series is complicated, and the sum of plagioclases is therefore given in Table 5-5. Also the maghemite/magnetite, and the goethite/hematite phases are presented as sums.

According to SKB´s requirements, a candidate tunnel backfill bentonite should have a montmorillonite content between 50 and 60%, with an accepted range of 45 to 90% (SKB 2010). According to the producer, Ashapura Minechem Co. Asha 2010 has a montmorillonite content of 69% (Appendix 2). Based on the standard Siroquant analyses performed, the average smectite content of the Asha 2010 samples is 74% (st.dev. 2.8%) and the range of variation is 69–79%. The value of d(060) is typical of the dioctahedral smectites, to which montmorillonite belongs, and montmorillonite is the dioctahedral smectite species available in the Siroquant database used for the quantitative modelling. However, a distinction between the smectites in the montmorillonite–beidellite series (dioctahedral smectites with predominantly octahedral and tetrahedral charge, respectively) cannot be made by a routine XRD-examination of random powders, but will require additional diagnostic tests of the purified smectite. A more comprehensive study of the Asha 2010 bentonite is presented in Olsson et al. (2013), where uncertainties in the identification/quantification of certain clay minerals at species level by use of Rietweld technique are discussed.

Table 5-5. Quantitative mineralogy of the samples of Asha 2010 evaluated by the Siroquant software according to the standard procedure. Sample Asha 2010-70 was ground in two batches (1 and 2) and scanned as five random powder preparations (A-C) for a repeatability test of the preparation and analysis of random powders.

Sample id	Smectite dioctahedral	Plagio-clase	Calcite	Cristo-balite	Gibb-site	Goethite/ hematite	Gypsum	Kaolin	Magnetite/ maghemite	Quartz	Rutile/ anatase
Asha 2010-10	79	< 1	3	< 1	< 1	6	1	8	2	< 1	< 1
Asha 2010-15	75	2	3	< 1	< 1	7	1	11	1	1	< 1
Asha 2010-40	77	< 1	3	1	< 1	7	1	10	2	1	< 1
Asha 2010-55	70	1	8	< 1	< 1	7	< 1	8	2	4	< 1
Asha 2010-60	69	< 1	4	1	< 1	8	1	14	2	1	< 1
Asha 2010-70:1A	74	< 1	4	< 1	< 1	6	1	11	2	2	< 1
Asha 2010-70:1B	75	< 1	5	< 1	< 1	7	< 1	10	1	1	< 1
Asha 2010-70:2A	74	< 1	3	< 1	< 1	7	1	11	2	1	< 1
Asha 2010-70:2B	76	< 1	4	< 1	< 1	6	1	9	2	2	< 1
Asha 2010-70:2C	74	< 1	3	< 1	< 1	7	1	11	2	1	< 1
Asha 2010-100	75	< 1	5	< 1	< 1	8	< 1	8	2	1	< 1
Mean (N=11)	**74**		**4**			**7**		**10**	**1.8**	**1.5**	
Std.dev.	**2.8**		**1.5**			**0.7**		**1.8**	**0.4**	**0.9**	
Min	**69**	**< 1**	**3**	**< 1**		**6**	**< 1**	**8**	**1**	**< 1**	
Max	**79**	**2**	**8**	**1**		**8**	**1**	**14**	**2**	**4**	

Ibeco 2011

Diffraction profiles of random powders of the samples of Ibeco 2011 are shown in Figure 5-8, in which the peak positions of the major accessory minerals are indicated together with the values d(001) and d(060) of the smectite. The smectite has predominantly divalent interlayer cations (cf. Section 5.2), which is consistent with a basal spacing around 1.50 nm. The value of d(060), 0.149 nm, is typical of the dioctahedral smectites, to which montmorillonite belongs.

All samples of Ibeco 2011 (N=5) contain high amounts of dolomite, $CaMg(CO_3)_2$, which together with calcite makes up more than 20% of the samples. Other major accessory minerals are plagioclase and quartz, and all together the accessory minerals constitute more than 30% of the bentonite.

Neither of the common potassium-bearing phases, such as mica/illite, K-feldspars or zeolites, can be detected in any of the XRD-traces, and yet the potassium content of the bentonite is fairly high (mean K_2O content 0.73% on LOI-free basis). However, previous, more detailed investigations of candidate tunnel backfill bentonite from the same producer (IBECO RWC BF 2004 and 2008; Olsson and Karnland 2009) indicated that the smectite of these bentonite batches were interstratified with up to 10% illitic layers. An identification of interstratified illite/smectite cannot be made by XRD-examination of random powders alone, but will require XRD-traces of oriented mounts of the purified clay mineral fraction for tests of the expansion behaviour, preferably together with chemical data for the same fraction. Lacking this information, a quantitative evaluation must be considered uncertain. For this reason, the results are reported as the mean composition of the five samples (Table 5-6), where the smectite content, evaluated by normalisation to 100%, may include also an unknown proportion of illite/smectite mixed-layers. However, the CEC of the Ibeco bentonite suggests that the smectite proportion is sufficiently high to match the requirements specified by SKB (a montmorillonite content between 50 and 60%, with an accepted range of 45 to 90%).

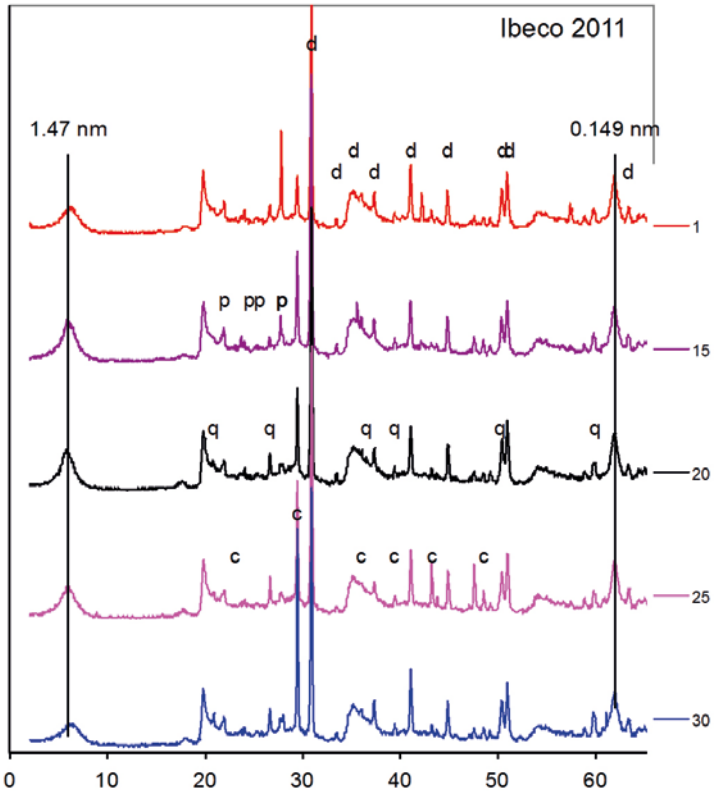

Figure 5-8. *XRD-profiles of random powders of Ibeco 2011. The position of the strongest peaks of the major accessory minerals is indicated: c=calcite; d=dolomite; p=Ca-plagioclase; q=quartz. The positions of the smectite peaks (001) at 1.47 nm and (060) at 0.149 nm are also indicated. CuKα radiation was used.*

Table 5-6. Average mineralogy determined using x-ray analysis of five samples of Ibeco 2011. Explanations of how these were developed are provided in the text.

Phase	Weight%
Smectite+illite/smectite	64
Calcite 1	4
Cristobalite	< 1
Dolomite	18
Gypsum	< 1
Kaolin	2
Plagioclase	8
Quartz	2

Asha 2012

The XRD analyses of Asha 2012 were performed and evaluated by CSIRO, Australia. Figure 5-9 shows an example of the XRD-profiles of one of the Asha 2012 samples. All XRD profiles are presented in Appendix 17.

The quantitative evaluation by use of the Siroquant program presented in Table 5-7 is based on XRD-profiles of Ca saturated samples. Soluble phases, like halite (NaCl) and gypsum ($CaSO_4 \times H_2O$), have been dissolved by this treatment but may be seen in most of the XRD-profiles of untreated samples (e.g. black curve in the upper graph of Figure 5-9). The relative mineral distributions of x-ray identified phases for all samples of Asha 2012 are shown in Figure 5-10.

The average smectite content of the Asha 2012 samples is 76% (st.dev. 1.3%) and the range is 74–79%, based on identified crystalline mineral phases. As a whole, the average mineralogy of Asha 2012 and Asha 2010 is very similar.

A comparison of the smectite content, liquid limit (Section 4.5) and CEC (Sectrion 4.6) is shown in Figure 5-11, where the ratio “sample value/population mean” for these parameters has been plotted for the samples of Asha 2012. As might be expected, a fairly good correspondence exists between the smectite content and the CEC. The correspondence between the smectite content and the liquid limit is not as clear and a number of “outliers” appear in the graph.

Asha 2012-380 micronised as received (black) and after Ca-saturation (red)

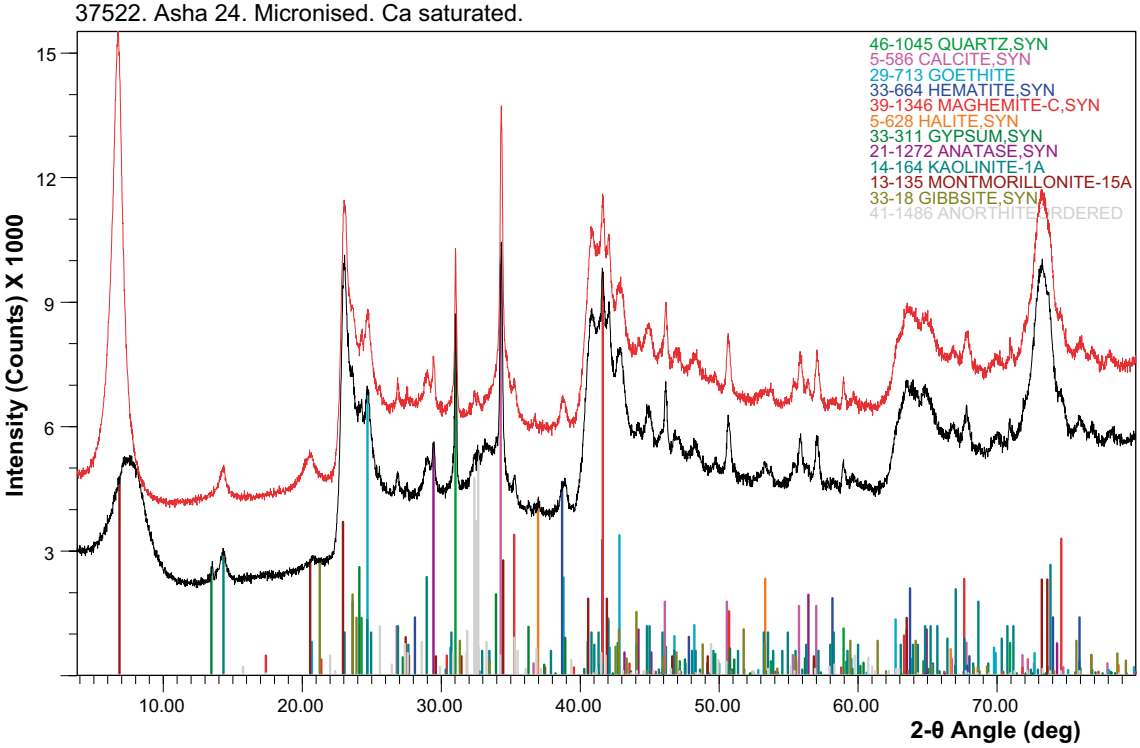

Asha 2012-380 <0.2 µm. Acetic acid treated and Ca saturated

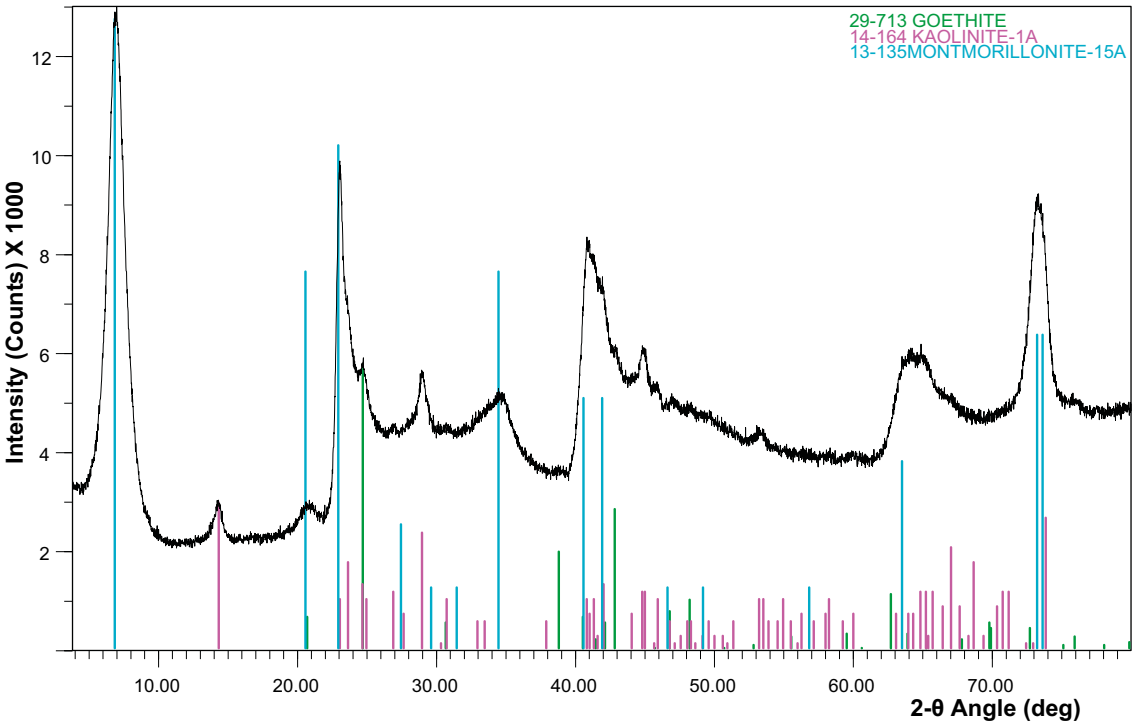

Figure 5-9. *Upper diagram: XRD-profiles of random powders of sample Asha 2012-380 as received and after Ca-saturation. Lower diagram: XRD-profile of random powder of the acetic acid treated and Ca-saturated < 0.2 µm fraction of Asha 2012-380. Co Kα radiation.*

Table 5-7. Quantitative mineralogy of the samples of Asha 2012 (Ca saturated sample).

Sample id	CSIRO id	Quartz	Albite/ Anorthite	Calcite	Maghemite	Anatase	Goethite/ Hematite	Smectite	Kaolin	Gibbsite
Asha 2012-1	37499	< 1	1	3	< 1	< 1	5	76	14	
Asha 2012-20	37500	2	< 1	3	< 1	< 1	5	75	14	
Asha 2012-40	37501	1	< 1	2	< 1	< 1	6	76	14	
Asha 2012-60	37502	1	< 1	2	< 1	< 1	5	77	14	
Asha 2012-100	37503	< 1	< 1	3	< 1	< 1	5	76	15	
Asha 2012-120	37504	1	< 1	2	< 1	< 1	5	77	14	< 1
Asha 2012-140	37505	1	< 1	2	< 1	< 1	5	74	17	
Asha 2012-160	37506	1		2	< 1	< 1	5	74	17	
Asha 2012-200	37507	1	< 1	2	< 1	< 1	5	75	16	
Asha 2012-220	37508	1	< 1	2	< 1	< 1	5	75	16	< 1
Asha 2012-240	37509	1	< 1	2	< 1	< 1	5	76	15	
Asha 2012-260	37510	1	< 1	2	< 1	< 1	5	77	14	
Asha 2012-300	37511	1	< 1	3	< 1	< 1	6	74	15	
Asha 2012-320	37512	1	< 1	2	< 1	< 1	6	75	15	< 1
Asha 2012-340	37513	1	< 1	3	< 1	< 1	5	76	13	1
Asha 2012-360	37514	1	< 1	3	< 1	< 1	5	74	16	< 1
Asha 2012-400	37515	1	< 1	4	< 1	< 1	5	76	13	< 1
Asha 2012-420	37516	3		3	< 1	< 1	7	78	8	< 1
Asha 2012-440	37517	1		3	< 1	< 1	7	77	11	< 1
Asha 2012-460	37518	1		4	< 1	< 1	6	75	14	< 1
Asha 2012-80	37519	2	< 1	3	< 1	< 1	7	76	11	< 1
Asha 2012-180	37520	1	< 1	3	< 1	< 1	5	78	12	
Asha 2012-280	37521	1	< 1	3	< 1	< 1	6	75	14	< 1
Asha 2012-380	37522	1	< 1	3	< 1	< 1	6	75	14	
Asha 2012-480	37523	1		2	< 1	< 1	8	79	9	< 1
Mean (N=25)		**1.2**		**2.6**			**5.6**	**76**	**14**	
st.dev.		**0.5**		**0.6**			**0.9**	**1.3**	**2.2**	
Min		**< 1**		**2**			**5**	**74**	**8**	
Max		**3**		**4**			**8**	**79**	**17**	
< 0.2 µm:										
Asha 2012-100	37503a						2	83	15	
Asha 2012-380	37522a						< 1	83	16	

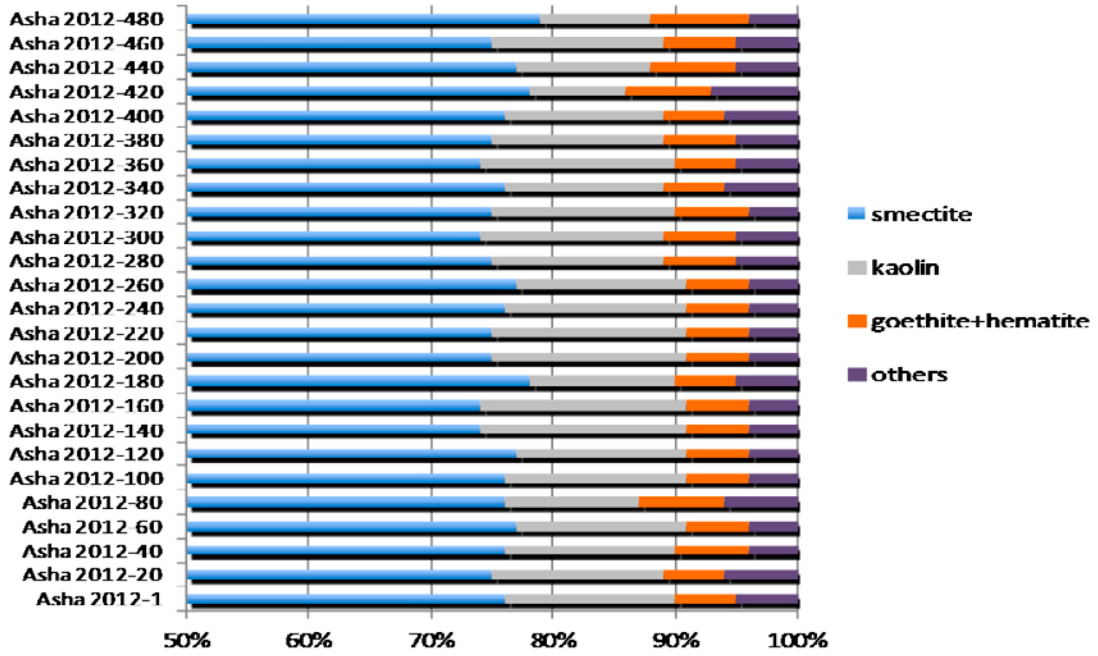

Figure 5-10. *The relative mineral distribution in all samples of Asha 2012.*

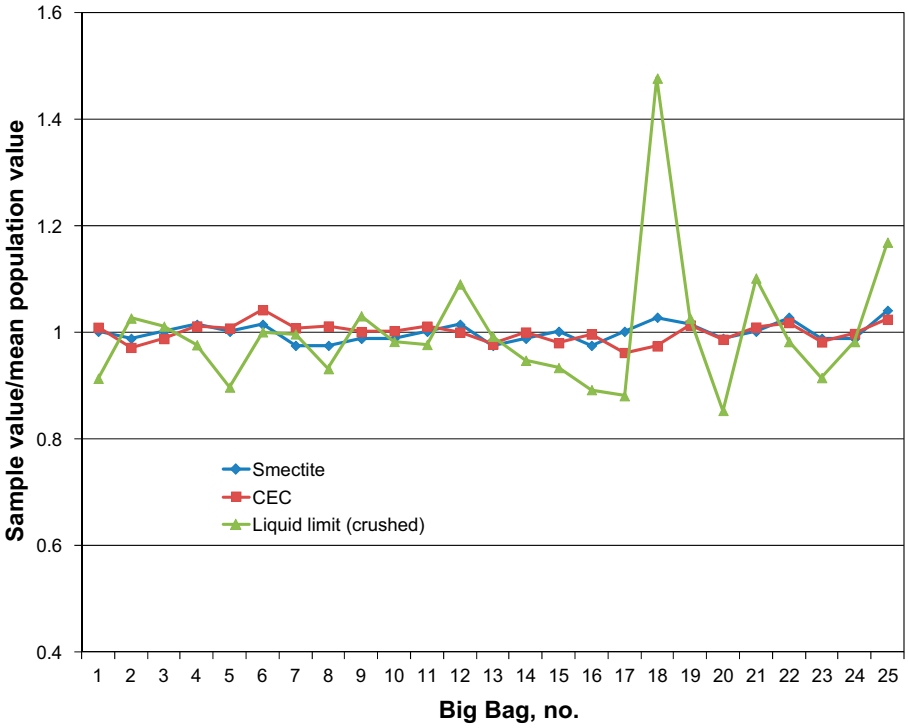

Figure 5-11. *Plot of the ratio "sample value/population mean" for the smectite content, CEC and liquid limit of the samples of Asha 2012.*

6 Hydro-mechanical tests

6.1 General

It is essential to be able to describe the behavior of the backfill material both during installation and when in place in the tunnel. An important parameter for the block handling during installation is the strength of the compacted blocks. The influence of expected conditions in deposition tunnels, i.e. high relative humidity, and how this will affect the blocks is also an important issue. Other important parameters are the compressibility of the saturated bentonite, the swelling pressure and hydraulic conductivity at different densities and with different water types used for the saturation of the samples.

6.2 Grain density

6.2.1 General

The grain density of a material is needed in calculations of e.g. the degree of saturation.

6.2.2 Method

The grain density of the bentonites was determined by use of volumetric flasks. After determining the volume of the flasks very carefully, dried material was mixed with 1 M NaCl solution in order to prevent swelling of the bentonite. When the mass of the solids, the total volume, the total mass (solids and flask) and the density of the liquid are known, it is possible to calculate the grain density of the material. The method is described in detail in Karnland et al. (2006).

6.2.3 Test matrix

The grain density was determined on five different samples for each of the three batches:

1. **Asha 2010.** All samples were taken from the same big bag (no. 113).
2. **Ibeco 2011.** All samples were taken from the same big bag (no. 1).
3. **Asha 2012.** Samples were taken from big bag no. 1, 60, 100, 160, and 200.

6.2.4 Results

The results of the measurements are provided in Table 6-1. The grain density of the Asha materials is significant higher than the Ibeco material. This increased density is attributed to the high iron content, see Section 5.4. The average grain density for Ibeco 2011 was 2,723 kg/m^3, for Asha 2010 2,917 kg/m^3 and for Asha 2012 2,928 kg/m^3. These values correspond well with previous determinations made on bentonites from the same areas e.g. Ibeco Seal and Deponit CAN can be compared with Ibeco 2011 and Asha 505 can be compared with Asha 2010 and Asha 2012, see data in Svensson et al. (2011).

Table 6-1. Results of the grain density determinations.

Batch of bentonite	Sample 1 kg/m^3	Sample 2 kg/m^3	Sample 3 kg/m^3	Sample 4 kg/m^3	Sample 5 kg/m^3	Average kg/m^3	Standard dev., kg/m^3
Asha 2010	2,937	2,886	2,918	2,905	2,938	2,917	22.1
Ibeco 2011	2,747	2,681	2,710	2,741	2,737	2,723	27.4
Asha 2012	2,930	2,935	2,928	2,916	2,930	2,928	7.2

6.3 Swelling pressure and hydraulic conductivity

6.3.1 Method

The hydraulic conductivity and swelling pressure were determined in special oedometers, see Figure 6-1. The specimens had a diameter of 50 mm and a height of 20 mm except for the lowest densities for which the diameter was 101 mm and the height 50 mm. The measurements were performed according to the following:

- The specimens of the as-delivered material were compacted in separate equipment to a specified dry density. After compaction the specimens were placed in the test cells, see Figure 6-1. For the samples with the lowest density, the material was transferred directly into the test cell.
- After mounting, the specimens were saturated from both top and bottom filters during continuous measurement of the swelling pressure with the load cell placed on top of the piston. The time needed to get stable conditions regarding the measured swelling pressure was about one week.
- After saturation, a water pressure gradient was applied across the specimen and the volume of the out-flowing water was measured. The volume was then used for calculating the hydraulic conductivity of the specimens. The gradient during the tests varied from 20 to 7,500 (corresponding to a pore pressure difference across the specimen of Δu = 20–1,500 kPa). No back-pressure was used in the tests.
- After finishing the hydraulic conductivity measurements the applied water pressure was decreased and the sample was then left for about one week.
- After the test the specimen were pressed out from the test cell and the water content and density were determined. The water content was determined by drying the sample in an oven for 24 h at a temperature of 105°C and the density was determined by weighing the sample, first in air and then submerged into paraffin oil.

The swelling pressure P_s was calculated from the measured force at zero water pressure according to:

$$P_s = \frac{F}{A} \tag{6-1}$$

where F is the axial force (N) and A is the cross section area of the sample (m^2). The accuracy of the measurements depends on the force transducer which is calibrated by use of special standard rings (SP calibrated).

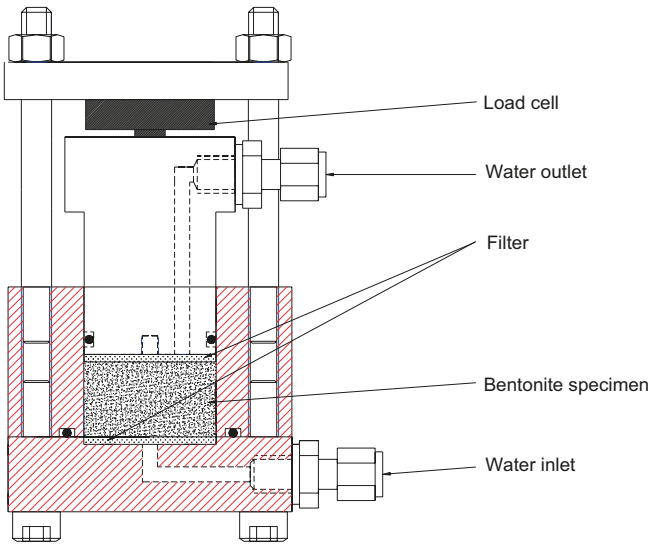

Figure 6-1. *Schematic of an oedometer used for measurement of the hydraulic conductivity and swelling pressure.*

The hydraulic conductivity was evaluated from the percolated water volume according to Darcy´s law:

$$k = \frac{V \times l}{A \times h \times t} \qquad (6\text{-}2)$$

where V is the percolated volume (m^3), l is the sample length (m), A is the sample area (m^2), h is the water pressure difference across the sample (mvp) and t is the time (s).

6.3.2 Water

The following water types were used in the tests:

- **Water 1**: water with a salinity of 1% (50/50 $NaCl/CaCl_2$).
- **Water 2**: water with a salinity of 3.5% (50/50 $NaCl/CaCl_2$).

The water type that is most likely to exist in the repository during the installation phase is type 1, but in order to study the influence of the salt content, water with a salinity of 3.5% was also tested.

6.3.3 Test matrix

The measurements were intended to study how swelling pressure and hydraulic conductivity vary with dry density for the different materials. For each of the tested materials, specimens were compacted in laboratory to different densities. A large number of measurements have been made:

- **Asha 2010**. The majority of the tests were made with material from big bag number 113 but some complementary tests were made with material from big bag number 125. Tests were performed with water salinities of 1% and 3.5%. In total, 14 samples were prepared and tested.
- **Ibeco 2011**. All tests were made with material from big bag number 1. Due to the achieved results which indicated high hydraulic conductivities at lower densities (see next section) complementary tests were made both with material from old batches and with ground material. The water used in the tests had a salinity of 1% and 3.5%. In total, 23 samples were prepared and tested.
- **Asha 2012**. The majority of the tests were made with material from big bag number 1 but some complementary tests were made with material from big bag number 200. The water used in the tests had a salinity of 1% and 3.5%. In total, 12 samples were prepared and tested.
- **Minelco**. A limited number of tests were made with this material. The material originated from a batch delivered to Äspö HRL several years ago. The water used in the tests had a salinity of 1%. In total, 5 samples were prepared and tested.

6.3.4 Results

General

A compilation of the results from the measurements is provided in Table 6-2 to 6-4. The results are also presented in diagrams, two for each tested material, where the swelling pressure and hydraulic conductivity, respectively, are plotted versus the dry density of each sample; see Figure 6-2 and 6-3. The results from the measurements of the Minelco material are presented in the same table and figure as the Asha material.

The material requirements, listed in the backfill production report (SKB 2010), states that the swelling pressure should be at least 100 kPa and the hydraulic conductivity should be less than 10^{-10} m/s. Modeling of the homogenization process in a backfilled tunnel has shown that the dry density of the bentonite closest to the rock wall (the pellet filled slot) can be as low as 1,370 kg/m^3 after homogenization (Åkesson et al. 2010). Using the requirements and the modeled lowest density as a basis when studying the data in Figure 6-2 to 6-3, the following observations can be made:

Asha 2010 and Asha 2012

The determined swelling pressure and the hydraulic conductivity for the two batches of material delivered from Ashapura during 2010 and 2012 are plotted versus the dry density, see Figure 6-2. There is a small difference between the two batches i.e. the determined swelling pressure of the material delivered 2012 is somewhat lower and the hydraulic conductivity somewhat higher when comparing with the 2010 batch. The swelling pressure for a density of 1,370 kg/m^3 is almost twenty times higher than the requirement, i.e. more than 2,000 kPa for the Asha 2010 batch, and the hydraulic conductivity is about two orders of magnitude lower than the required, i.e. about 10^{-12} m/s. Corresponding values for the Asha 2012 is a swellling pressure about six times higher than the requirement and about ten times lower hydraulic conductivity than required.

Minelco

The results obtained for the Minelco specimens are almost the same as for Asha 2010 for both swelling pressure and hydraulic conductivity. The test matrix for the Minelco material only included five samples and all tests were performed with a water salinity of 1%.

Ibeco 2011

The determined swelling pressure and the hydraulic conductivity for Ibeco 2011 are plotted versus the dry density, see Figure 6-3. The behavior of the material was not as expected. The swelling pressure at the lowest modeled density is about four times higher than the requirements i.e. about 400 kPa. This is, however, about five to ten times lower than the expected swelling pressure based on results from earlier investigations of material delivered with the same trade name in 2004 and 2008 (Johannesson et al. 2010, Olsson and Karnland 2009). The scatter for the measured hydraulic conductivities for densities below 1,370 kg/m^3 is very high. The evaluated hydraulic conductivity varies from $2 \cdot 10^{-11}$ to $1 \cdot 10^{-7}$. The large variation might be the result of piping that may have occured in some of the specimens. The phenomenon has, however, not been observed in earlier studies of this material at these densities and due to the unexpected results some extra tests were made with material from old batches. The results from the measurements using material from old batches showed that it was the new material that behaved differently. In order to investigate if any cementation of the material had affected the results, two samples (one from batch 2008 and one from batch 2011) were crushed and then tested regarding swelling pressure and hydraulic conductivity, see Table 6-3. There was no obvious effect of the crushing regarding the swelling pressure and only a minor effect regarding the hydraulic conductivity.

The differences between the various Ibeco batches are large, regarding both swelling pressure and hydraulic conductivity. The batch delivered 2004 seems to be of the highest quality although this batch had an equally high carbonate content (24%) as Ibeco 2011 (only a few measurements were made and all at rather low densities). The Ibeco batch delivered in 2008 also meets the requirements for a back-fill clay, even if the margin regarding the hydraulic conductivity is smaller than for the 2004 batch.

The swelling pressure for Ibeco 2011 is about one order of magnitude lower compared to the material delivered 2008. The hydraulic conductivity is about one order of magnitude higher than for the 2008 batch for the density interval 1,370 to 1,600 kg/m^3, but still below the specified performance, 10^{-10} m/s. At lower densities the scatter in hydraulic conductivity for the 2011 batch is very high. In six of the tests performed at densities below 1,370 kg/m^3, the measured hydraulic conductivity was between 10^{-7} and 10^{-8} m/s. Even if these six samples have densities lower than what is expected from the modeling, the high hydraulic conductivity indicates that this batch is abnormal.

The gradients used in the tests on the Ibeco 2011 materials were small but this is not believed to be an explanation for the behavior observed. The smectite content determined for this batch is rather low, see Section 6.5, but according to the requirements in the backfill production report (SKB 2010) (45 to 90%) it is high enough. This leaves some other mechanism to cause the behavior, one possible mechanism is the presence of some cementitious material(s) (either crystalline e.g. calcite/dolomite, or amorphous precipitate). Such cementation may be partially removed by the crushing and grinding of the bentonite to fine particle size, which would be consistent with the observed change in liquid limit results presented in Figure 4-3.

Table 6-2. Compilation of results from measurements of swelling pressure and hydraulic conductivity for Asha 2010 and Minelco.

Material	Big Bag no.	Dry density kg/m³	Gradient	Hydraulic conductivity m/s	Swelling pressure kPa	Water	Remark
Asha 2010	113	1,158	50	3.7E–10	137	1%	
Asha 2010	125	1,163	50	4.5E–10	150	1%	
Asha 2010	113	1,164	100	7.9E–11	268	1%	
Asha 2010	113	1,272	2,500	2.6E–12	1,198	1%	
Asha 2010	113	1,400	2,500	7.7E–13	1,969	1%	
Asha 2010	113	1,488	5,000	4.7E–13	2,964	1%	
Asha 2010	113	1,549	5,000	2.3E–13	4,579	1%	
Asha 2010	125	1,584	7,500	1.4E–13	8,032	1%	
Asha 2010	113	1,139	50	7.0E–09	136	3.5%	
Asha 2010	113	1,168	100	1.6E–09	214	3.5%	
Asha 2010	113	1,272	1,750	7.3E–12	685	3.5%	
Asha 2010	113	1,311	1,750	1.4E–12	1,621	3.5%	
Asha 2010	113	1,539	7,500	3.3E–13	5,131	3.5%	
Asha 2010	113	1,574	7,500	2.3E–13	5,581	3.5%	
MINELCO	n/a	1,182	750	3.2E–11	329	1%	
MINELCO	n/a	1,270	750	5.6E–12	833	1%	
MINELCO	n/a	1,368	4,000	5.4E–13	1,846	1%	
MINELCO	n/a	1,471	5,000	3.2E–13	4,593	1%	
MINELCO	n/a	1,497	5,000	1.8E–13	4,997	1%	

Table 6-3. Compilation of results from measurements of swelling pressure and hydraulic conductivity for Ibeco RWC BF2011 and some references from older deliveries.

Material	Big Bag no.	Dry density kg/m³	Gradient	Hydraulic conductivity m/s	Swelling pressure kPa	Water	Remark
IBECO RWC BF 2011	1	1,135	50	5.8E–08	38	1%	
IBECO RWC BF 2011	1	1,195	100	2.9E–08	89	1%	
IBECO RWC BF 2011	1	1,203	100	3.2E–08	123	1%	
IBECO RWC BF 2011	1	1,245	100	1.6E–09	127	1%	
IBECO RWC BF 2011	1	1,280	100	2.0E–10	189	1%	
IBECO RWC BF 2011	1	1,296	500	1.2E–10	361	1%	
IBECO RWC BF 2011	1	1,300	100	1.6E–08	275	1%	
IBECO RWC BF 2011	1	1,323	500	2.4E–11	323	1%	
IBECO RWC BF 2011	1	1,332	100	2.1E–07	310	1%	
IBECO RWC BF 2011	1	1,347	250	8.3E–11	363	1%	
IBECO RWC BF 2011	1	1,369	1,000	1.8E–11	528	1%	
IBECO RWC BF 2011	1	1,455	1,000	1.3E–12	1,084	1%	
IBECO RWC BF 2011	1	1,530	4,500	4.0E–13	2,099	1%	
IBECO RWC BF 2011	1	1,582	4,500	2.0E–13	3,279	1%	
IBECO RWC BF 2011	1	1,210	100	7.3E–08	84	3.5%	
IBECO RWC BF 2011	1	1,413	1,500	7.6E–12	604	3.5%	
IBECO RWC BF 2011	1	1,492	1,500	9.5E–13	1,178	3.5%	
IBECO RWC BF 2011	1	1,567	5,000	2.6E–13	2,532	3.5%	
IBECO RWC BF 2011	1	1,625	5,000	1.4E–13	4,221	3.5%	
IBECO RWC BF 2004	n/a	1,321	1,500	3.4E–12	712	1% salt	
IBECO RWC BF 2008	n/a	1,313	1,500	1.4E–11	1,202	1% salt	
IBECO RWC BF 2008	n/a	1,334	250	1.0E–12	1,224	1% salt	Crushed
IBECO RWC BF 2011	n/a	1,346	250	7.6E–12	329	1% salt	Crushed

Table 6-4. Compilation of results from measurements of swelling pressure and hydraulic conductivity for Asha 2012.

Material	Big Bag no.	Dry density kg/m³	Gradient	Hydraulic conductivity m/s	Swelling pressure kPa	Water	Remark
Asha 2012	1	1,061	20	2.1E–08	29	1%	
Asha 2012	200	1,063	20	1.1E–08	22	1%	
Asha 2012	1	1,180	100	5.2E–10	163	1%	
Asha 2012	1	1,342	1,000	3.7E–12	937	1%	
Asha 2012	1	1,438	1,000	8.8E–13	1,829	1%	
Asha 2012	1	1,545	4,000	3.4E–13	4,308	1%	
Asha 2012	1	1,631	4,000	1.4E–13	8,000	1%	
Asha 2012	200	1,652	4,000	5.3E–14	10,659	1%	
Asha 2012	1	1,095	20	1.38549E–07	18	3.5%	
Asha 2012	200	1,172	50	1.20789E–09	114	3.5%	
Asha 2012	1	1,368	500	8.2475E–12	686	3.5%	
Asha 2012	1	1,658	2,500	1.20318E–13	10,052	3.5%	

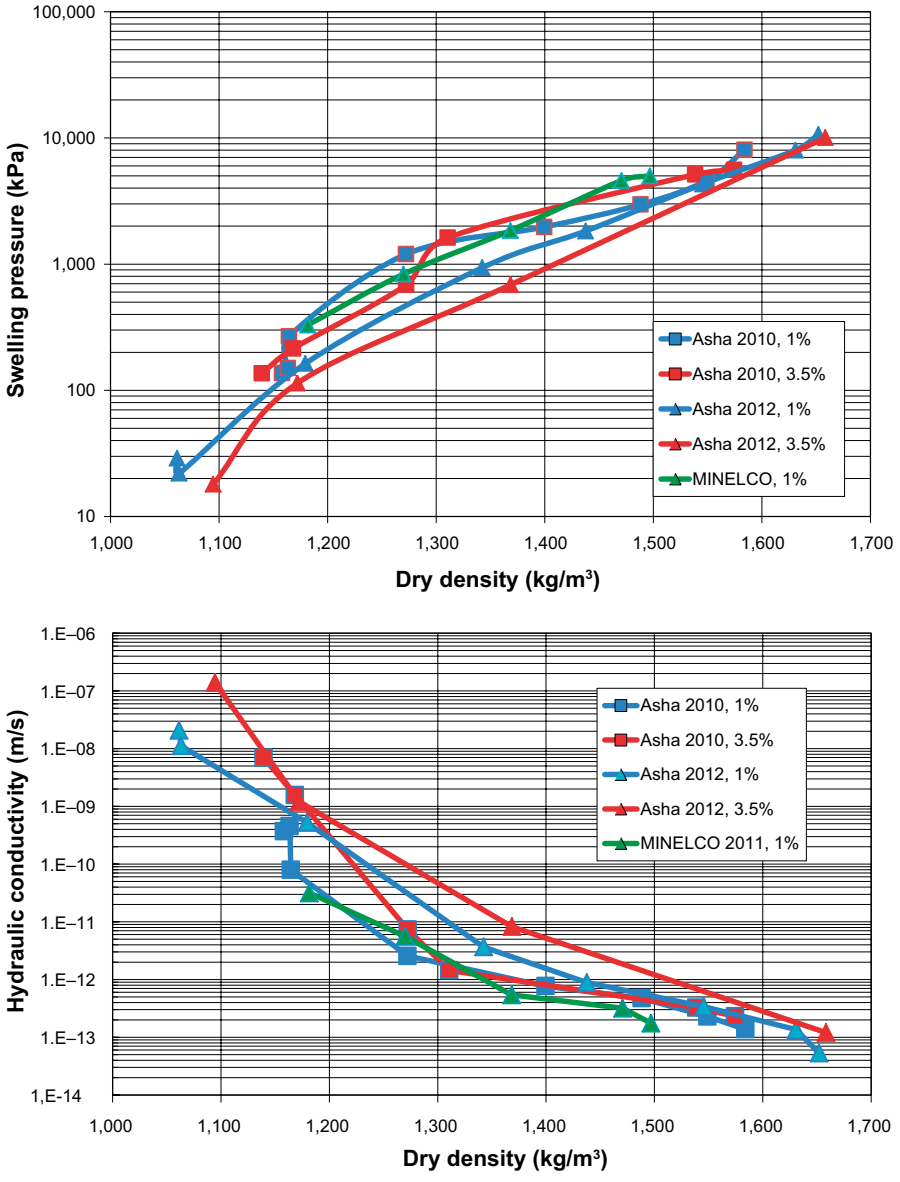

Figure 6-2. *Swelling pressure (upper) and hydraulic conductivity (lower) plotted versus dry density for the Asha 2010, Asha 2012 and Minelco.*

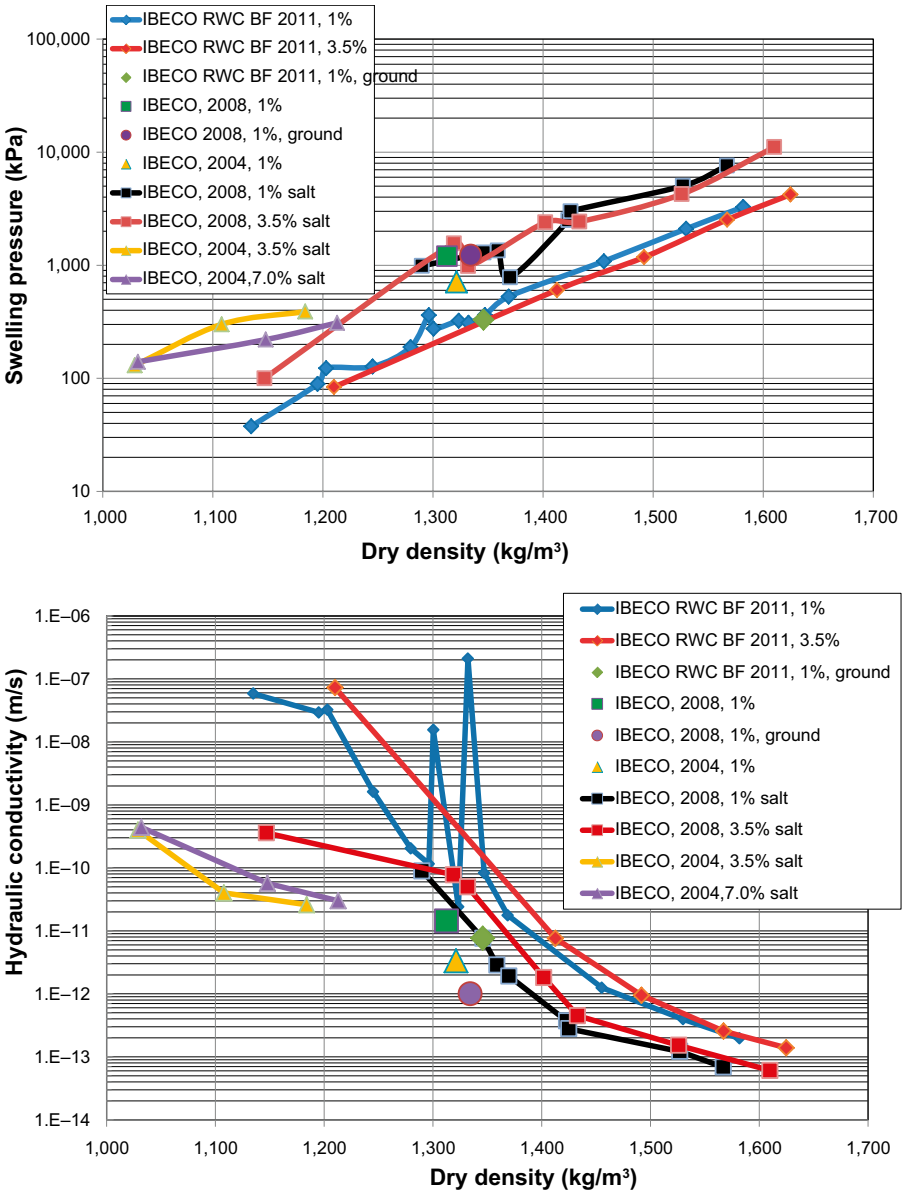

Figure 6-3. *Swelling pressure (upper) and hydraulic conductivity (lower) plotted versus dry density for the IBECO 2011 material.*

6.4 Compressibility of the saturated backfill

6.4.1 Method

The compressibility of the saturated clay was determined with oedometer tests. The equipment used for the tests is shown in Figure 6-4. The material was compacted into the oedometer ring and the piston was placed on top of the specimen. The samples were saturated through the two filters at a constant vertical stress of about 200 kPa. The water used for the tests had a salinity of 1 and 3.5% (50/50 $NaCl/CaCl_2$). When the specimens were completely saturated the vertical load was increased in steps during continuous measurement of the displacement of the specimen. The following approximate load steps were used; 400, 800, 1,600 and 3,200 kPa.

6.4.2 Test matrix

This test type was only performed with the Asha material delivered in 2010, big bag no. 113. Two tests were made, one where the sample was saturated with water with a salinity of 1% and one saturated with water with a salinity of 3.5%.

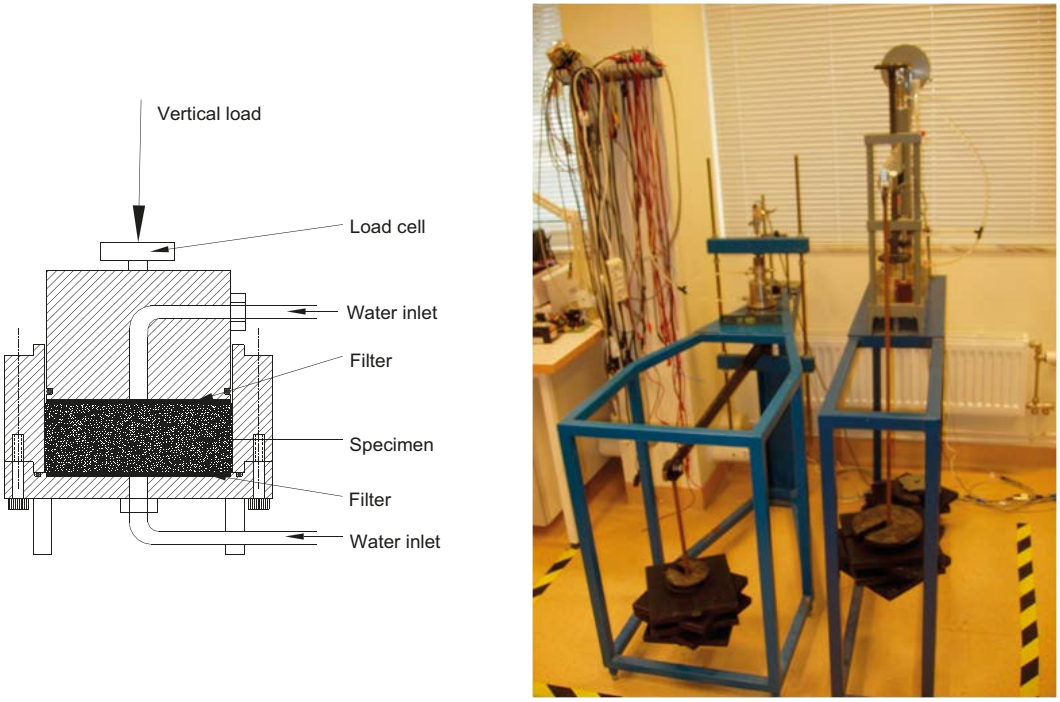

Figure 6-4. Left: *Schematic drawing of the test cell.* ***Right****: Photo of the test equipment used for the oedometer tests.*

6.4.3 Results

The measured data from the different load steps in the two oedometer tests is provided in Figure 6-5 and 6-6. For each of the tests the void ratio as function of time is plotted. The curves have a typical shape for this type of test made on clays. The curve can be divided into three steps, see Figure 6-5. Part 1 of the curve can be interpreted as a small elastic deformation of the material (instant and small). Part 2 of the curve represents the consolidation of the material when the increased pore water pressure caused by the increased load dissipates. The consolidation is time dependent and normally represents a large part of the deformation of the material. The rate of consolidation is a function of the hydraulic conductivity and the bulk modulus of the material. Part 3 of the deformation represents the creep of the sample (creep in the particle skeleton). This deformation is also time-dependent, but compared with the consolidation much smaller.

After finishing the tests, the density and water content of the specimens were determined. From these data, the dry density, the density at saturation and the void ratio could be calculated. The data received from the tests are listed in Table 6-5.

The final densities at the different load steps are plotted as a function of the vertical stress for the two tests in Figure 6-7. The figure indicates that the deformation of the samples is almost proportional to the vertical stress up to 3,200 kPa. The densities achieved at the different load steps are somewhat higher for the sample saturated with water with a salinity of 3.5% compared to the sample saturated with water with a salinity of 1%, which is consistent with the swelling pressure-density relationships exhibited by bentonite.

Table 6-5. Data determined after termination of tests.

Test no.	Final vertical stress kPa	Saturated density kg/m^3	Dry density kg/m^3	Void ratio
Test 1, 1% salt	3,395	1,890	1,366	1.100
Test 2, 3.5% salt	3,129	1,912	1,400	1.050

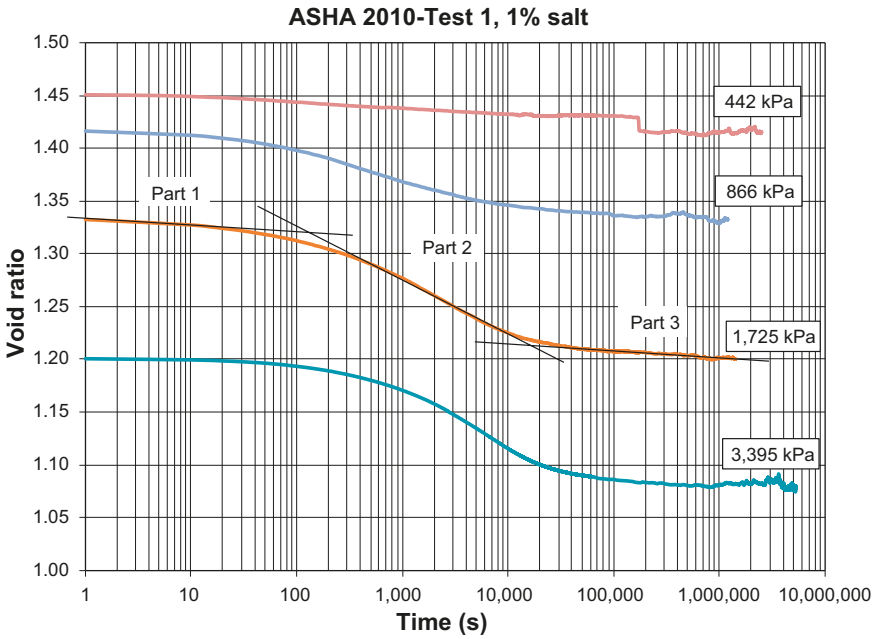

Figure 6-5. *Void ratio as function of time for the four load steps in Test 1.*

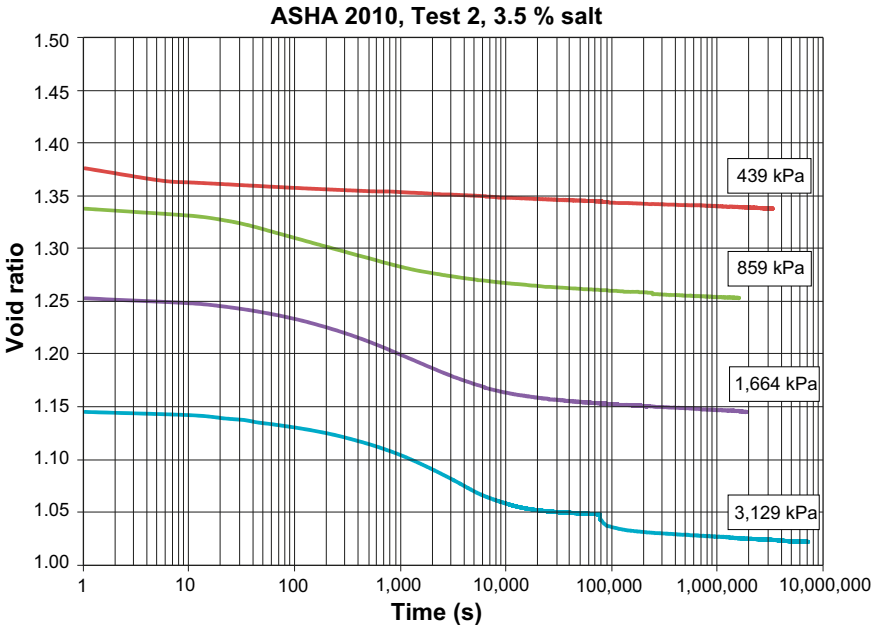

Figure 6-6. *Void ratio as function of time for the four load steps in Test 2.*

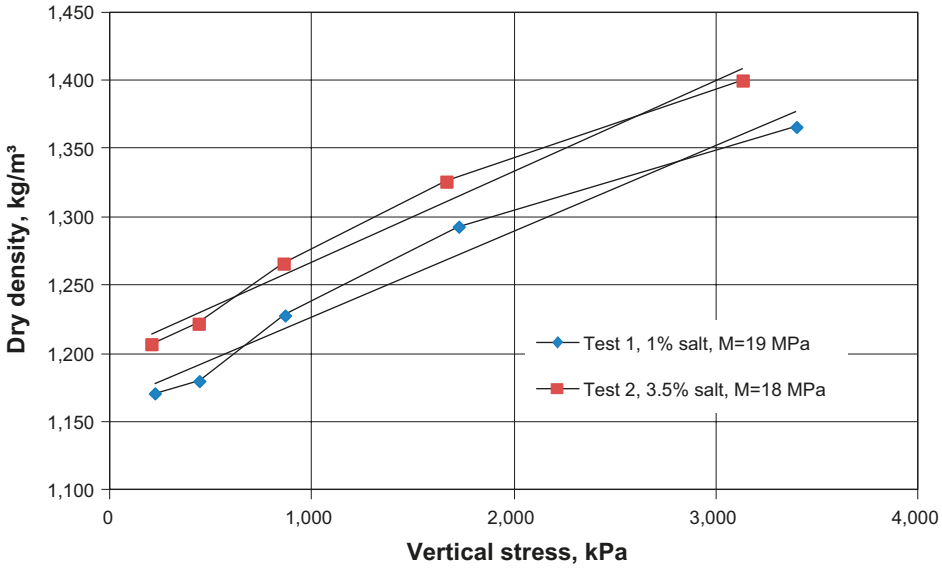

Figure 6-7. *Dry density plotted as function of the vertical stress for the two tests performed with two different water salinities.*

The compression modulus was evaluated according to Equation 6-3 within the measured stress interval.

$$M = \frac{\delta\sigma}{\delta\varepsilon} \tag{6-3}$$

where

M = compression modulus (MPa)

σ = vertical stress (MPa)

ε = vertical strain (%)

The compression moduli are almost the same for both samples, 19 MPa and 18 MPa respectively, which means that the salinity of the pore water does not discernibly affect the compressibility of the material.

6.5 Determining the strength of compacted blocks

6.5.1 General

The strength of the compacted blocks is important both for the handling of the blocks in order to avoid damage and pieces falling off, but also for assessment of calculated stresses when high loads act on the blocks in the tunnel (for instance caused by high swelling pressure from the buffer in a deposition hole). Two types of tests have been used for determining the block strength:

- Unconfined one dimensional compression tests.
- Beam tests.

6.5.2 Unconfined one dimensional compression tests

Method

In the unconfined one dimensional compression tests, compacted samples were compressed in vertical direction until failure occurred and the compressive strength of the material was determined from the maximum applied load. The tests were made in following steps:

- Small specimens were compacted (Ø 35 mm, h 70 mm). In order to minimize the density variations cross the sample a lubricated mold was used (Molycote).
- A specimen was placed in a load frame and compressed by applying a vertical constant deformation rate of ~0.09 mm/min with continuous measurement of the vertical load and the deformation of the specimen (see Figure 6-8).
- The strength of the specimen was evaluated according to Equation 6-4.

$$\sigma_{max} = \frac{F_{max}}{A} \tag{6-4}$$

where

σ_{max} = Maximum Deviator stress (kPa)

A = Area of the sample determined before test start (m)

F_{max} = Maximum applied vertical load (kN)

The evaluation of Young´s modulus (E) was made with Equation 6-5. The evaluation was made in the stress range 1,000 kPa to 2,000 kPa.

$$E = \frac{\Delta\sigma_v}{\Delta\varepsilon_v} \tag{6-5}$$

Test matrix

This test was only done using material from the batch delivered from Ashapura in 2012 (Asha 2012). The specimens were compacted with the following parameters varied:

1. Two different compaction pressures, 25 and 50 MPa.
2. Four different water contents, as-delivered, 20%, 22% and 24%.

Each specimen was manufactured in triplicate and the tests were done three times in order to ensure consistent results were obtained.

Figure 6-8. *Test arrangement for determination of the shear strength of pre-compacted samples of backfill material.*

Results

Altogether twenty-four tests were performed. The results from the measurements of all samples are provided in Figure 6-9 and the evaluated stress at failure for each sample is shown in Figure 6-10. The influence of density on the maximum stress at failure is obvious and so is the influence of the water content. The dry density obtained in this small scale is somewhat higher than what has been obtained in full scale. The results show, however, that the water content chosen for the full scale block manufacturing, 20%, seems to be suitable also regarding the strength of the blocks. The results from the tests are summarized in Table 6-6 together with the evaluated E-modulus.

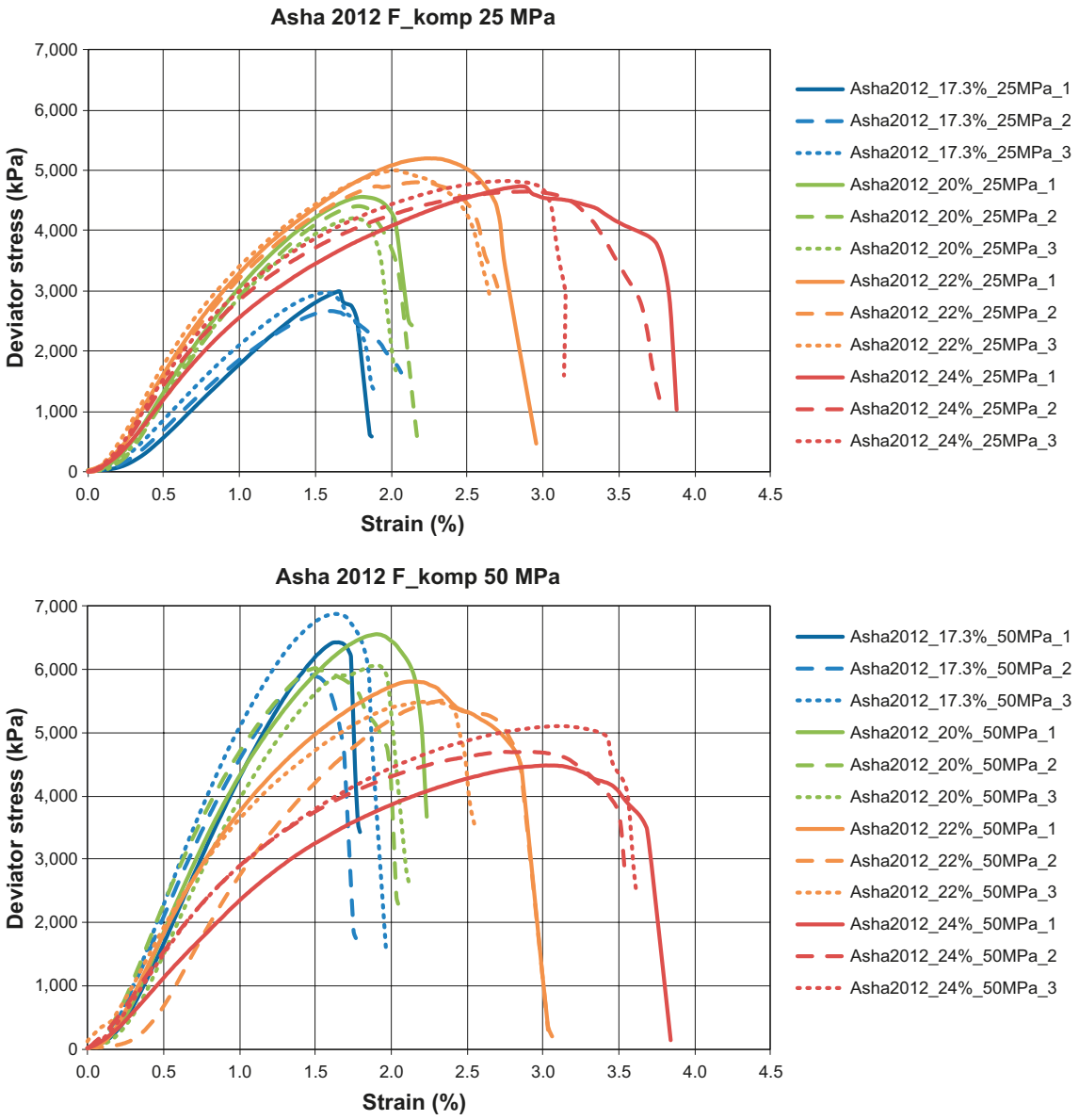

Figure 6-9. *The deviator stress plotted versus strain for the unconfined compression tests made on Asha 2012 material.* ***Upper:*** *Samples compacted with 25 MPa.* ***Lower:*** *Samples compacted with 50 MPa.*

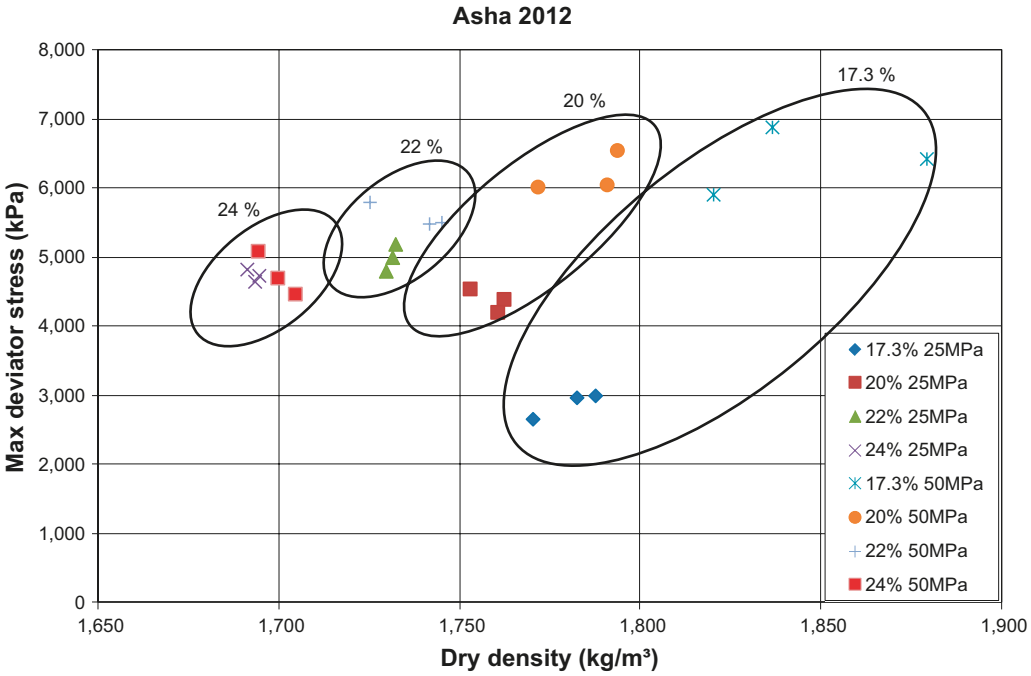

Figure 6-10. *The deviator stress at failure as function of the dry density for the unconfined compression tests made on Asha 2012 material.*

Table 6-6. Compilation of data from the unconfined one dimensional compression tests.

Test No	Test ID	Dry density kg/m³	Water content %	Max deviator stress kPa	Strain at failure %	E-modulus MPa
1	Asha2012_17.3%_25MPa_1	1,787	17.3	3,003	1.65	241
2	Asha2012_17.3%_25MPa_2	1,770	17.5	2,664	1.60	223
3	Asha2012_17.3%_25MPa_3	1,782	17.4	2,975	1.56	249
4	Asha2012_20%_25MPa_1	1,753	20.0	4,551	1.81	391
5	Asha2012_20%_25MPa_2	1,762	19.6	4,400	1.78	382
6	Asha2012_20%_25MPa_3	1,760	19.7	4,212	1.76	379
7	Asha2012_22%_25MPa_1	1,732	21.9	5,197	2.26	409
8	Asha2012_22%_25MPa_2	1,730	22.2	4,807	2.18	399
9	Asha2012_22%_25MPa_3	1,731	21.8	5,005	2.04	433
10	Asha2012_24%_25MPa_1	1,694	23.2	4,741	2.85	303
11	Asha2012_24%_25MPa_2	1,693	23.4	4,654	2.88	349
12	Asha2012_24%_25MPa_3	1,691	23.7	4,832	2.78	376
13	Asha2012_17.3%_50MPa_1	1,879	14.2	6,433	1.66	522
14	Asha2012_17.3%_50MPa_2	1,820	17.5	5,916	1.46	553
15	Asha2012_17.3%_50MPa_3	1,836	17.0	6,891	1.63	645
16	Asha2012_20%_50MPa_1	1,793	19.5	6,557	1.90	565
17	Asha2012_20%_50MPa_2	1,772	19.6	6,027	1.50	605
18	Asha2012_20%_50MPa_3	1,791	19.8	6,059	1.92	528
19	Asha2012_22%_50MPa_1	1,725	21.8	5,805	2.13	488
20	Asha2012_22%_50MPa_2	1,745	21.7	5,512	2.34	439
21	Asha2012_22%_50MPa_3	1,742	21.6	5,492	2.21	453
22	Asha2012_24%_50MPa_1	1,704	23.1	4,477	3.02	251
23	Asha2012_24%_50MPa_2	1,700	23.4	4,709	2.88	330
24	Asha2012_24%_50MPa_3	1,694	23.2	5,098	3.08	346

6.5.3 Beam tests

Method

A second type of test was used to determine the tensile strength of specimens of backfill material. The sample preparation was made in two different ways:

1. Small specimens were compacted in the laboratory (Ø 50 mm, h 20 mm). From these samples beams were sawn out (axbxc ~10×20×35 mm^3).
2. Cores were drilled out from backfill blocks manufactured in full scale at Höganäs Bjuf AB. From these cores, beams with the same dimensions as above were sawn out at different levels of the block.

- The beams were forced to failure by applying a constant deformation rate of 0.10 mm/min at the middle of the beam. The load and the displacement were measured continuously; see drawing and photo provided in Figure 6-11.
- The tensile stress (σ_t) and the strain (ε_t) were evaluated with the following equations:

$$\sigma_t = \frac{6Qc}{4ba^2} \tag{6-6}$$

$$\varepsilon_t = \frac{a\omega 6}{c^2} \tag{6-7}$$

where

Q = vertical force

a = sample height

b = sample width

c = the length between the support points

ω = the vertical displacement at the middle of the beam

Test matrix

These tests were completed on materials from the two batches from Asha. The tests can be divided into three main series:

1. **Asha 2010 as-delivered.** Specimens were compacted in the laboratory to different densities. From these samples, beams were sawn out. In total, 13 samples were tested.
2. **Asha 2010 crushed.** About 20 tons of this material was crushed in order to improve the block quality (Sandén and Andersson 2012). Cores were drilled from the blocks manufactured with this material, and from these cores, beams were sawn out and used for the tests. In total, 31 samples were tested.
3. **Asha 2012 as delivered.** Samples were compacted in the laboratory and beams were sawn out from these samples. In total, 37 samples were tested. The samples were manufactured with different water content and compaction pressure.

Results

A selection of representative results from the tensile strength measurements is shown in Figure 6-12 and the rest of the results are provided in Appendix 16. The influence of the initial water content is obvious when comparing the driest samples, 17% water content, and the wettest, 24% water content. A compilation of all results from the tests is provided in Tables 6-7 to 6-9. In Figure 6-13, the maximum tensile strength evaluated from the different tests is plotted as a function of the dry density. Even though there is scatter in the results, it is clearly shown in the figure that the strength increases with increasing density but also with increasing water content of the samples.

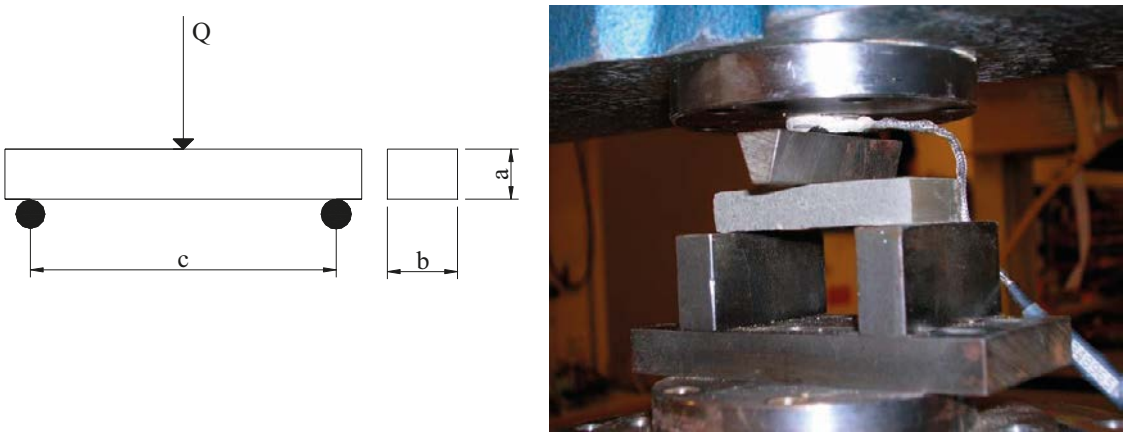

Figure 6-11. *Test arrangement for determination of the tensile strength.*

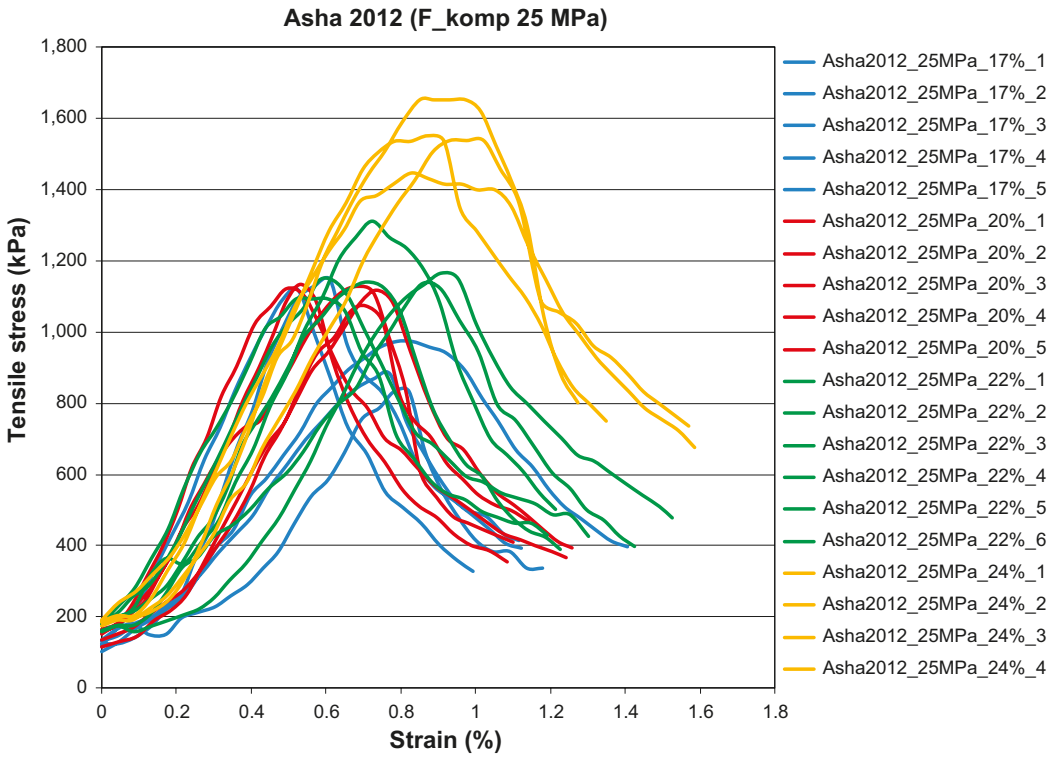

Figure 6-12. *Example of results from the beam tests performed with material from the batch Asha 2012. The samples shown in the figure were compacted in laboratory with a pressure of 25 MPa and with different water contents.*

There are obvious differences in block strength between materials from the two batches. The tensile strength of blocks compacted with the as-delivered Asha 2010 is below 400 kPa for dry densities between 1,700 to 1,750 kg/m^3 (w=15–16%) which should be compared to the as-delivered Asha 2012 (w=17%) where all measurements show a strength higher than 800 kPa. It should be noted that after crushing the Asha 2010 material to a more suitable granule size distribution (green circles and blue diamonds) and increasing the water content somewhat, the strength increased markedly. The behavior indicates that there might be some cementation in the material. A possible explanation is that the crushing breaks up cemented granules which might affect the behavior of the material regarding e.g. water suction. The quality of blocks manufactured with crushed material was improved e.g. the edges were more stable and it was easier to saw out the beams used in the strength tests.

Table 6-7. Compilation of the tensile strength results from beam tests with the Asha 2010 material as-delivered. The samples were compacted in the laboratory to different densities.

Test ID	Comp. Pressure MPa	Water cont. %	Dry density kg/m³	Strain at failure %	Max Tensile strength kPa
8	n/a	15.5	1,749	0.68	350
9a	n/a	15.2	1,733	0.75	472
9b	n/a	15.5	1,747	0.60	284
10a	n/a	15.6	1,781	0.76	631
10b	n/a	15.3	1,767	0.83	501
11a	n/a	15.1	1,788	0.76	628
11b	n/a	15.9	1,785	0.72	711
12a	n/a	15.0	1,822	0.79	974
12b	n/a	15.8	1,816	0.69	973
13a	n/a	15.2	1,839	0.60	918
13b	n/a	15.2	1,823	0.79	1,026
14a	n/a	14.2	1,865	0.66	1,117
14b	n/a	15.0	1,879	0.66	1,137

Table 6-8. Compilation of the tensile strength results from beam tests with the Asha 2010 material after crushing and compaction to form blocks. The samples tested were sawn from cores taken from the compacted blocks.

Test ID	Comp. Pressure MPa	Water cont. %	Dry density kg/m³	Strain at failure %	Max Tensile strength kPa
13_1A	36	17.8	1,774	0.40	734
13_1B	36	18.3	1,763	0.55	710
13_1C	36	18.6	1,778	0.55	958
13_2A	36	17.6	1,792	0.47	954
13_2B	36	17.0	1,795	0.04	284
13_2C	36	16.8	1,806	0.56	1,274
13_5A	36	18.6	1,780	0.54	1,133
13_5C	36	18.2	1,777	0.62	732
13_5D	36	18.3	1,775	0.51	954
17_1A	38	22.3	1,758	0.84	1,492
17_1B	38	21.8	1,763	0.93	1,702
17_1C	38	21.9	1,766	0.76	1,570
17_1D	38	22.2	1,754	0.77	1,533
17_2A	38	22.9	1,727	0.75	1,428
17_2B	38	22.4	1,747	0.68	1,358
17_2C	38	22.6	1,738	0.54	1,142
17_2D	38	22.5	1,748	0.95	1,611
17_5A	38	22.2	1,749	0.75	1,315
17_5B	38	21.7	1,770	0.69	1,286
17_5C	38	22.0	1,747	0.57	1,462
17_5D	38	23.0	1,730	0.75	1,516
33_1A	27	17.5	1,784	0.51	847
33_1B	27	17.6	1,773	0.62	945
33_1C	27	18.4	1,782	0.57	1,061
33_1D	27	17.0	1,834	0.28	1,238
33_2A	27	16.8	1,791	0.49	981
33_2B	27	17.8	1,778	0.49	915
33_2C	27	18.7	1,761	0.45	684
33_2D	27	18.8	1,774	0.75	1,059
33_5A	27	17.8	1,764	0.48	933
33_5D	27	17.8	1,765	0.52	837

Table 6-9. Compilation of the tensile strength results from beam tests with the Asha 2012 material. The samples were compacted in laboratory with different compaction pressures and different water contents.

Test ID	Comp. Pressure MPa	Water cont. %	Dry density kg/m³	Strain at failure %	Max Tensile strength kPa
Asha2012_25MPa_17%_1	25	17.3	1,726	0.83	972
Asha2012_25MPa_17%_2	25	17.3	1,734	0.77	883
Asha2012_25MPa_17%_3	25	17.3	1,742	0.82	832
Asha2012_25MPa_17%_4	25	17.3	1,739	0.52	1,118
Asha2012_25MPa_17%_5	25	17.3	1,759	0.61	1,145
Asha2012_25MPa_20%_1	25	20.0	1,729	0.73	1,118
Asha2012_25MPa_20%_2	25	20.0	1,717	0.71	1,072
Asha2012_25MPa_20%_3	25	20.0	1,708	0.68	1,129
Asha2012_25MPa_20%_4	25	20.0	1,733	0.49	1,122
Asha2012_25MPa_20%_5	25	20.0	1,731	0.53	1,133
Asha2012_25MPa_22%_1	25	22.0	1,714	0.91	1,166
Asha2012_25MPa_22%_2	25	22.0	1,717	0.61	1,093
Asha2012_25MPa_22%_3	25	22.0	1,713	0.71	1,140
Asha2012_25MPa_22%_4	25	22.0	1,703	0.62	1,143
Asha2012_25MPa_22%_5	25	22.0	1,709	0.72	1,310
Asha2012_25MPa_22%_6	25	22.0	1,699	0.86	1,137
Asha2012_25MPa_24%_1	25	24.0	1,696	0.87	1,551
Asha2012_25MPa_24%_2	25	24.0	1,693	1.02	1,537
Asha2012_25MPa_24%_3	25	24.0	1,689	0.83	1,448
Asha2012_25MPa_24%_4	25	24.0	1,688	0.97	1,650
Asha2012_50MPa_17%_1	50	17.3	1,785	0.66	1,691
Asha2012_50MPa_17%_2	50	17.3	1,788	0.60	1,099
Asha2012_50MPa_17%_3	50	17.3	1,816	0.78	1,619
Asha2012_50MPa_17%_4	50	17.3	1,797	0.62	1,820
Asha2012_50MPa_17%_5	50	17.3	1,811	0.51	1,454
Asha2012_50MPa_20%_1	50	20.0	1,802	0.75	1,509
Asha2012_50MPa_20%_2	50	20.0	1,752	0.65	1,014
Asha2012_50MPa_20%_3	50	20.0	1,772	0.96	1,547
Asha2012_50MPa_20%_4	50	20.0	1,759	0.77	1,137
Asha2012_50MPa_22%_1	50	22.0	1,758	0.83	1,622
Asha2012_50MPa_22%_2	50	22.0	1,755	0.99	1,405
Asha2012_50MPa_22%_3	50	22.0	1,749	1.24	1,677
Asha2012_50MPa_22%_4	50	22.0	1,760	0.96	1,955
Asha2012_50MPa_24%_1	50	24.0	1,705	1.26	1,793
Asha2012_50MPa_24%_2	50	24.0	1,706	1.21	1,576
Asha2012_50MPa_24%_3	50	24.0	1,714	1.01	1,777
Asha2012_50MPa_24%_4	50	24.0	1,708	1.31	1,858

At present, based on current information regarding backfill block compaction at full scale, the blocks are likely to be manufactured at a water content of 20%. The compaction tests associated with full-sized blocks have shown that their dry density will be about 1,700 to 1,750 kg/m^3 (the required density is 1,650 to 1,750 kg/m^3). Based on the results of the current tensile tests, the maximum tensile strength of the blocks will be about 1,000 to 1,200 kPa.

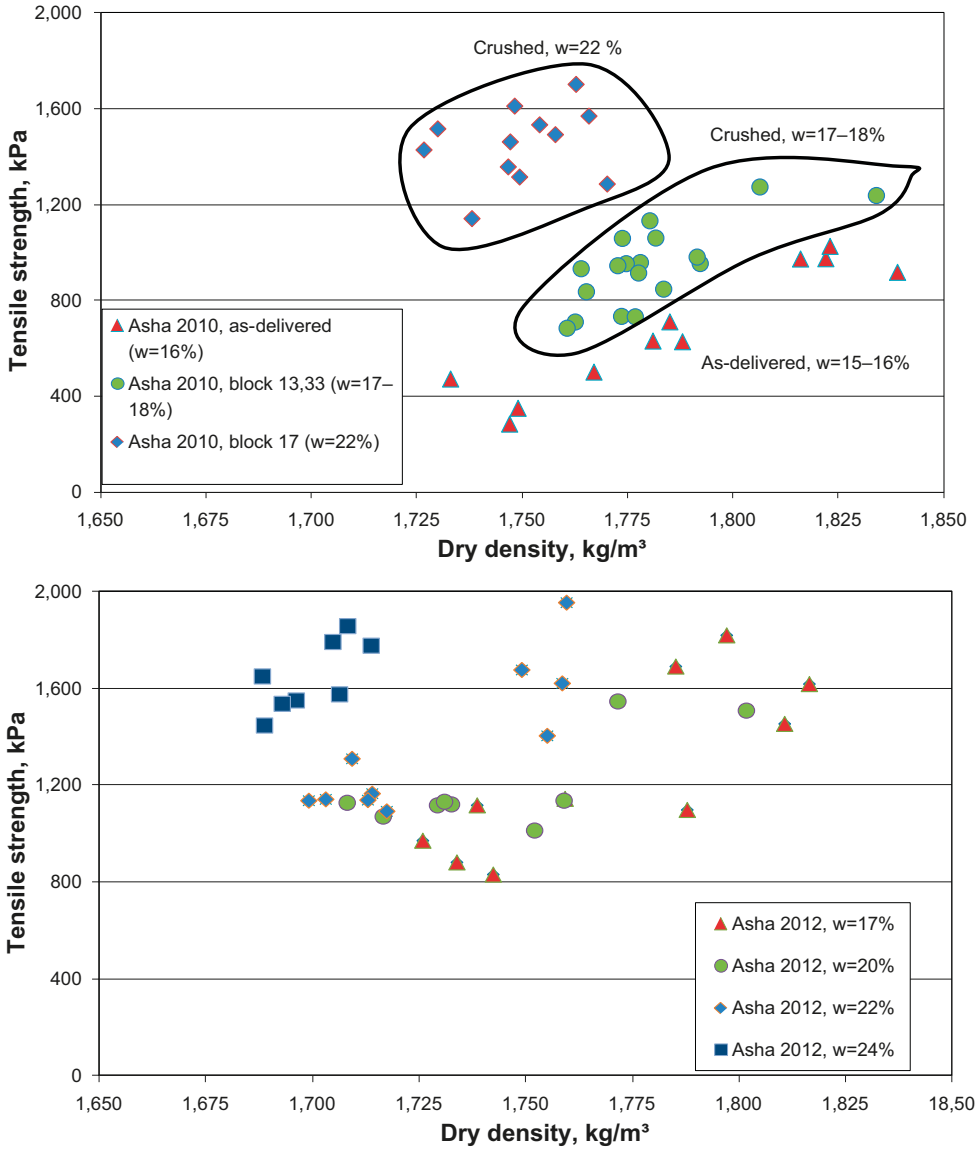

Figure 6-13. *The maximum tensile strength at failure for the beam tests plotted as a function of the dry density of the specimens.* ***Upper****: Samples prepared in the laboratory from the Asha 2010 as-delivered (red the dots) and samples from the same material but instead drilled out from compacted blocks manufactured with crushed material (green and blue dots).* ***Lower****: Samples prepared in the laboratory with Asha 2012 material with different water contents.*

6.6 Relative humidity induced swelling

6.6.1 General

The backfill blocks can absorb water from the atmosphere after emplacement (depending on local humidity conditions). This may cause swelling and cracking of the blocks. The swelling and cracking of the blocks may affect the ability of the installation equipment to lift and stack blocks in a stable manner and thereby influence the possibilities to fill the tunnel with the required number of blocks. The issue was previously investigated in the KBS-3H project regarding buffer material (Sandén et al. 2008b) and backfill materials (Johannesson et al. 2010, Sandén et al. 2008a).

6.6.2 Terminology

The water content *w* used is defined as mass of water per mass of dry substance in %. The dry mass is obtained from drying the wet specimen at 105°C for 24h, see Section 4.3. The relative humidity *RH* is the ratio between the partial vapor pressure and the vapor pressure at saturation in %.

6.6.3 Method

General

Specimens of Asha 2010 were compacted from crushed material. After compaction the specimens were put in jars and exposed to the climate generated inside the jars. The water uptake and swelling (volume expansion) were measured continuously and the cracking of the surfaces studied. Different climates were chosen for the specimens, which all had the same initial water content and dry density. Four identical specimens were made for each climate;

- two specimens was used to determine the water absorption rate (prefix A-),
- two specimens was used for studying the swelling/volume expansion (prefix V-).

In addition one reference specimen was used for measurement of the initially obtained distribution of density and water content.

The specimens were compacted in a mould with diameter d = 50 mm to a height of about 40 mm. Each specimen was subsequently sawn to the desired height, h = 30 mm. At the end of testing each specimen was divided into three disks: closest to the water surface, middle and top (furthest from water). One half of each disk was used to determine the water content and the other half to determine the density. The density was calculated from a volume determined by weighing the specimens above and submerged into paraffin oil.

Test equipment

Determination of the water absorption rate. The prepared specimens were suspended in a special vessel (jar made of acrylic plastic with an air-tight lid) and shown to the left in Figure 6-14. The specimen was covered with a rubber membrane and two O-rings to prevent the specimen from slipping. The bottom of the vessel was filled with de-ionized water or a saturated salt solution. Only the base of each specimen was exposed to the air above the surface of the solution. The specimen was attached to a vertical rod, which passed through the lid. This design made it possible to weigh the specimen without taking it out of the jar. In order to seal off the hole when no weighing was being performed a sealing washer was mounted. The distance between the exposed bentonite surface and the water surface was held constant during the test period. The specimens were weighed at selected intervals and after each weighing the amount of absorbed water could be calculated and hence the water absorption rate determined.

Swelling/volume expansion. The specimens were placed in a cage on a fine net over the chosen solution (de-ionized water or saturated salt solution) in the same type of vessel made of acrylic plastic as described above. The set-up is shown to the right in Figure 6-14. The specimens were weighed and taken out and measured with a slide caliper at preselected intervals. The surfaces were observed for evidence of cracking.

The height of each specimen was measured from the bottom of the specimen holder to the top of the specimen on the opposite sides of the specimen. The results are displayed as the average of each measurement pair. The diameter was measured a few millimeters from the top of the specimen.

6.6.4 Test matrix

The specimens in the two series were carried out at two different *RH* values. High relative humidity, approximately 100%, was achieved using de-ionized water in the jars. A lower relative humidity of 75.5% was achieved using a saturated salt solution of NaCl in the jar (Greenspan 1977). The specimens were placed at laboratory room climate, 22°C ± 1°C. The specimens were placed 45 mm above the solution in the jars.

For all specimens Asha 2010 material (crushed) was compacted with a uniaxial compaction pressure of 36 MPa. The initial water content for all specimens was 20% and the dry density was 1,700 kg/m^3.

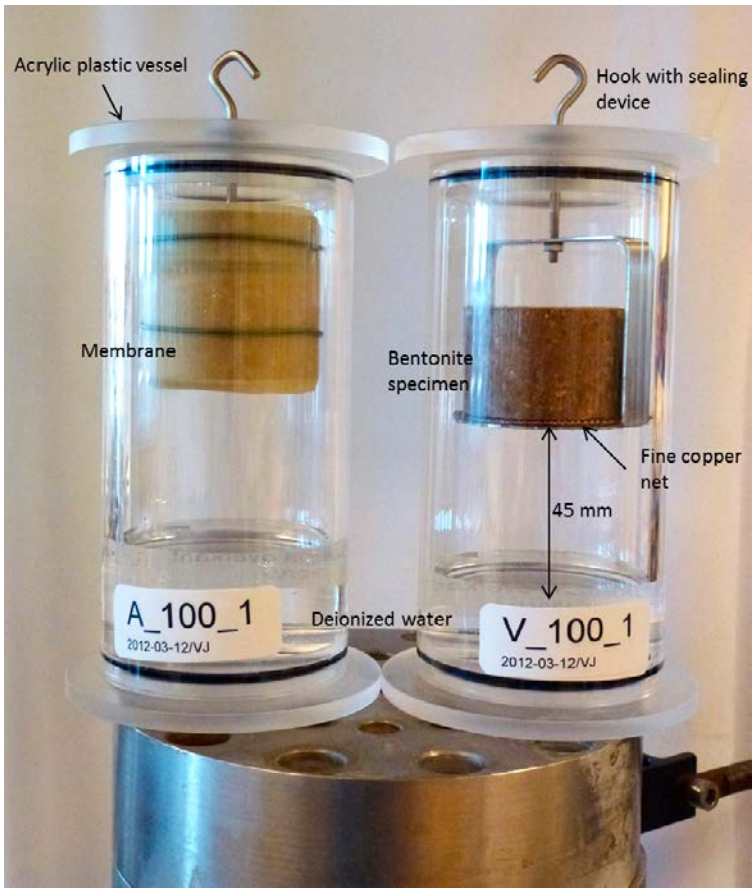

Figure 6-14. *Equipment used for measuring water absorption rate and swelling.*

6.6.5 Results

General

The tests operated for about 90 days and the samples were not assumed to have reached steady state or equilibrium.

Water absorption

Figure 6-15 shows the cumulative mass of water absorbed for the specimens that were weighed. In the diagrams the initial weight at time zero corresponds to the specimens' weight directly after compaction and before they were placed in the vessels and water was added. The total increases in mass were also calculated from the initial and final mass of the specimens. Good agreement was seen and the difference was less than 1.0 g for the four specimens shown in Figure 6-15.

The absorption rate for the specimens is shown in Figure 6-16 and Figure 6-17 where the calculations were based on tangential changes between two measurements and accumulated change from the start, respectively. The cross section area was assumed to remain constant during the test.

The measured initial and final water contents of all specimens are shown in Figure 6-18, not only from the specimens with prefix A-.

Swelling/volume expansion

The changes in height and diameter during the test period are shown in Figures 6-19 and 6-20. The height and diameter at time zero correspond to measurements of the specimens before water was added to the vessel.

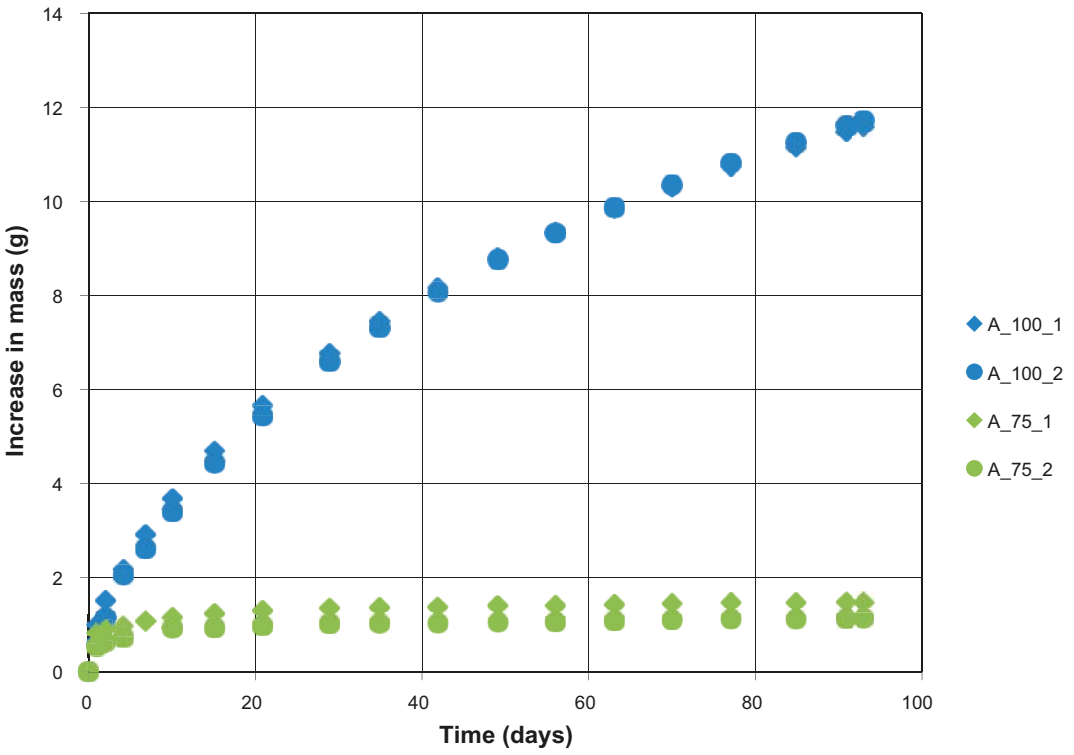

Figure 6-15. *Water absorption from series A.*

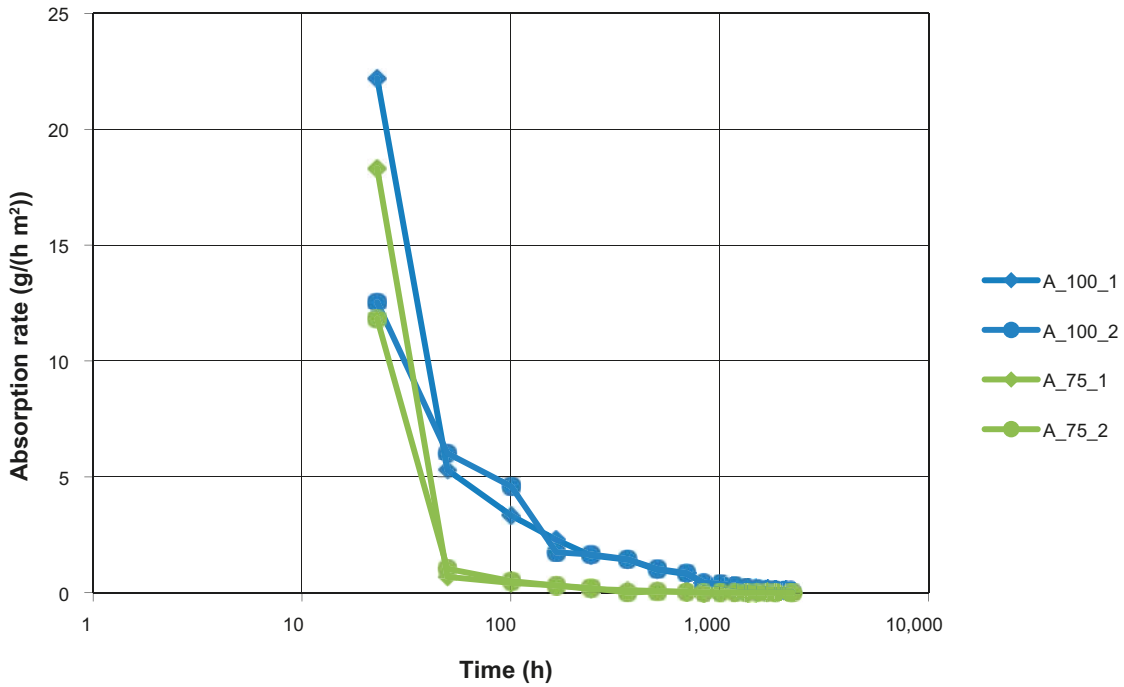

Figure 6-16. *Water absorption rate plotted versus time. The evaluation was based on tangential changes between measurements.*

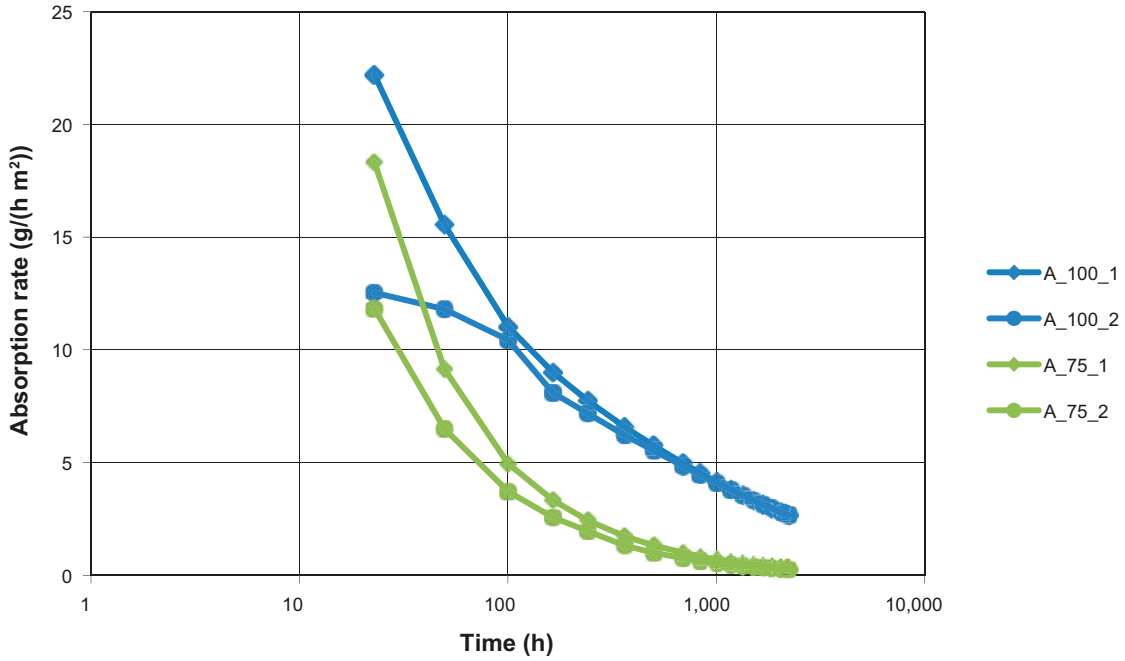

Figure 6-17. *Water absorption rate plotted versus time. The evaluation was based on accumulated change from the start.*

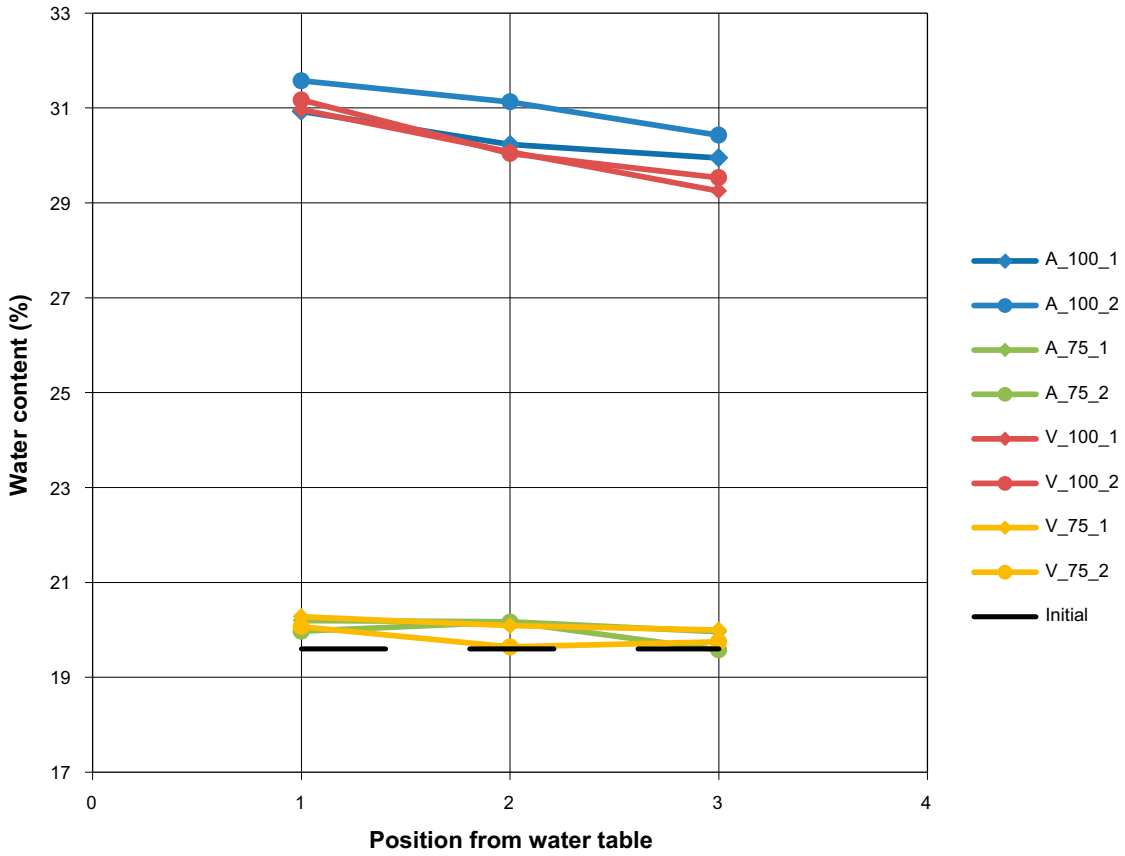

Figure 6-18. *Initial and final water contents. The values are plotted versus position from the water table where the numbers 1, 2 and 3 mean near the water table, in the middle and on top, respectively.*

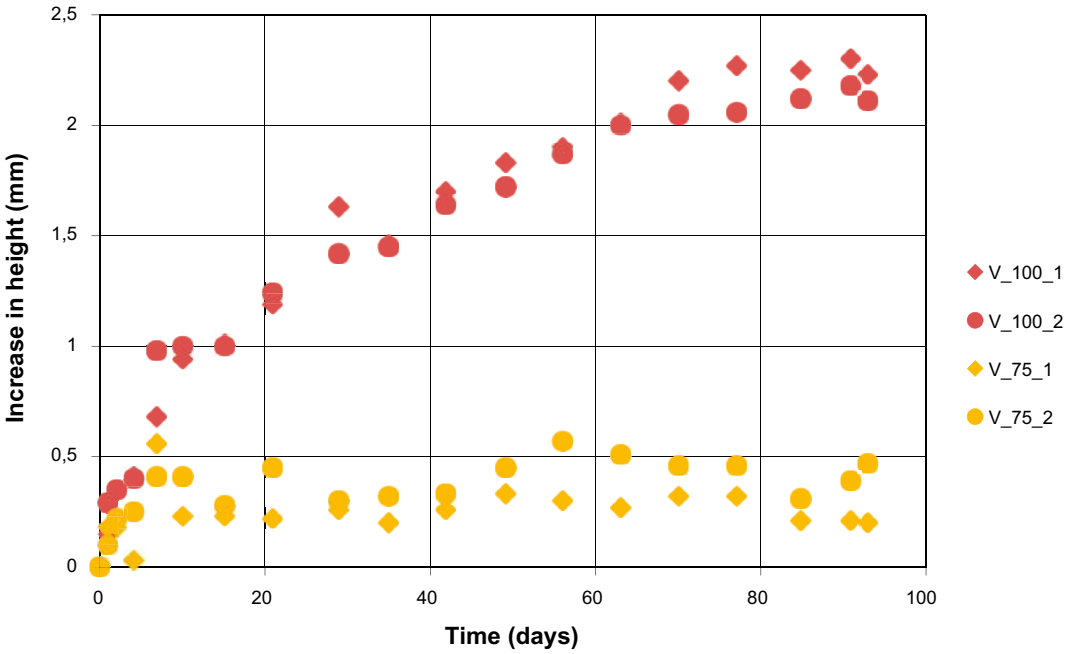

Figure 6-19. *Change in specimen height as result of water absorption. (The diagram shows the average of the measurements taken at each time.)*

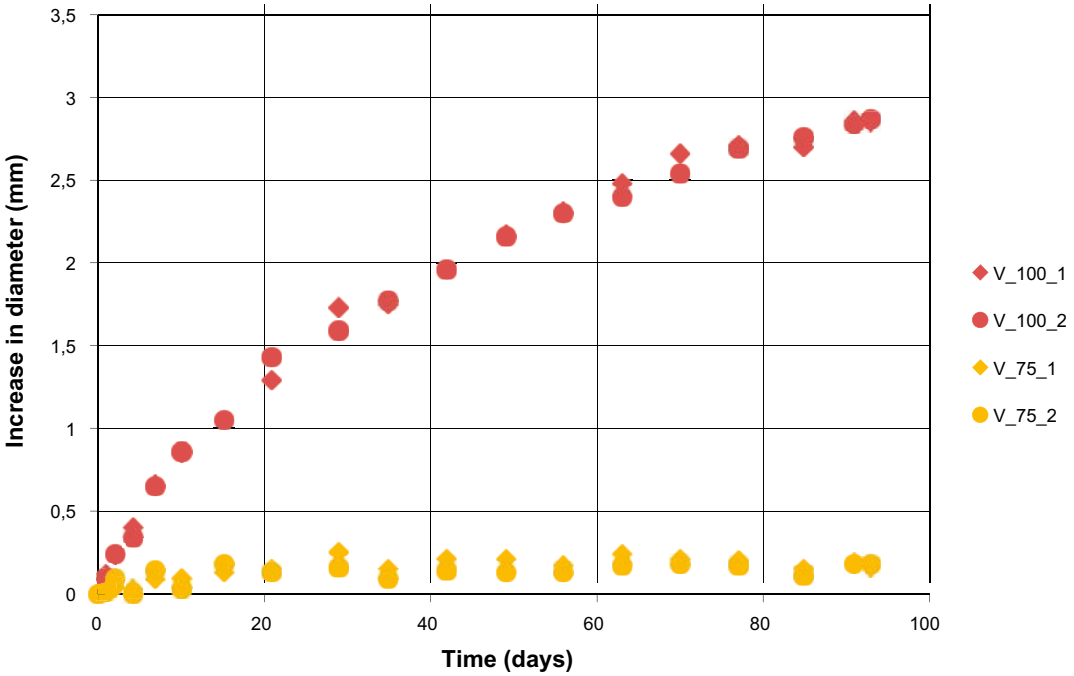

Figure 6-20. *Change in specimen diameter as result of water absorption.*

The final height and diameter were measured and could also be calculated from the initial values and added to the changes shown in Figure 6-19 and 6-20. The differences between the calculated and measured values were less than 0.3 mm and 0.2 mm for the height and diameter, respectively. Figure 6-21 shows the dry densities before and at the end of the tests for all specimens, not only from the specimens with prefix V-.

Cracking

Cracking of the specimens was observed mainly on one specimen V_100_1, Figure 6-22. The cracking was first visible after 49 days. On the duplicate, cracking was observed after 70 days.

6.6.6 Comments and conclusions

The following observations were made:

Absorption

- No large difference in absorption was seen between the two specimens of the same type.
- The absorption rate of the specimens placed at high relative humidity was higher than of the specimens placed at the lower relative humidity where almost no water was absorbed.
- After 93 days the water content gradient in the specimens placed at high relative humidity was less than 2% along the initially 3 cm high specimens.

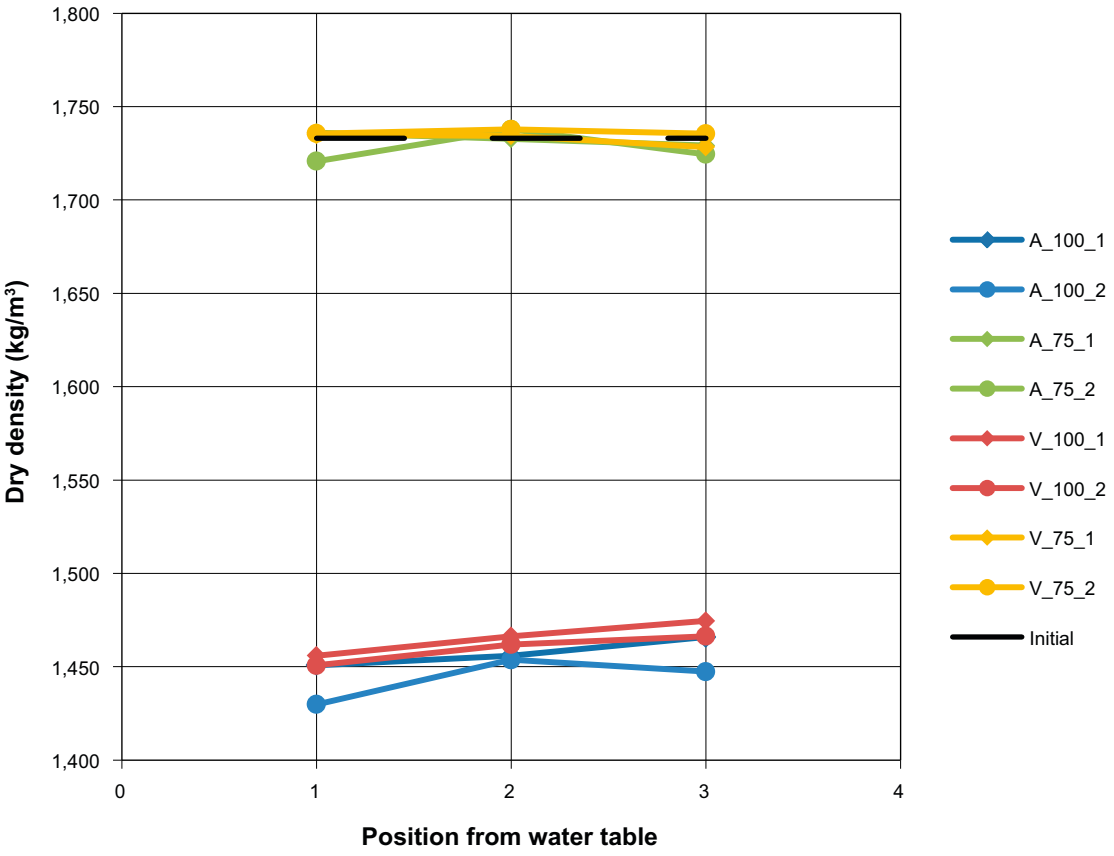

Figure 6-21. *Initial dry densities compared with the corresponding dry densities at the end of the tests.*

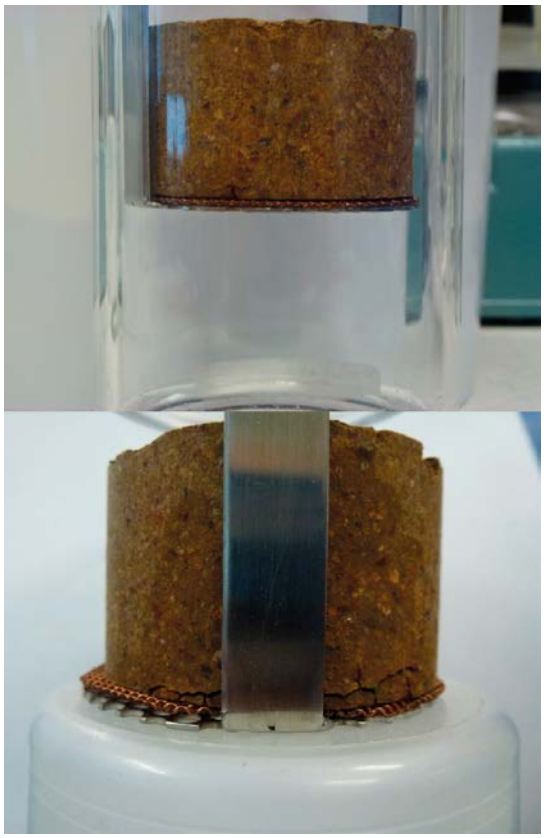

Figure 6-22. *Cracking of specimen V_100_1 after 49 (upper) and 90 (lower) days, respectively.*

Swelling

- No large difference in swelling was seen between the two specimens of the same type.
- The swelling of the specimens placed at high relative humidity was larger than of the specimens placed at the lower relative humidity.
- After 93 days the dry density gradient in the specimens placed at high relative humidity was less than 25 kg/m^3 along the initially 3 cm high specimens.
- After 93 days the dry densities of specimens placed at lower relative humidity was almost the same as their as-placed condition.

Cracking

- No cracking was observed on specimens with only the bottom surface exposed to the climate.
- Cracking was observed on both specimens with all surfaces exposed to high relative humidity.

The results from the tests showed that compacted blocks of Asha with a water content of 20% seemed to be in equilibrium with its surroundings when the relative humidity was 75%, i.e. the water absorption was small, there was almost no swelling and there were no indications of cracking during the 93 days of testing.

Similar tests, but with another material, were performed by Sandén et al. (2008a). In the present study, however, both absorption and swelling was somewhat smaller than observed in the previous study. In a study presented by Sandén et al. (2008b) a scale effect was observed, larger block was seen to be more prone to cracking than smaller specimens. Since cracking was observed on small specimens in the present study (at a relative humidity of 100% and after 49 days) it is recommended that investigations are made on larger blocks in addition.

6.7 Relative humidity induced swelling, tests performed with full scale blocks

6.7.1 General

Backfill blocks will be exposed to different relative humidities during the installation time. The relative humidity is expected to vary from very low, in vented tunnels, to very high in tunnels with water inflow and stagnant air. It is of great importance that the blocks can be lifted (vacuum tool) and handled by the robot during the installation. In order to check the influence of relative humidity on the block stability, tests have been made at full scale using blocks of predetermined quality regarding water content and density.

6.7.2 Method and test matrix

The backfill blocks used in the test were manufactured at Höganäs Bjuf AB of material from the Asha 2012 batch. Each block had a mass of about 228 kg and the dimensions were 500×570×400 mm. The dry density of the blocks was between 1,700 to 1,750 kg/m^3 and the water content about 20%. After manufacturing, the blocks were stored, wrapped in plastic, for about four months. It was not possible to visually see any differences on the block before and after the storage.

In the test, three blocks were placed in three different climate rooms with controlled relative humidities at the Technical University of Lund. The target relative humidities were 55, 75 and 95%, respectively, but the registered relative humidities in the chambers during testing were closer to 60, 72 and 94% (Figure 6-24). In addition, one block was placed in a room without climate control, where the relative humidity was very low, 18%, at the beginning of the test. The original plan was to test two blocks at each relative humidity, but this was not possible due to limited access to and space in the climate rooms. For the same reason the duration of the test was relatively short.

Each block was weighed and measured before test start. During the test period the blocks were taken out of the climate-controlled room at regular intervals in order to check how the climate had affected the weight and dimensions, and also to peform lift tests using a vacuum tool of the same type as the robot will use (Figure 6-23). The blocks were also visually inspected, especially regarding formation of cracks.

6.7.3 Results

Climate chamber

The relative humidity and temperature in the climate rooms were monitored by use of small battery-powered loggers (Tinytag). The loggers were placed on the block surface in order to check that micro climates did not develop. When the bentonite equilibrates against ambient relative humidity, moisture is either absorbed or desorbed and if the transport of moisture in the air is limited, a micro climate may develope close to the bentonite surface. RH in the room environment (18%) was registered with a Vaisala RH sensor placed a few meters from the block. The registered relative humidity and temperature from the four tests is provided in Figure 6-24. The dips in the RH curves depend on the control procedure when blocks were taken out from the rooms for weighing, control of dimensions and test of the vacuum tool.

For simplicity, the intended relative humidity in each of the climate rooms has been used in the following descriptions of the different tests.

Detailed test data can be found in Sicada, Field Note nr: Äspö 3060. Sicada is SKB's internal databse system for storing of experimental data.

Figure 6-23. *Photo showing a block taken out from a climate chamber for control. A vacuum lifting device is used to lift the block from the pallet to the balance.*

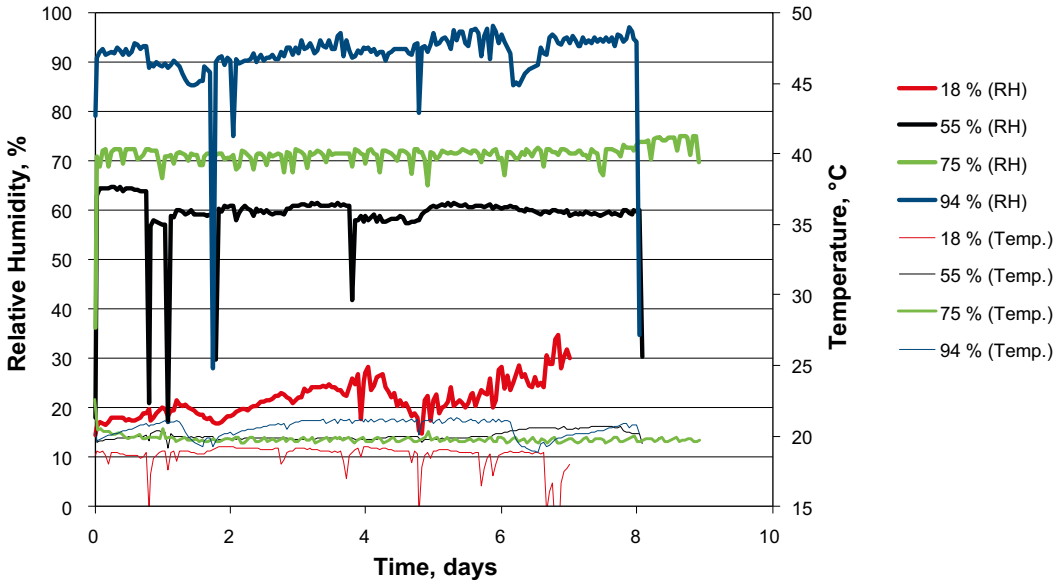

Figure 6-24. *Registered relative humidity and temperature plotted versus time for the four tests.*

Block stability

General

Previous determinations of retention curves have shown that Asha bentonite (another batch: Asha 230, 2008) with a water content of 20% is in equilibrium with a relative humidity of about 75% (Johannesson et al. 2008, p 38). Accordingly, the backfill blocks can be expected to be very stable at this relative humidity (see also the results from the relative humidity induced swelling in Section 6.6). At lower humidity the blocks will dry out and at higher humidity they will take up water from the air.

18% relative humidity environment (room climate)

A few small cracks could be observed on the block surfaces already after 16 hours. The number of cracks increased the following days and after seven days there was a very distinct pattern of cracks all over the block (Figure 6-25). The lifting tests with the vacuum tool showed, however, that it was possible to lift the block also after four days, but after one week there was too much leakage through the cracks and it was no longer possible to lift the block with the tool.

During the test time there was a loss of weight of about 2.5 kg, corresponding to 1.1% of the block weight (Figure 6-29 and 6-30). The changes in dimensions were, however, rather small (Figure 6-31 and 6-32). The block dimensions (height, width and length) had decreased by about one mm in all directions after one week.

Figure 6-25. *Photos of the block placed in 18% RH taken at different times (24 h, 42 h, 64 h and 7 days) after test start.*

55% relative humidity environment

As with the blocks exposed to 18% relative humidity environment, the 55% relative humidity blocks developed some small cracks that could be observed within 24 hours. The number of cracks was, however, evidently smaller than for the block placed in RH 18% . The number of cracks continued to increase the following days and after seven days there was a very evident pattern of cracks all over the block (Figure 6-26). It was possible to lift the block with the vacuum tool without any problem during the whole test duration, i.e. eight days.

The weight loss during the course of testing was about 1.2 kg, corresponding to 0.55% of the block weight (Figure 6-29 and 6-30), and the block dimensions had decreased with between 0.5 to 0.8 mm after eight days (Figure 6-31 and 6-32).

75% relative humidity environment

A first small crack was observed in the blocks exposed to 75% relative humidity after 45 h. The number of cracks increased the following days, but after nine days the number of cracks was still limited and the block looked rather unaffected by the environment (Figure 6-27). No lifting tests were performed with this block since the tool was not available, but judged by the visual characteristics of the block there should be no problem to lift it with the vacuum tool also after nine days.

The weight loss was about 0.5 kg, corresponding to 0.2% of the block weight (Figure 6-29 and 6-30), and the block dimensions had decreased with a few tenths of a millimeter after nine days (Figure 6-31 and 6-32).

Figure 6-26. *Photos of the block placed in 55% taken at different times (24 h, 48 h, 90 h and 8 days) after test start.*

Figure 6-27. *Photos of the block placed in 75% taken at different times (24 h, 45 h, 5 days and 9 days) after test start. (There is a small damage on the bottom-left side of the block due to the block handling before test).*

94% relative humidity environment

In contrast to the other three blocks tested, the block absorbed water from the air when exposed to 94% relative humidity. The block looked unaffected after two days, but then a ring-shaped crack started to develop on the top surface, and later, new cracks of the same shape started to develop on the sides of the block. After ninety hours test it was no longer possible to lift the block with the vacuum tool.

The block increased in mass by about 1.6 kg during the test, corresponding to 0.7% of the total mass (Figure 6-29 and 6-30). The block dimensions increased with between 0.5 to 1 mm the first two days, but after that the block swelled rather rapidly and all dimensions had increased with 6 to 7 mm after eight days (Figure 6-31 and 6-32).

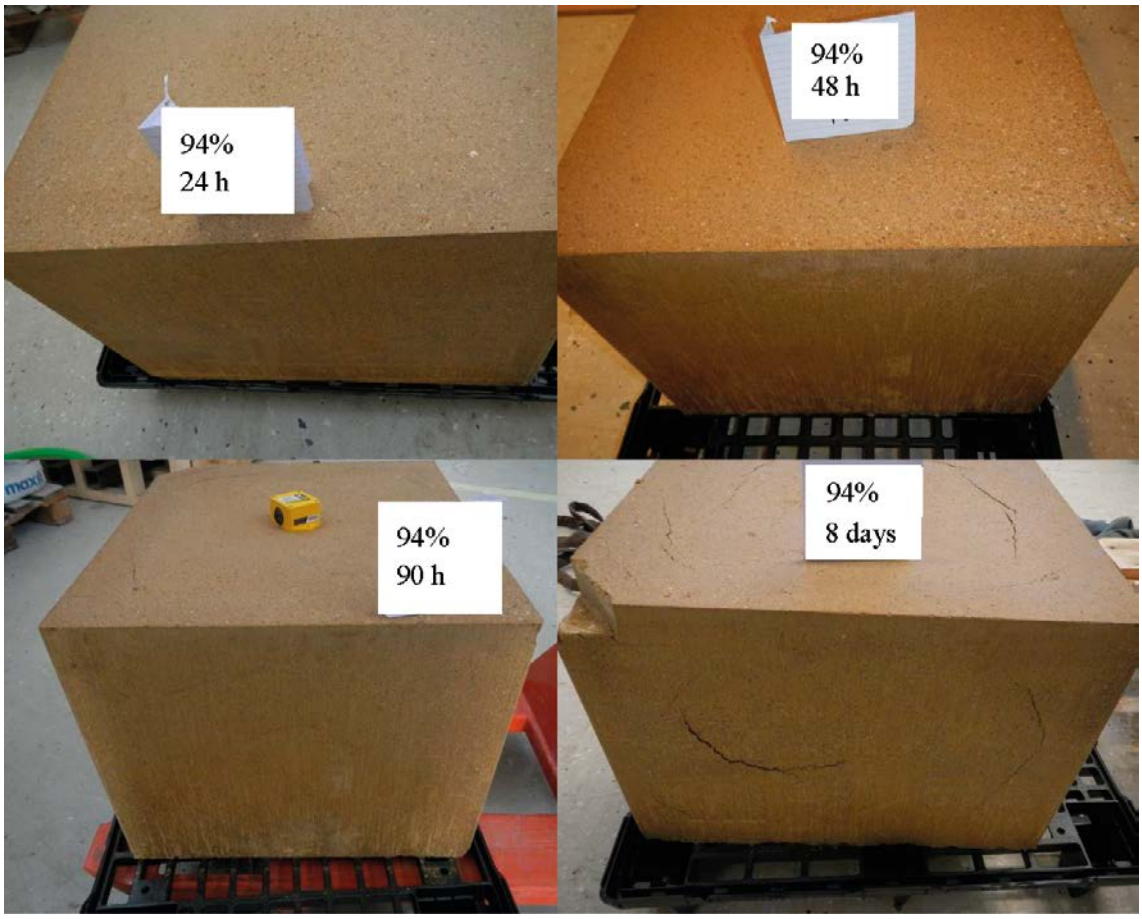

Figure 6-28. *Photos of the block placed in 94% taken at different times (24 h, 48 h, 90 h and 8 days) after test start.*

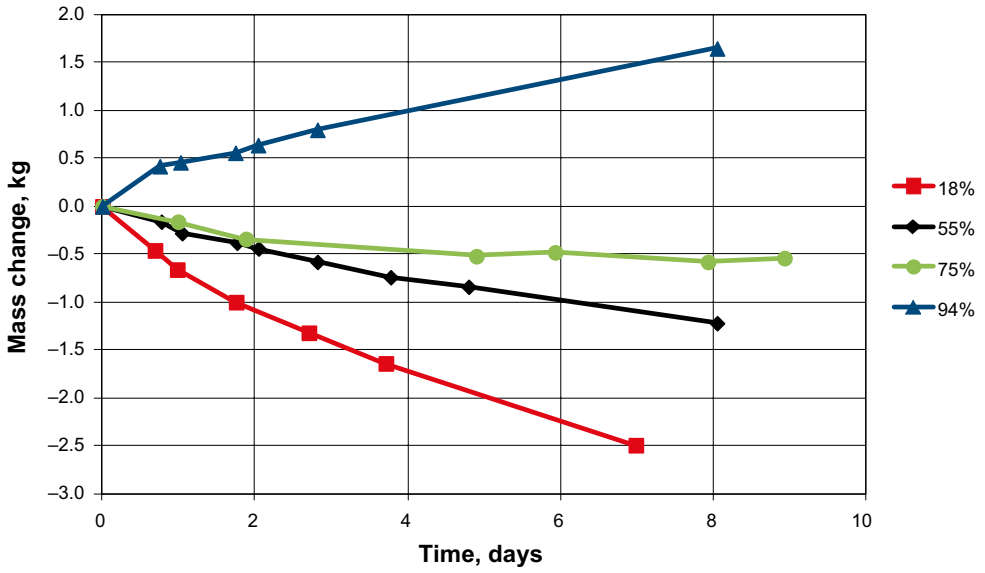

Figure 6-29. *Mass change plotted versus time for the four blocks placed in different climates.*

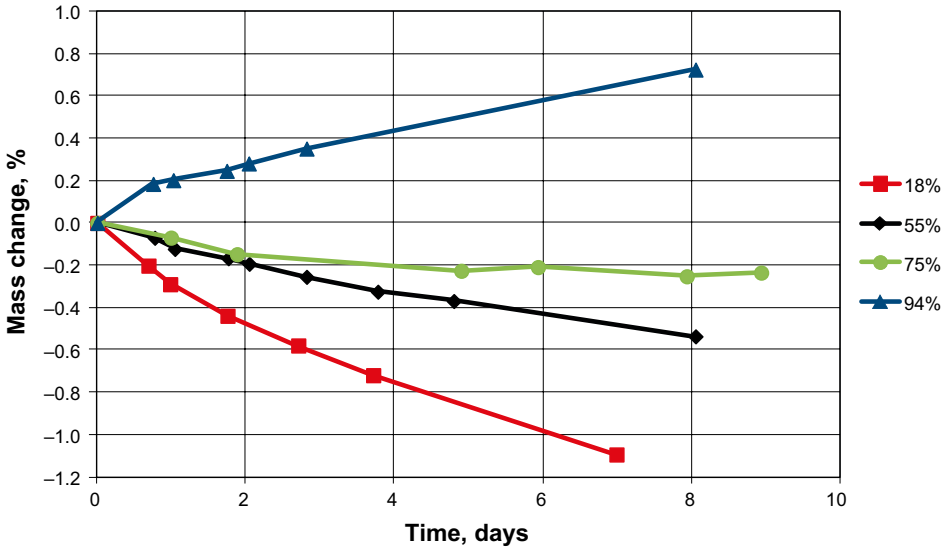

Figure 6-30. Mass change in percent plotted versus time for the four blocks placed in different climates.

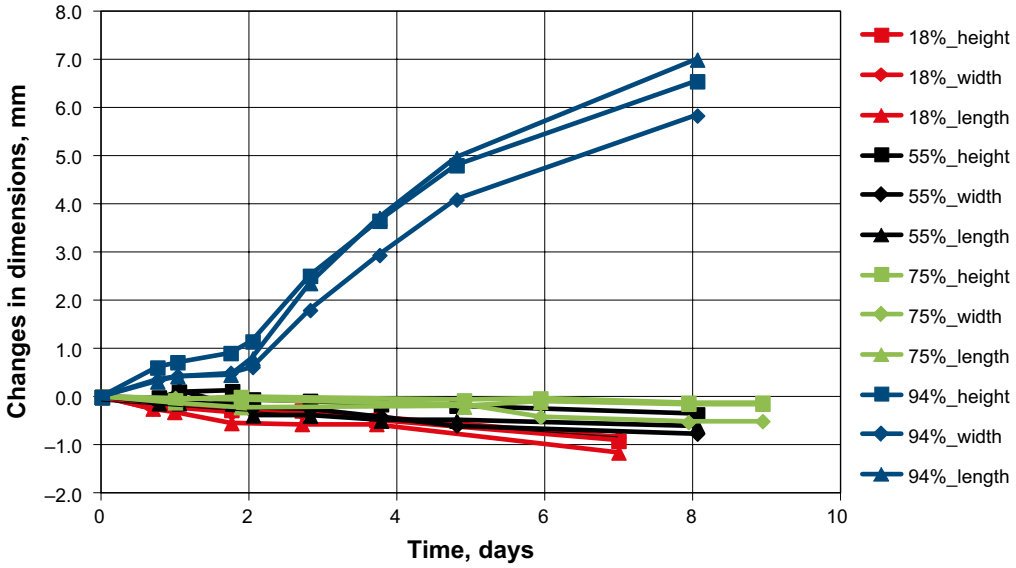

Figure 6-31. Changes in block dimensions plotted versus time for the four blocks placed in different climates.

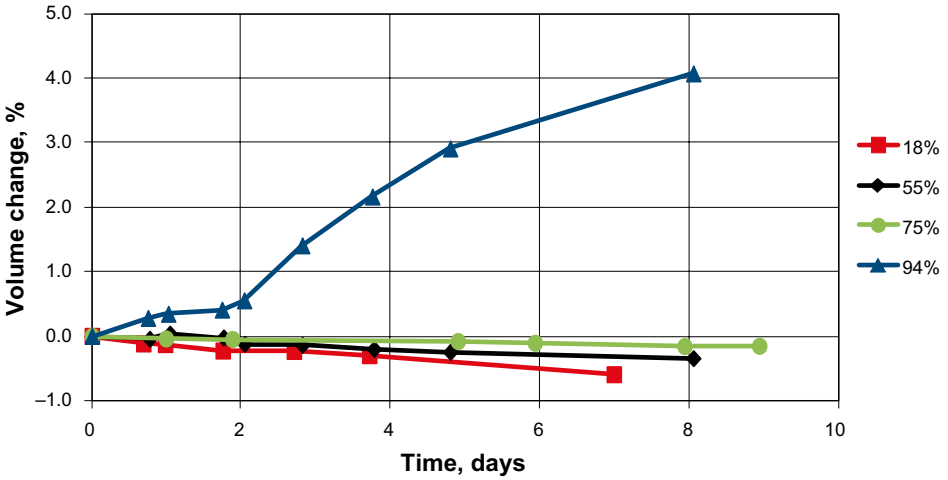

Figure 6-32. *Volume changes plotted versus time for the four blocks placed in different climates.*

6.7.4 Comments and conclusions

Based on the performed test series the following comments can be made:

1. Backfill blocks manufactured to the desired density and moisture conditions will be strongly affected by the environmental conditions around them. The relative humidity in the surrounding air, during storage and installation will be the dominating influence on block stability.
2. When the blocks are exposed to relative humidities below approximately 75% they will loose weight and the dimensions will decrease in all directions.
3. When the blocks are exposed to relative humidities higher than approximately 75% they will increase in weight and the dimensions will increase in all directions.
4. At very dry conditions (RH=18%), the blocks will start to crack on the surface within 24 hours. The first cracks will, however, not influence the ability to handle the blocks with a vacuum lifting tool. After about four days of exposure, however, the cracks will be too many and too deep for handling the block with vacuum tool.
5. At high humidity (RH=94%) the blocks will be almost unaffected for about two days but will then start to crack and swell, and after another day or two it will not be possible to handle the blocks in a secure way.

The tests have shown that the backfill blocks will be strongly affected by the humidity of the surrounding air during exposure. Despite this fact, a main conclusion, can be drawn:

- Backfill blocks of the tested quality will be possible to handle and install in a block pile, independent of the relative humidity (20 to 94%) also after 48 hours of exposure. If the exposure lasts for longer time, the lifting and handling of the blocks will be unsure.

The storing of backfill blocks after manufacturing is of great importance. It is recommended that the blocks are stored either in sealed vessels, in a climate-controlled room or wrapped in plastic. Alternatively, the backfill blocks should, immediately after manufacturing be transported to the tunnel for installation, thereby avoiding stability issues.

7 Summary of results and conclusions

7.1 Acceptance control

The acceptance control of the three bentonite batches examined in this study included the following measurements:

- Water content.
- Swell index.
- Liquid limit (added in the control of Asha 2012).
- CEC (Cation Exchange Capacity).
- Granule size distribution (added in the control of Asha 2012).

7.1.1 Water content

The requirement regarding water content was set to 16±1.5% for the as-delivered bentonite batches. The water content is defined as mass of water per mass of dry substance in %. This definition is used in this report and is common in geotechnical contexts.

The two batches from Asha had water contents that on average were very close to the required specification, although the variation within the batches was large. The batch from Ibeco had higher water content which was subsequently determined to be the result of incorrect understanding of water content definition on the part of the producer. This example shows that it is very important to define the water content unambiguously when ordering bentonite and also not to assume an understanding of technical terminology by the suppliers.

7.1.2 Swell index

The Ibeco bentonite has a lower swelling potential, 4.0 ml/g on average, compared to the two batches from Asha (5.1 ml/g in average for the batch delivered 2010 and 7.3 ml/g in average for the batch delivered in 2012). This difference is also reflected in the liquid limit.

7.1.3 Liquid limit

The liquid limit was used as part of the acceptance control for the Asha 2012 batch. A few determinations of the liquid limit were made, for comparison purposes, on samples taken from the two other batches of bentonite.

The variation in the liquid limit of samples from the Asha 2012 batch was large, ranging from 265% to 120%. The Asha 2012 batch was shipped to Sweden in two rounds (big bag 1 to 300 in the first round, big bag 301 to 500 in the second) and it is clear that the variation in liquid limits increases significantly for the material delivered in the second round. This difference in the results remained when the tests were repeated with a somewhat modified preparation technique.

7.1.4 CEC

The average CEC of the Ibeco 2011 bentonite was 65 meq/100 g. Both batches of Asha bentonite had higher mean CEC-values, 85 and 87 meq/100 g, which are consistent with their higher smectite proportion.

The scatter in the CEC determination was similar for the samples of the Ibeco 2011 and the Asha 2012 bentonite. In contrast, the CEC of the samples of Asha 2010 ranged from 79 to 96 meq/100 g, which was significantly larger than the scatter in the Cu-trien method, as demonstrated by repeatability tests. The scatter is attributable to the heterogeneity of the bentonite in the batch Asha 2010.

7.1.5 Granule size distribution

The granule size distribution is important in the manufacturing of backfill blocks in full scale, because of its effects on the strength and physical stability of the blocks.

The requirements regarding the granule size distribution when ordering the two first batches, Asha 2010 and Ibeco 2011, were not clearly enough defined, resulting in problems with subsequent use in block manufacturing and other testing. The only requirements provided for the bentonite materials delivered were

- Granule size distribution between 0–5 mm.
- Maximum 20% particle size < 0.063 mm.

The batch Ibeco 2011 fulfilled these requirements, but the Asha 2010 batch deviated significantly, having about 20% of granules or aggregates with a size larger than 5 mm. These granules were hard and the full-scale blocks produced using this bentonite tended to have very brittle edges.

Compaction tests with crushed Asha 2010 bentonite gave good results, and the order for the Asha 2012 batch therefore included a requirement that the granule size should be finer than 3 mm. The acceptance control of the new batch included determinations of the granule size distribution of twenty-five samples from different big bags. The results showed that the granule size distribution was very similar to those of the Asha 2010 batch. A visual inspection indicated that the material had been crushed between two rollers with gap set at 3 mm. This procedure had disintegrated, or reshaped, the large granules but at the same time new, platy granules had formed with a thickness of 3 mm. The newly formed granules seemed, however, somewhat softer, and later compaction tests have shown that the block quality was improved.

These results highlight the need to carefully define the granularity of the bentonite purchased and to ensure that these specifications are met.

7.2 Chemical and mineralogical analyses

7.2.1 Exchangeable cations

All samples of Asha bentonite (N=9 for Asha 2010; N=5 for Asha 2012) were sodium-dominated (~50%), and had calcium as the second most abundant cation. However, the variation between individual samples was significantly larger than the scatter in a repeatability test performed on one of the Asha samples, consistent with the heterogeneous character of the Asha bentonite.

The Ibeco-bentonite (N=4), which contains > 20% Ca/Mg carbonates, was calcium-dominated (45%), and the proportions of sodium and magnesium were almost equal. Potassium was a minor component of the cation pool in all samples, but the proportion was higher in the Ibeco bentonite than in the Asha bentonite. The variation between individual samples was small, consistent with the homogeneous character of the Ibeco bentonite.

7.2.2 Chemical composition of the bentonites

Sulphur and carbon. The total sulphur content was close to or below the detection limit (0.02%) in all samples of Asha 2010 (N=7). The samples of Ibeco 2011 (N=5) had higher total sulphur content, but the maximum value was still low, 0.11% S. The highest total sulphur content (0.19% S) was found among the samples of Asha 2012 (N=5). Gypsum was detected by XRD-analysis in several of these samples, suggesting that the major fraction of sulphur exists as sulphate.

The total carbon content of the samples of Asha 2010 (0.41–0.95% C) was more or less equal to the acid soluble carbon content, suggesting that the predominant source of carbon is a carbonate phase. The maximum acid-soluble carbon content corresponded stoichiometrically to 8% $CaCO_3$.

The samples of Ibeco 2011 had the highest content of acid-soluble carbon (3.04–3.49% C), parallel with high MgO and CaO contents. Hence, also in this bentonite carbonates – in this case Ca/Mg carbonates – were the predominant source of carbon.

The total carbon content of the samples of Asha 2012 (0.54–0.70% C) was systematically somewhat higher than the acid-soluble carbon content, which suggested that organic matter might exist. The acid-insoluble carbon content (i.e. total minus acid-soluble C) was low, 0.24% C at a maximum.

***Major oxides*.** Due to large variations in LOI, comparisons of the major oxide composition were based on ratios of the oxides (SiO_2/Al_2O_3, Al_2O_3/Fe_2O_3 and Al_2O_3/MgO). In contrast to the Ibeco samples, the Asha samples displayed a significant scatter in these ratios, again demonstrating the heterogeneity of these bentonite batches. A repeatability test performed on five subsamples of one of the Asha samples showed that the analytical scatter was small.

7.2.3 X-ray diffraction analysis

The mineralogical composition was determined by X-ray diffraction analysis of randomly oriented powders at two laboratories using different equipment and slightly different sample preparation. Both laboratories used the commercial package SIROQUANT for quantitative evaluation of the mineralogy.

Asha 2010

Consistent with the scatter in the chemical data, the XRD-analysis clearly showed that the content of accessory minerals, mainly kaolin, calcite, quartz and crystalline iron oxides/oxyhydroxides, varied among the samples. Based on a standard Siroquant modelling the average mineralogy of Asha 2010 was:

74% smectite, 10% kaolin, 7% goethite/hematite, 4% calcite, 1.8% magnetite/maghemite and 1.5% quartz. Other crystalline phases detected were all below 1%.

The value of d(060) of the smectite in the Asha bentonite is typical of the dioctahedral smectites, to which montmorillonite belongs, but a distinction between the smectites in the montmorillonite–beidellite series at a species level cannot be made by XRD-examination of random powders alone.

Ibeco 2011

All samples of Ibeco 2011 (N=5) contain high amounts of dolomite, which together with calcite makes up more than 20% of the samples. Other major accessory minerals are plagioclase and quartz. No potassium-bearing phase could be detected, and yet the potassium content of the bentonite is fairly high (mean K_2O content 0.73% on LOI-free basis). However, previous, more detailed investigations of backfill bentonite from the same producer (IBECO 2004 and 2008) indicated that the smectite in these batches was interstratified with up to 10% illitic layers. Interstratified illite/smectite may consequently exist also in the bentonite Ibeco 2011, but the identification by XRD-examination of random powders alone is uncertain. Hence, the reported smectite content might include also an unknown proportion of illite/smectite mixed-layers. The CEC of the Ibeco bentonite suggests, however, that the smectite proportion is sufficiently high to match the requirements specified in SKB (2010). According to the Siroquant modelling the average mineralogy of Ibeco 2011 was:

64% smectite+smectite/illite mixed layers, 18% dolomite, 8% plagioclase, 4% calcite, 2% quartz, 2% kaolin.

Asha 2012

The XRD analyses of Asha 2012 were performed and evaluated at CSIRO, Australia. According to their quantitative evaluation the average mineralogy of Asha 2012 was:

76% smectite, 14% kaolin, 5.6% goethite/hematite, 2.6% calcite, 1.2% quartz. Other crystalline phases detected were all below 1%.

Hence, despite the heterogeneity of the Asha bentonite, the average mineralogy of the two batches was similar, and the smectite content in all laboratory samples conforms to the nominal range stipulated for the reference backfill material.

7.3 Hydro-mechanical tests

The hydro-mechanical tests have included the following determinations:

- Grain density of the bentonite.
- Swelling pressure and hydraulic conductivity.
- Compressibility of the saturated backfill.
- Strength of compacted blocks
  - Unconfined one dimensional compression tests.
  - Beam tests.
- Relative humidity induced swelling.

7.3.1 Grain density

The average grain density for Ibeco 2011 was 2,723 kg/m^3, for Asha 2010 2,917 kg/m^3, and for Asha 2012 2,928 kg/m^3 (N=5 for each batch). These values correspond to previous determinations made on bentonites of the same origin and the density differences between the Ibeco and Asha materials is attributed to the presence of iron minerals in Asha, which results in a higher grain density.

7.3.2 Swelling pressure and hydraulic conductivity

The material requirements prescribe that the swelling pressure should be at least 100 kPa and the hydraulic conductivity should be less than 10^{-10} m/s. Modeling of the homogenization process in a backfilled tunnel has shown that the dry density of the bentonite closest to the rock wall can be as low as 1,370 kg/m^3. The requirements and the modeled lowest density were used as a basis for the assessment of the three bentonite batches.

Asha 2010

The swelling pressure for a density of 1,370 kg/m^3 was about twenty times higher than the requirement, i.e. 2,000 kPa, and the hydraulic conductivity two orders of magnitude lower than the required 10^{-10} m/s. The results are consistent and typical of a bentonite with high smectite content.

Ibeco 2011

The swelling pressure at the lowest modeled density was about four times as high as the requirements, i.e. about 400 kPa (1% salinity, 50/50 Na/Ca). This is, however, about five to ten times lower than the swelling pressure determined in earlier investigations of material delivered with the same trade name in 2004 and 2008. The scatter in the measured hydraulic conductivity for dry densities below 1,370 kg/m^3 was very high. The evaluated hydraulic conductivity varied from $2 \cdot 10^{-11}$ to $1 \cdot 10^{-7}$. The large variation might depend on piping in some of the specimens. The phenomenon has, however, not been observed in earlier studies of this material at these densities and due to the unexpected results some extra tests were made with material from the old batches. The results of these measurements showed large differences between the different batches, regarding both swelling pressure and hydraulic conductivity. The batch delivered 2004 seems to be of the highest quality, but the batch delivered 2008 also fulfills the swelling and hydraulic requirements set for the backfill.

The swelling pressure for Ibeco 2011 (1% salinity, 50/50 Na/Ca) was about one order of magnitude lower than the material delivered in 2008. The hydraulic conductivity was about one order of magnitude higher than for the 2008 batch for the density range 1,350 to 1,600 kg/m^3, but at densities lower than this, the scatter in hydraulic conductivity for the 2011 batch was very high. In six of the tests performed at the density interval 1,135–1,332 kg/m^3, the hydraulic conductivity was between 10^{-7} and 10^{-8} m/s. Although these tests are performed at densities below what is expected after homogenization, they indicate that the Ibeco 2011 batch is of lower quality, regarding the hydraulic conductivity, compared with e.g. the batch delivered in 2004. The gradients used in the tests were small and the smectite content is sufficiently high to match the requirements (45 to 90%; cf. XRD-analysis).

Asha 2012

The swelling pressure for a density of 1,320 kg/m^3 was about six times higher than the requirement and the hydraulic conductivity was about ten times lower than the required 10^{-10} m/s.

7.3.3 Compressibility of the saturated backfill

Two oedometer tests were performed, both with Asha 2010 bentonite, one saturated with water with 1% salinity and the other with 3.5% salinity. The curves showing the compression after applying a new load step plotted versus time have a typical shape for this type of tests made on bentonite clays.

The deformation of the samples were almost proportional to the vertical stress up to 3,200 kPa, which was the maximum stress applied in the tests. The densities achieved at the different load steps were somewhat higher for the sample saturated with water with a salinity of 3.5% compared to the sample saturated with water with a salinity of 1%, which is logical. The evaluated compression modules were almost the same for both samples, 19 MPa and 18 MPa respectively, which means that the salinity of the pore water in the range of interest (< 3.5% TDS) does not discernably affect the compressibility of the material.

7.3.4 Strength of compacted blocks

Unconfined one-dimensional compression tests

Altogether twenty-four tests were performed on the Asha 2012 material. Specimens were compacted with different compaction pressures, 25 and 50 MPa, and with four different water contents (as-delivered, 20%, 22%, and 24%). Each specimen was manufactured in triplicate. The results showed that there was a clear influence of density on the maximum stress at failure and also of the water content of the samples.

The results also showed that the blocks manufactured at full scale using Asha, with water content of 20% and with a dry density of 1,700 to 1,750 kg/m^3, will have rather high strength, maximum deviator stress of about 4,000 kPa, and a calculated E-modulus of about 400 MPa.

Beam tests

Tests were made with samples from both batches from Asha. Samples were compacted in laboratory but also sawed out from blocks manufactured in full scale. The scatter in the determined strength is large, but it is clear that the strength increases with increasing density and also with increasing water content of the samples.

There were obvious differences in block strength between materials from the two batches. For dry densities between 1,700 to 1,750 kg/m^3 the determined strength of compacted blocks of Asha 2010 bentonite as-delivered was below 400 kPa (w=15–16%), which should be compared to the as-delivered Asha 2012 (w=17%) for which all measurements show a strength higher than 800 kPa. After crushing the Asha 2010 material to a more suitable granule size distribution, the strength increased markedly also for this material.

According to the present status of the backfill block compaction at full scale, the blocks will have a water content of 20%. The compaction tests have shown that the dry density will be about 1,700 to 1,750 kg/m^3 (the required density is 1,650 to 1,750 kg/m^3). This should give a maximum tensile strength of about 1,000 to 1,200 kPa.

7.3.5 Relative humidity induced swelling of blocks

Small scale laboratory tests

Compacted specimens of crushed Asha 2010 with 50 mm diameter and 30 mm height were placed in vessels with a relative humidity of either 100% or 75%. The initial water content was 20% and the initial dry density was approximately 1,700 kg/m^3. One test series were performed with the aim of determining water uptake and another with the aim of determining expansion and cracking.

The results from the tests showed that compacted blocks of Asha with a water content of 20% seemed to be well in equilibrium with a relative humidity of 75%, i.e. the water absorption was small, there was almost no swelling and there were no indications of cracks. Similar tests, but with another material, were performed by Sandén et al. (2008a). In the present study, both absorption and swelling was somewhat smaller. In a study presented by Sandén et al. (2008b) a scale effect was observed; larger blocks were seen to be more vulnerable to cracking than smaller specimens. Since cracking was already observed on small specimens in the present study (at a relative humidity of 100% and after 49 days) it was recommended that larger blocks should be tested in addition.

Full scale tests with backfill blocks

The tests showed that the full-sized backfill blocks are very sensitive to the surrounding relative humidity. There seems, however, to be a difference between the tests performed in laboratory scale and the tests performed in full scale. The full scale blocks are more prone to cracking after rather short exposure to the atmosphere. The reason for this is probably that the stresses are smaller in small specimens since expansion is not prevented by interlocking particle effects.

One main conclusion from the full scale tests is that, independent of the relative humidity (18 to 94%), the blocks will be possible to handle and install (lifting with vacuum tool) after 48 hours exposure to this environment. If the exposure lasts longer, the ability to lift and handle the blocks will be uncertain.

The storing of backfill blocks after manufacturing is of great importance in ensuring their physical stability. It is recommended that the blocks are stored either in sealed vessels or wrapped in plastic. Alternatives are e.g. that the blocks are stored in a climate controlled room or that the backfill blocks are transported to the tunnel for installation immediately after manufacturing.

7.4 Conclusions

A number of hydro-mechanical and chemical-mineralogical methods, relevant to quality assessment of bentonite, were used to test the three bentonite batches Ibeco 2011, Asha 2010 and Asha 2012. This testing was done in order to evaluate their conformity to the requirements placed on bentonites for tunnel backfill material and also to assess whether manufactured backfill blocks were of acceptable quality.

The Ibeco 2011 batch was a homogeneous bentonite, which fulfilled the requirements regarding granule size distribution. The swell index, liquid limit and CEC indicated that the amount of smectite was moderate but sufficiently high to match the requirements, 45–90 wt%, placed on a backfill bentonite and this was confirmed by a quantitative evaluation of the mineralogy. The behaviour of the Ibeco 2011 material in the swelling pressure and hydraulic conductivity tests was, however, unexpected and did not conform to the requirements. Due to this fact the material properties determined for Ibeco 2011 were compared with the results for bentonite with the same commercial name delivered in 2004 and 2008 (Table 7-1), and the swelling pressure and hydraulic conductivity of the latter were re-tested. The results indicated that the swelling pressure of Ibeco 2011 was about ten times lower than those of the other batches. The hydraulic conductivity at low densities (< 1,370 kg/m^3) suggested that the bentonite of the batch 2011 sealed poorly against the walls of the sample holder, which resulted in piping.

The chemical and mineralogical investigations of Ibeco 2011 showed that the content of potentially cementitious material, such as carbonates, was high, more than 20%, and this may affect the hydraulic behavior. However, the batch from 2004 had an equally high carbonate content (Table 7-1) but had not shown such behavior in hydraulic conductivity tests performed at even lower densities.

The investigations of the bentonite delivered 2004 and 2008 had also shown that illitic interlayers existed in the smectite. The mineralogical investigation of Ibeco 2011 was less detailed, including only X-ray scans of random powders of bulk samples. Because interstratified illite/smectite cannot be quantified or identified with certainty from XRD-profiles of this type of preparations there is an uncertainty regarding the smectite content. However, based on the potassium content of the

bentonite, the evaluated smectite content, 64%, may include 5–7% illitic interlayers at most. Hence, the difference between the batches in amounts or composition of the smectite seems small and is an unlikely explanation of their very different hydraulic behavior (Table 7-1).

A certain variation can be seen in other material parameters of the different bentonite batches from Ibeco, but at present no firmly confirmed explanation of the unusual hydraulic behavior of Ibeco 2011 can be given.

A material like Ibeco 2011 would not have been approved by the acceptance control in the KBS-3V-repository. However a rejection of a material delivery is undesired and could cause interruptions in the backfill production. SKB continius the work with further characterization of bentonite materials and development of more precise material specifications to avoid materials that doesn't conform to the requirements.

In the as-received state both batches of the Asha bentonite were heterogeneous materials. The requirements regarding granule size distribution were not fulfilled by any of the batches, and the variation between individual samples from the same batch was significant. Backfill blocks produced at full scale using as-received Asha 2010 were in general of unacceptable quality, and this fact stresses the need to carefully define and check the granularity of the bentonite purchased.

Moreover, a parallel investigation of Asha 2010 demonstrated that the coarse aggregations found in the bentonite had higher smectite proportion than the fine-grained matrix of the bentonite and the mineralogy differed with respect to abundance and type of accessory minerals. Accordingly, a risk exists for sampling errors yielding laboratory samples of poor representativeness if granules are segregated by size during handling and/or sampling of the 1,250 kg sacks with bentonite. In order to reduce such errors a sampling plan designed for heterogeneous materials should be applied.

The swell index, liquid limit and CEC indicated that the smectite content of both batches was fairly high, but large variations were also observed in these material parameters, consistent with the heterogeneity of the bentonite. A quantitative evaluation of the mineralogy confirmed that the variation was large but that the average smectite content of the two batches was similar, 74 and 76%. Hence, the smectite content was in the same range as that of the Asha batches delivered in 2004 and 2008 (Table 7-1) and conformed to the nominal range stipulated for the reference backfill material, 50–60 wt% with an accepted variation within 45–90 wt%. In the requirements, the smectite is, however, defined as montmorillonite. Like montmorillonite, the smectite in the Asha batches 2010 and 2012 was dioctahedral, but the performed analyses did not include determination of the charge distribution for distinguishing the members in the montmorillonite–beidellite series at species level.

The swelling pressure of both batches of Asha bentonite was well above the requirement and the hydraulic conductivity one to two orders of magnitude lower than the required, 10^{-10} m/s. The results are consistent and typical of a bentonite with high smectite content.

Table 7-1. Compilation of material parameters determined for different batches from Ibeco and Asha. n.d. = not detected. Data is compiled from Johannesson and Nilsson (2006), Johannesson (2008), Johannesson et al. (2010), Olsson and Karnland (2009) and from the new investigations presented in this report.

Material	Liquid limit %	Free swelling ml	Smectite %	Illite-Smectite (not detectable) %	Carbonate %	CEC meq/100 g	Exchangeable cations			
							Ca %	K %	Mg %	Na %
Ibeco RWC-BF, 2004	150	5	64	5–10	24	73	41	2.7	48	9
Ibeco RWC-BF, 2008	122	4.4	73	< 3 %	< 1 %	71	44	2.2	24	31
Ibeco RWC-BF, 2011	116	4	64	Inclusive possible I-S	22	65	45	1.9	25	29
Asha 230, 2004	180	8.4	78	n.d.	n.d.	97	31	0.4	13	56
Asha 230, 2008	473	13.5	80	n.d.	n.d.	89	9	0.5	11	80
Asha NW BFL-L, 2010	198	5.1	74	n.d.	4	87	28	0.7	17	48
Asha NW BFL-L, 2012	160	7.3	76	n.d.	2.6	85	31	0.5	13	47

According to the present design the backfill blocks will have a density between 1,700–1,750 kg/m^3 and a water content of 20%. Tests performed on full-scale backfill blocks with this density and water content suggested that the strength of such blocks will be sufficiently high. Other tests in which full-scale blocks were exposed to relative humidities between 20 and 94% during about one week showed that the blocks could stand 48 hours of exposure, irrespective of relative humidity, and still be handled and lifted with a vacuum tool. However, if the exposure was longer than 2–4 days, cracking and/or swelling occurred, and the blocks could no longer be lifted with the tool. The results stress that the environmental demands will be high on the storage environment needed for blocks.

References

SKB's (Svensk Kärnbränslehantering AB) publications can be found at www.skb.se/publications.

Ammann L, Bergaya F, Lagaly G, 2005. Determination of the cation exchange capacity of clays with copper complexes revisited. Clay Minerals 40, 441–453.

ASTM D 5890-11. Standard test method for swell index of clay mineral component of geosynthetic clay liners. West Conshohocken, PA: ASTM International.

Belyayeva N I, 1967. Rapid method for the simultaneous determination of the exchange capacityand content of exchangeable cations in solonetzic soils. Soviet Soil Science, 1409–1413.

Brindley G W, Brown G, 1980. Crystal structures of clay minerals and their X-ray identification. London: Mineralogical Society. (Mineralogical Society Monograph 5).

Dohrmann R, Genske D, Karnland O, Kaufhold S, Kiviranta L, Olsson S, Plötze M, Sandén T, Sellin P, Svensson D, Valter M, 2012a. Interlaboratory CEC and exchangeable cation study of bentonite buffer materials: II. Alternative methods. Clays and Clay Minerals 60, 176–185.

Dohrmann R, Genske D, Karnland O, Kaufhold S, Kiviranta L, Olsson S, Plötze M, Sandén T, Sellin P, Svensson D, Valter M, 2012b. Interlaboratory CEC and exchangeable cation study of bentonite buffer materials: I. Cu(II)-triethylenetetramine method. Clays and Clay Minerals 60, 162–175.

Greenspan L, 1977. Humidity fixed points of binary saturated aqueous solutions. Journal of Research of the National Bureau of Standards A. Physics and Chemistry 81A, 89–96.

Jackson M L, 1975. Soil chemical analysis: advanced course. 2nd ed. Madison,WI: Parallel Press.

Johannesson L-E, 2008. Backfill and closure of the deep repository, Phase 3 – pilot tests to verify engineering feasibility. Geotechnical investigations made on unsaturated backfill materials. SKB R-08-131, Svensk Kärnbränslehantering AB.

Johannesson L-E, Nilsson U, 2006. Deep repository – engineered barrier systems. Geotechnical behaviour of candidate backfill materials. Laboratory tests and calculations for determining performance of the backfill. SKB R-06-73, Svensk Kärnbränslehantering AB.

Johannesson L-E, Sandén T, Dueck A, 2008. Deep repository – engineered barrier system. Wetting and homogenization processes in backfill materials. Laboratory tests for evaluating modeling parameters. SKB R-08-136, Svensk Kärnbränslehantering AB.

Johannesson L-E, Sandén T, Dueck A, Ohlsson L, 2010. Characterization of a backfill candidate material, IBECO-RWC-BF. Baclo Project – Phase 3. Laboratory tests. SKB R-10-44, Svensk Kärnbränslehantering AB.

Karnland O, Olsson S, Nilsson U, 2006. Mineralogy and sealing properties of various bentonites and smectite-rich clay materials. SKB TR-06-30, Svensk Kärnbränslehantering AB.

Mehra O P, Jackson M L, 1960. Iron oxide removal from soils and clays by a dithionite-citrate system buffered with sodium bicarbonate. In proceeding of the 7th National conference on Clays and Clay Minerals, 317–327.

Meier L P, Kahr G, 1999. Determination of the cation exchange capacity (CEC) of clay minerals using the complexes of copper(II) ion with triethylenetetraamine and tetraethylenepentamine. Clays and Clay Minerals 47, 386–388.

Olsson S, Karnland O, 2009. Characterisation of bentonites from Kutch, India, and Milos, Greece – some candidate tunnel back-fill materials? SKB R-09-53, Svensk Kärnbränslehantering AB.

Olsson S, Karnland O, Svensson D, Lundgren C, 2013. Chemical and mineralogical characterization of the Indian tunnel backfill bentonite Asha NW BFL-L 2010. SKB R-13-48, Svensk Kärnbränslehantering AB.

Rietveld H M, 1969. A profile refinement method for nuclear and magnetic structures. Journal of Applied Crystallography 2, 65–71.

Sandén T, Andersson L, 2012. Optimization of backfill pellet properties ÅSKAR DP2. Laboratory tests. SKB R-12-18, Svensk Kärnbränslehantering AB.

Sandén T, Börgesson L, Dueck A, Goudarzi R, Lönnqvist M, 2008a. Deep repository – Engineered barrier system. Erosion and sealing processes in tunnel backfill materials investigated in laboratory. SKB R-08-135, Svensk Kärnbränslehantering AB.

Sandén T, Börgesson L, Dueck A, Goudarzi R, Lönnqvist M, Nilsson U, Åkesson M, 2008b. KBS-3H. Description of buffer tests in 2005–2007. Results of laboratory tests. SKB R-08-40, Svensk Kärnbränslehantering AB.

SKB, 2010. Design, production and initial state of the backfill and plug in deposition tunnels. SKB TR-10-16, Svensk Kärnbränslehantering AB.

Svensson D, Dueck A, Nilsson U, Olsson S, Sandén T, Lydmark S, Jägerwall S, Pedersen K, Hansen S, 2011. Alternative buffer material. Status of ongoing laboratory investigation of reference material and test package 1. SKB TR-11-06, Svensk Kärnbränslehantering AB.

SIS-CEN ISO/TS 17892-12:2007. Geotechnical investigation and testing – Laboratory testing of soils – Part 12: Determiniation of Atterbergs limits. Stockholm: Swedish Standards Institute.

Taylor J C, Matulis C E, 1994. A new method for Rietveld clay analyses. Part I. Use of a universal measured standard profile for Rietveld quantification of montmorillonites. Powder Diffraction 9, 119–123.

Åkesson M, Kristensson O, Börgesson L, Dueck A, Hernelind J, 2010. THM modeling of buffer, backfill and other system components. Critical processes and scenarios. SKB TR-10-11, Svensk Kärnbränslehantering AB.

Ibeco RWC-BF 2010

Data sheet

S&B Industrial Minerals GmbH

IBECO®

IBECO RWC-BF

Beschreibung	Description	Description
Natürlicher Calziumbentonit mit mittlerem Montmorillonitgehalt	Calcium bentonite natural with a medium montmorillonite content	Bentonite calcique naturelle à moyen teneur en montmorillonite

Anwendung	Application	Application
Als Dicht- und Versatzmaterial für Untertage-Deponien	As sealing and backfilling material for underground repositories	Comme cachetage et matériel de remblai pour les dépôts souterrains

	Technische Durchschnittswerte	Technical values (average)	Valeur techniques (moyenne)		
w	Wassergehalt ISO 787/2	Water content	Teneur d'eau	16 ± 1,5	%
ρ_s	Dichte DIN 51057	Specific density	Poids spécifique	2,65	g/cm³
	Schüttdichte DIN 53466	Bulk density	Densité apparente tassée	1020 ± 50	g/l
	Körnung	Grain size	Granulation	0 – 5	mm
	Siebrückstand auf Sieb 0,063 mm DIN 53734	Dry screen residue on sieve 0,063 mm	Refus au tamis (voie sèche) 0,063 mm	> 80	%
	Methylenblau-Adsorption VDG P69	Methylen-blue-adsorption	Adsorption du bleu de méthylène	300 ± 30	mg/g
CEC	Kationenaustauschkapazität	Cation exchange capacity	Capacité d'échange de cations	60 ± 10	mval/ 100g
w_A	Wasseraufnahmevermögen Enslin-Neff, DIN 18132	Water absorption capacity	Capacité d'absorption d'eau	150± 30	%
	Quellvolumen	Swelling index	Gonflement	≥ 7	ml/2g
w_L	Fließgrenze DIN 18122	Liquid limit	Limite de liquidité	115	%
w_P	Ausrollgrenze DIN 18122	Plastic limit	Limite de plasticité	33	%
I_p	Plastizitätszahl (errechnet)	Plasticity index (calculated)	Indice de plasticité (calculée)	82	%

Lieferform	Delivery	Livraison
• Lose per Silo-Lkw • In Säcken, auf Paletten, geschrumpft • In Big Bags	• Bulk per road tanker • In bags on pallets, shrink wrapped • In big bags	• Vrac en camion-silo • En sacs sur palette filmée • En big bags

Da wir auf die Verwendung unseres Produktes keinen Einfluss nehmen können, beschränkt sich unsere Haftung auf diese Produktinformation.	The values listed are indicative and are not to be construed as rigid specifications.	Les renseignements contenus dans cette fiche technique sont fournis à titre indicatif et ne peuvent engager notre responsabilité.

S&B Industrial Minerals GmbH
- Geschäftsbereich IBECO -
Ruhrorter Straße 72 • D – 68219 Mannheim • Tel.+49 6 21 / 8 04 27-0 • Fax +49 6 21 / 8 04 27-50

DKOC 08.12

Asha NW BFL-L 2010

Data sheet

Note: Under the heading “Description of goods” the wrong material is described. The right material is within parenthesis.

ASHAPURA MINECHEM LIMITED

LABORATORY TEST REPORT OF
FINAL INSPECTION REPORT

QR / AIL / QA / 22
REV. 0

CERTIFICATE OF ANALYSIS

INVOICE NO.	:	AML/CONT/0192/2010-11 Date : 26.10.2010
BUYER	:	SVENSK KARNBRANSLEHANTERING AB ASPOLABORATORIET BOX 929, SE-572 29 OSKARSHAMN.
DESCRIPTION OF GOODS	:	12.500 MT ATTAPULGITE POWDER . (ASHA NW BFL-L)
PACKING	:	200 BAGS X 1.25 MT JUMBO BAGS 2 BAGS ON 1 PALLET.
LOADING PORT	:	MUNDRA, INDIA
DISCHARGE PORT	:	MALMO PORT, SWDEN
MARKING	:	FRONT SIDE: FOR ASHA NW BFL-L BACKSIDE POUCH MARKING REQUIRED AS ASHA NW BFL-L BAG NO. LOT NO.

Parameters	Requirement	Results
Moisture Content	15 - 17 %	15.40%
Montmorillonite	55% Min	69.20%
Granules Size	0.5 --- 10 mm	OK

For ASHAPURA MINECHEM LTD.

AUTHORIZED SIGNATORY

Appendix 3

Asha 2010 water content

Big Bag no.	Water content %	Big Bag no.	Water content %	Big Bag no.	Water content %
1	17.97	71	19.19	141	16.34
2	15.71	72	15.20	142	16.51
3	17.04	73	15.06	143	16.21
4	17.64	74	15.62	144	15.87
5	17.02	75	14.38	145	16.32
6	18.36	76	14.22	146	16.95
7	16.09	77	15.50	147	17.43
8	15.79	78	15.69	148	17.55
9	16.10	79	17.06	149	18.60
10	16.24	80	16.77	150	16.04
11	15.48	81	16.23	151	17.49
12	15.69	82	16.77	152	18.16
13	16.35	83	17.87	153	20.09
14	15.67	84	15.90	154	17.26
15	16.22	85	15.59	155	15.12
16	15.87	86	14.81	156	16.17
17	17.49	87	15.51	157	16.35
18	16.38	88	15.59	158	15.79
19	15.85	89	16.73	159	15.57
20	15.86	90	15.25	160	18.23
21	16.41	91	16.74	161	18.14
22	16.41	92	15.43	162	17.19
23	16.87	93	15.52	163	16.59
24	16.90	94	15.58	164	17.53
25	15.23	95	15.80	165	17.47
26	18.01	96	16.33	166	18.16
27	17.10	97	16.64	167	15.22
28	17.49	98	15.62	168	17.64
29	17.10	99	18.40	169	19.02
30	15.65	100	18.15	170	16.36
31	15.84	101	16.68	171	15.55
32	14.32	102	15.90	172	16.30
33	17.09	103	16.73	173	14.65
34	16.01	104	16.61	174	15.54
35	15.02	105	16.15	175	16.32
36	15.26	106	16.43	176	16.25
37	15.60	107	15.88	177	16.41
38	15.09	108	16.70	178	17.18
39	15.44	109	15.76	179	19.21
40	14.96	110	15.75	180	19.34
41	15.07	111	15.50	181	16.69
42	13.81	112	13.33	182	18.35
43	17.14	113	15.82	183	16.04
44	14.03	114	14.22	184	16.79
45	16.67	115	15.54	185	16.67
46	16.05	116	13.68	186	16.06
47	14.22	117	15.32	187	14.59
48	15.56	118	17.19	188	15.24
49	14.96	119	16.16	189	15.77
50	16.45	120	14.40	190	15.66
51	15.02	121	16.37	191	16.02
52	17.12	122	18.39	192	14.25
53	16.51	123	17.26	193	17.37
54	16.98	124	16.91	194	18.52
55	14.73	125	15.03	195	18.70
56	18.59	126	15.66	196	15.83
57	15.86	127	16.92	197	17.18
58	14.15	128	15.19	198	15.27
59	15.72	129	14.01	199	15.67
60	16.06	130	17.67	200	15.63
61	15.08	131	15.34		
62	14.50	132	15.97		
63	16.82	133	15.50		
64	15.73	134	16.04		
65	13.34	135	16.82		
66	14.14	136	17.31		
67	16.80	137	16.04		
68	15.57	138	18.66		
69	13.45	139	18.31		
70	14.41	140	15.87		

Appendix 4

Ibeco 2011 water content

Big Bag no.	Water content %	Big Bag no.	Water content %
1	21.00	43	20.90
2	20.80	44	20.60
3	19.50	45	20.50
4	19.90	46	22.20
5	18.90	47	20.80
6	19.30	48	21.80
7	20.80	49	19.50
8	19.00	50	20.70
9	19.10	51	19.70
10	20.70	52	20.90
11	19.30	53	19.90
12	21.00	54	21.60
13	20.70	55	20.60
14	18.50	56	20.20
15	19.00	57	21.70
16	21.40	58	20.30
17	19.60	59	19.00
18	20.30	60	20.20
19	20.60	61	19.90
20	19.80	62	19.80
21	20.40	63	20.90
22	20.00	64	19.00
23	21.80	65	19.60
24	20.70	66	20.10
25	19.60	67	21.10
26	19.80	68	20.90
27	19.10	69	20.10
28	19.90	70	21.10
29	20.40	71	21.60
30	20.60	72	19.90
31	20.10	73	17.90
32	19.50	74	19.60
33	20.00	75	17.90
34	19.60	76	19.60
35	21.30	77	21.50
36	20.80	78	21.10
37	21.00	79	20.70
38	19.90	80	21.10
39	21.00	81	21.50
40	20.70		
41	21.00		
42	19.10		

Appendix 5

Asha 2012 water content

Big Bag no.	Water content %	Big Bag no.	Water content %	Big Bag no.	Water content %	Big Bag no.	Water content %
1	16.80	76	16.90	151	15.20	226	15.40
2	16.30	77	16.80	152	14.30	227	15.60
3	15.80	78	16.80	153	15.40	228	15.40
4	15.30	79	16.50	154	15.70	229	16.10
5	17.29	80	14.90	155	15.50	230	15.71
6	16.60	81	15.50	156	14.70	231	17.10
7	17.70	82	17.10	157	16.50	232	17.20
8	18.30	83	15.90	158	15.00	233	17.10
9	16.40	84	17.60	159	16.10	234	14.00
10	17.53	85	15.20	160	16.10	235	16.30
11	15.60	86	17.20	161	16.00	236	16.00
12	17.20	87	16.40	162	15.50	237	15.40
13	16.10	88	17.40	163	16.30	238	15.90
14	15.50	89	17.10	164	16.20	239	16.00
15	14.90	90	17.37	165	16.00	240	17.30
16	15.70	91	16.20	166	16.20	241	16.80
17	15.70	92	17.40	167	16.00	242	15.30
18	16.20	93	15.90	168	15.10	243	15.40
19	16.10	94	16.60	169	15.70	244	17.10
20	14.70	95	16.10	170	17.26	245	16.80
21	16.40	96	16.30	171	16.20	246	17.10
22	16.90	97	15.40	172	15.80	247	16.90
23	15.40	98	16.30	173	18.70	248	17.20
24	16.20	99	16.30	174	16.20	249	16.80
25	16.80	100	15.60	175	14.30	250	17.15
26	18.00	101	15.80	176	14.70	251	17.20
27	17.40	102	14.20	177	13.40	252	15.10
28	15.80	103	16.90	178	17.40	253	16.30
29	15.50	104	16.50	179	15.80	254	16.60
30	17.05	105	16.60	180	16.20	255	15.30
31	16.90	106	16.50	181	16.10	256	16.60
32	16.50	107	17.00	182	15.90	257	17.00
33	18.60	108	14.40	183	14.70	258	17.10
34	17.40	109	16.10	184	15.60	259	16.00
35	17.50	110	15.81	185	15.90	260	17.00
36	14.90	111	15.20	186	16.00	261	17.10
37	15.60	112	15.60	187	17.00	262	15.40
38	14.20	113	15.30	188	16.80	263	15.30
39	15.70	114	14.90	189	17.40	264	14.70
40	15.80	115	15.20	190	16.78	265	14.70
41	16.40	116	15.90	191	15.20	266	17.10
42	16.30	117	15.30	192	14.70	267	16.10
43	16.00	118	15.70	193	17.50	268	16.10
44	16.50	119	16.70	194	16.80	269	14.10
45	16.50	120	16.90	195	16.60	270	15.56
46	15.50	121	15.80	196	17.10	271	16.80
47	16.50	122	16.10	197	15.90	272	16.40
48	15.60	123	15.40	198	16.00	273	15.70
49	16.90	124	15.90	199	14.40	274	14.20
50	16.79	125	15.90	200	17.30	275	14.50
51	17.00	126	16.80	201	15.50	276	14.60
52	16.20	127	15.40	202	15.10	277	16.10
53	15.80	128	15.70	203	15.60	278	17.20
54	16.90	129	16.50	204	14.40	279	17.00
55	14.60	130	16.56	205	16.10	280	16.80
56	17.00	131	14.50	206	16.50	281	15.70
57	17.00	132	15.60	207	15.30	282	16.00
58	15.70	133	17.00	208	17.00	283	16.40
59	16.30	134	14.70	209	15.80	284	16.80
60	16.30	135	15.70	210	15.93	285	16.80
61	16.70	136	14.60	211	15.50	286	17.80
62	16.10	137	15.10	212	13.70	287	16.30
63	17.40	138	14.90	213	15.40	288	15.50
64	17.20	139	15.30	214	16.70	289	16.50
65	16.60	140	15.00	215	14.90	290	16.58
66	16.30	141	15.00	216	15.90	291	16.00
67	16.90	142	16.00	217	15.70	292	15.40
68	17.70	143	14.70	218	16.50	293	16.20
69	15.90	144	15.60	219	17.20	294	15.20
70	17.60	145	16.40	220	16.60	295	17.50
71	17.50	146	15.10	221	16.20	296	16.10
72	16.60	147	15.90	222	16.90	297	16.40
73	17.00	148	15.60	223	17.20	298	15.40
74	17.20	149	16.50	224	17.00	299	15.90
75	17.20	150	16.55	225	15.80	300	15.50

Big Bag no.	Water content %	Big Bag no.	Water content %	Big Bag no.	Water content %
301	17.30	376	17.80	451	17.65
302	16.30	377	16.16	452	17.17
303	17.20	378	15.74	453	14.58
304	16.50	379	15.96	454	14.89
305	14.20	380	16.44	455	16.96
306	17.70	381	17.67	456	16.36
307	16.20	382	17.61	457	15.41
308	15.50	383	17.22	458	13.29
309	16.00	384	17.78	459	15.66
310	16.76	385	17.71	460	16.16
311	17.70	386	18.29	461	16.03
312	15.30	387	18.29	462	17.60
313	16.00	388	15.06	463	15.72
314	16.70	389	15.43	464	16.75
315	16.40	390	16.41	465	15.69
316	16.20	391	17.24	466	19.56
317	16.40	392	16.54	467	16.07
318	14.70	393	16.63	468	17.49
319	16.90	394	12.73	469	16.56
320	16.40	395	15.82	470	17.05
321	16.40	396	16.98	471	15.59
322	14.58	397	15.73	472	17.03
323	14.16	398	17.05	473	15.73
324	17.73	399	14.89	474	14.66
325	17.42	400	16.57	475	15.95
326	15.65	401	15.82	476	17.12
327	17.68	402	15.47	477	24.95
328	16.86	403	17.53	478	17.96
329	17.11	404	13.27	479	16.57
330	15.53	405	16.97	480	17.25
331	12.67	406	14.66	481	15.69
332	16.43	407	16.10	482	16.04
333	14.88	408	17.27	483	17.93
334	17.20	409	16.74	484	13.03
335	12.79	410	17.07	485	17.57
336	16.74	411	15.50	486	13.51
337	15.69	412	14.55	487	17.16
338	17.48	413	16.15	488	16.81
339	14.92	414	17.01	489	17.06
340	16.08	415	14.74	490	12.51
341	19.03	416	16.90	491	16.43
342	16.50	417	15.78	492	17.09
343	17.90	418	16.03	493	16.12
344	17.89	419	17.37	494	18.04
345	16.88	420	12.75	495	16.53
346	18.76	421	14.13	496	15.38
347	16.96	422	15.85	497	17.98
348	16.38	423	14.30	498	12.85
349	17.04	424	16.22	499	15.45
350	17.17	425	17.01	500	12.53
351	13.78	426	12.83		
352	17.08	427	15.23		
353	17.93	428	15.23		
354	13.98	429	16.00		
355	16.23	430	16.86		
356	14.25	431	12.62		
357	15.39	432	17.06		
358	16.66	433	17.39		
359	16.23	434	15.44		
360	16.77	435	15.17		
361	17.27	436	16.60		
362	15.83	437	12.40		
363	17.91	438	13.25		
364	14.33	439	17.02		
365	15.76	440	17.08		
366	12.65	441	17.73		
367	16.83	442	15.66		
368	15.06	443	18.09		
369	16.28	444	14.76		
370	17.71	445	17.31		
371	14.76	446	16.91		
372	14.25	447	16.37		
373	16.26	448	16.64		
374	17.69	449	16.05		
375	16.12	450	19.53		

Appendix 6

Asha 2010 swell index

Big Bag no.	Swell index ml/g
5	5.2
10	4.5
15	4.8
20	4.5
25	4.8
30	5.1
35	4.7
40	5.0
45	5.8
50	4.9
55	4.3
60	4.8
65	4.7
70	6.4
75	5.1
80	4.8
85	6.4
90	4.8
95	4.4
100	4.9
101	6.1
106	5.8
111	5.7
116	4.4
121	4.2
126	5.4
131	6.1
136	4.2
141	5.5
146	4.5
151	5.5
156	6.1
161	4.9
166	4.2
171	4.8
176	5.8
181	4.9
186	5.6
191	4.9
196	5.8

Appendix 7

Ibeco 2011 swell index

Big Bag no.	Swell index ml/g
1	4.2
6	4.0
11	4.2
16	4.2
21	4.0
26	4.1
31	3.7
36	3.6
41	4.5
46	4.6
51	4.0
56	4.0
61	3.8
66	3.6
71	3.7
76	3.7
81	3.5

Appendix 8

Asha 2012 swell index

Big Bag no.	Swell index ml/g
5	6.3
10	6.9
30	7.2
50	6.9
70	7.5
90	8.3
110	7.6
130	7.7
150	7.7
170	8.5
190	7.1
210	7.2
230	7.6
250	7.2
270	7.8
290	7.1
310	7.8
330	8.1
350	7.2
370	6.5
390	7.2
410	6.9
430	7.3
450	7.1
470	6.6

Appendix 9

Asha 2010 and Ibeco 2011 liquid limit

Material-Big Bag no.	Liquid limit %
Ibeco 2011	116
Asha 2010-113	193
Asha 2010-113	227
Asha 2010-113	208
Asha 2010-113	197
Asha 2010-125	176
Asha 2010-125	187

Appendix 10

Asha 2012 liquid limit

Crushed material		Material as-delivered	
Big Bag no.	Liquid limit %	Big Bag no.	Liquid limit %
1	163.4	1	137.9
5	215.4	5	179.4
10	191.0	10	158.2
20	183.6	20	167.0
30	177.4	30	157.0
40	180.9	40	135.6
50	165.3	50	144.6
60	174.6	60	145.2
70	200.5	70	166.5
80	197.0	80	174.3
90	171.2	90	153.3
100	160.5	100	155.8
110	190.0	110	163.8
120	179.0	120	161.7
130	186.4	130	161.2
140	178.3	140	160.2
150	174.6	150	152.6
160	166.7	160	150.8
170	174.8	170	156.6
180	175.7	180	164.7
190	187.1	190	170.7
200	184.4	200	166.7
210	181.1	210	134.9
220	175.8	220	156.4
230	182.8	230	183.3
240	174.7	240	152.6
250	176.7	250	152.9
260	195.1	260	166.2
270	178.8	270	150.5
280	163.6	280	141.2
290	162.4	290	121.6
300	177.5	300	155.5
310	209.6	310	180.5
320	169.4	320	132.8
330	246.1	330	216.3
340	167.0	340	158.0
350	214.8	350	179.7
360	159.6	360	122.1
370	172.9	370	138.2
380	175.7	380	143.1
390	233.8	390	190.4
400	157.6	400	125.7
410	219.4	410	205.9
420	264.1	420	225.1
430	218.6	430	181.1
440	183.6	440	177.4
450	141.4	450	120.2
460	152.6	460	158.4
470	265.3	470	202.2
480	209.1	480	166.9

Appendix 11

Asha 2010 CEC

Big Bag no.	CEC meq/100 g	Big Bag no.	CEC meq/100 g
5	93.2	105	83.4
5	94.5	105	82.8
10	86.9	110	86.8
10	86.2	110	86.7
15	82.3	113	85.0
15	81.1	113	84.0
20	85.7	113	85.4
20	84.7	113	85.4
25	84.1	113	83.6
25	86.2	115	86.7
30	82.8	115	85.9
30	83.0	120	79.1
35	81.8	120	80.8
35	82.5	125	88.8
40	86.0	125	88.5
40	85.8	125	89.1
45	94.3	125	88.3
45	93.9	125	89.4
50	84.0	130	92.7
50	86.1	130	92.0
55	79.0	135	94.0
55	80.0	135	95.0
60	87.7	140	80.0
60	87.9	140	81.3
65	79.1	145	84.0
65	79.3	145	83.7
70	84.2	155	85.4
70	83.8	155	86.5
70	83.7	160	93.1
70	82.6	160	93.5
70	83.3	165	92.3
75	90.9	165	90.2
75	90.7	170	83.4
80	95.3	170	84.1
80	95.6	175	87.2
85	87.6	175	87.2
85	88.5	180	95.7
90	91.2	180	96.0
90	90.4	185	84.2
95	89.3	185	84.7
95	89.8	190	81.3
100	88.6	190	80.5
100	92.0	195	95.7
		195	95.8
		200	82.6
		200	82.4

Appendix 12

Ibeco 2011 CEC

Big Bag no.	CEC meq/100 g
1	66.7
1	66.8
5	62.4
5	63.3
10	65.3
10	63.2
15	62.5
15	63.7
20	66.2
20	66.2
25	64.4
25	62.3
30	62.3
30	61.6
35	66.2
35	66.6
40	63.3
40	64.1
41	65.2
41	65.3
46	64.2
46	64.6
51	67.1
51	68.0
56	68.2
56	68.7
61	64.2
61	65.3
66	68.1
66	68.7
71	64.9
71	66.9
76	65.6
76	64.0
81	68.3
81	67.4

Appendix 13

Asha 2012 CEC

Big Bag no.	CEC meq/100 g	Big Bag no.	CEC meq/100 g
1	85.34	260	84.53
1	85.62	260	84.90
5	84.64	270	84.35
5	85.07	270	83.51
10	85.94	280	83.37
10	84.14	280	82.95
20	82.96	290	83.50
20	81.60	290	83.23
30	83.48	300	82.92
30	84.26	300	82.72
40	83.50	310	87.05
40	83.90	310	87.10
50	83.37	320	82.35
50	83.58	320	83.71
60	85.81	330	85.09
60	85.54	330	84.52
70	84.92	340	85.64
70	85.66	340	83.18
80	85.35	350	86.84
80	85.68	350	85.26
90	82.82	360	81.45
90	84.08	360	81.49
100	85.47	370	82.76
100	85.24	370	85.58
110	84.03	380	85.10
110	83.36	380	83.86
120	87.93	390	87.74
120	88.63	390	88.03
130	84.96	400	82.64
130	83.95	400	82.40
140	84.67	410	87.08
140	86.11	410	84.83
150	84.69	420	85.09
150	84.84	420	86.60
160	85.73	430	87.56
160	85.62	430	86.74
170	84.30	440	85.45
170	83.05	440	85.15
180	85.95	450	85.57
180	86.51	450	85.16
190	86.19	460	83.13
190	85.06	460	84.00
200	84.99	470	87.94
200	84.58	470	86.99
210	83.22	480	86.40
210	83.54	480	87.10
220	85.02		
220	84.85		
230	84.45		
230	83.59		
240	84.79		
240	86.51		
250	85.87		
250	84.73		

Appendix 14

Asha 2010 and Ibeco 2011 granule size distribution

Screen size mm	Sample Asha 2010-113	Asha 2010-125
16	100.0	100.0
8	97.5	98.1
4	78.6	93.5
2	58.6	70.5
0.5	21.8	42.4
0.25	11.7	10.4
0.125	4.7	5.3
0.075	2.3	2.6

Screen size mm	Sample Ibeco 1	Ibeco 2	Ibeco 3
8	100.0	100.0	100.0
4	98.4	98.2	98.6
2	68.9	67.9	77.4
0.5	15.1	14.2	26.9
0.25	6.6	6.3	12.4
0.125	1.9	1.7	3.1
0.075	0.5	0.5	0.8

Appendix 15

Asha 2012 granule size distribution

Screen size	Sample				
mm	Asha 2012-1	Asha 2012-20	Asha 2012-40	Asha 2012-60	Asha 2012-80
16	100.0	100.0	100.0	100.0	100.0
8	85.3	92.0	87.3	94.2	88.1
4	61.8	78.0	72.2	76.7	70.2
2	35.8	57.2	50.6	51.6	45.9
1	16.1	34.9	28.8	28.2	25.1
0.5	8.0	20.8	16.5	15.3	14.3
0.25	4.3	11.4	8.8	7.7	7.5
0.125	2.0	4.6	3.7	3.1	3.0
0.075	1.1	2.5	2.1	1.7	1.6

Screen size	Sample				
mm	Asha 2012-100	Asha 2012-120	Asha 2012-140	Asha 2012-160	Asha 2012-180
16	100.0	100.0	100.0	100.0	100.0
8	71.6	75.6	87.7	92.9	90.6
4	42.7	53.2	67.7	71.6	70.5
2	19.4	32.4	44.2	45.5	47.3
1	7.2	16.3	23.9	25.5	25.3
0.5	3.3	8.6	13.1	15.3	13.2
0.25	1.7	4.4	6.6	8.7	6.3
0.125	0.8	1.8	2.5	3.8	2.2
0.075	0.5	1.0	1.3	2.0	1.1

Screen size	Sample				
mm	Asha 2012-200	Asha 2012-220	Asha 2012-240	Asha 2012-260	Asha 2012-280
16	100.0	100.0	100.0	100.0	100.0
8	86.2	93.8	95.3	92.3	94.3
4	64.4	73.0	78.6	70.9	75.6
2	40.0	51.3	55.6	46.4	51.8
1	22.2	31.5	33.5	24.9	29.4
0.5	13.7	19.2	19.9	13.2	17.0
0.25	8.4	10.5	10.7	6.3	9.0
0.125	4.0	4.1	4.2	2.3	3.5
0.075	2.1	1.9	1.8	1.1	1.5

Screen size	Sample				
mm	Asha 2012-300	Asha 2012-320	Asha 2012-340	Asha 2012-360	Asha 2012-380
16	100.0	100.0	100.0	100.0	100.0
8	90.6	93.0	89.7	90.7	85.4
4	67.2	76.3	74.5	74.2	71.7
2	44.6	54.2	49.4	52.0	51.2
1	25.2	32.5	26.3	29.2	29.7
0.5	15.0	20.0	15.0	16.7	17.0
0.25	8.4	11.3	8.2	8.8	8.8
0.125	3.8	4.9	3.7	3.6	3.5
0.075	2.2	2.8	2.2	2.0	1.9

Screen size	Sample				
mm	Asha 2012-400	Asha 2012-420	Asha 2012-440	Asha 2012-460	Asha 2012-480
16	100.0	100.0	100.0	100.0	100.0
8	90.1	95.8	89.8	97.6	87.1
4	70.7	80.5	70.9	76.8	64.6
2	45.6	58.6	46.3	53.0	38.2
1	23.3	36.3	25.7	32.4	18.4
0.5	12.7	22.7	15.1	20.3	9.7
0.25	6.5	13.4	8.4	11.4	5.1
0.125	2.7	6.4	3.7	4.7	2.4
0.075	1.5	3.9	2.2	2.6	1.5

Asha 2010 and 2012 beam tests

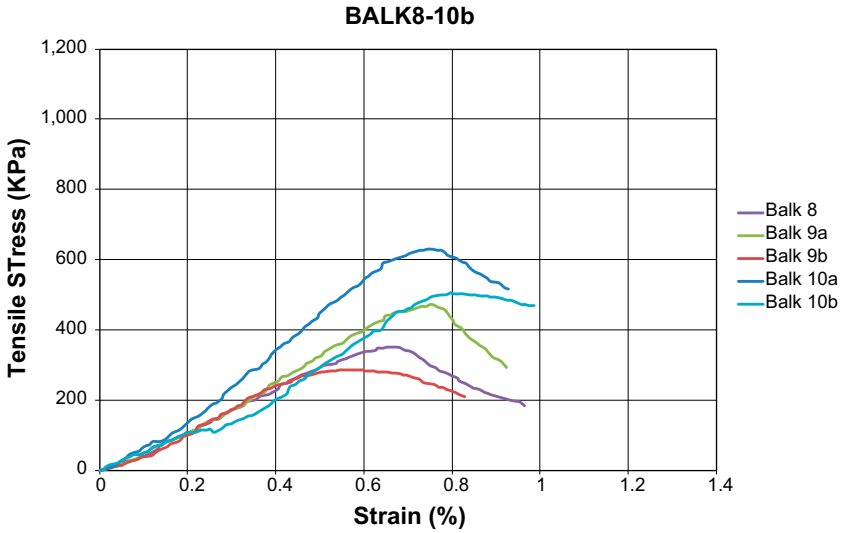

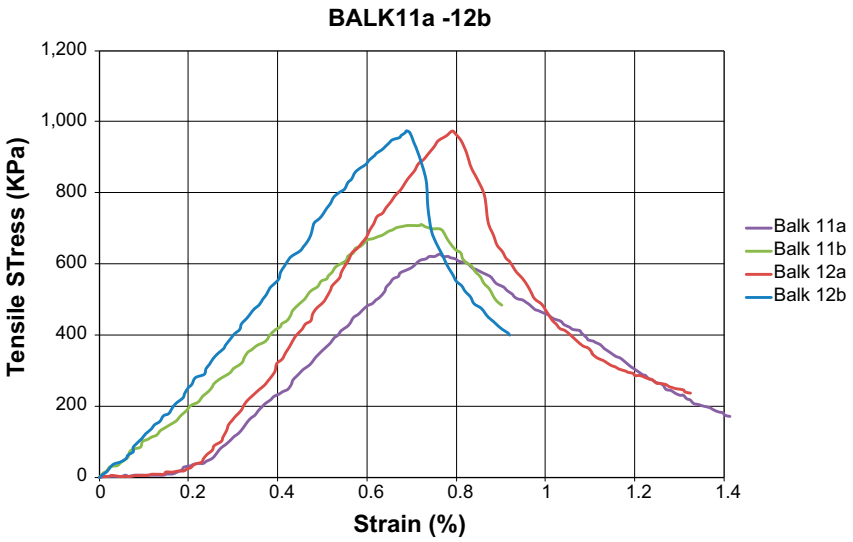

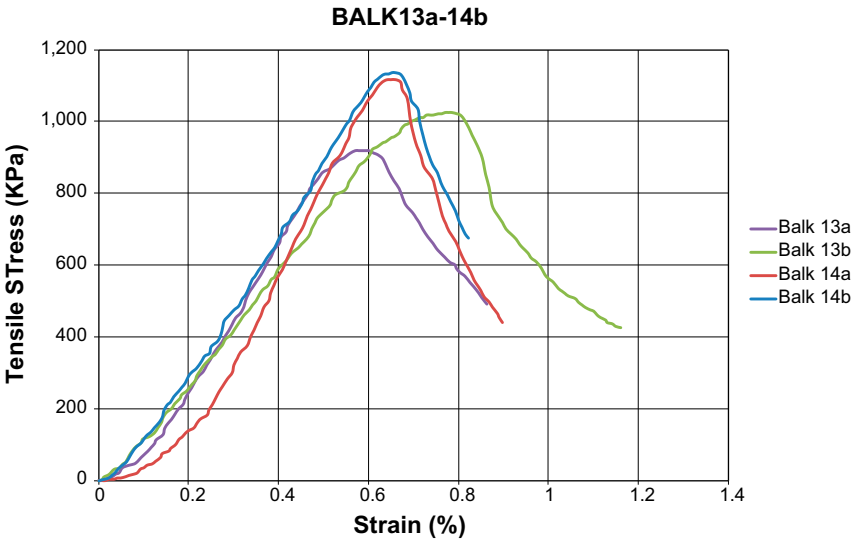

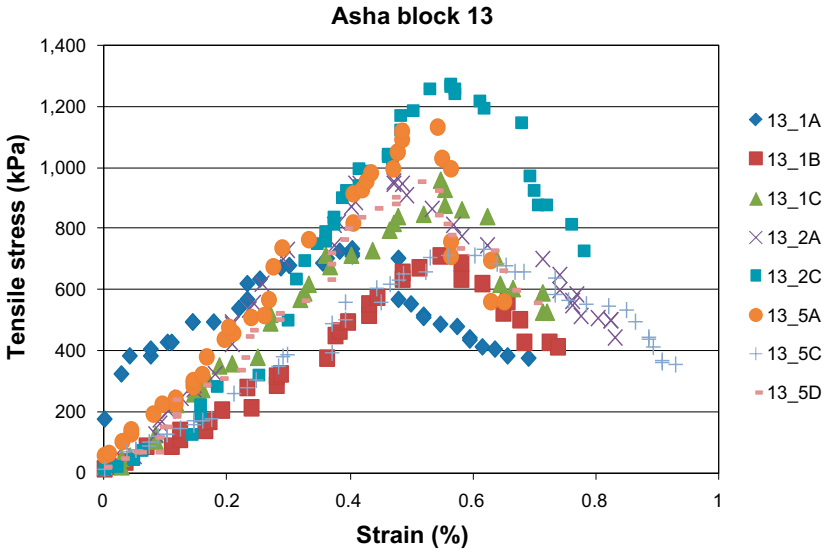
Asha block 13
Tensile stress (kPa)
Strain (%)
13_1A
13_1B
13_1C
13_2A
13_2C
13_5A
13_5C
13_5D

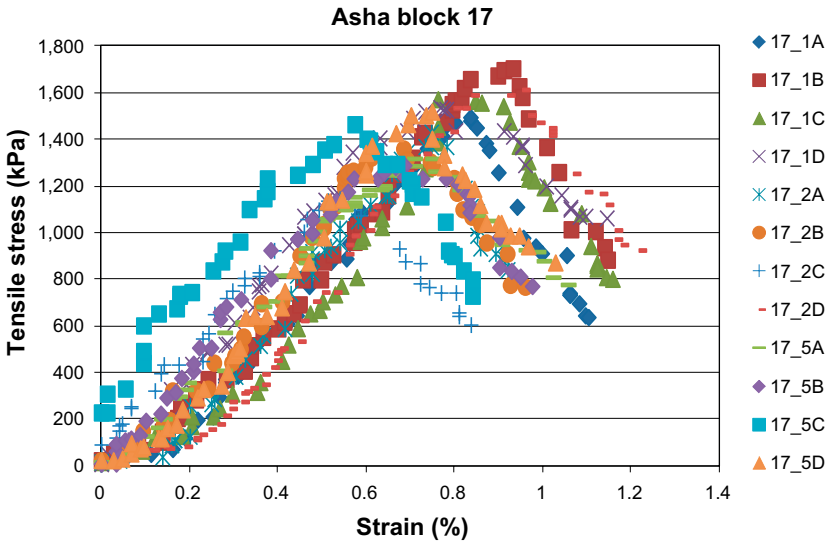
Asha block 17
Tensile stress (kPa)
Strain (%)
17_1A
17_1B
17_1C
17_1D
17_2A
17_2B
17_2C
17_2D
17_5A
17_5B
17_5C
17_5D

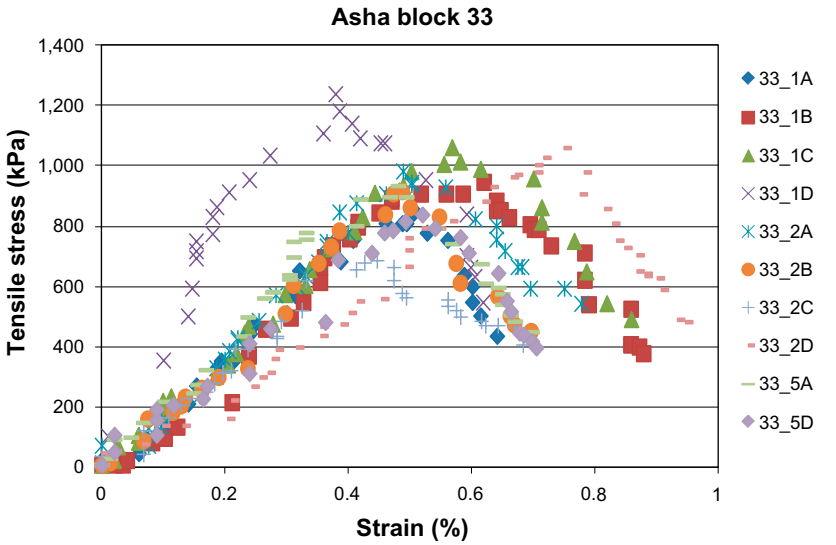
Asha block 33
Tensile stress (kPa)
Strain (%)
33_1A
33_1B
33_1C
33_1D
33_2A
33_2B
33_2C
33_2D
33_5A
33_5D

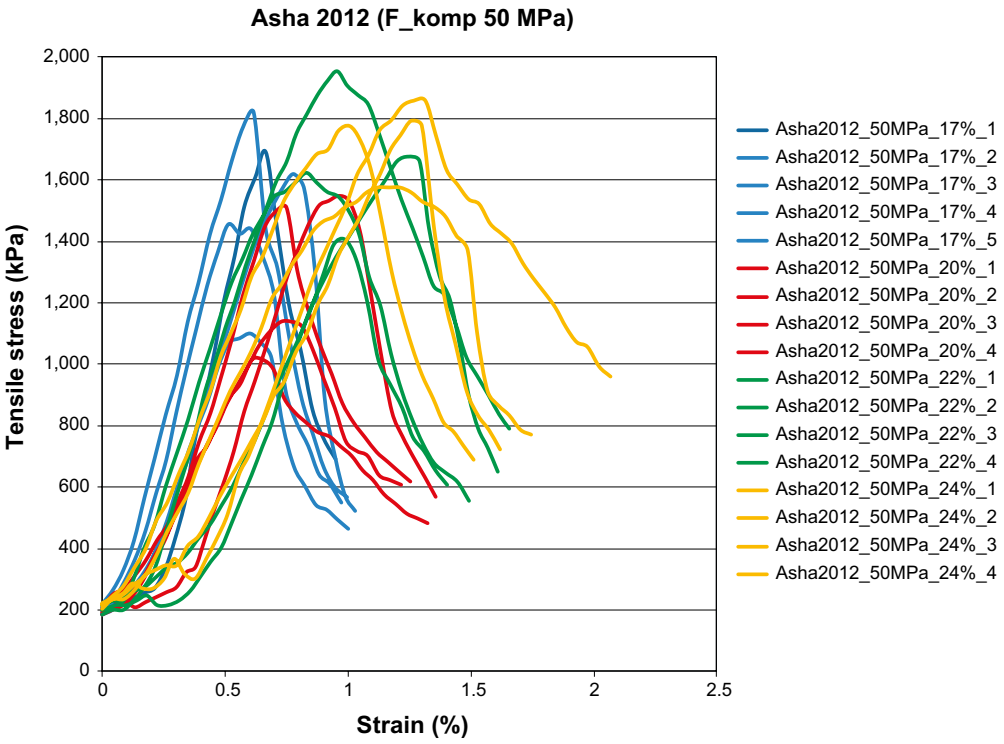
Asha 2012 (F_komp 50 MPa)
Tensile stress (kPa)
2,000
1,800
1,600
1,400
1,200
1,000
800
600
400
200
0
0
0.5
1
1.5
2
2.5
Strain (%)
Asha2012_50MPa_17%_1
Asha2012_50MPa_17%_2
Asha2012_50MPa_17%_3
Asha2012_50MPa_17%_4
Asha2012_50MPa_17%_5
Asha2012_50MPa_20%_1
Asha2012_50MPa_20%_2
Asha2012_50MPa_20%_3
Asha2012_50MPa_20%_4
Asha2012_50MPa_22%_1
Asha2012_50MPa_22%_2
Asha2012_50MPa_22%_3
Asha2012_50MPa_22%_4
Asha2012_50MPa_24%_1
Asha2012_50MPa_24%_2
Asha2012_50MPa_24%_3
Asha2012_50MPa_24%_4

XRD profiles of samples of Asha 2012

Asha 2012 Big bag no. 1

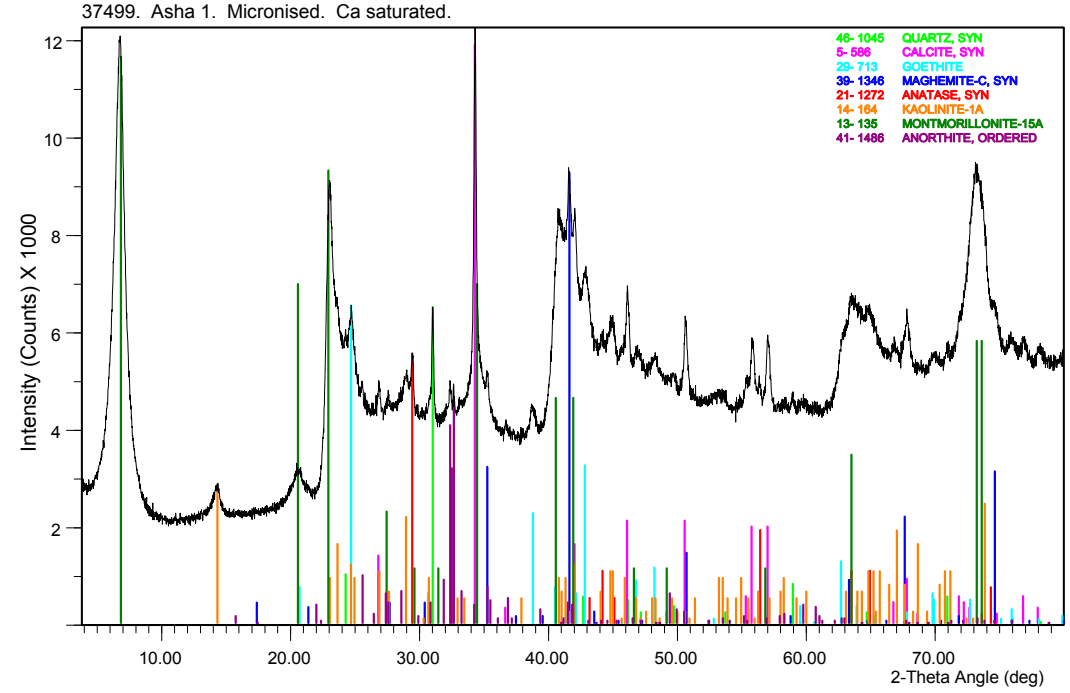

Asha 2012 Big bag no. 1

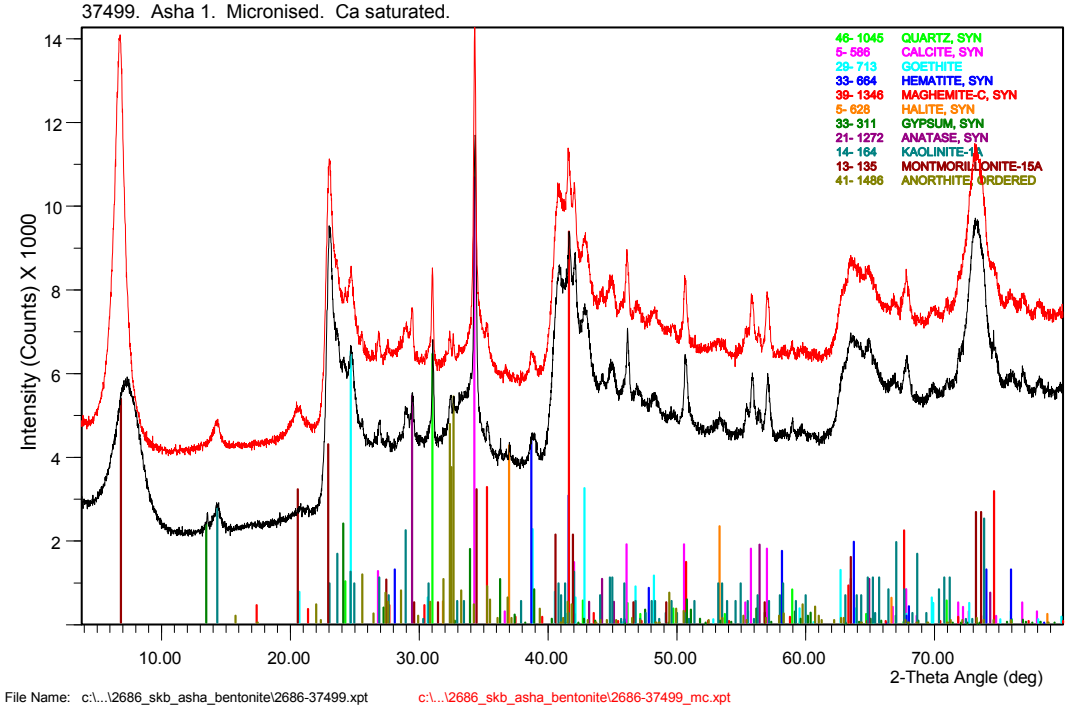

Asha 2012 Big bag no. 20

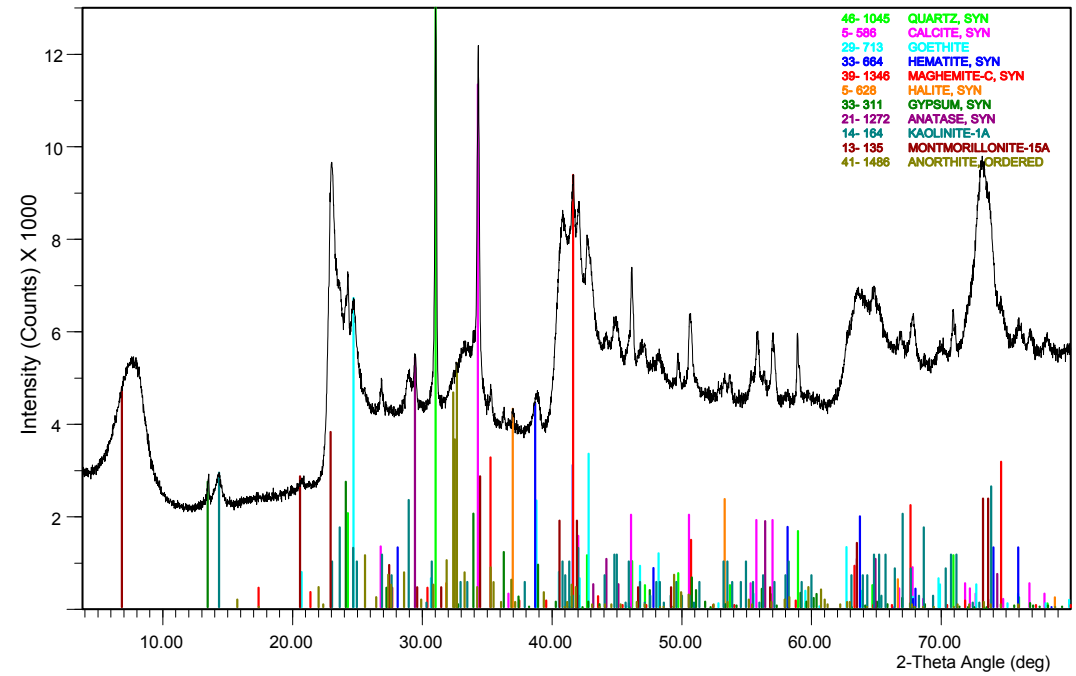

Asha 2012 Big bag no. 20

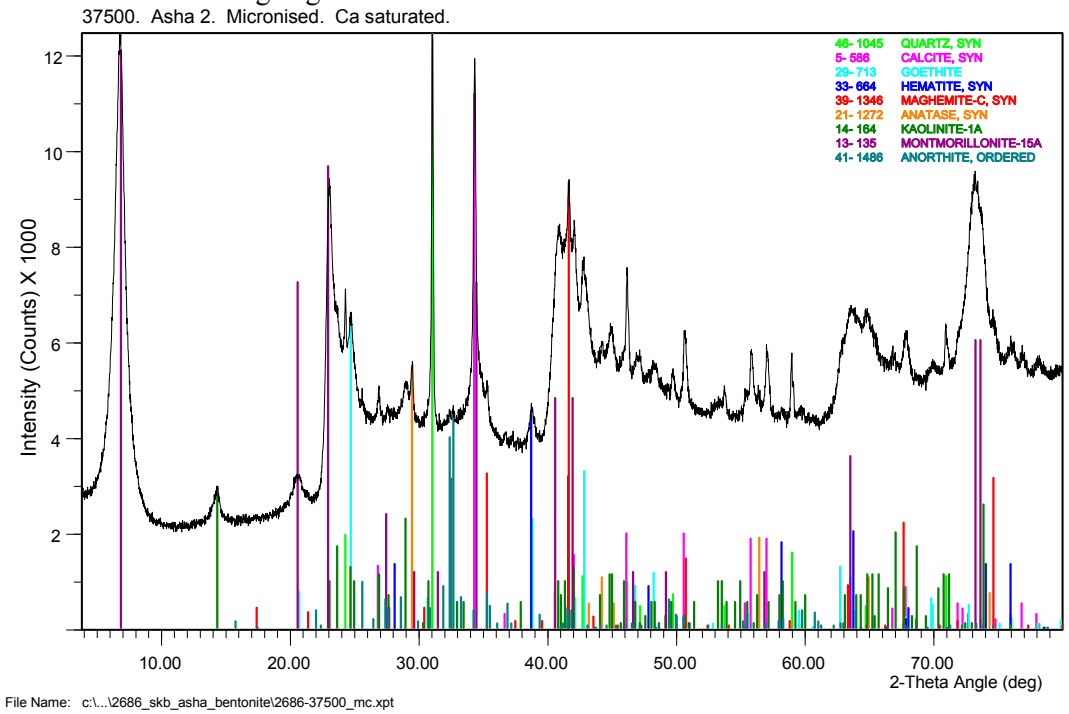

Asha 2012 Big bag no. 20

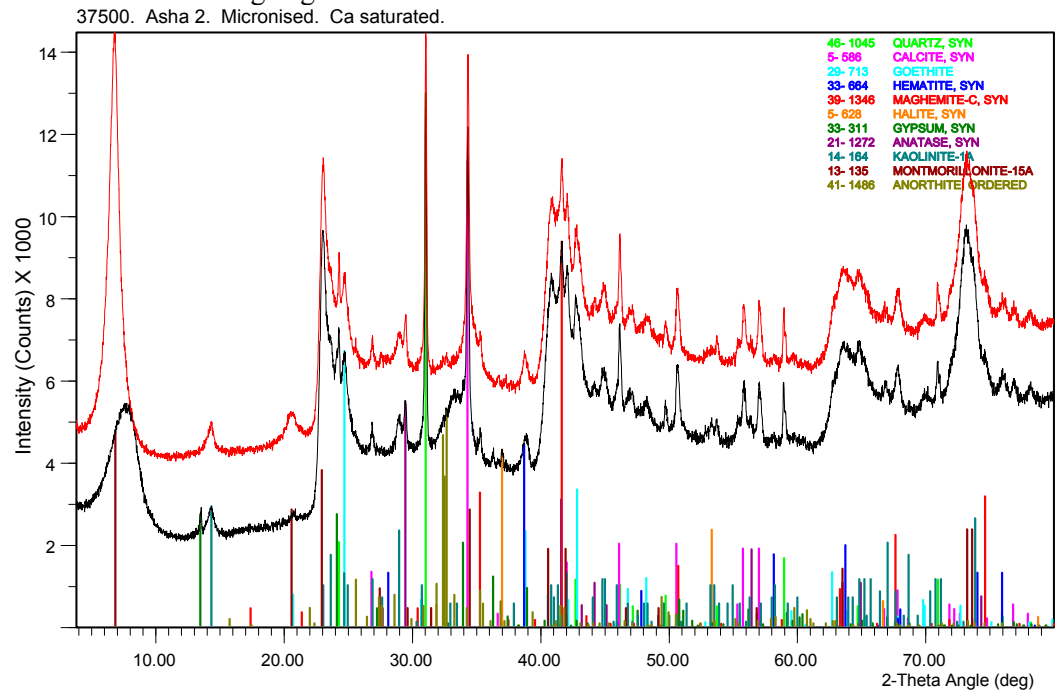

Asha 2012 Big bag no. 40

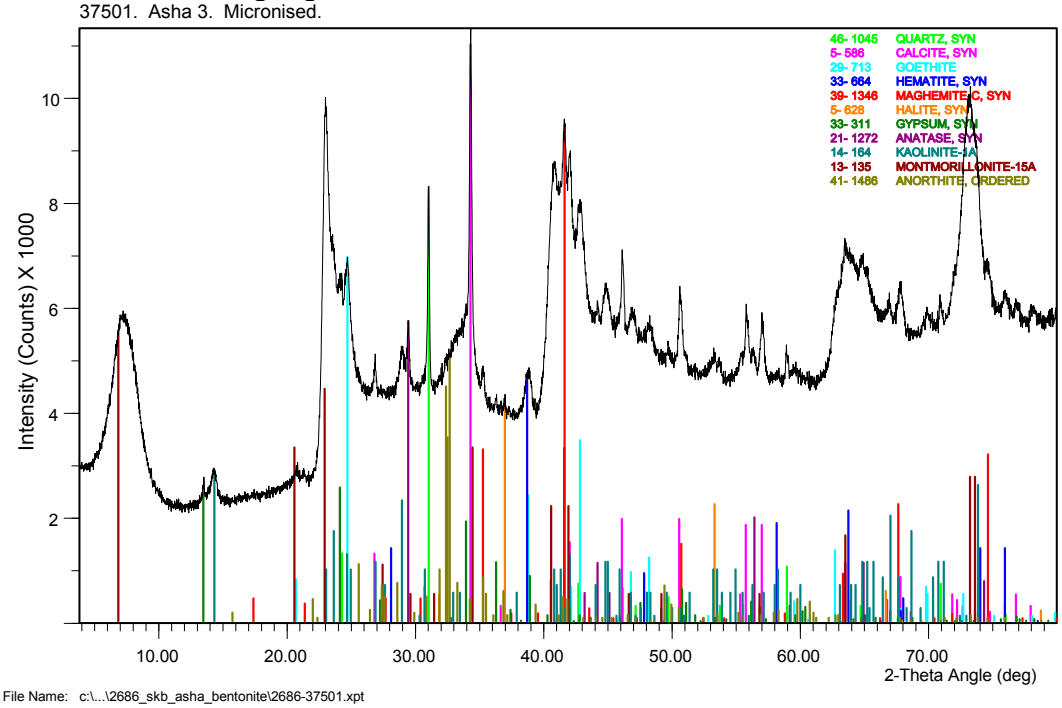

Asha 2012 Big bag no. 40

37501. Asha 3. Micronised. Ca saturated.

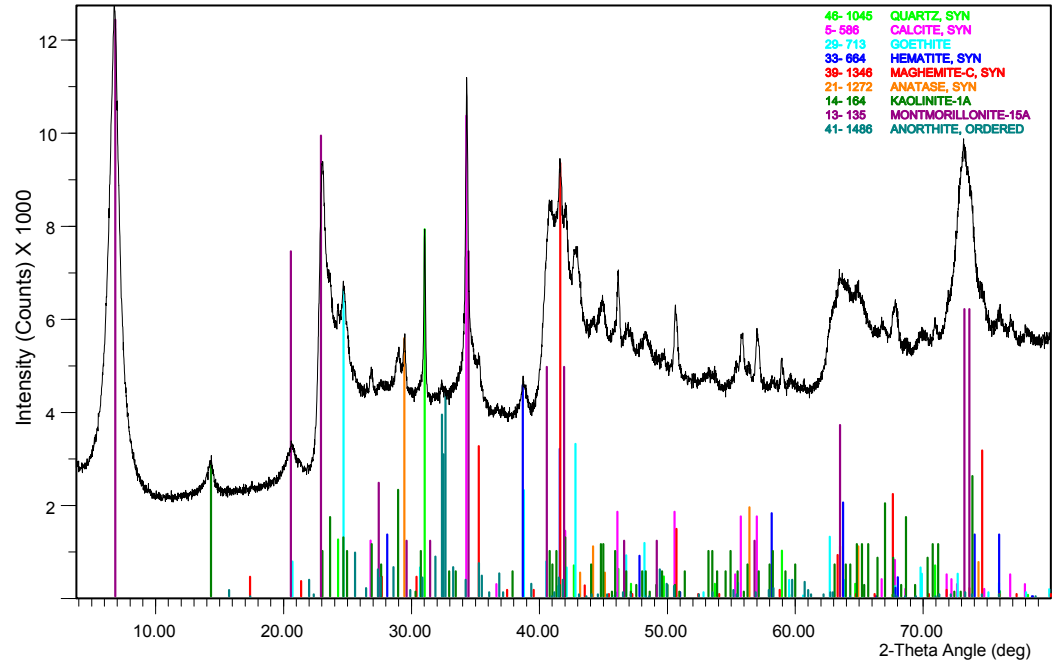

File Name: c:\...\2686_skb_asha_bentonite\2686-37501_mc.xpt

Asha 2012 Big bag no. 40

37501. Asha 3. Micronised. Ca saturated.

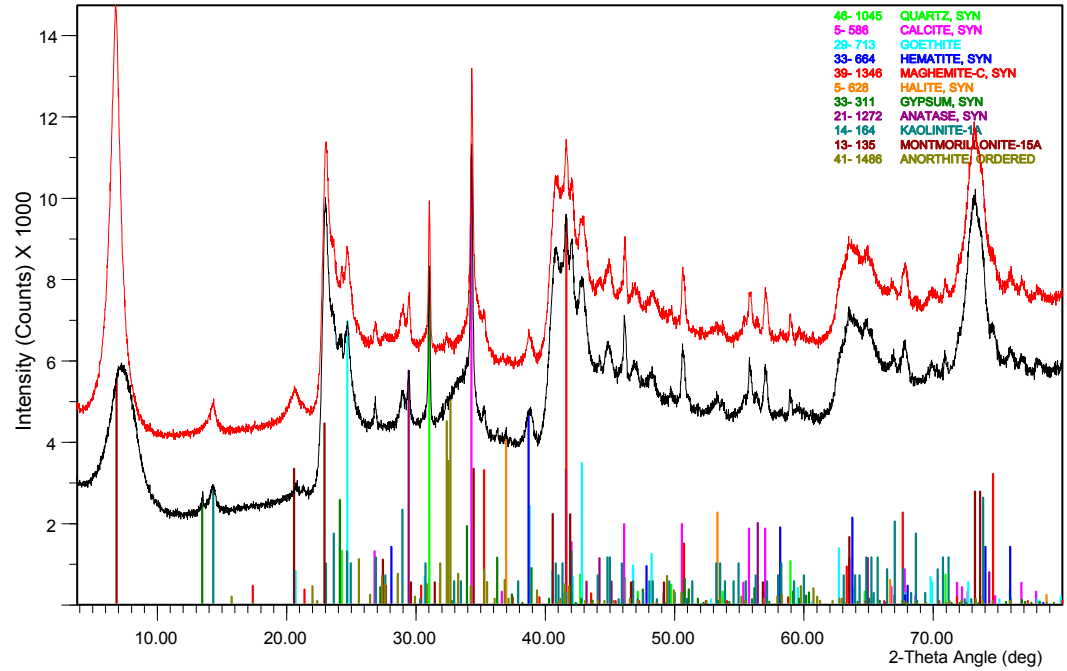

File Name: c:\...\2686_skb_asha_bentonite\2686-37501.xpt c:\...\2686_skb_asha_bentonite\2686-37501_mc.xpt

Asha 2012 Big bag no. 60

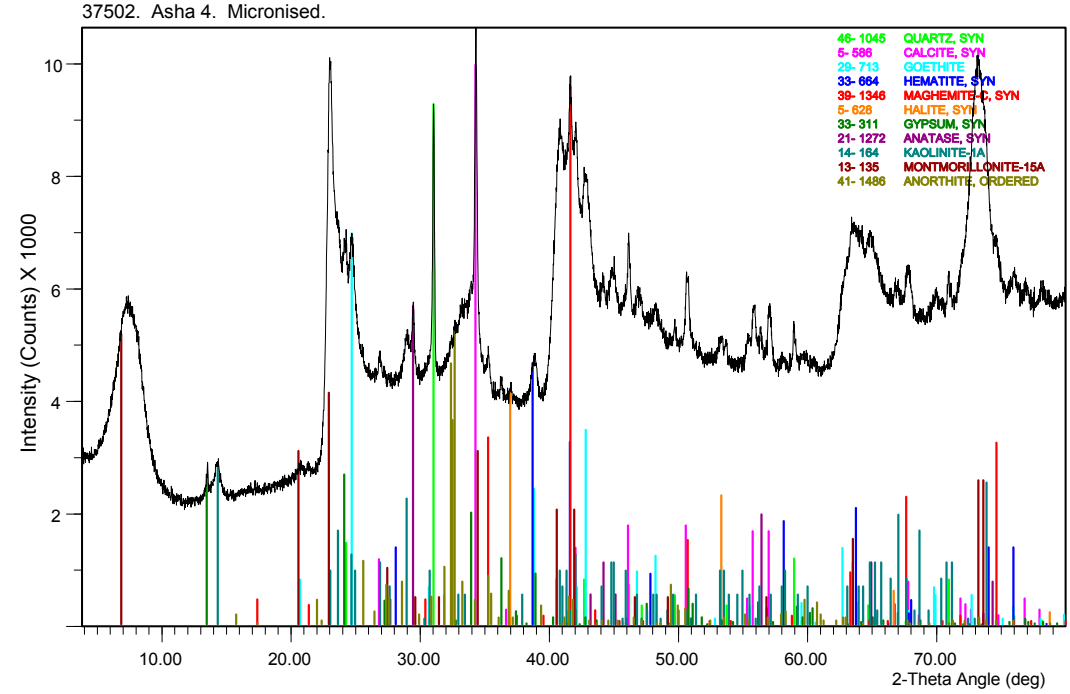

Asha 2012 Big bag no. 60

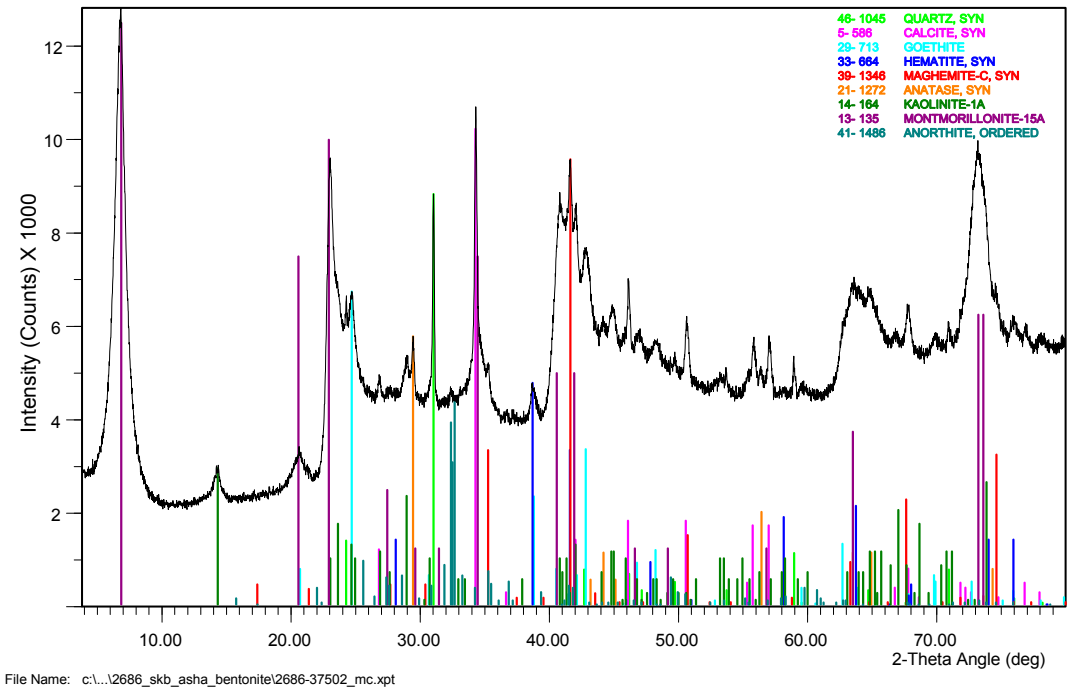

Asha 2012 Big bag no. 60

37502. Asha 4. Micronised. Ca saturated.

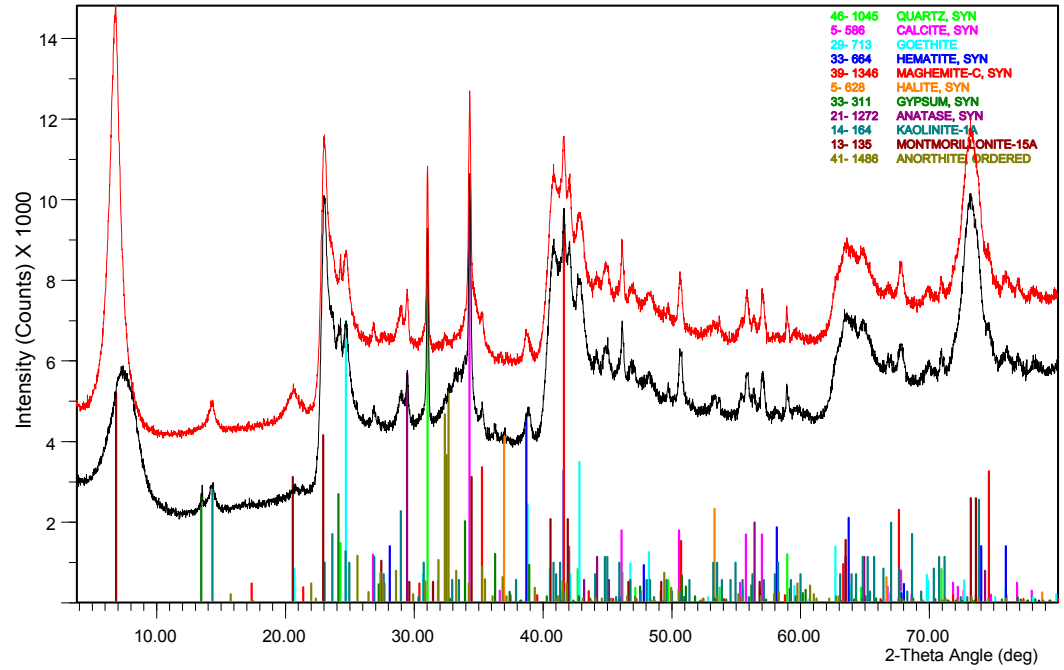

File Name: c:\...\2686_skb_asha_bentonite\2686-37502.xpt c:\...\2686_skb_asha_bentonite\2686-37502_mc.xpt

Asha 2012 Big bag no. 100

37503. Asha 5. Micronised.

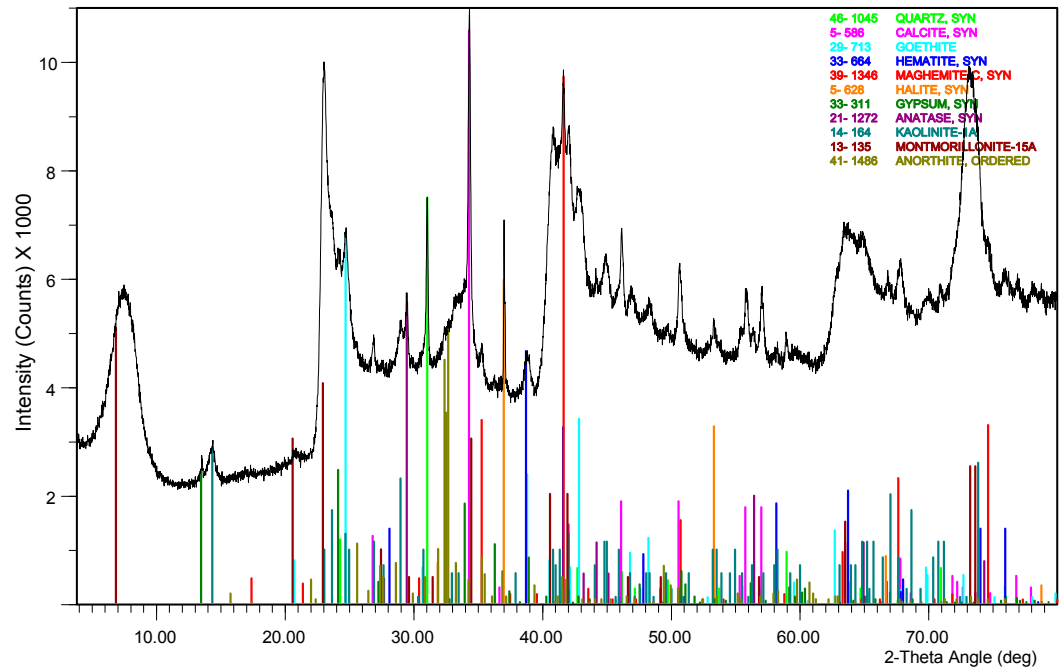

File Name: c:\...\2686_skb_asha_bentonite\2686-37503.xpt

Asha 2012 Big bag no. 100

37503. Asha 5. Micronised. Ca saturated.

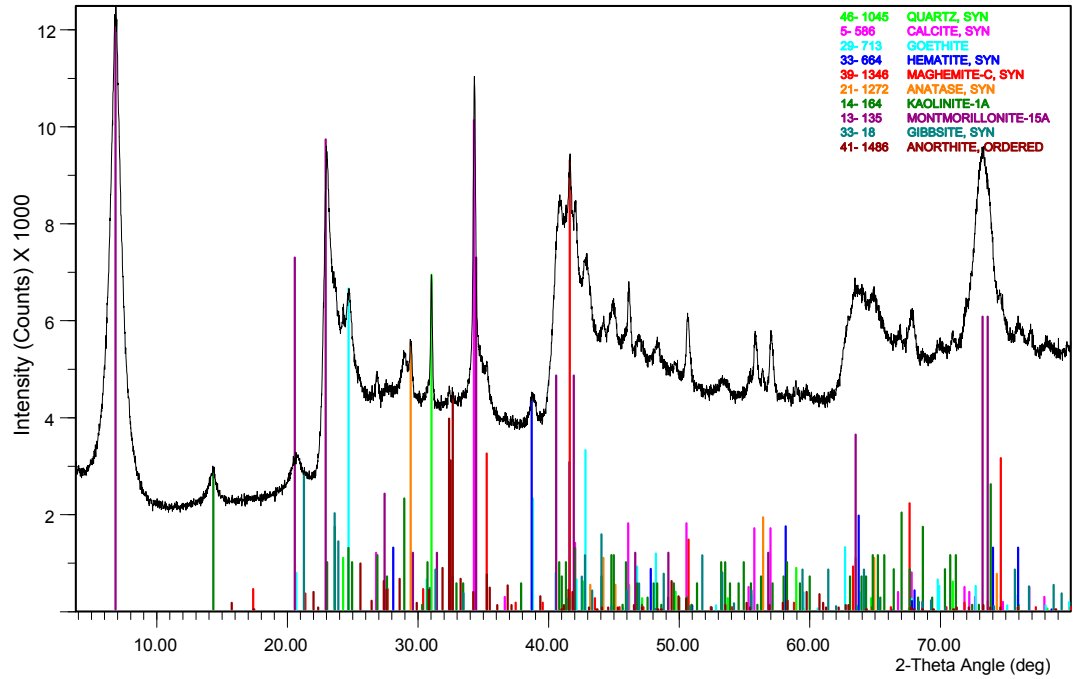

File Name: c:\...\2686_skb_asha_bentonite\2686-37503_mc.xpt

Asha 2012 Big bag no. 100

37503. Asha 5. Micronised. Ca saturated.

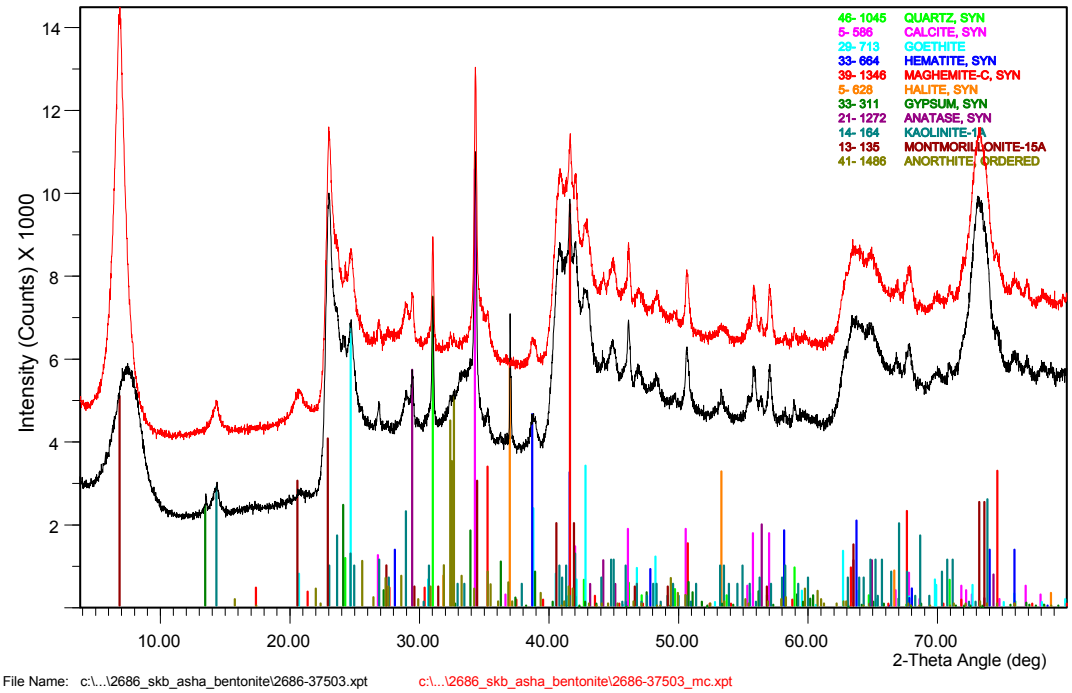

File Name: c:\...\2686_skb_asha_bentonite\2686-37503.xpt c:\...\2686_skb_asha_bentonite\2686-37503_mc.xpt

Asha 2012 Big bag no. 100

37503. Asha 5. >0.2um.

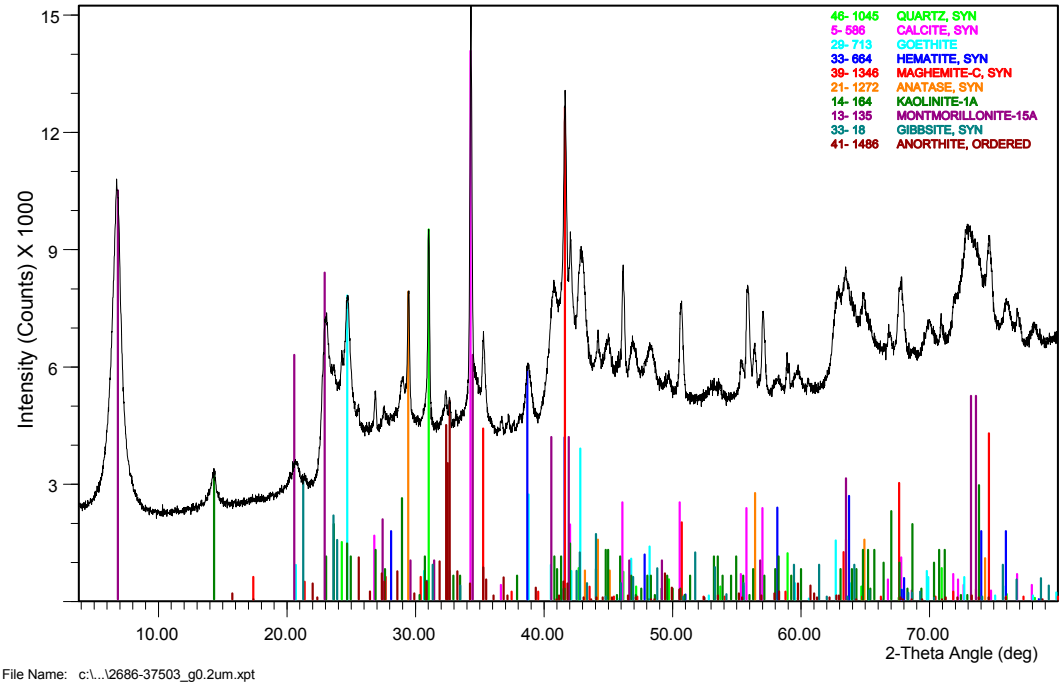

File Name: c:\...\2686-37503_g0.2um.xpt

Asha 2012 Big bag no. 100

37503. Asha 5. <0.2um. Acetic acid treated. Ca saturated.

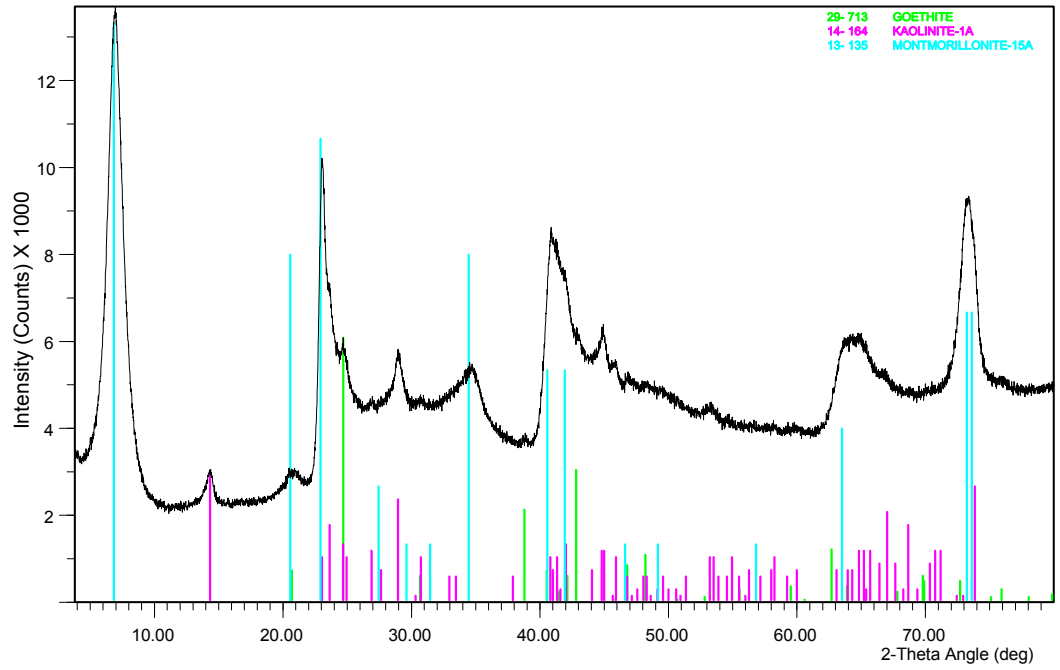

File Name: c:\...\2686-37503_l0.2um.xpt

Asha 2012 Big bag no. 120

37504. Asha 6. Micronised.

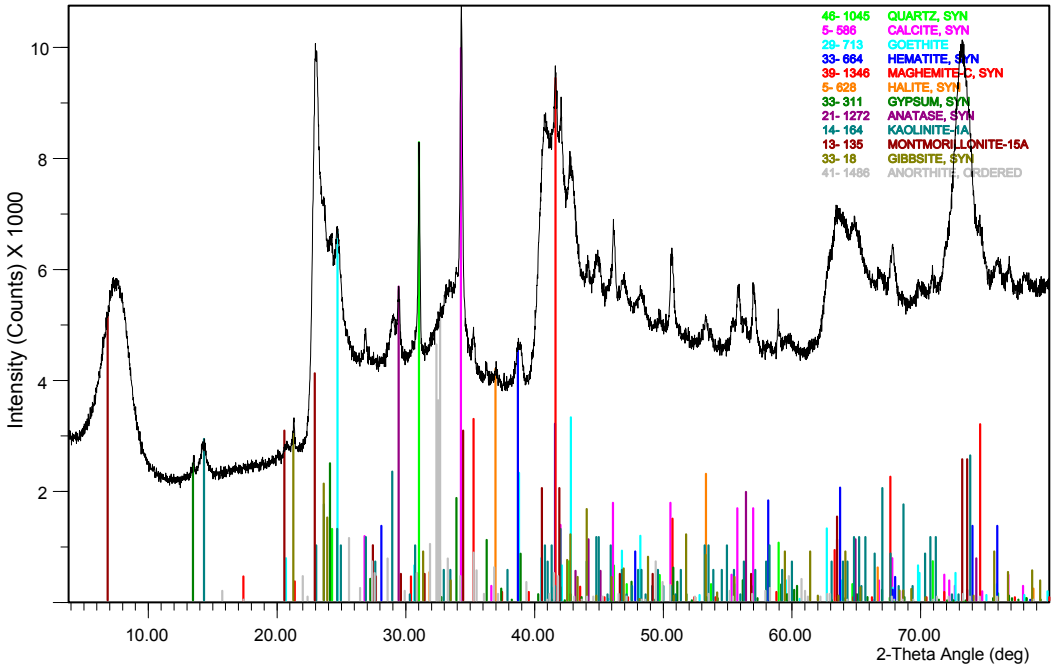

File Name: c:\...\2686_skb_asha_bentonite\2686-37504.xpt

Asha 2012 Big bag no. 120

37504. Asha 6. Micronised. Ca saturated.

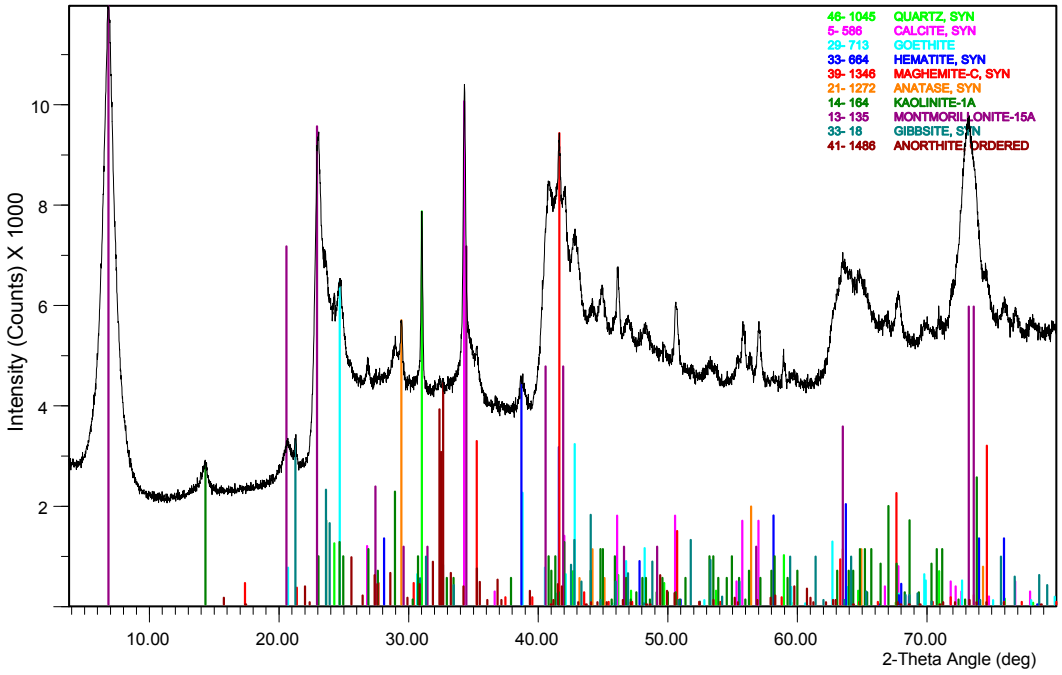

File Name: c:\...\2686_skb_asha_bentonite\2686-37504_mc.xpt

Asha 2012 Big bag no. 120

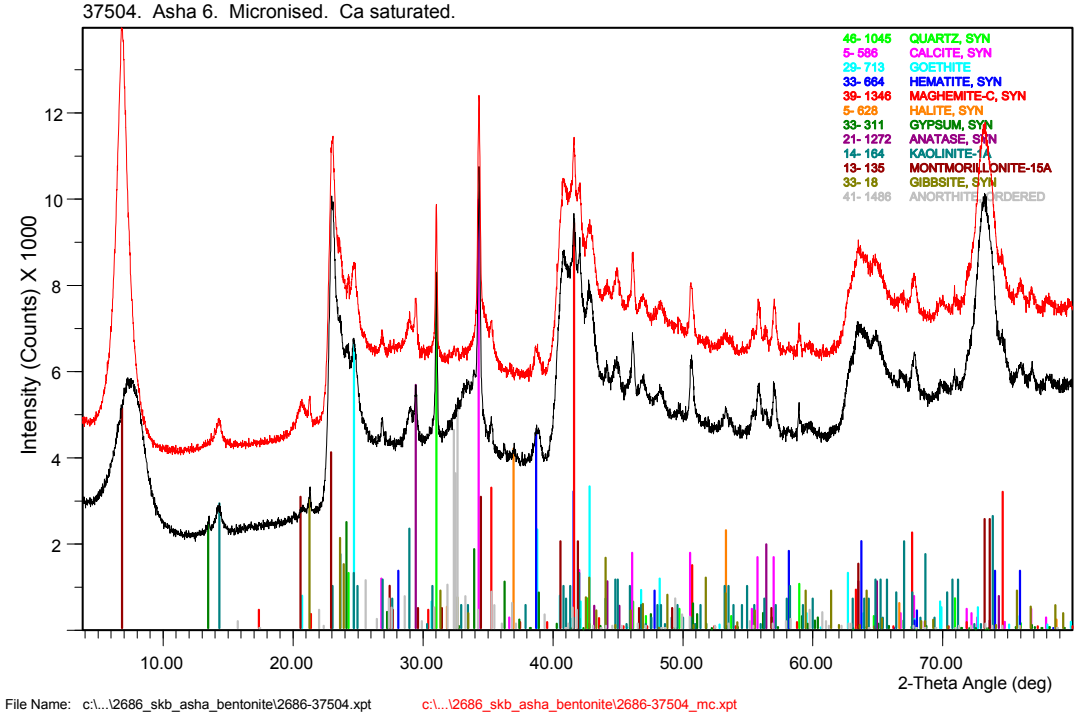

Asha 2012 Big bag no. 140

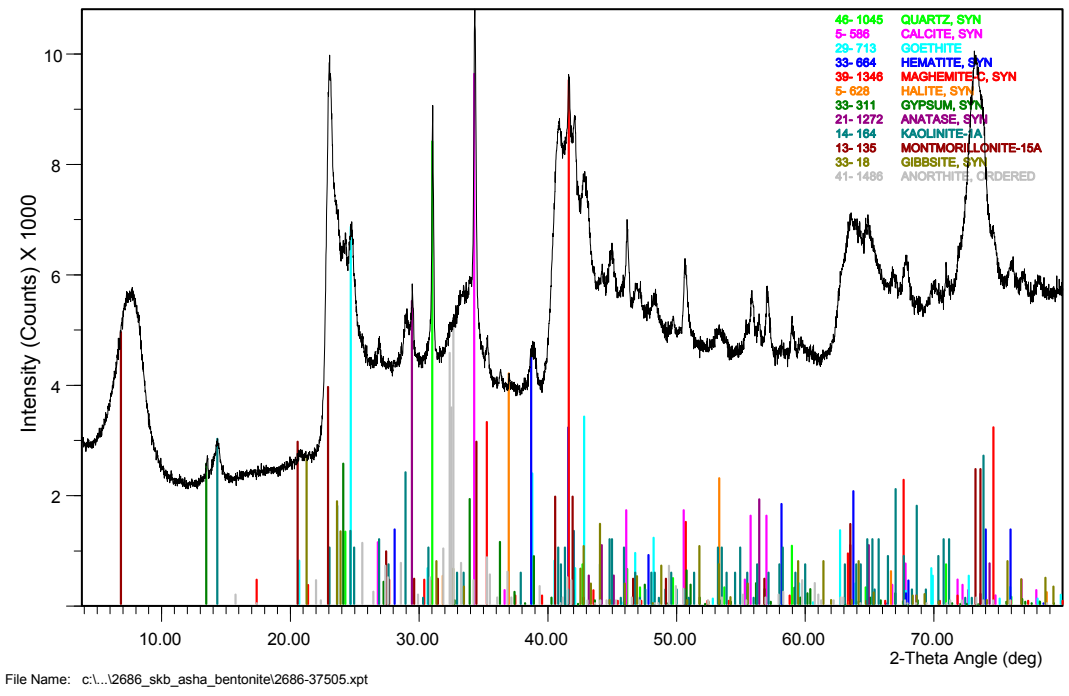

Asha 2012 Big bag no. 140

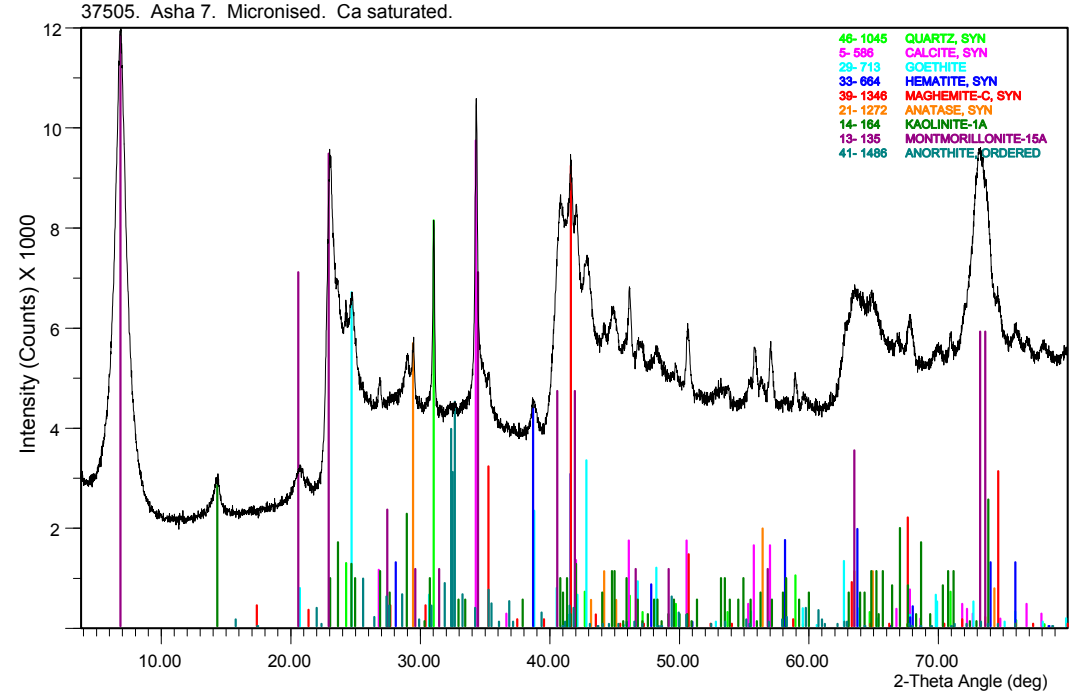

Asha 2012 Big bag no. 140

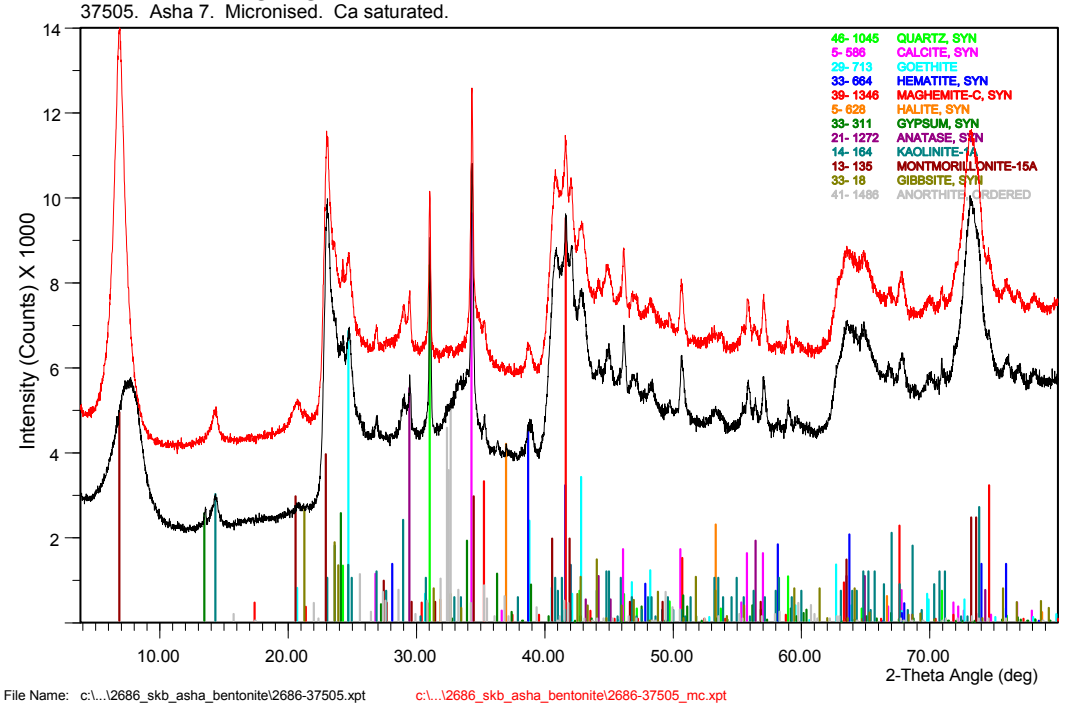

Asha 2012 Big bag no. 160

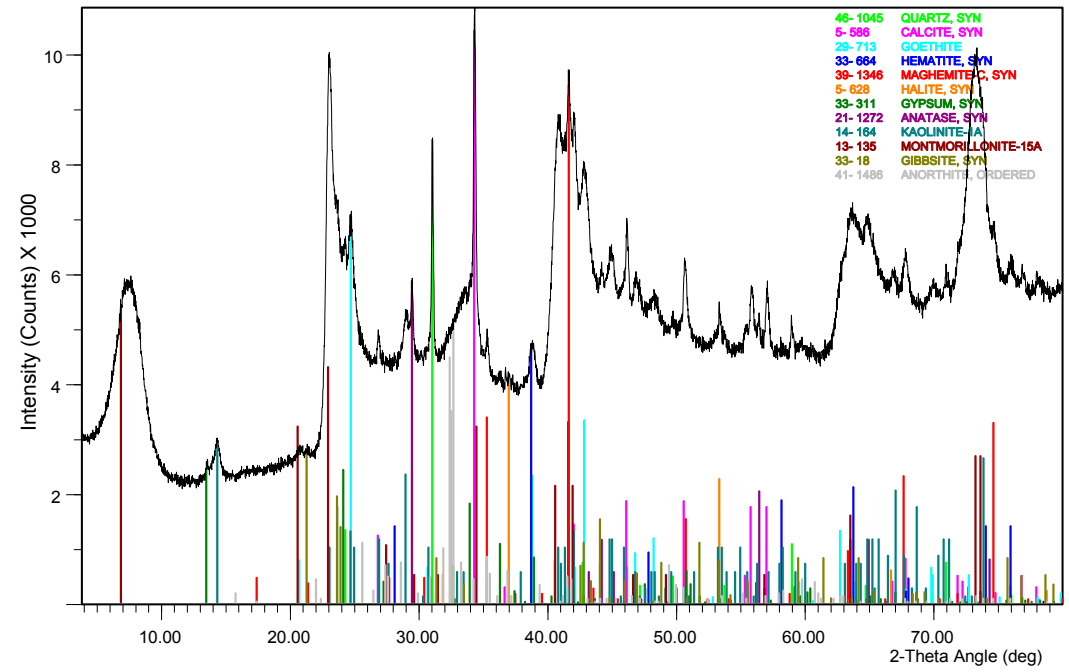

File Name: c:\...\2686_skb_asha_bentonite\2686-37506.xpt

Asha 2012 Big bag no. 160

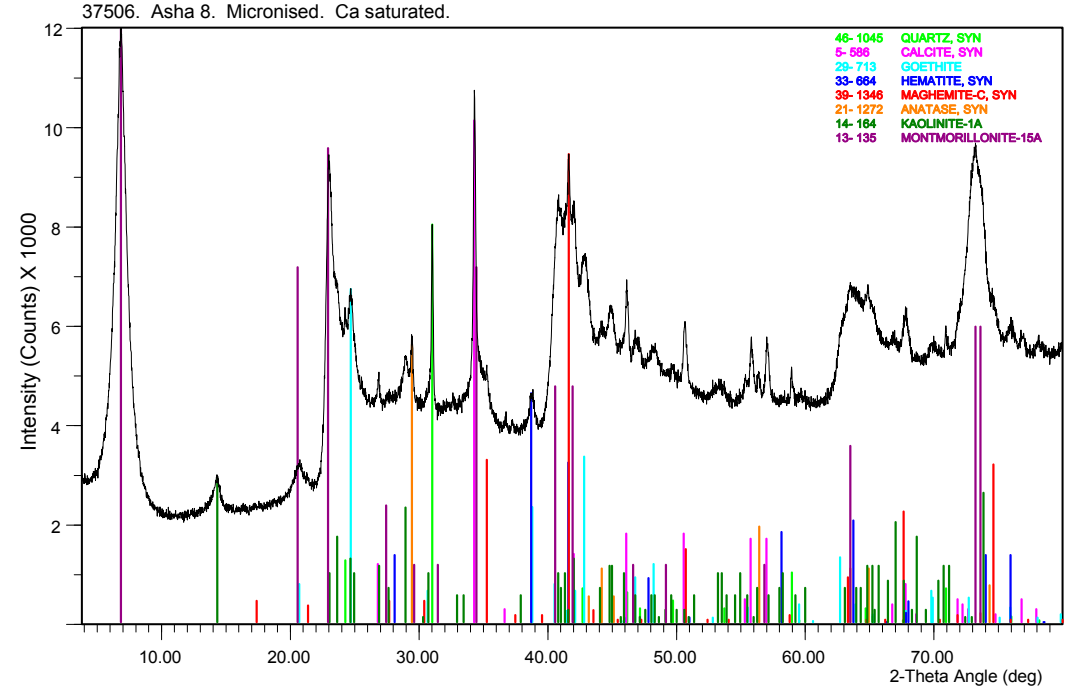

File Name: c:\...\2686_skb_asha_bentonite\2686-37506_mc.xpt

Asha 2012 Big bag no. 160

37506. Asha 8. Micronised. Ca saturated.

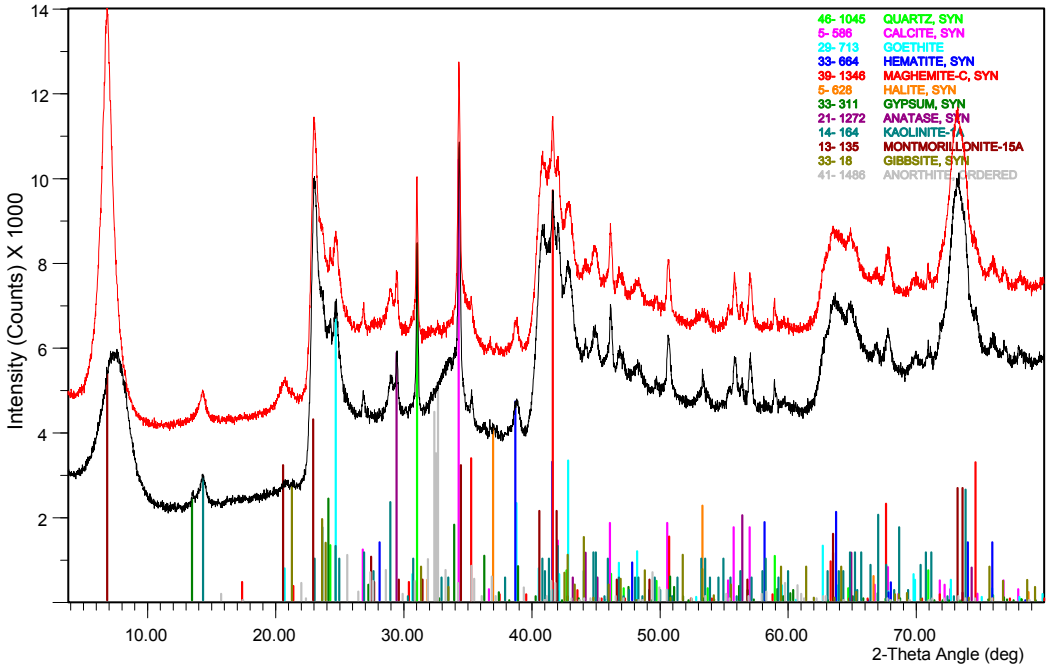

File Name: c:\...\2686_skb_asha_bentonite\2686-37506.xpt c:\...\2686_skb_asha_bentonite\2686-37506_mc.xpt

Asha 2012 Big bag no. 200

37507. Asha 9. Micronised.

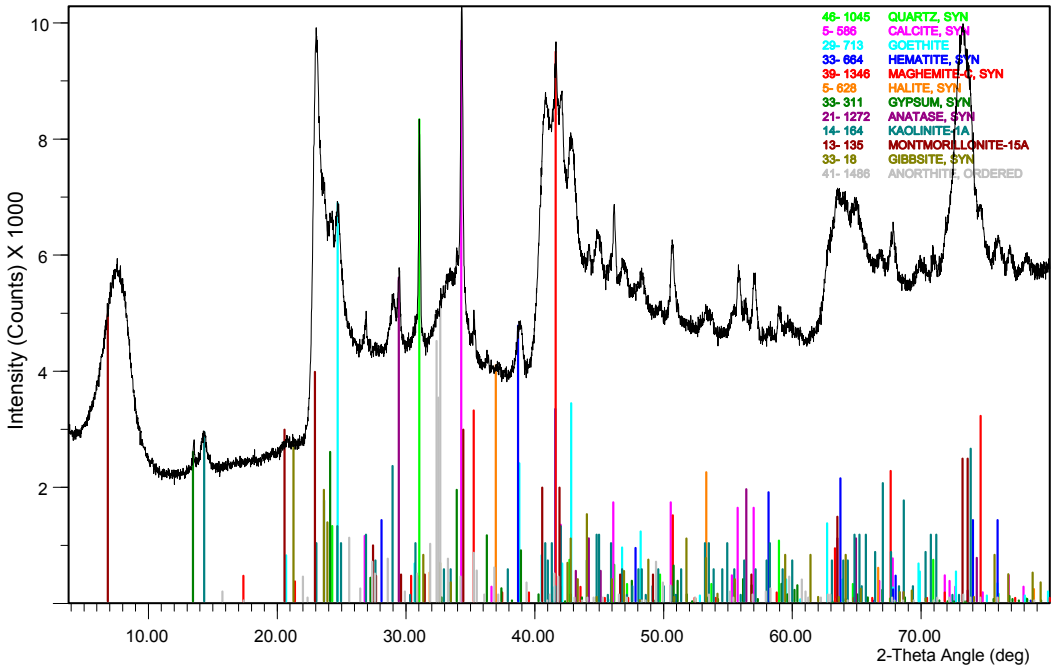

File Name: c:\...\2686_skb_asha_bentonite\2686-37507.xpt

Asha 2012 Big bag no. 200

37507. Asha 9. Micronised. Ca saturated.

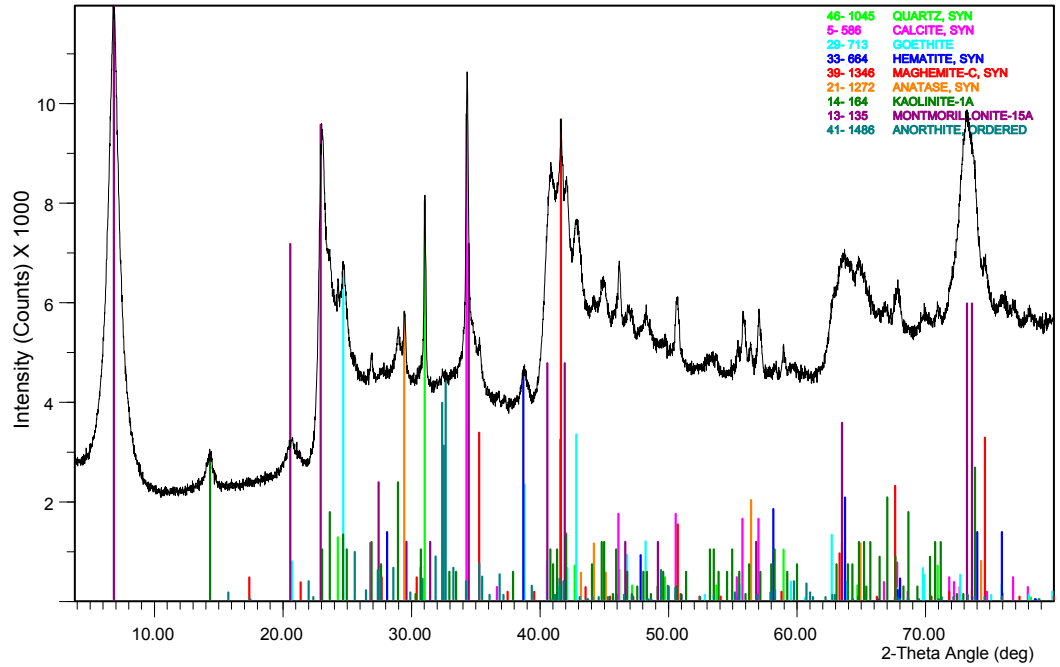

File Name: c:\...\2686_skb_asha_bentonite\2686-37507_mc.xpt

Asha 2012 Big bag no. 200

37507. Asha 9. Micronised. Ca saturated.

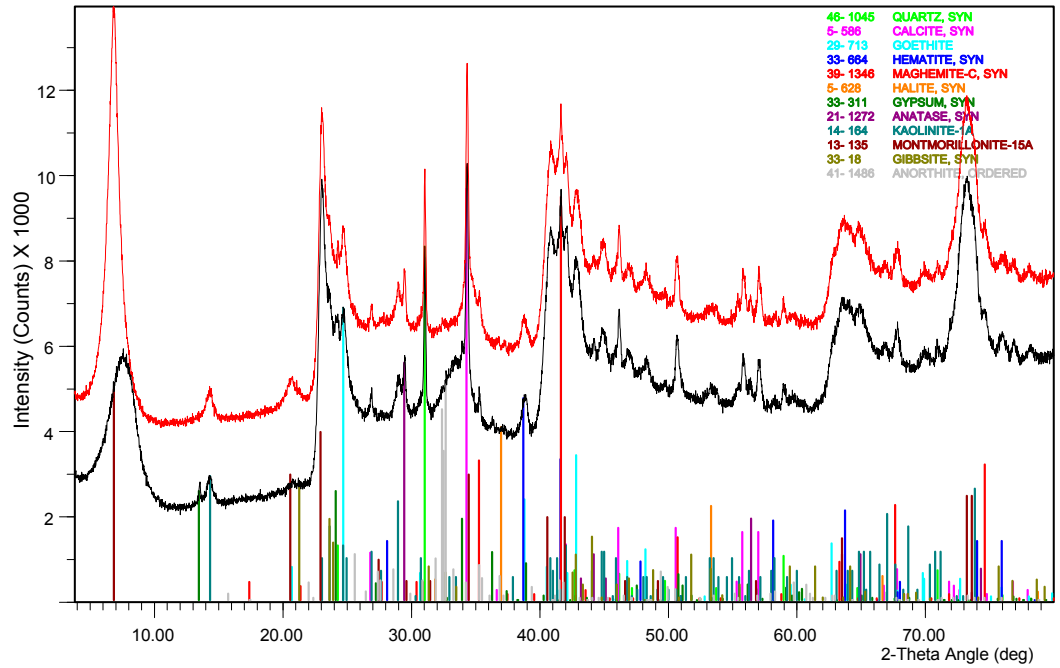

File Name: c:\...\2686_skb_asha_bentonite\2686-37507.xpt c:\...\2686_skb_asha_bentonite\2686-37507_mc.xpt

Asha 2012 Big bag no. 220

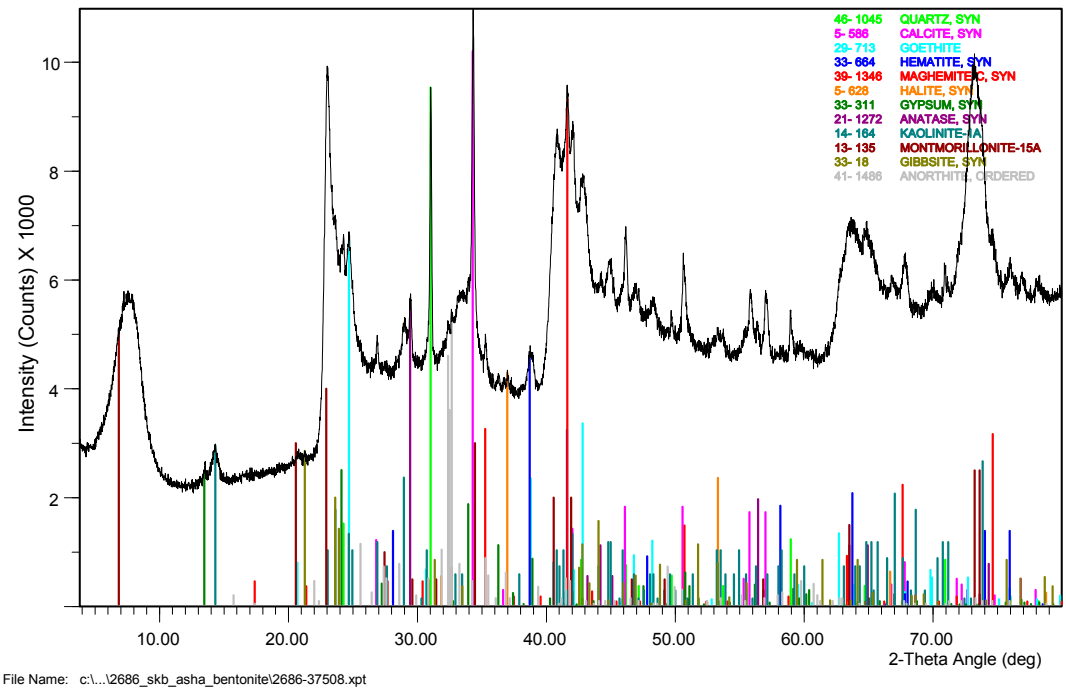

File Name: c:\...\2686_skb_asha_bentonite\2686-37508.xpt

Asha 2012 Big bag no. 220

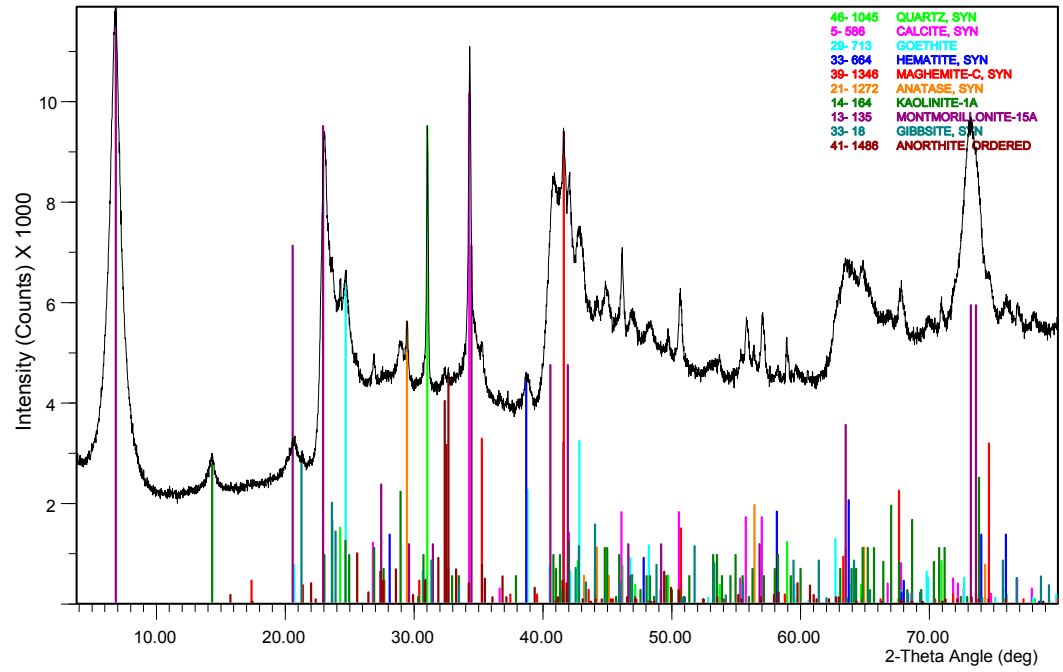

File Name: c:\...\2686_skb_asha_bentonite\2686-37508_mc.xpt

Asha 2012 Big bag no. 220

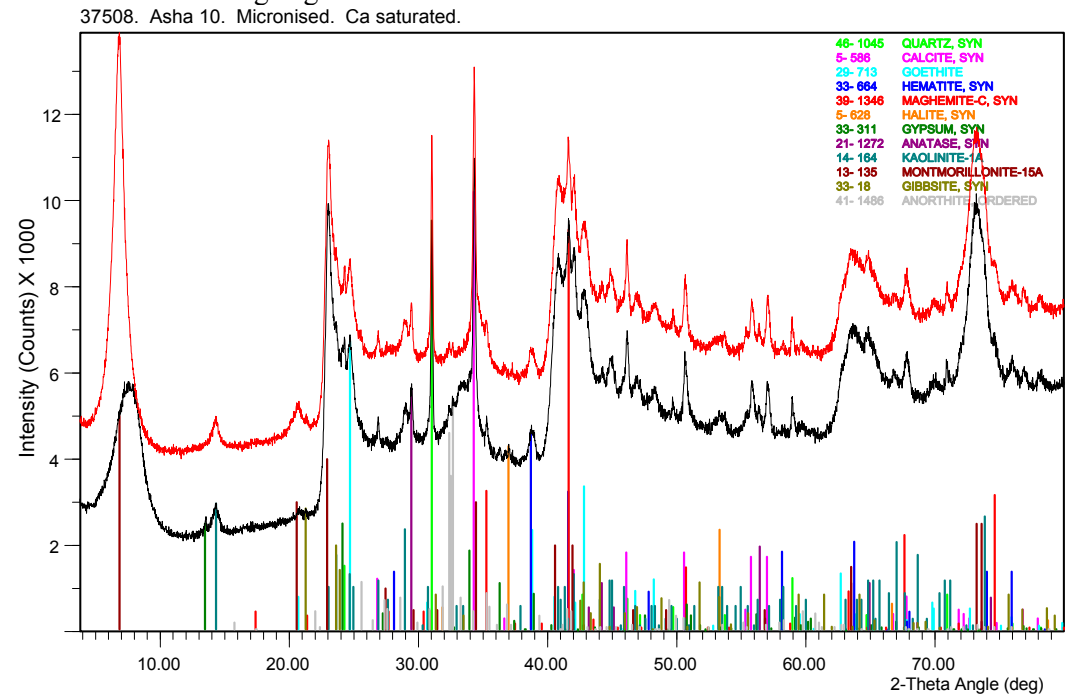

Asha 2012 Big bag no. 240

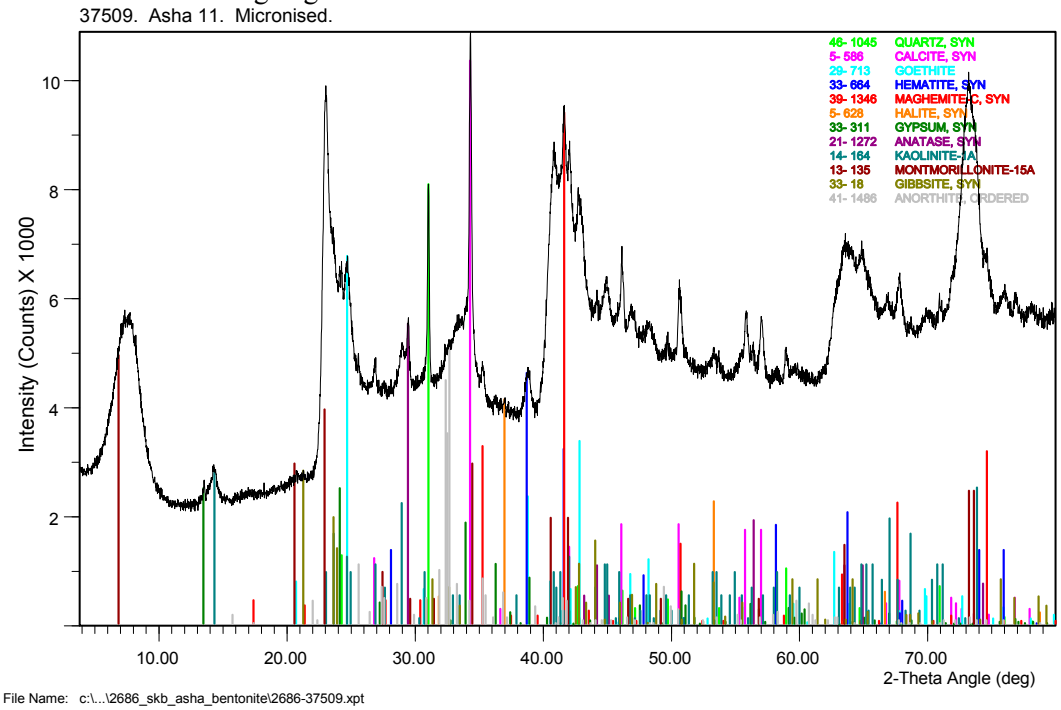

Asha 2012 Big bag no. 240

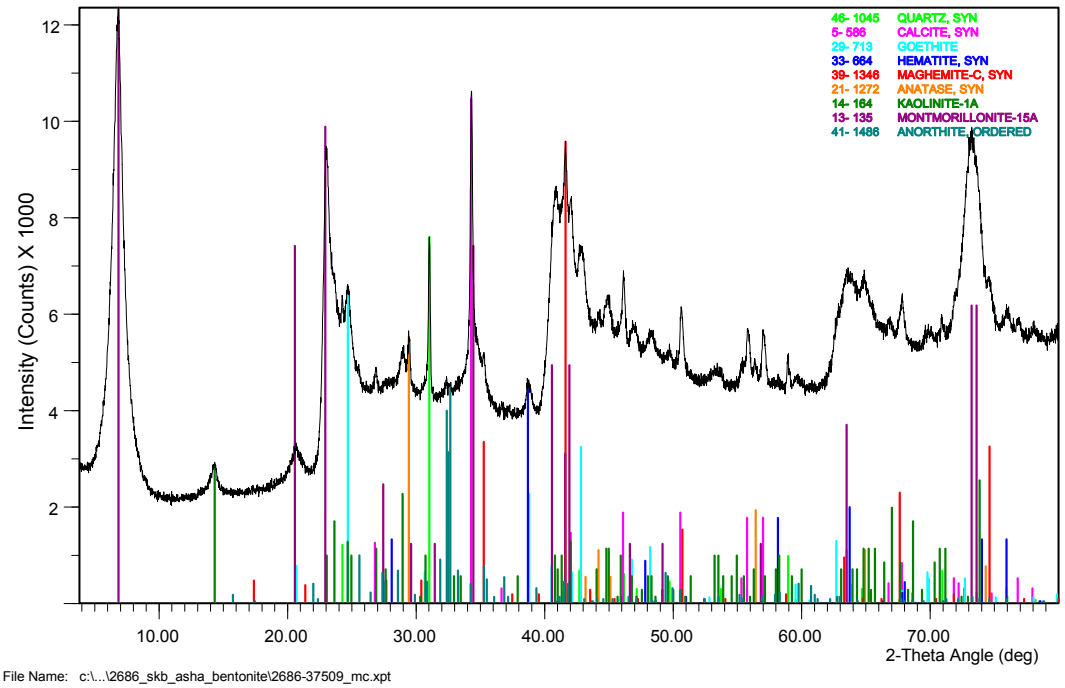

File Name: c:\...\2686_skb_asha_bentonite\2686-37509_mc.xpt

Asha 2012 Big bag no. 240

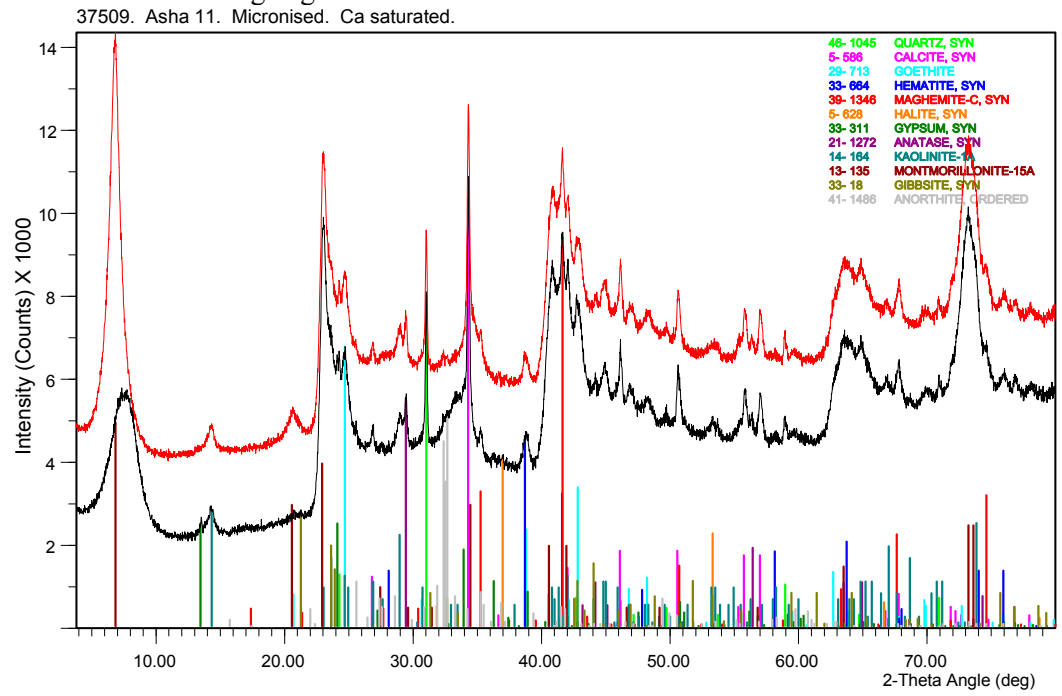

File Name: c:\...\2686_skb_asha_bentonite\2686-37509.xpt c:\...\2686_skb_asha_bentonite\2686-37509_mc.xpt

Asha 2012 Big bag no. 260

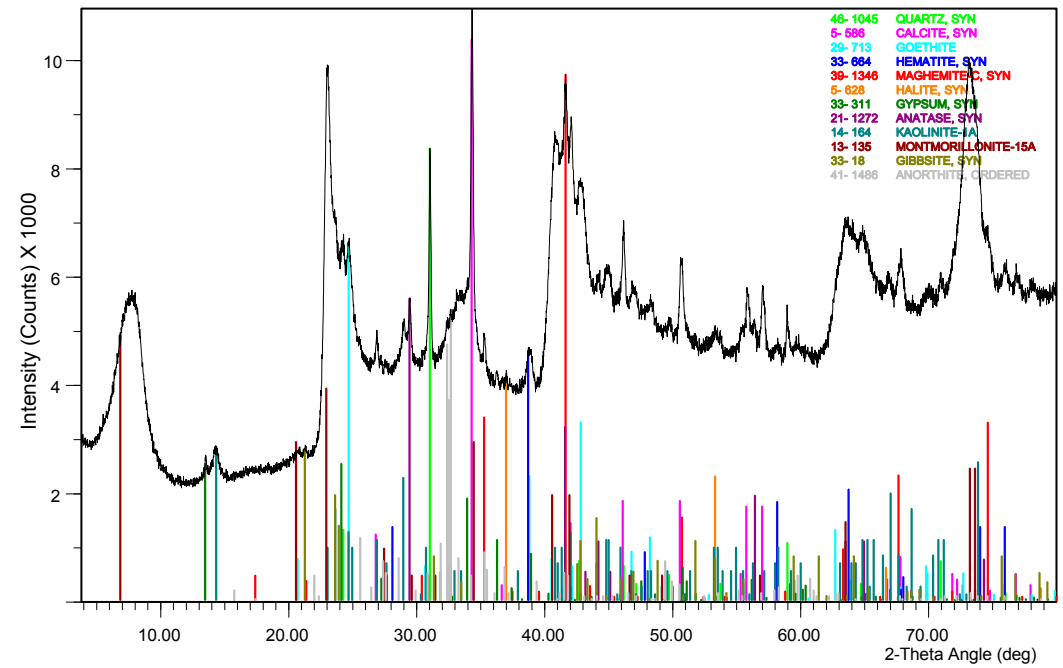

File Name: c:\...\2686_skb_asha_bentonite\2686-37510.xpt

Asha 2012 Big bag no. 260

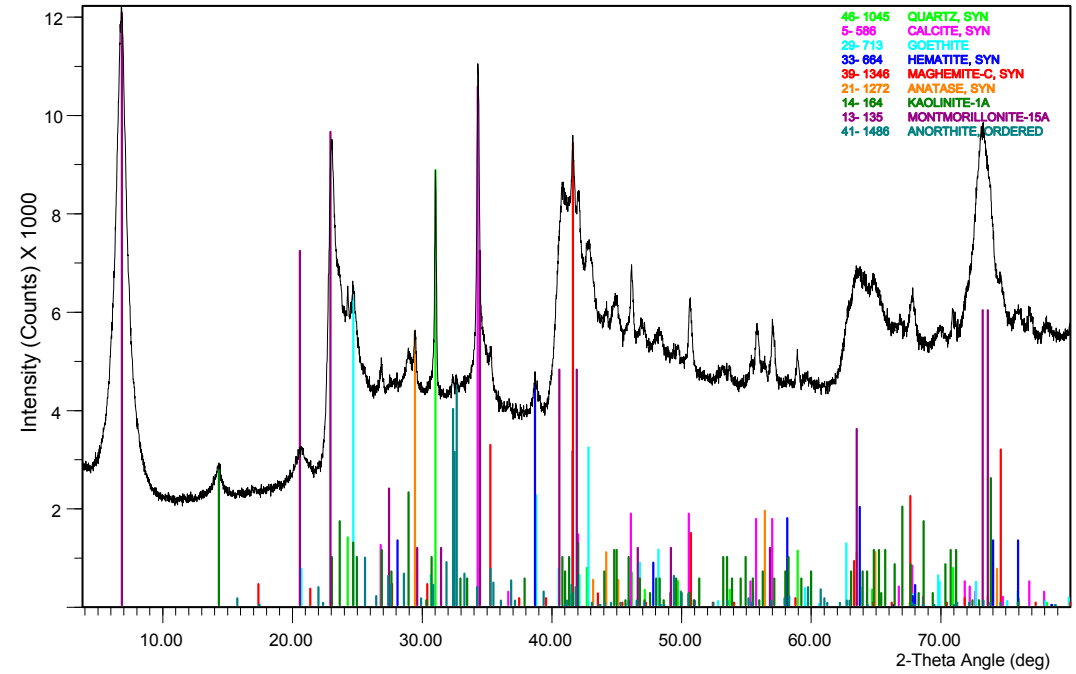

File Name: c:\...\2686_skb_asha_bentonite\2686-37510_mc.xpt

Asha 2012 Big bag no. 260

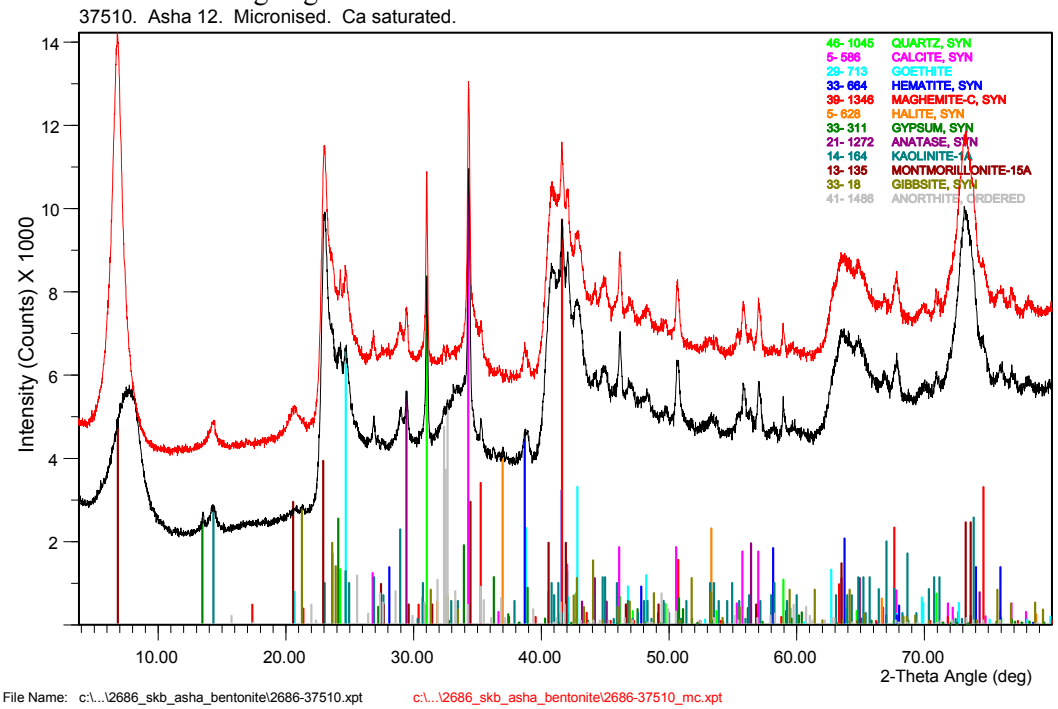

Asha 2012 Big bag no. 300

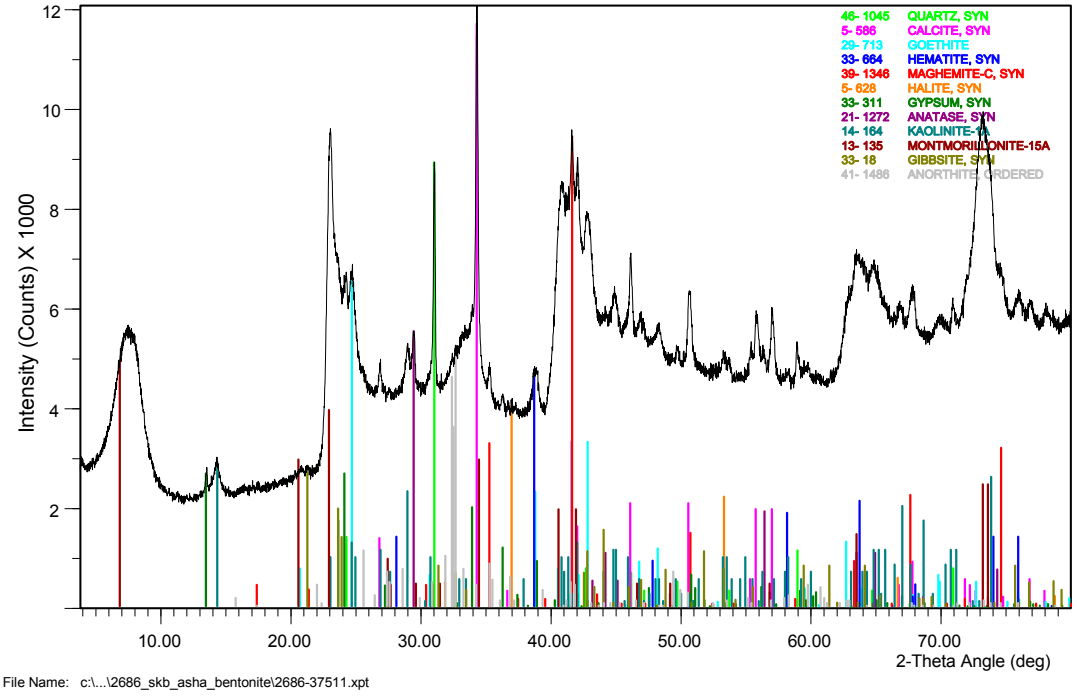

Asha 2012 Big bag no. 300

37511. Asha 13. Micronised. Ca saturated.

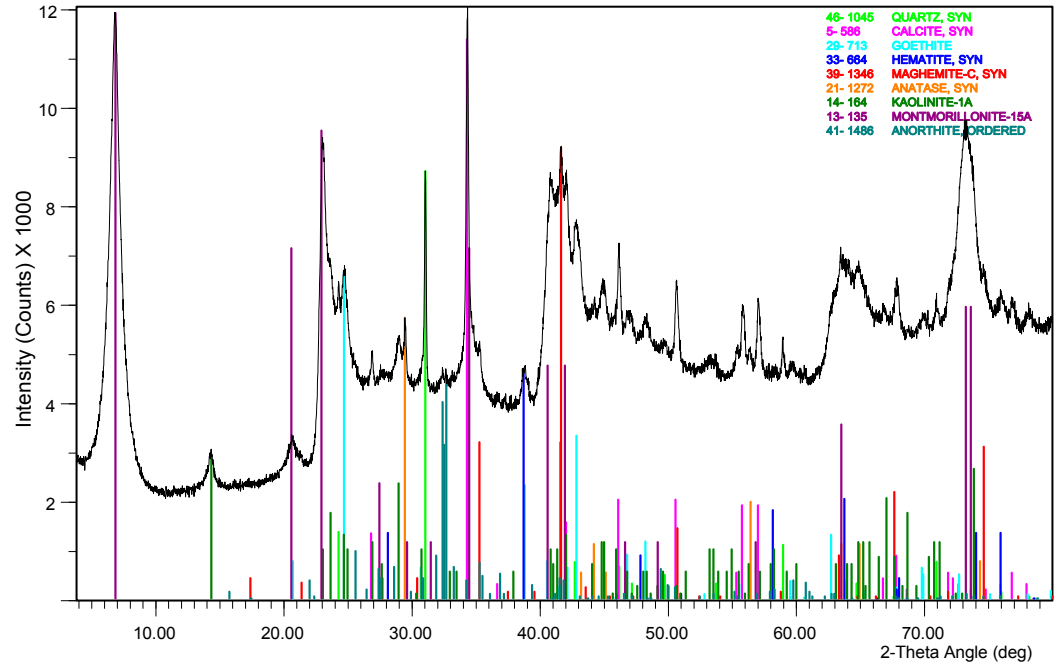

File Name: c:\...\2686_skb_asha_bentonite\2686-37511_mc.xpt

Asha 2012 Big bag no. 300

37511. Asha 13. Micronised. Ca saturated.

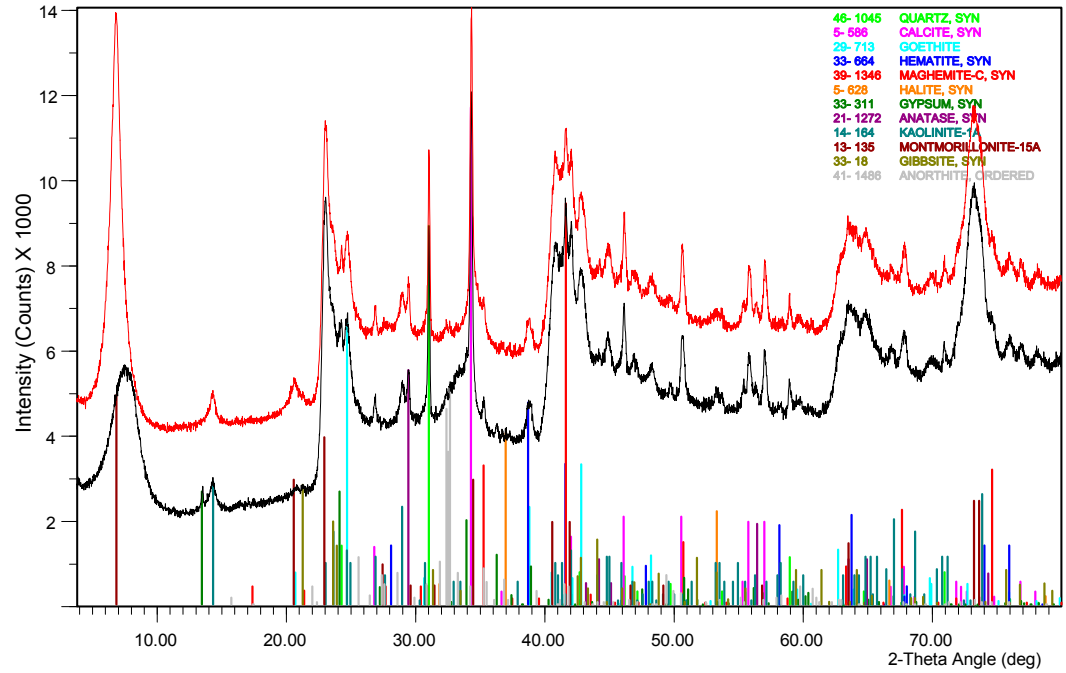

File Name: c:\...\2686_skb_asha_bentonite\2686-37511.xpt c:\...\2686_skb_asha_bentonite\2686-37511_mc.xpt

Asha 2012 Big bag no. 320

37512. Asha 14. Micronised.

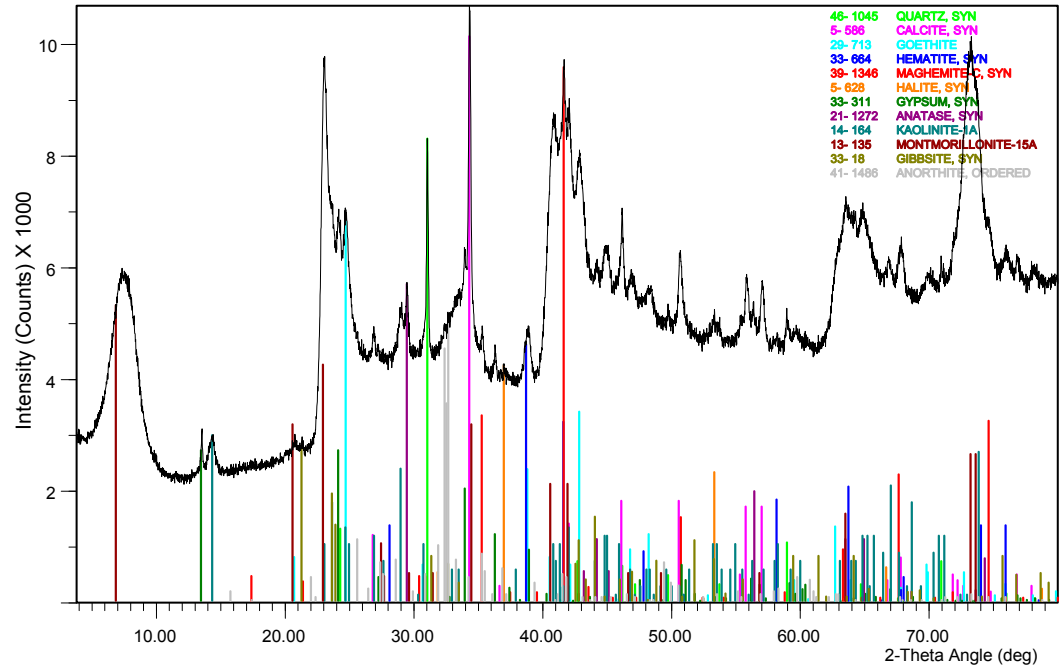

File Name: c:\...\2686_skb_asha_bentonite\2686-37512.xpt

Asha 2012 Big bag no. 320

37512. Asha 14. Micronised. Ca saturated.

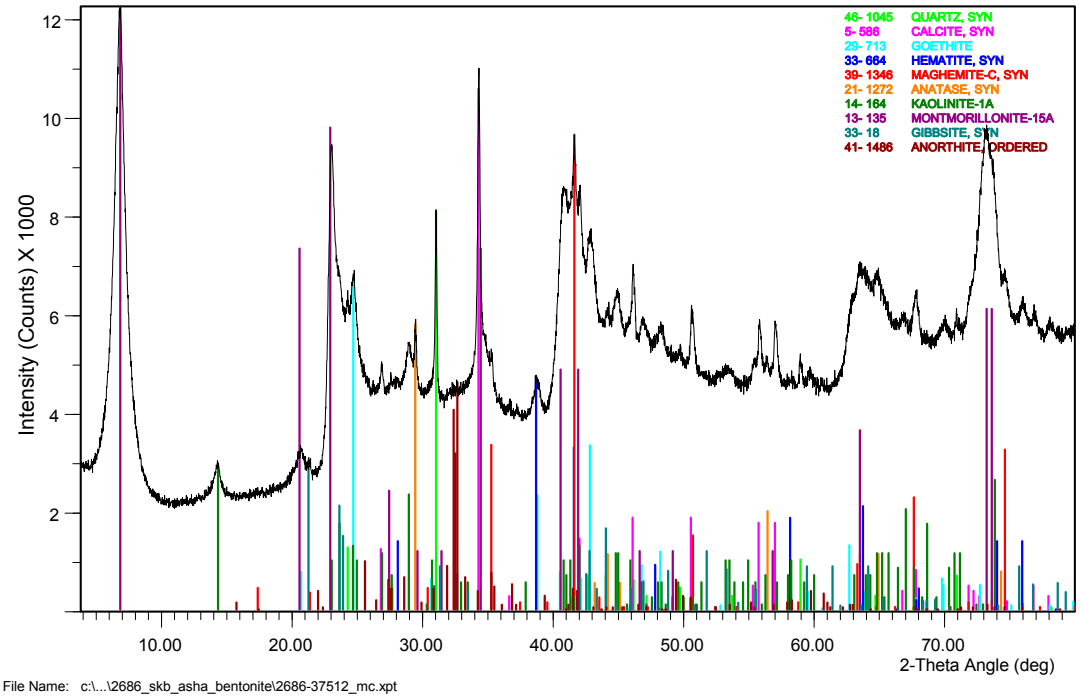

File Name: c:\...\2686_skb_asha_bentonite\2686-37512_mc.xpt

Asha 2012 Big bag no. 320

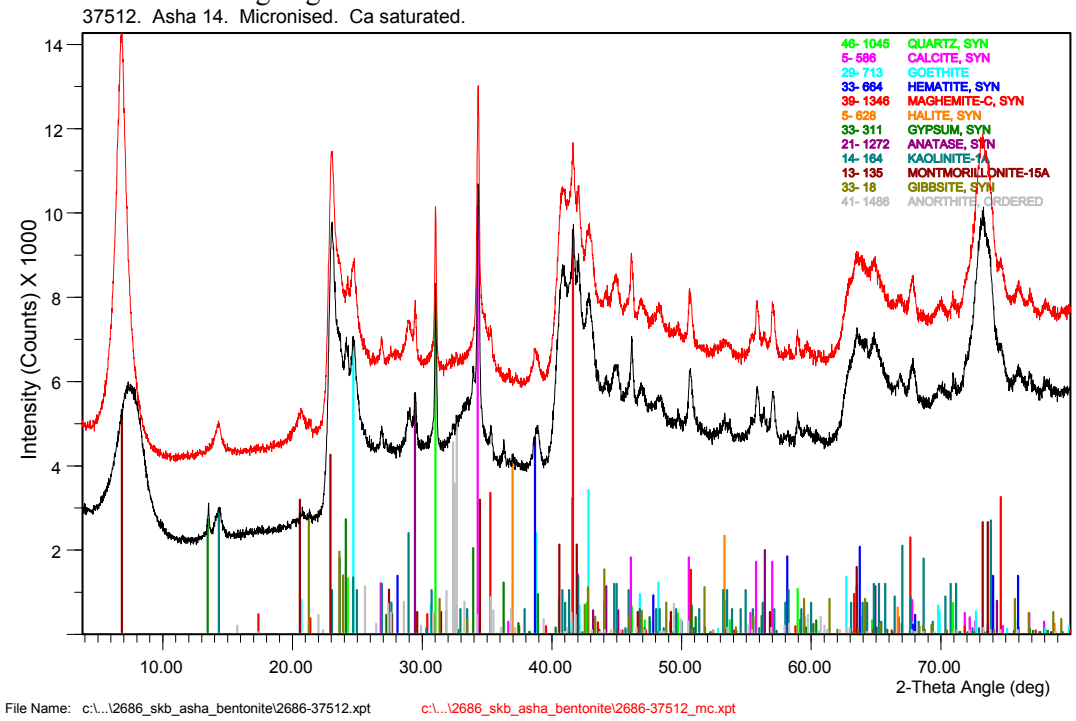

Asha 2012 Big bag no. 340

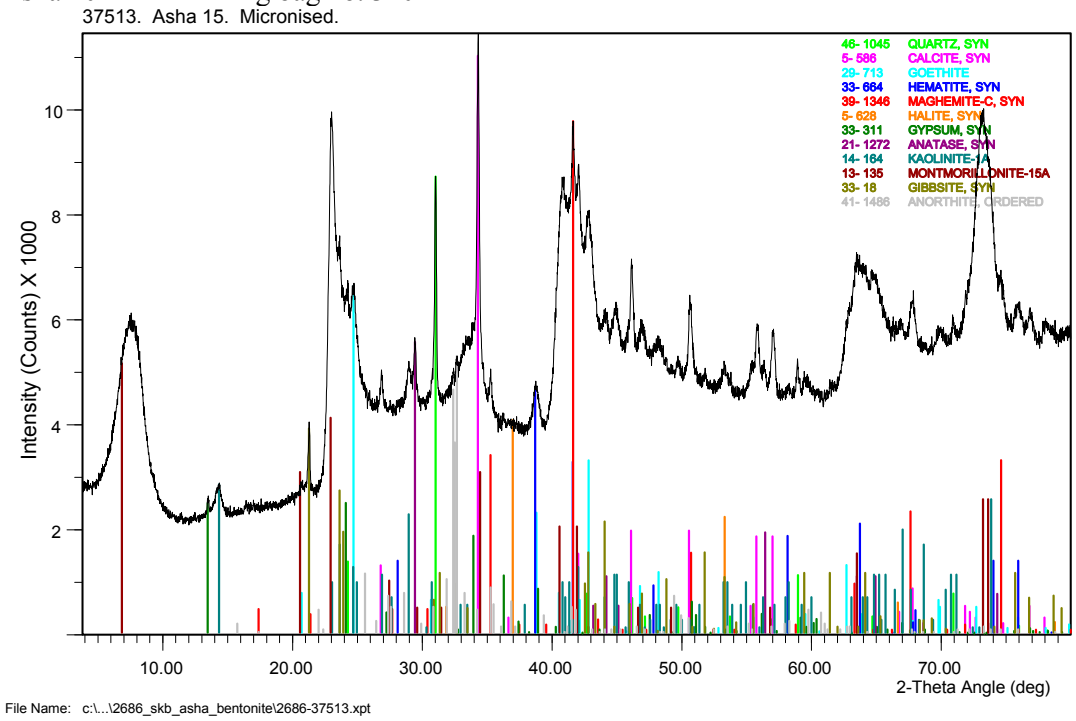

Asha 2012 Big bag no. 340

37513. Asha 15. Micronised. Ca saturated.

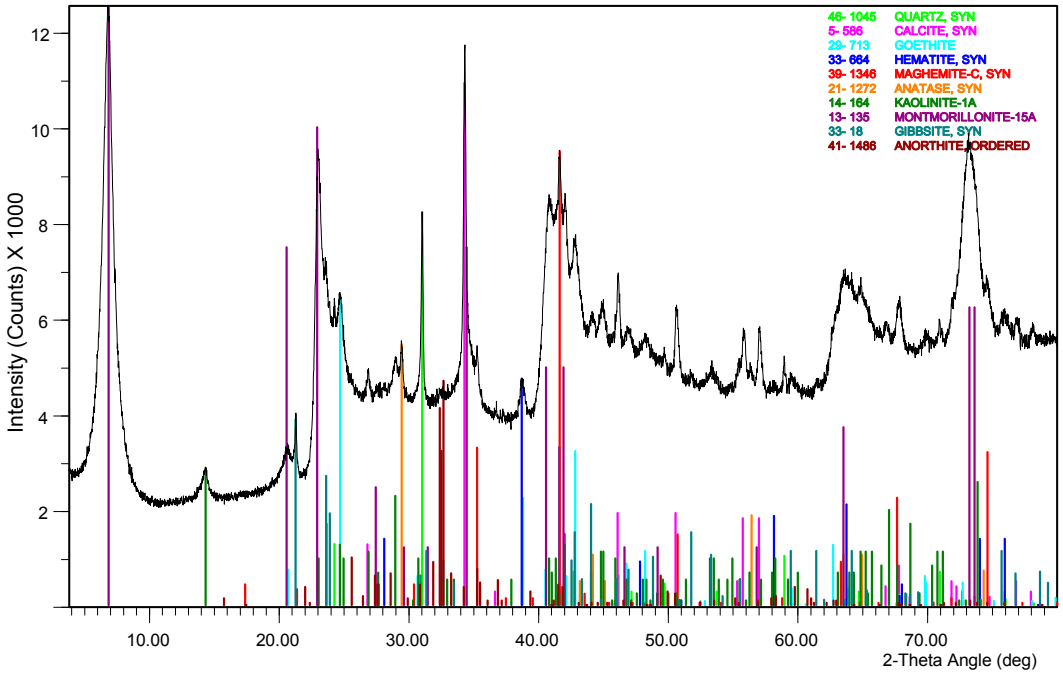

File Name: c:\...\2686_skb_asha_bentonite\2686-37513_mc.xpt

Asha 2012 Big bag no. 340

37513. Asha 15. Micronised. Ca saturated.

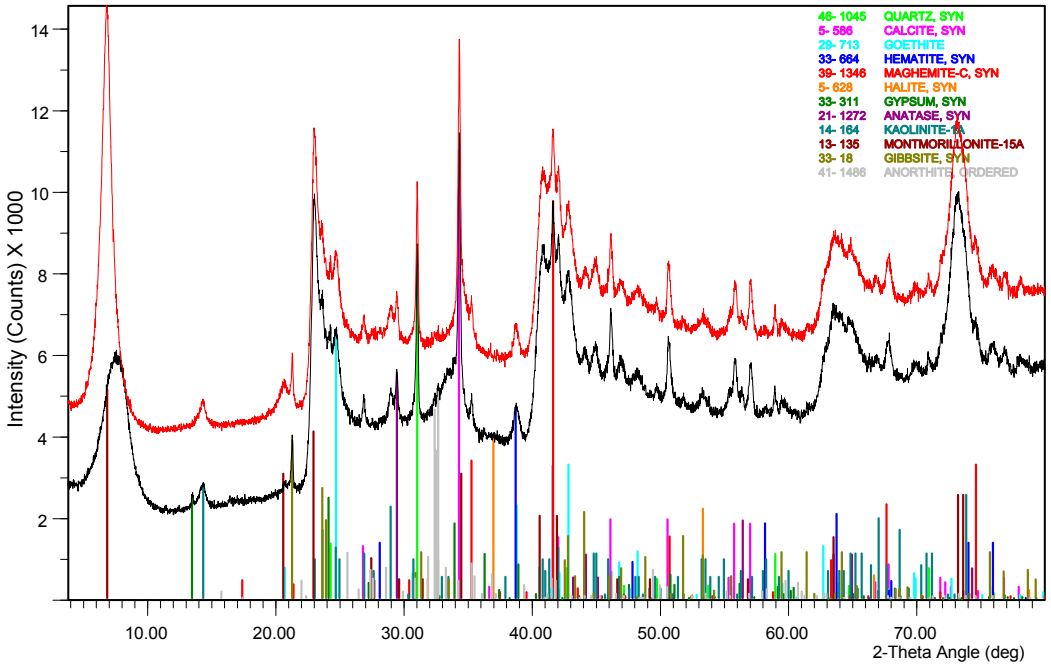

File Name: c:\...\2686_skb_asha_bentonite\2686-37513.xpt c:\...\2686_skb_asha_bentonite\2686-37513_mc.xpt

Asha 2012 Big bag no. 360

37514. Asha 16. Micronised.

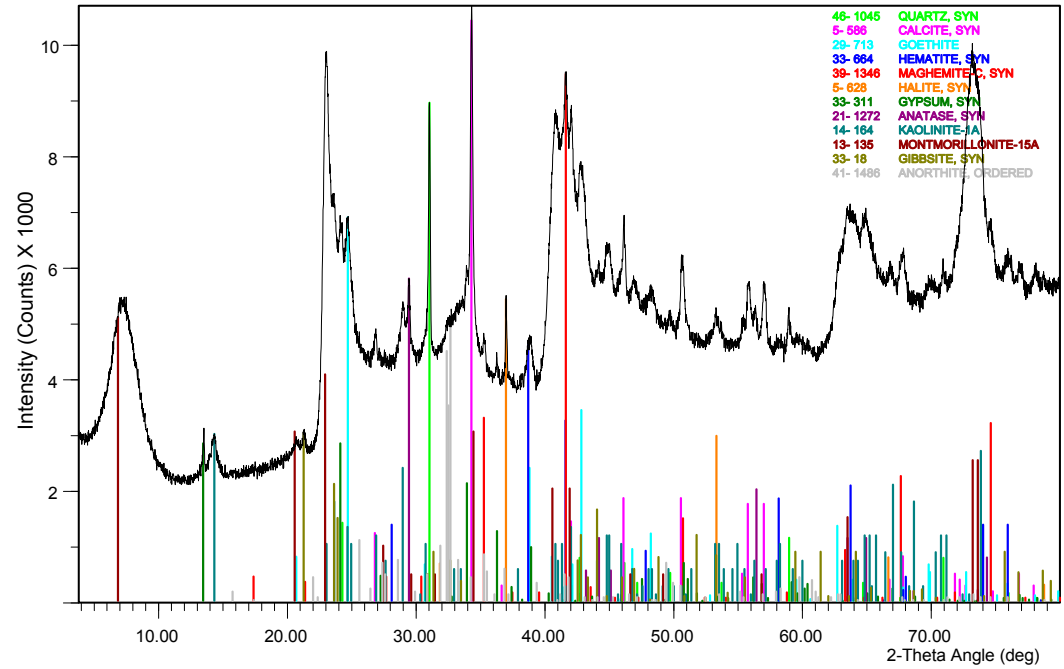

File Name: c:\...\2686_skb_asha_bentonite\2686-37514.xpt

Asha 2012 Big bag no. 360

37514. Asha 16. Micronised. Ca saturated.

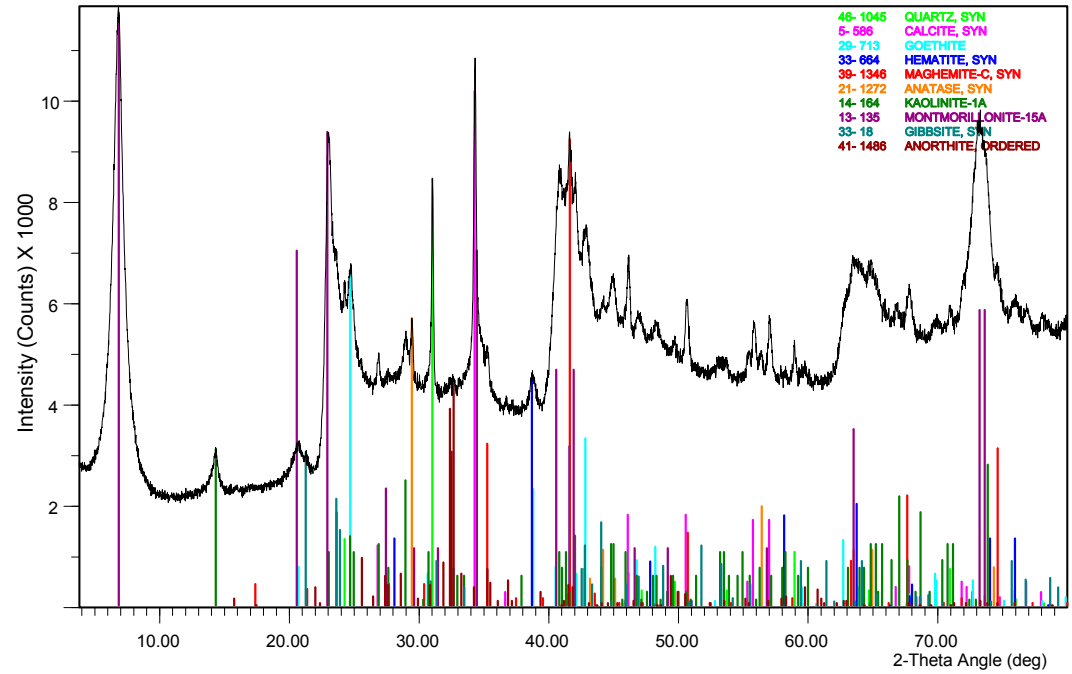

File Name: c:\...\2686_skb_asha_bentonite\2686-37514_mc.xpt

Asha 2012 Big bag no. 360

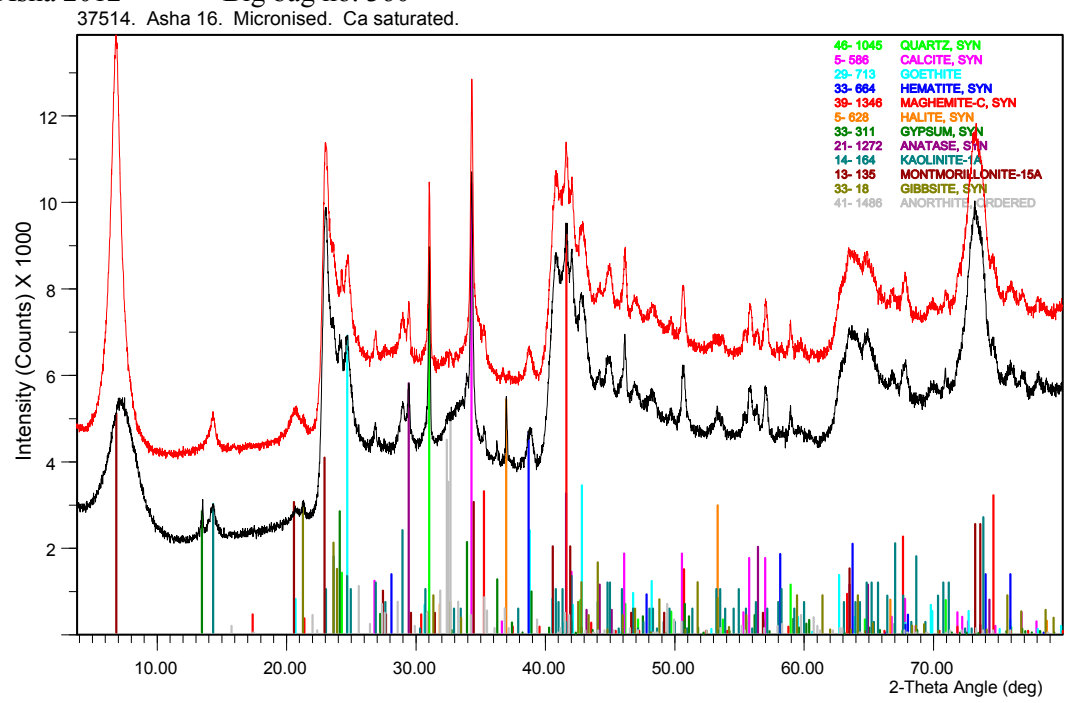

Asha 2012 Big bag no. 400

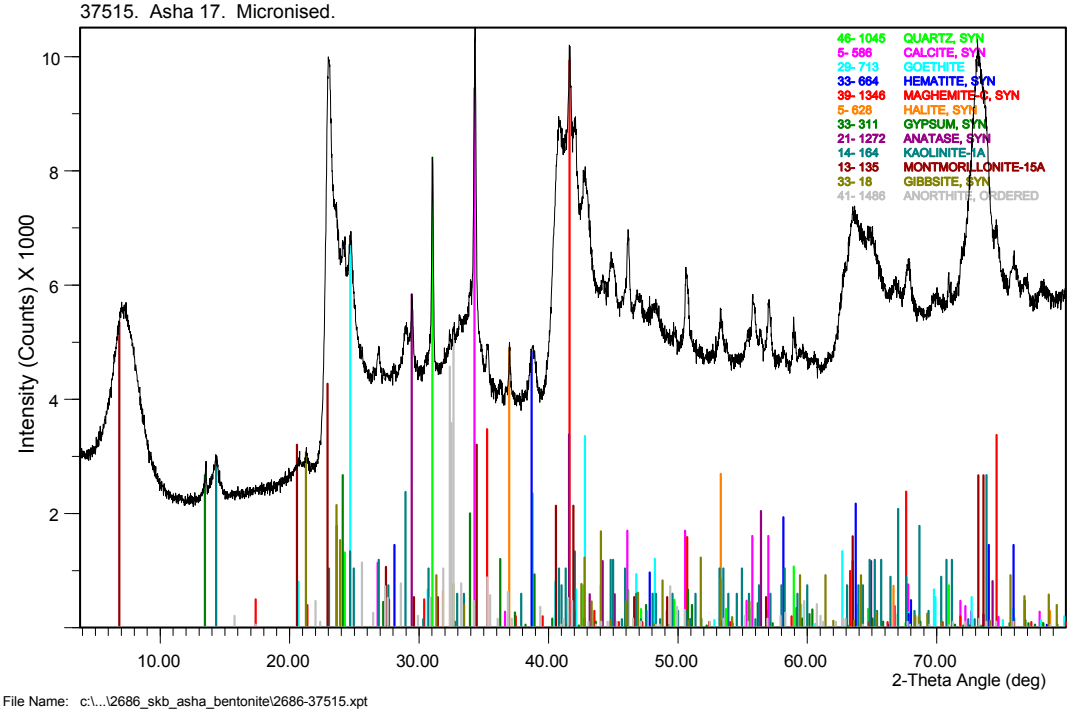

Asha 2012 Big bag no. 400

37515. Asha 17. Micronised. Ca saturated.

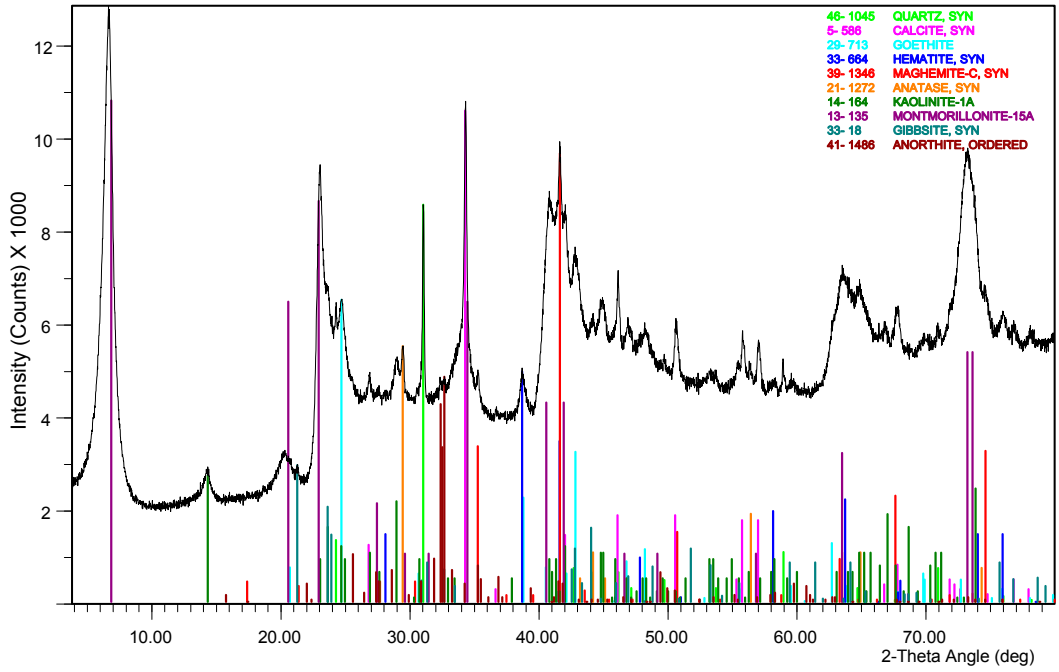

File Name: c:\...\2686_skb_asha_bentonite\2686-37515_mc.xpt

Asha 2012 Big bag no. 400

37515. Asha 17. Micronised. Ca saturated.

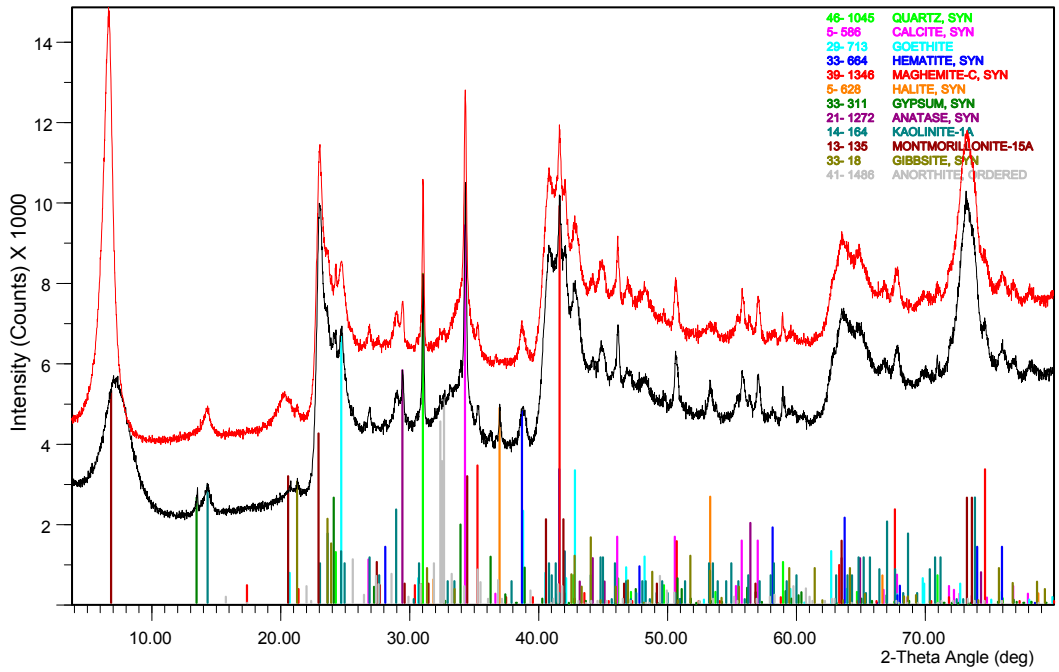

File Name: c:\...\2686_skb_asha_bentonite\2686-37515.xpt c:\...\2686_skb_asha_bentonite\2686-37515_mc.xpt

Asha 2012 Big bag no. 420

37516. Asha 18. Micronised.

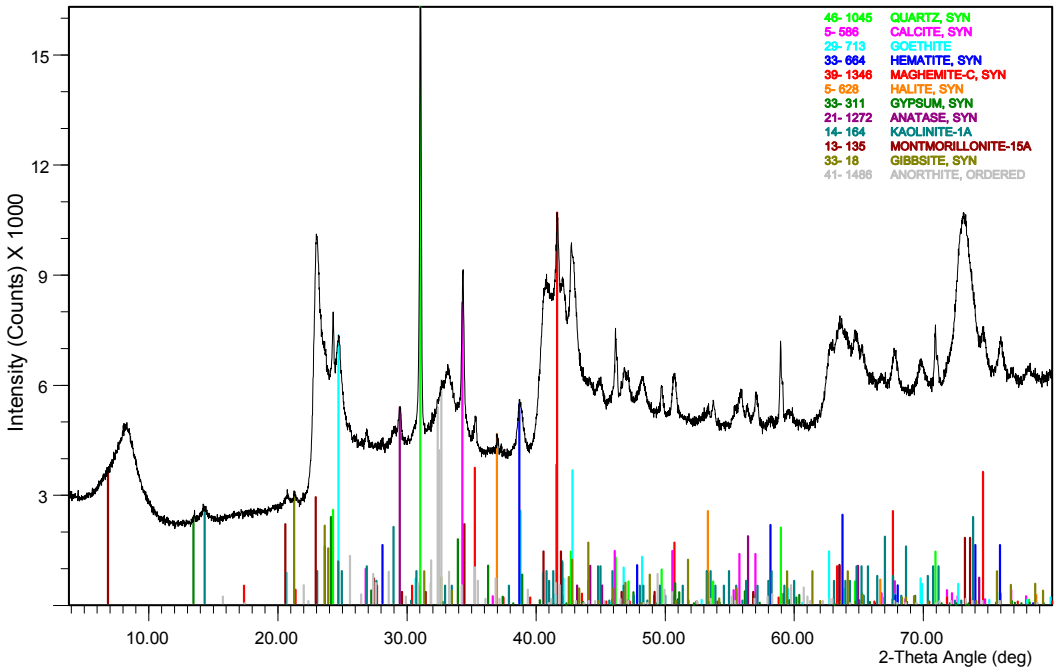

File Name: c:\...\2686_skb_asha_bentonite\2686-37516.xpt

Asha 2012 Big bag no. 420

37516. Asha 18. Micronised. Ca saturated.

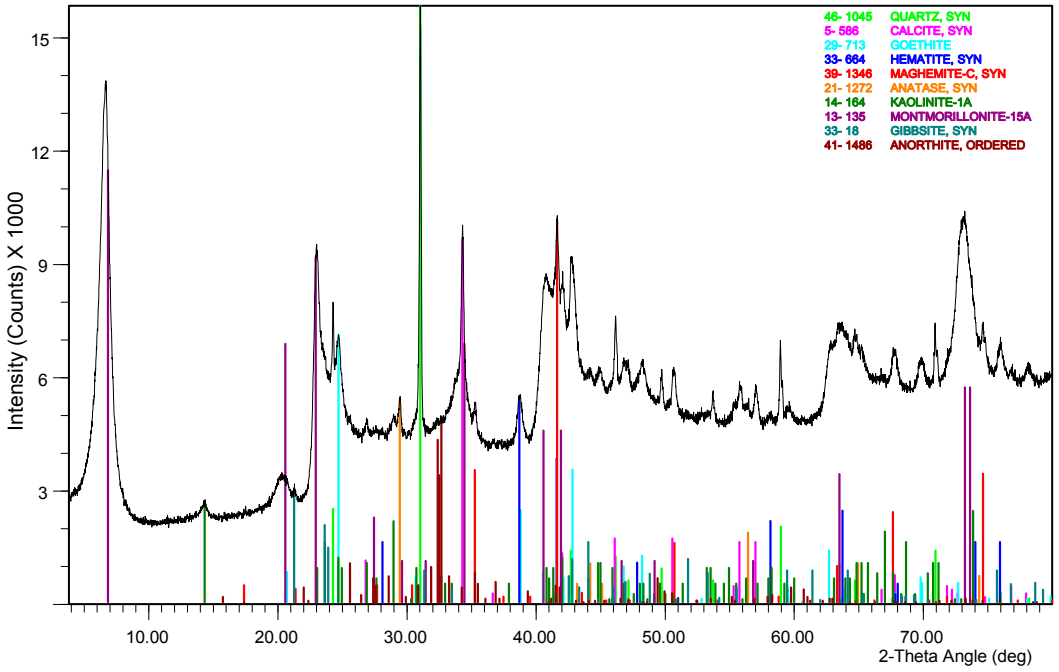

File Name: c:\...\2686_skb_asha_bentonite\2686-37516_mc.xpt

Asha 2012 Big bag no. 420

37516. Asha 18. Micronised. Ca saturated.

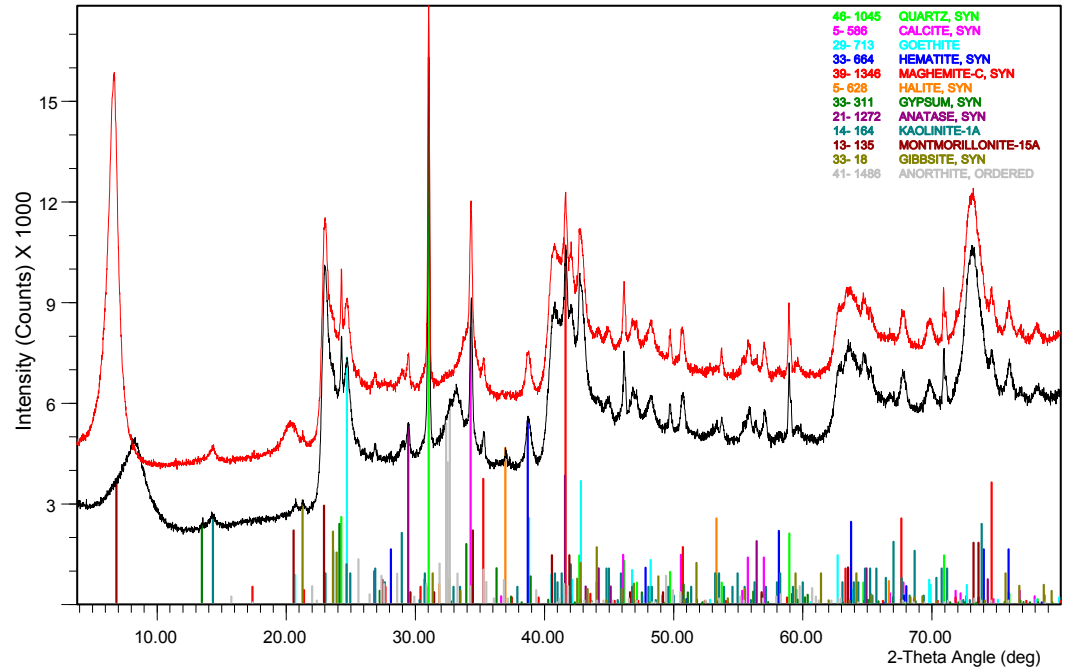

File Name: c:\...\2686_skb_asha_bentonite\2686-37516.xpt c:\...\2686_skb_asha_bentonite\2686-37516_mc.xpt

Asha 2012 Big bag no. 440

37517. Asha 19. Micronised.

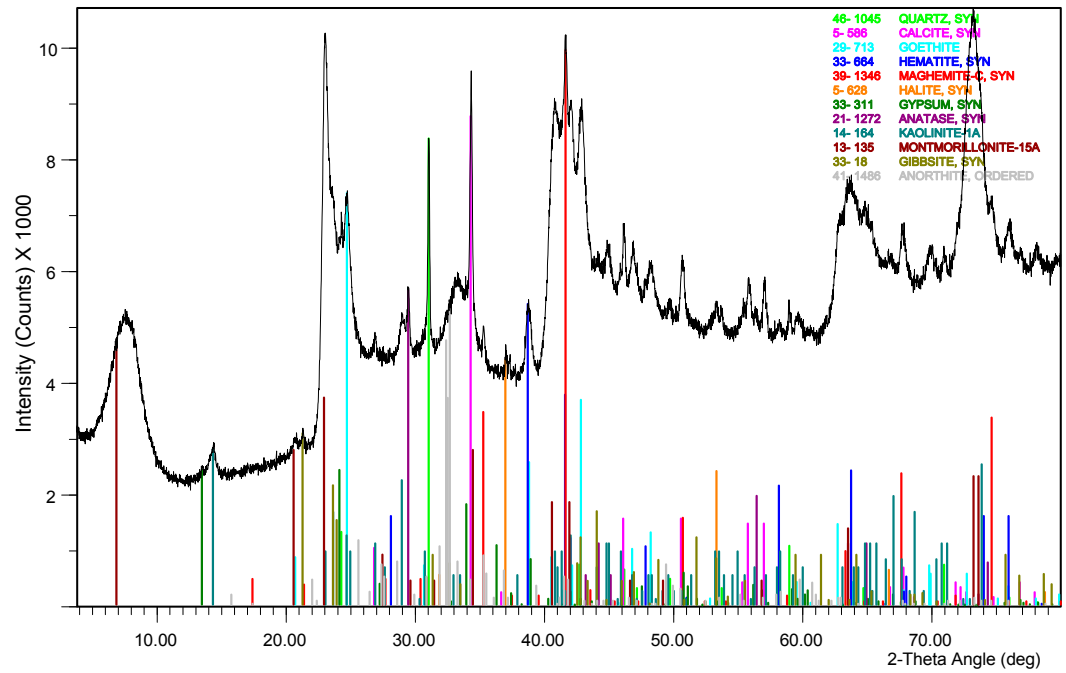

File Name: c:\...\2686_skb_asha_bentonite\2686-37517.xpt

Asha 2012 Big bag no. 440

37517. Asha 19. Micronised. Ca saturated.

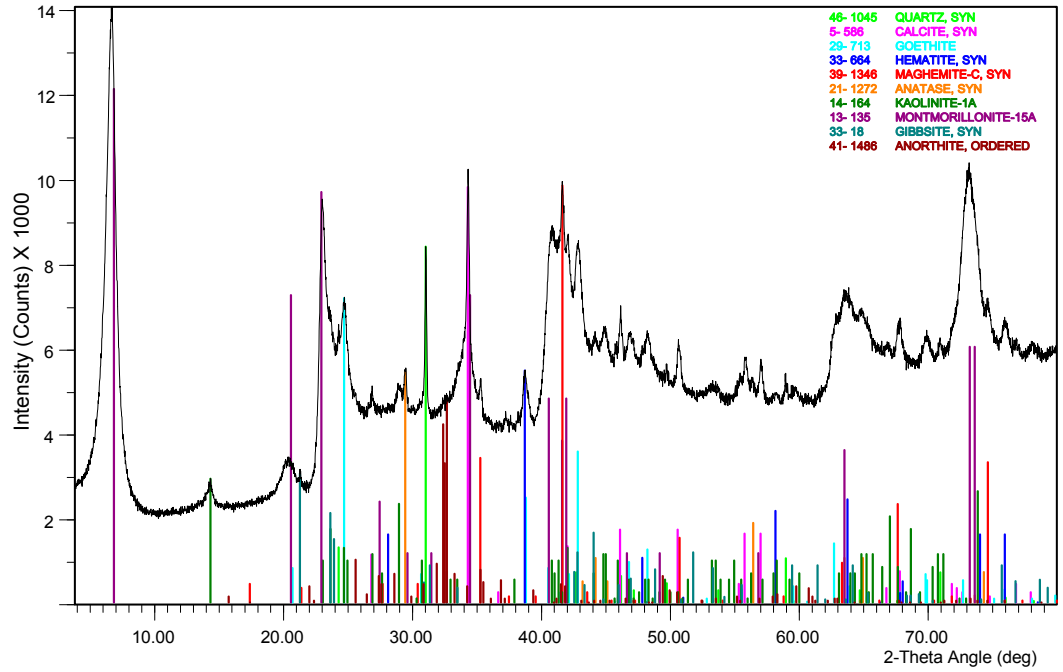

File Name: c:\...\2686_skb_asha_bentonite\2686-37517_mc.xpt

Asha 2012 Big bag no. 440

37517. Asha 19. Micronised. Ca saturated.

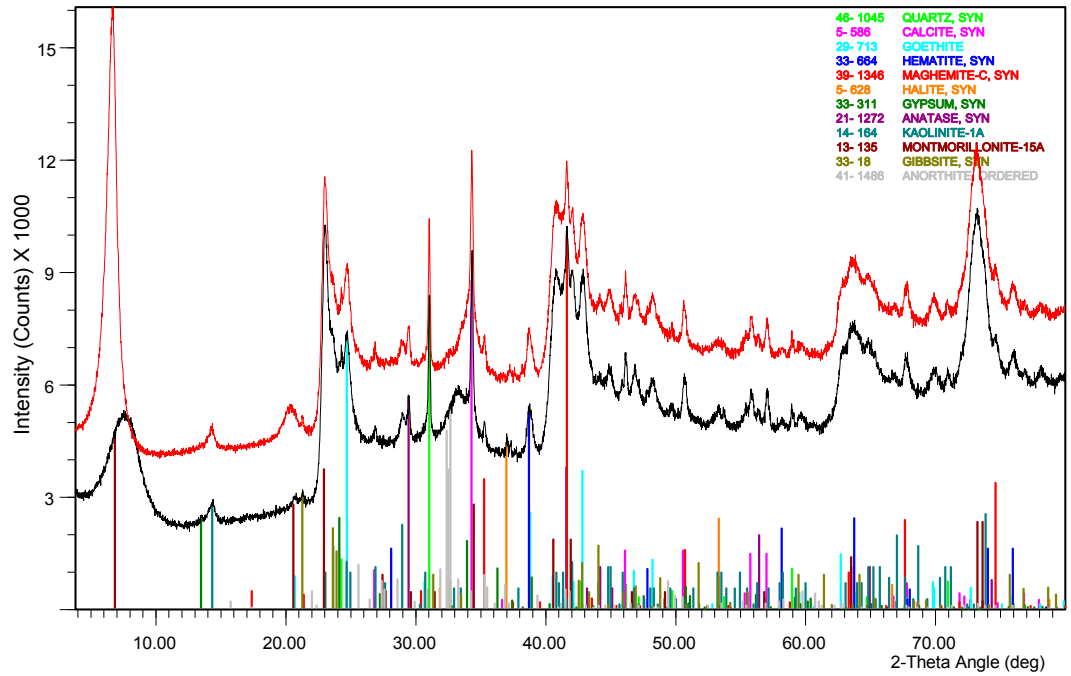

File Name: c:\...\2686_skb_asha_bentonite\2686-37517.xpt c:\...\2686_skb_asha_bentonite\2686-37517_mc.xpt

Asha 2012 Big bag no. 460

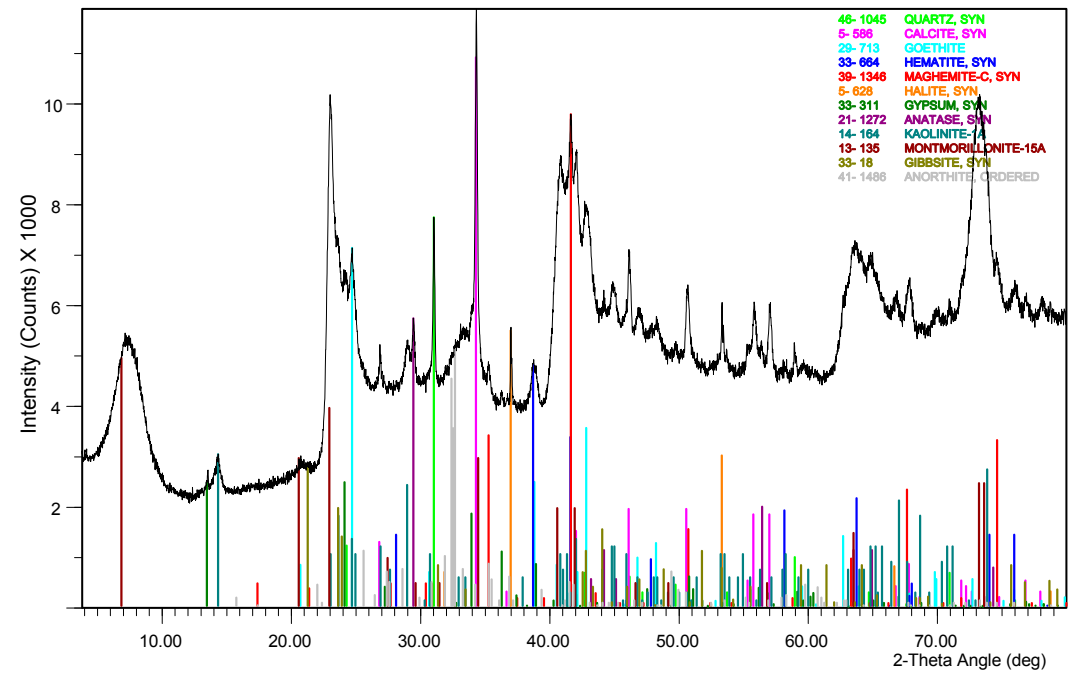

Asha 2012 Big bag no. 460

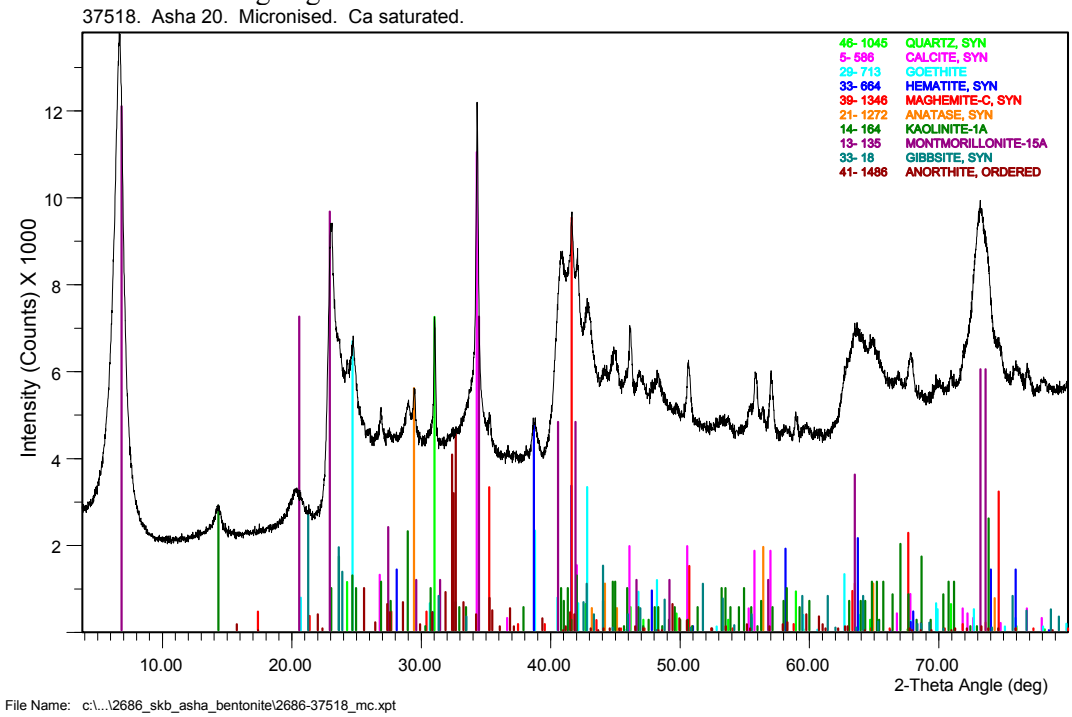

Asha 2012 Big bag no. 460

37518. Asha 20. Micronised. Ca saturated.

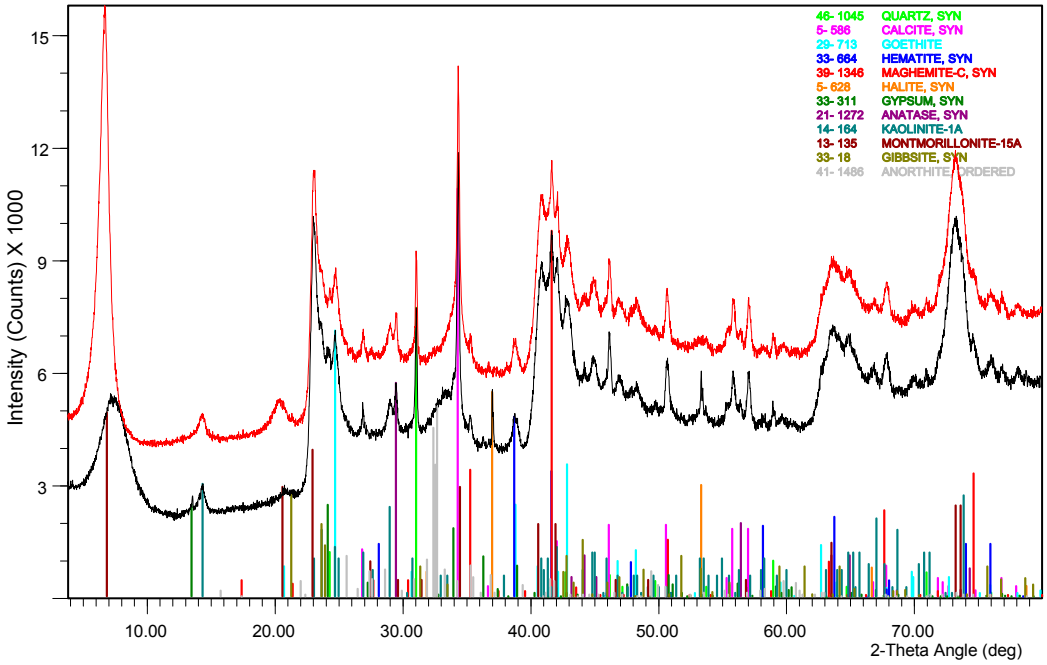

File Name: c:\...\2686_skb_asha_bentonite\2686-37518.xpt c:\...\2686_skb_asha_bentonite\2686-37518_mc.xpt

Asha 2012 Big bag no. 80

37519. Asha 21. Micronised.

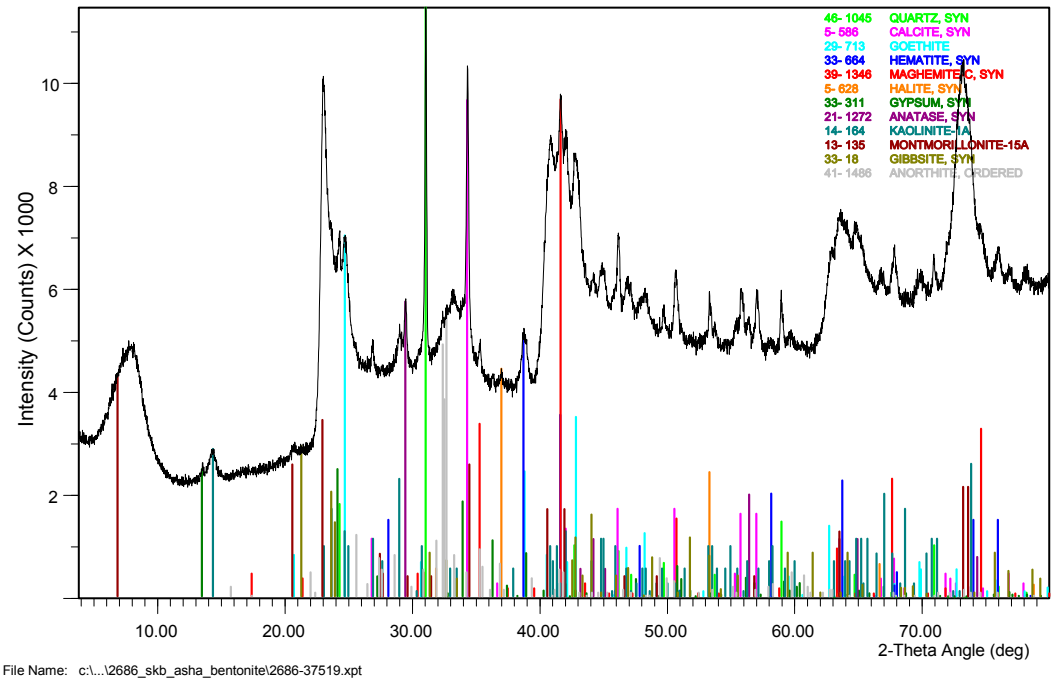

File Name: c:\...\2686_skb_asha_bentonite\2686-37519.xpt

Asha 2012 Big bag no. 80

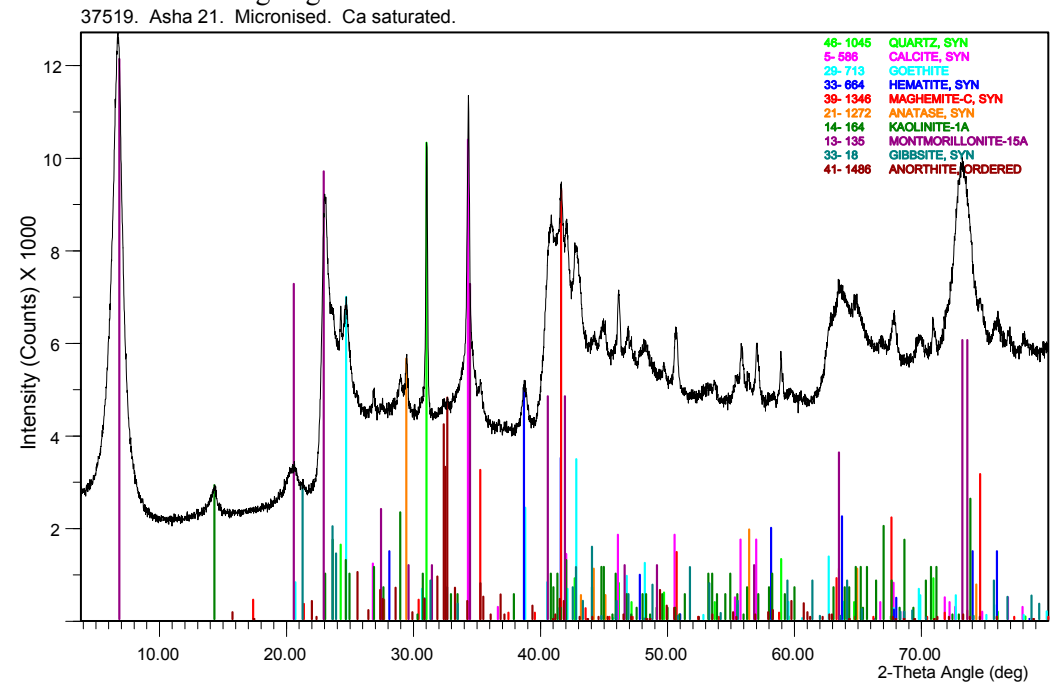

Asha 2012 Big bag no. 80

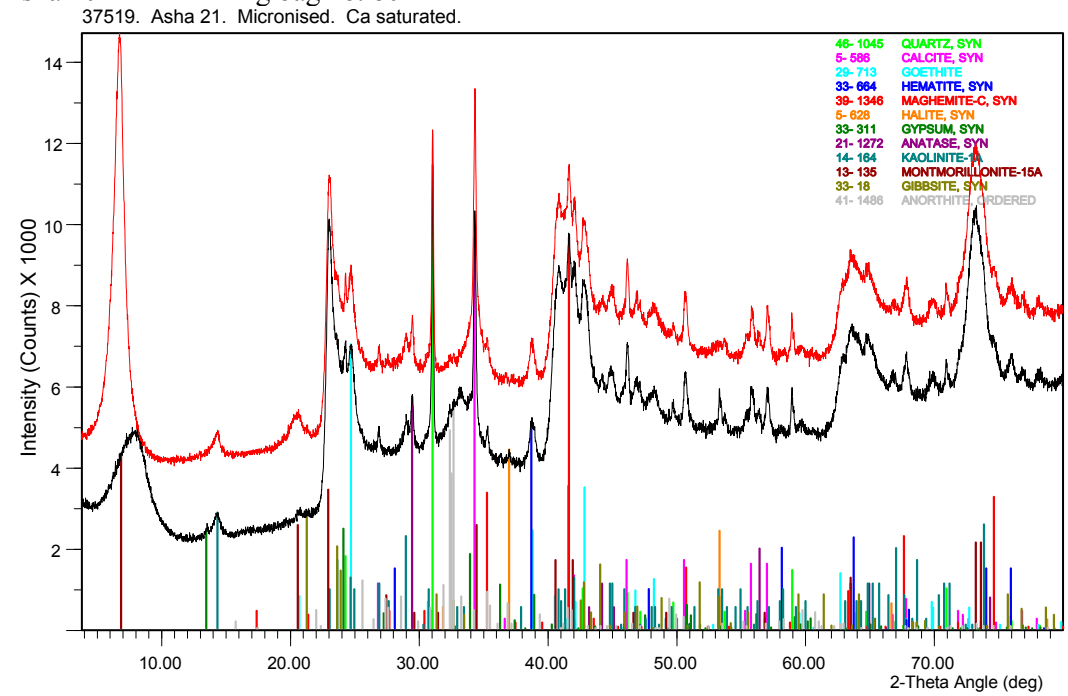

Asha 2012 Big bag no. 180

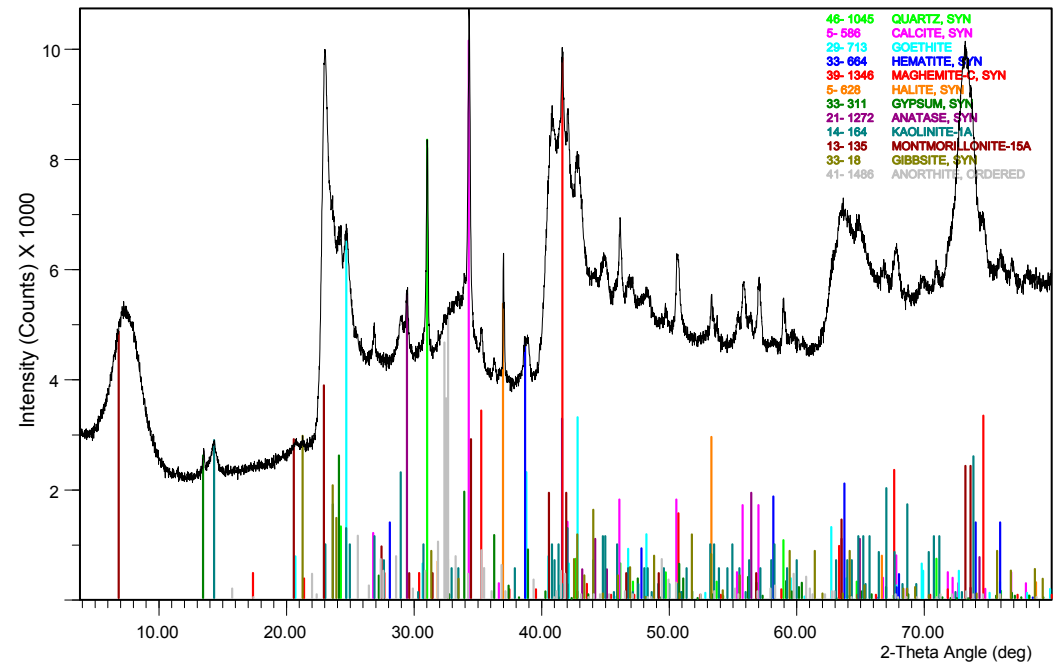

File Name: c:\...\2686_skb_asha_bentonite\2686-37520a.xpt

Asha 2012 Big bag no. 180

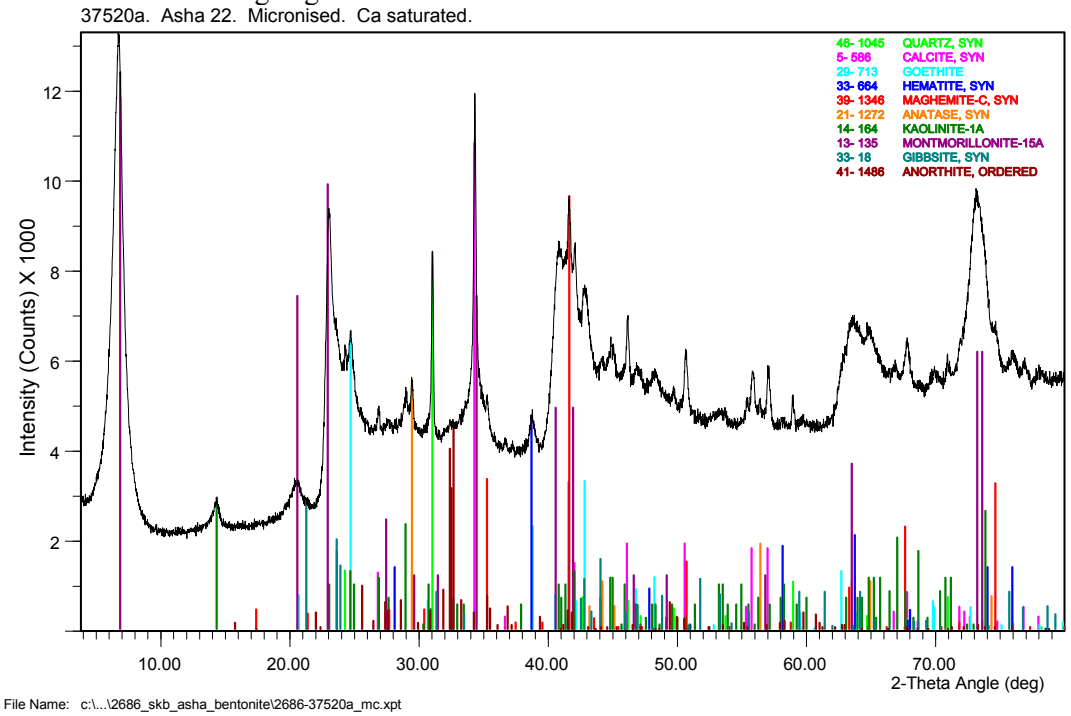

File Name: c:\...\2686_skb_asha_bentonite\2686-37520a_mc.xpt

Asha 2012 Big bag no. 180

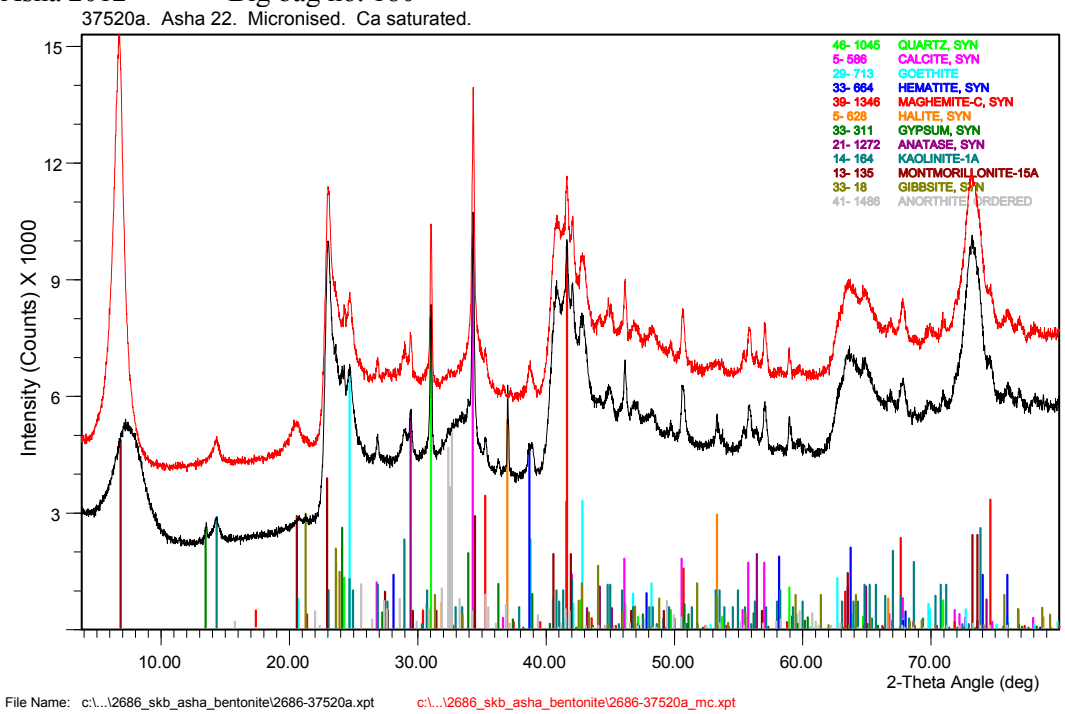

Asha 2012 Big bag no. 280

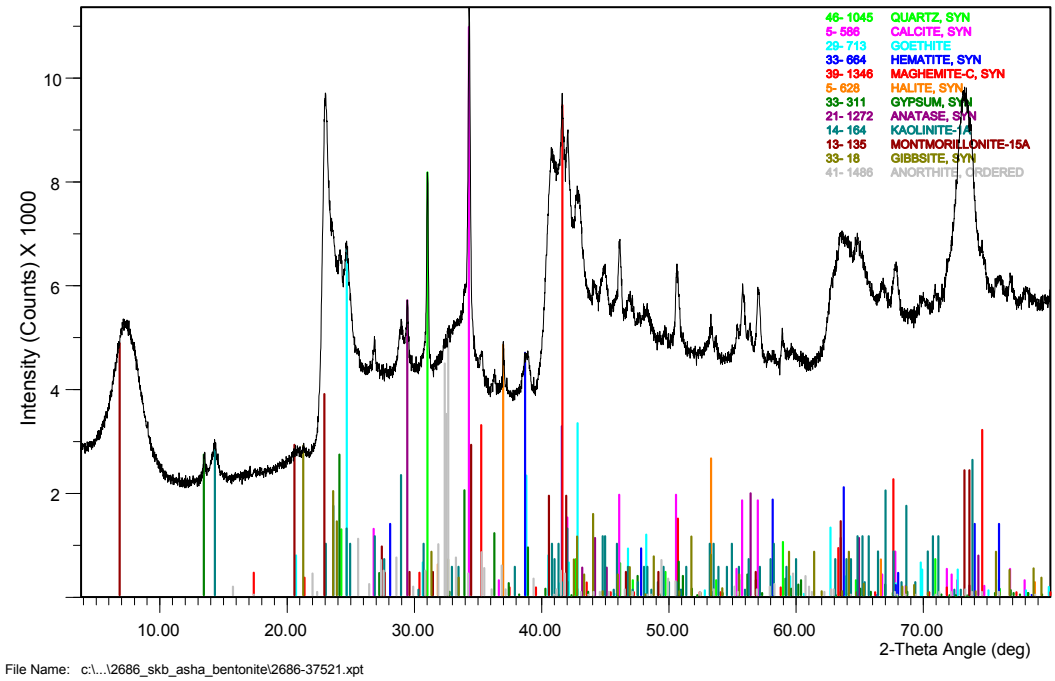

Asha 2012 Big bag no. 280

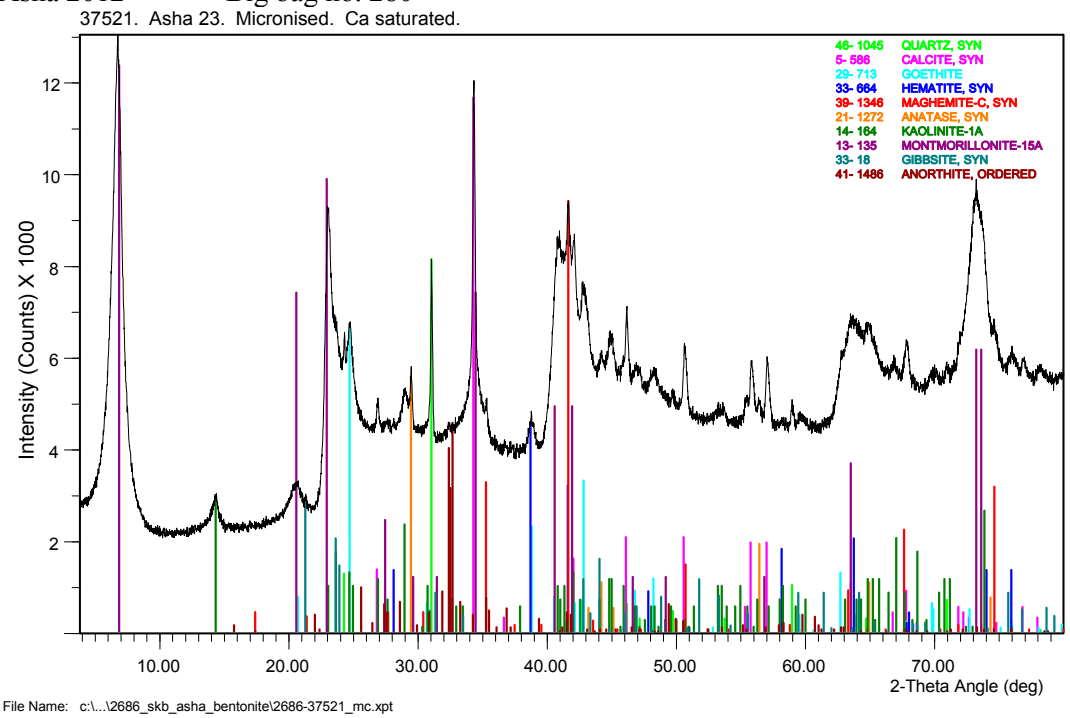

Asha 2012 Big bag no. 280

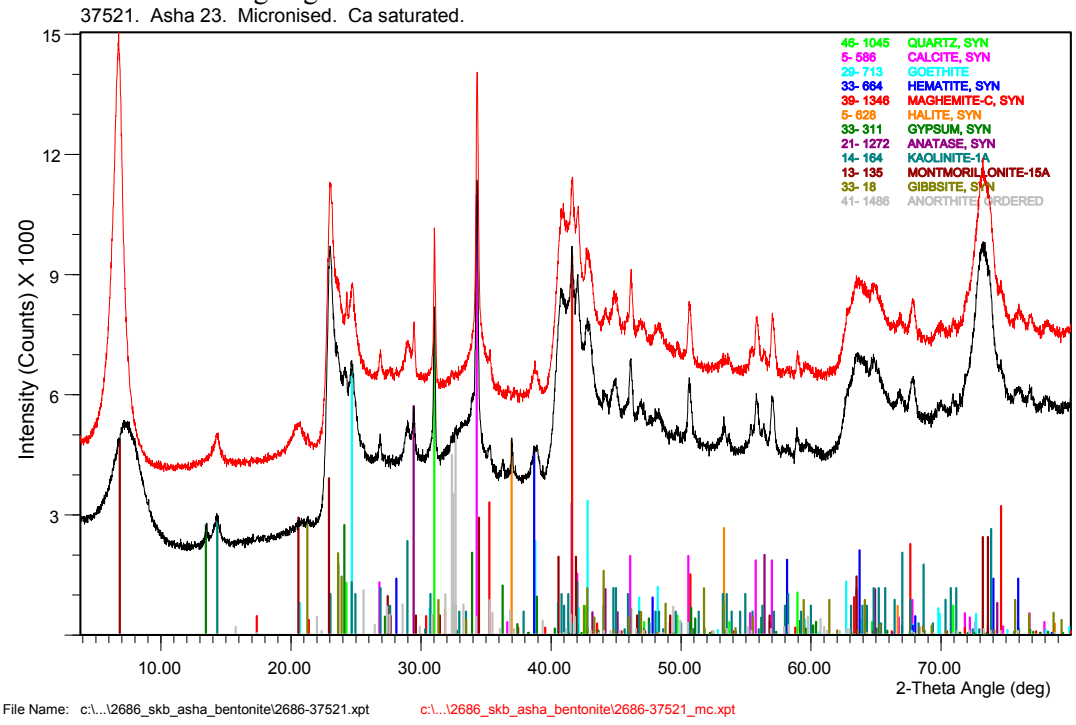

Asha 2012 Big bag no. 380

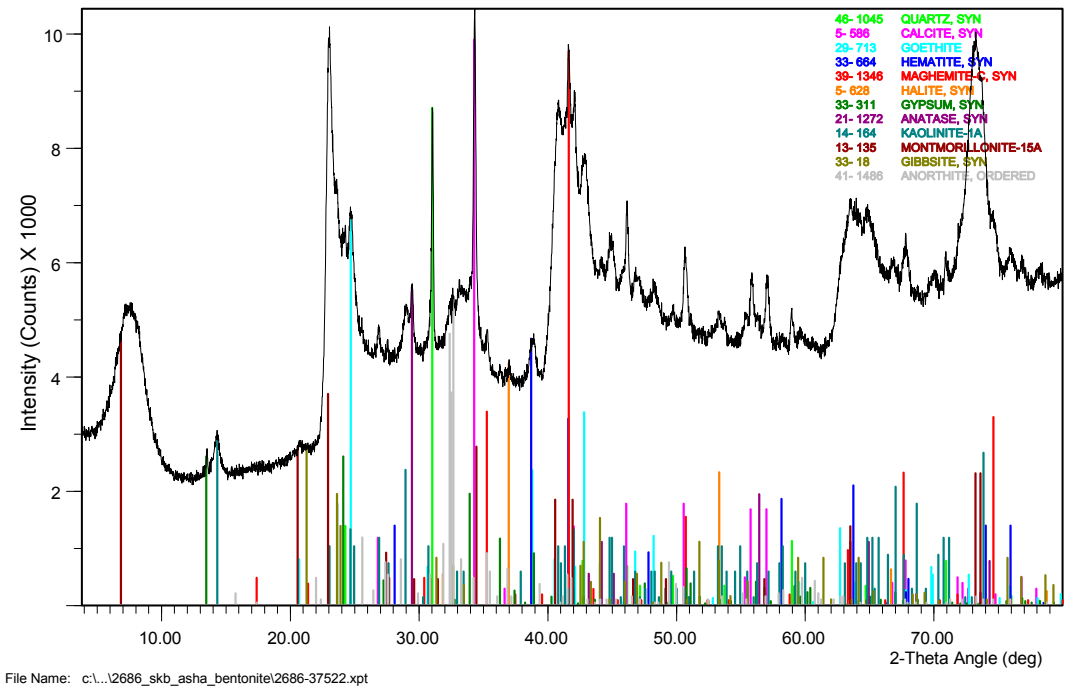

File Name: c:\...\2686_skb_asha_bentonite\2686-37522.xpt

Asha 2012 Big bag no. 380

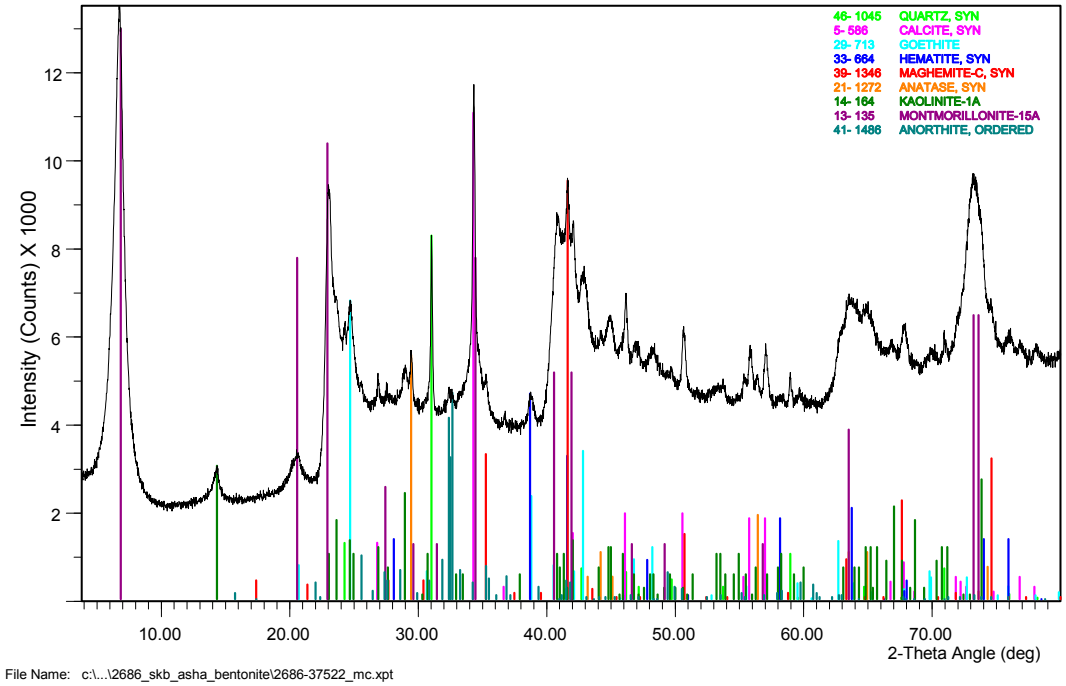

File Name: c:\...\2686_skb_asha_bentonite\2686-37522_mc.xpt

Asha 2012 Big bag no. 380

37522. Asha 24. Micronised. Ca saturated.

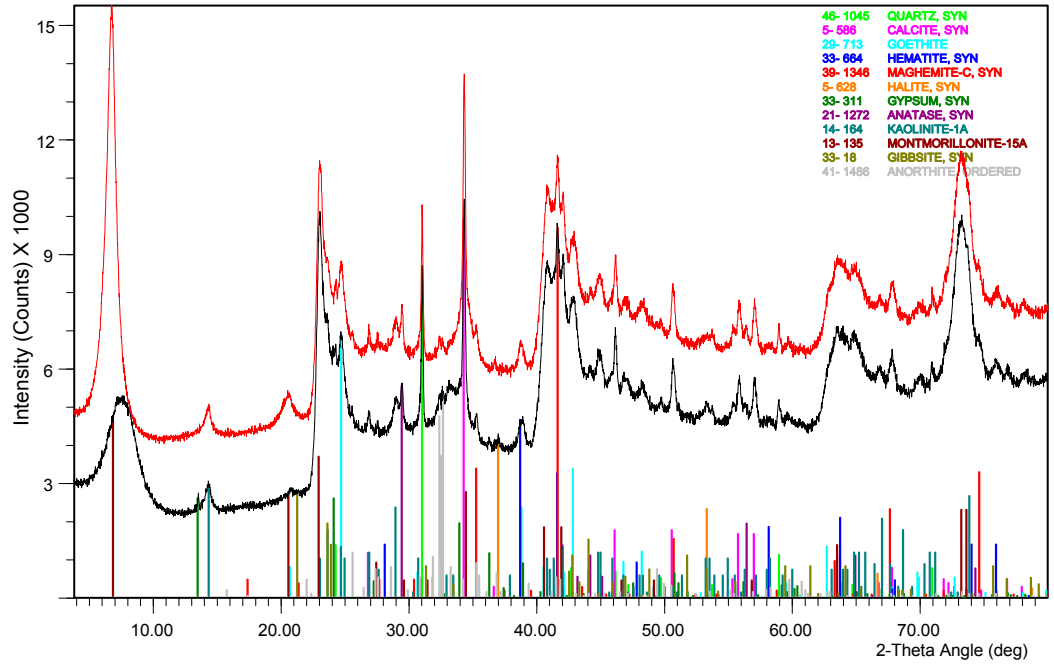

File Name: c:\...\2686_skb_asha_bentonite\2686-37522.xpt c:\...\2686_skb_asha_bentonite\2686-37522_mc.xpt

Asha 2012 Big bag no. 380

37522. Asha 24. >0.2um.

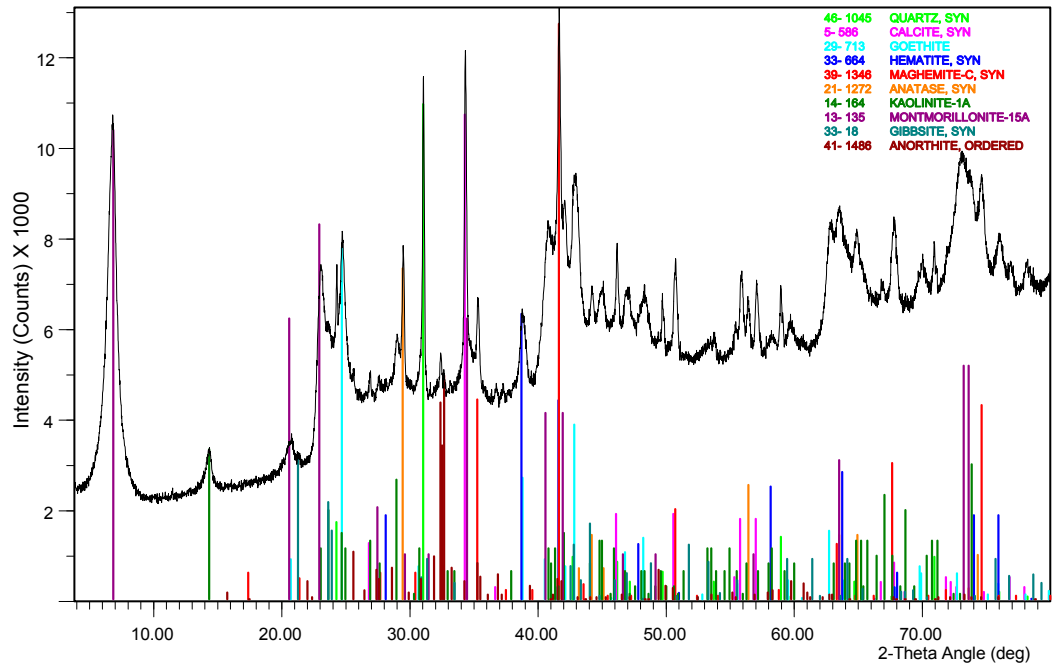

File Name: c:\...\2686-37522_g0.2um.xpt

Asha 2012 Big bag no. 380

37522. Asha 24. <0.2um. Acetic acid treated. Ca saturated.

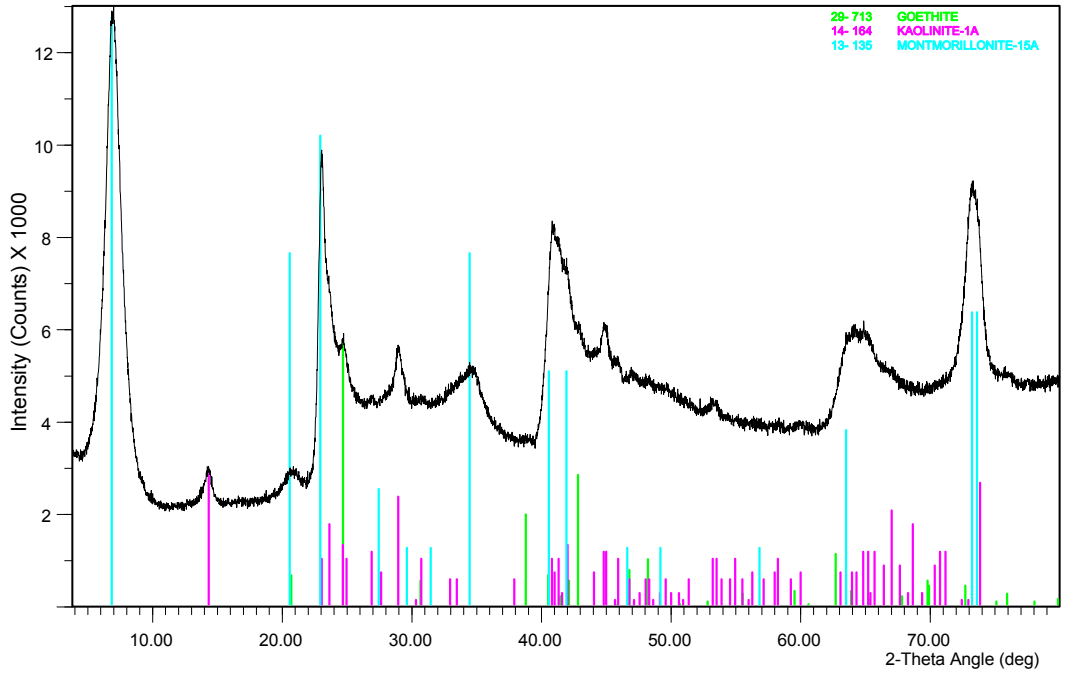

File Name: c:\...\2686-37522_l0.2um.xpt

Asha 2012 Big bag no. 480

37523. Asha 25. Micronised.

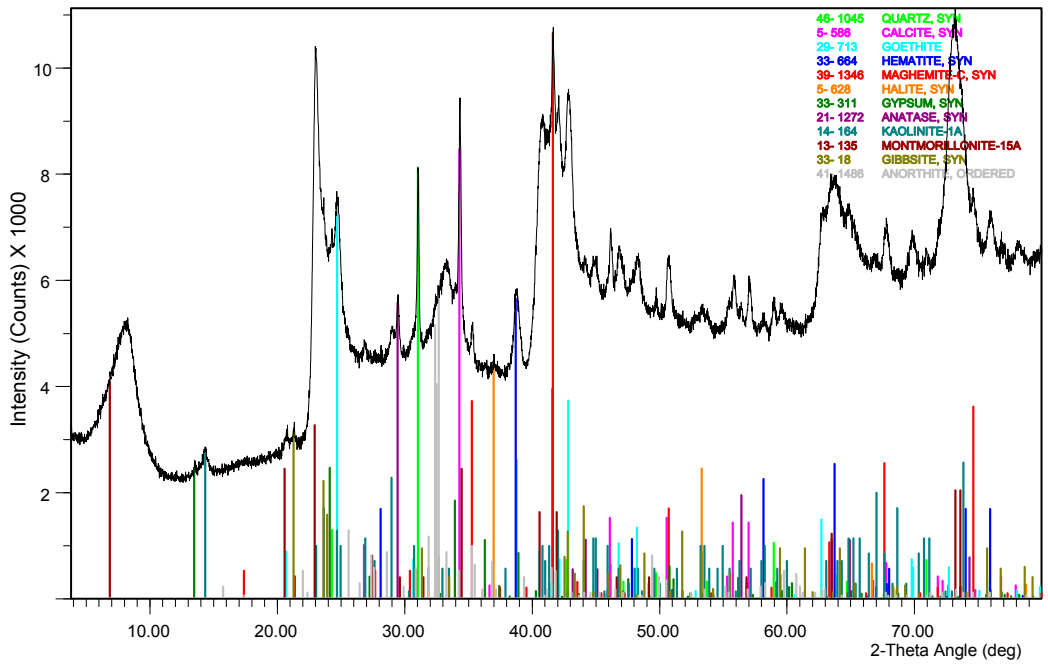

File Name: c:\...\2686_skb_asha_bentonite\2686-37523.xpt

Asha 2012 Big bag no. 480

37523. Asha 25. Micronised. Ca saturated.

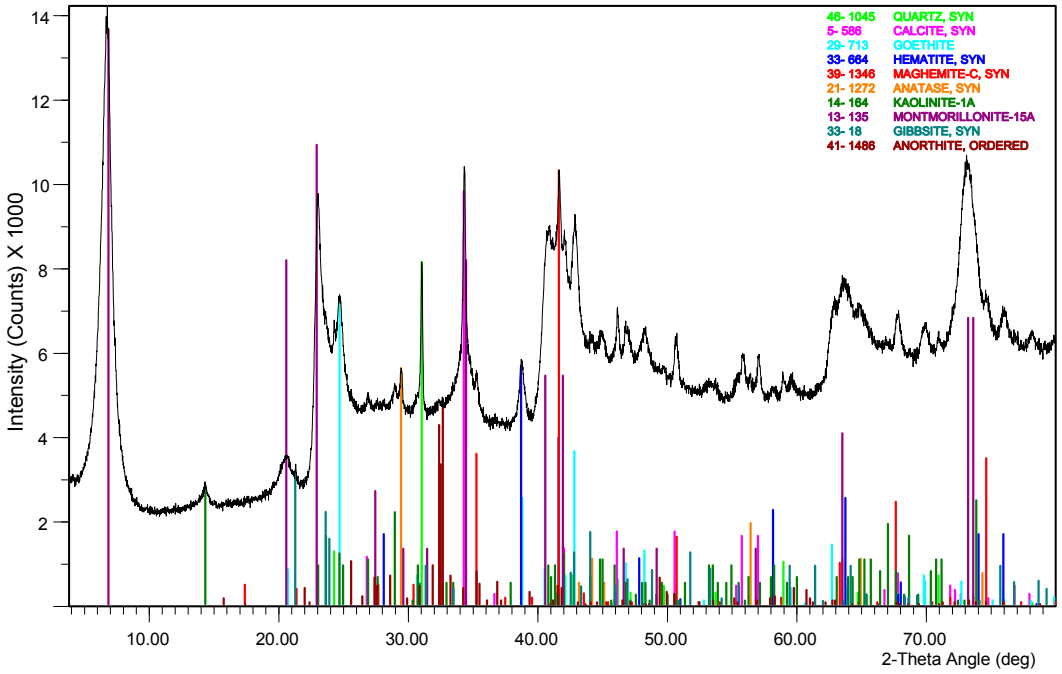

File Name: c:\...\2686_skb_asha_bentonite\2686-37523_mc.xpt

Asha 2012 Big bag no. 480

37523. Asha 25. Micronised. Ca saturated.

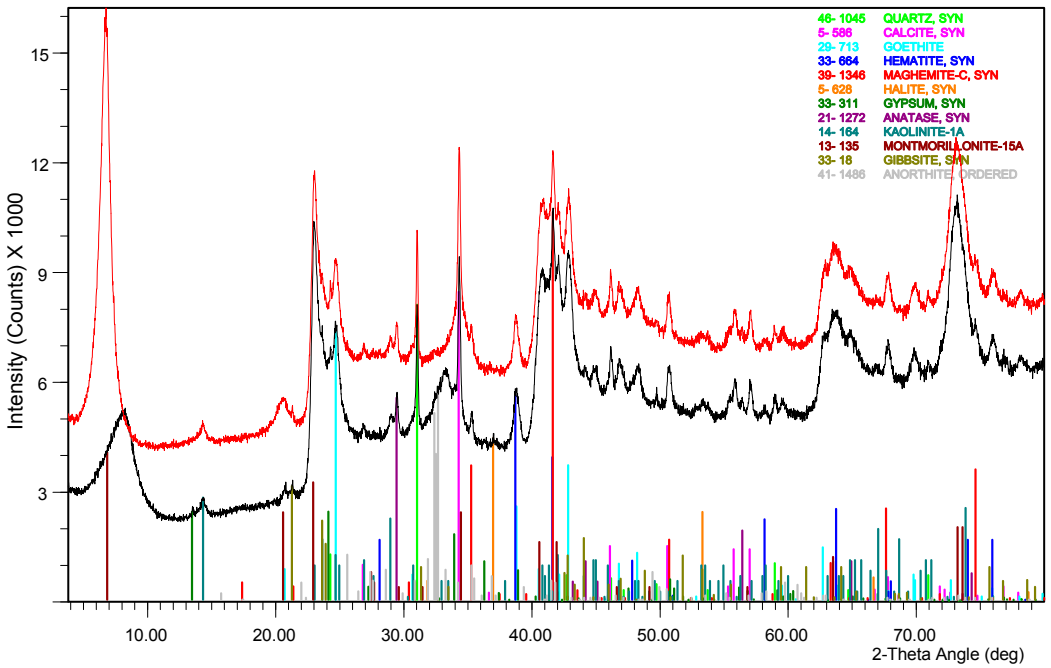

File Name: c:\...\2686_skb_asha_bentonite\2686-37523.xpt c:\...\2686_skb_asha_bentonite\2686-37523_mc.xpt